Underfoot Pressure Equalisation as an Explanation for Extreme Heteropody

ELEANOR CATHERINE STRICKSON

A thesis submitted in partial fulfilment of the requirements of Liverpool John Moores University for the degree of Doctor of Philosophy

January 2020

Table of Contents

Acknowledgements

First and foremost, I would like to thank Liverpool John Moores University for awarding me a Faculty of Science PhD Scholarship, without which I would not have been able to move to Liverpool and start this PhD, never mind doing it for three years while keeping myself fed and clothed. Thanks also for awarding me with the oral presentation prize for the school of Natural Sciences and Psychology. It really helped boost my confidence at a pivotal point in my life. I would also like to thank LJMU for allowing me to go to conferences everywhere from Manchester to Australia, where I met and discussed science with many amazing people. Thanks also to the Carl Gans Collections and Charitable Fund, for awarding me a travel grant to go and present my research at ICVM 2019 in Prague, and saving me from having to stay in a 20 person room in an all-girls party hostel for a multi-day conference.

Thank you to my co-supervisors, David Wilkinson at Lincoln University, at John Hutchinson at the Royal Veterinary College, Hatfield, for their help and advice, and especially to John for providing the bulk of the CT scan data used for chapter 2 and its corresponding Journal of Anatomy paper. I had a blast working with it. Thanks, on the topic of chapter 2, to David Blackburn at the Florida Museum of Natural History for providing us with frog CT scans to use, and to Diego Sustiata and two anonymous reviewers for reviewing the paper for submission, and ultimately helping us get it published.

A special thank you should go out to the NHS, without which I would not be here finishing this PhD. I went in for multiple hospital visits, for surgeries, surgical revisions, road traffic accidents, the works. Thank God for the NHS. Thanks especially to Dr. Rashid and Dr. Morley at Charing Cross Hospital for literally cutting me up and stitching me back together multiple times this year, and to Susan Wilder for giving me CBT at the darkest point in my life since my teenage years. I honestly would not be alive, never mind finishing this PhD, if

it wasn’t for your intervention. You guys are literal lifesavers. Thank you too to Jeremy Corbyn for trying to save it as an institution. You tried, bud.

On a lighter note, thank you to my friends for helping me through this and putting up with long periods of absence followed by being back in your life sporadically, and my parents, for supporting me and lifting me up when I needed it. Thank you especially to Karin Moejes and Ryan Marek for having my back and being there for me when I needed it most. I love you guys. Honourable mentions go to Alice Manterfield, Naomi Wain, Jack Warburton, and Heather Burton. Thanks also to Marta Zaher, for giving me back my confidence as a scientist when it was completely lost, for giving me somewhere to write up, and for all that other stuff that’s best left out of an acknowledgements section. I love you.

Lastly, thanks to the co-operative for spotting me to star in an ad campaign. Without that opportunity I wouldn’t have been able to afford rent, or to finish writing up, never mind getting onto Nottingham’s 30 under 30 list. Thank you for standing up for trans rights, and for the rights of all oppressed peoples, and thank you to everyone else who does too. Solidarity. Together, we shall overcome. Until then, the fight continues.

“The philosophers have only interpreted the world, in various ways; the point is to change it.”

– Karl Marx

“Everyone thinks that courage is about facing death without flinching. But almost anyone can do that. Almost anyone can hold their breath and not scream for as long as it takes to die. True courage is about facing life without flinching. I don't mean the times when the right path is hard, but glorious at the end. I'm talking about enduring the boredom, the messiness, and the inconvenience of doing what is right.”

– Robin Hobb

List of Tables and Equations

List of Figures

Abstract

Heteropody is the phenomenon in which the manus and pes of quadrupedal animals differ substantially in size and shape. The term is most often used in reference to the extreme foot size differences present in fossils and trackways of some non-avian dinosaurs, particularly sauropods. Previous studies have asserted the possibility that extreme heteropody developed in these animals as a mechanism to equalise underfoot pressure, compensating for unusually anterior/posterior centre of mass positions. This thesis sets out to test this hypothesis by answering the following questions:

1. Can skeletal surface area predict soft tissue foot surface area?
2. Is antero-posterior centre of mass position correlated with heteropody in extant taxa?
3. Do underfoot forces and pressures in extant taxa indicate the presence of a pressure equalisation mechanism?
4. Is there evidence in the fossil record for a link between centre of mass and extreme heteropody in dinosaurs?

These questions were answered using the corresponding methods:

1. Using CT scans of the feet of extant animals and a custom Matlab script to derive underfoot surface area for skeletal and soft tissue and if they correlate.
2. Using digitized skeletons and convex hulls of quadrupedal extant animals to gather centre of mass and heteropody data for a range of extant animals, and seeing how they correspond with CoM positions.
3. Combining new pressure mat recordings with recordings in the literature for quadrupedal animals and seeing how they correspond with CoM positions.
4. Gathering heteropody data from sauropodomorph fossil trackways and some quadrupedal dinosaur body fossils, and testing how they correspond with previously established CoM position estimates.

From these lines of enquiry, no link between CoM position and heteropody was definitively established. Results for live animal studies showed more signal for a correlation than in skeleton-only studies, and dinosaur trackway analysis showed potential for a link in sauropodomorphs, but neither of these studies provided enough evidence to establish a correlation between CoM and heteropody in tetrapods. This thesis does not support the hypothesis that heteropody is used as a pressure equalisation mechanism in tetrapods, especially as a universal rule. This thesis also found that soft tissue underfoot surface area is highly predictable from skeletal underfoot surface area. In addition, it found that underfoot surface area based on soft tissue is larger in forefeet compared to hindfeet that would be expected from skeletal surface area alone.

Declaration

No portion of the work referred to in the thesis has been submitted in support of an application for another degree or qualification of this or any other university or other institute of learning

Chapter 1

Introduction

1.1 Mass Distribution and Stability of Posture

The distribution of mass across an animal's limbs is linked to its stability, both during locomotion and when standing. The stability of each animal during locomotion, and its ability to support its own body weight, is a product of several anatomical and biomechanical factors, such as overall posture and the position of the limbs, distribution of mass throughout the body, the ability of the limbs to support that mass, and locomotory mode (Full et al., 2002; Hildebrand, 1980). An organism must be able to support its own weight and to be able to be able to carry its mass through locomotion without injury, (Gray, 1944; Biewener, 2005).

During locomotion, the movements of an animal's limbs are restricted to those that will keep the animal stable, lest the animal trip and fall, causing possible physiological damage, such as broken limbs and infection, and risking predation (Hildebrand, 1980; Eng and Winter 1993; Buchner et al., 2000; Pfau et al., 2006).

Quadrupedal animals, when opting for a slow walk where stability is guaranteed, have the option of using three feet to form 'triangles of stability' – where (for example) three feet are on the ground at a time, and body mass is therefore supported by three limbs at once, with the animal in question's centre of mass lying along the longest edge of these triangles (Figure 1.1) (Hildebrand, 1980; Henderson, 2006). This ensures stability in the animal by maximising support for the animal's mass, and allowing the animal to selectively use the most favourable combinations of these feet for balancing. The result is a stable walk, however, having 3 limbs on the ground at a time limits gait options, and thus this option is far from universally used (McGhee and Frank, 1968; Alexander, 2003). The

same principle can be applied when building quadrupedal robots, or robots with more than four legs, to keep them stable during movement (Cho et al., 1995), and is found in hexapodal locomotion where ‘tripods’ alternate (Lee et al., 1988; Ting et al., 1994).

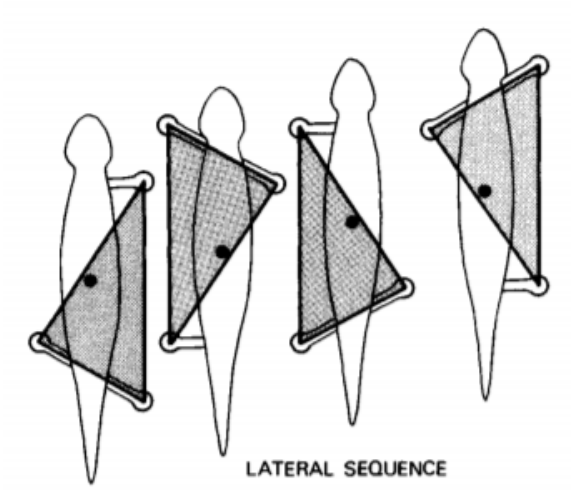

Figure 1.1 Visualisation of how three limbs on the ground at a time in quadrupeds (eg. salamander) can act to form triangles of support in a sprawling animal, and the relationship of these triangles of support with centre of mass positions. The black dot on each animal represents the animal’s centre of mass. From Hildebrand (1980).

In quadrupedal animals, the forelimb and the hindlimb can be utilised for different functional roles in locomotion. This is observed, for example, in primates and felines, where the hindlimbs apply the majority of the propulsive forces in steady state locomotion, while the forelimbs serve to provide the majority of forces used to brake or manoeuvre (Granatosky et al., 2018). Across quadrupedal mammals this pattern is consistent, with forelimbs bearing more weight, providing more vertical support, and providing the majority of the braking/backward forces, and hindlimbs providing the majority of the forward/propulsive forces: the so-called ‘hindlimb drive’ model (Demes et al., 1994). This model applies primarily to steady state locomotion. When an animal is accelerating, all four limbs can be net contributors to propulsion (Demes and Günther, 1989). These roles

appear functionally consistent regardless of mass distribution on the limbs, as observed across a number of different species of quadrupeds (Lee et al., 2004).

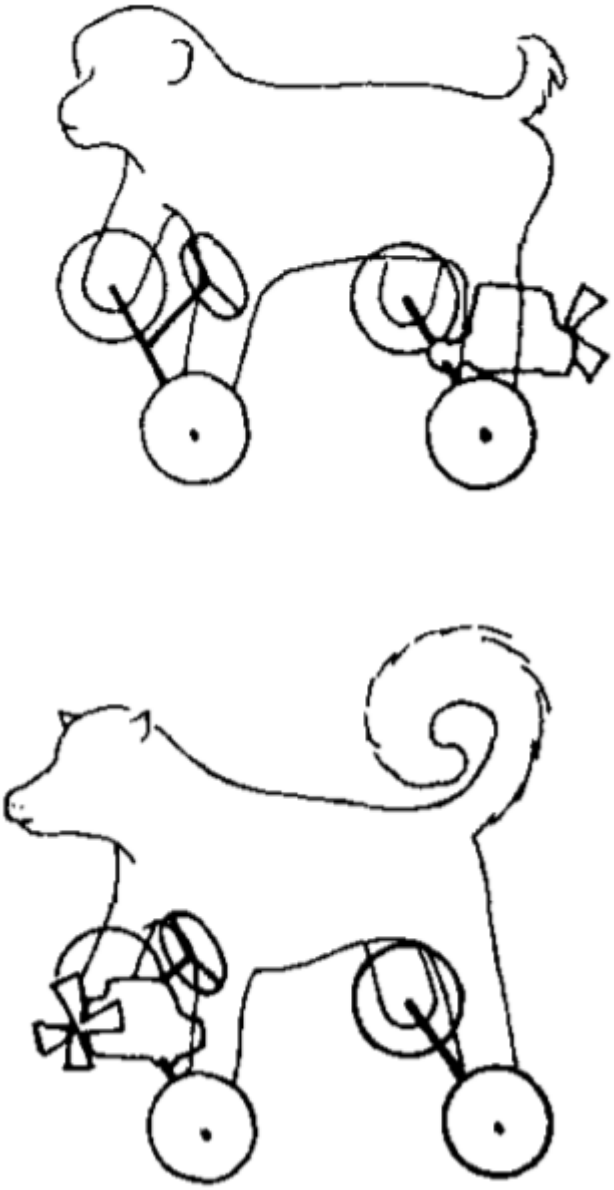

Figure 1.2 Simplified illustration of a primate quadruped (above) which uses hindlimb driven locomotion when moving at steady states, and non-primate quadruped (below) which, in contrast, primarily uses forelimbs for propulsion when moving at steady states, exposing them to higher forces. The propeller in the figure represents the limbs providing most of the propulsive force in locomotion in steady state locomotion, while the steering wheel represents the limbs most involved in determining the direction of locomotion in the same state from Kimura (1979).

The autopodia – the manus (the forefoot), and the pes (the hindfoot) – and their shape and posture, are important in determining the locomotory abilities of an animal. Since they are located at the ends of the limbs, they play a large role in both supporting an organism's mass, and accelerating/braking during movement (Huson, 1991; Wright, et al., 2012). Since animals with autopodia have diversified to fill a huge swath of ecological niches, from flying to swimming to burrowing, grasping, slashing, heavy load bearing, and more, there is incredible variety in the shape, size, and utility of autopodia, all while it is still necessary to retain efficient ability of the autopodia to support an animal's body weight, and allow it to move. Arboreal animals require hands that can grasp branches, fossorial animals often develop large claws for digging, semi-aquatic animals can evolve webbed feet for more efficient propulsion during paddling or swimming (Shimer, 1903; Osburn, 1903; Lull, 1904; Lehmann, 1963; Patel et al., 2015).

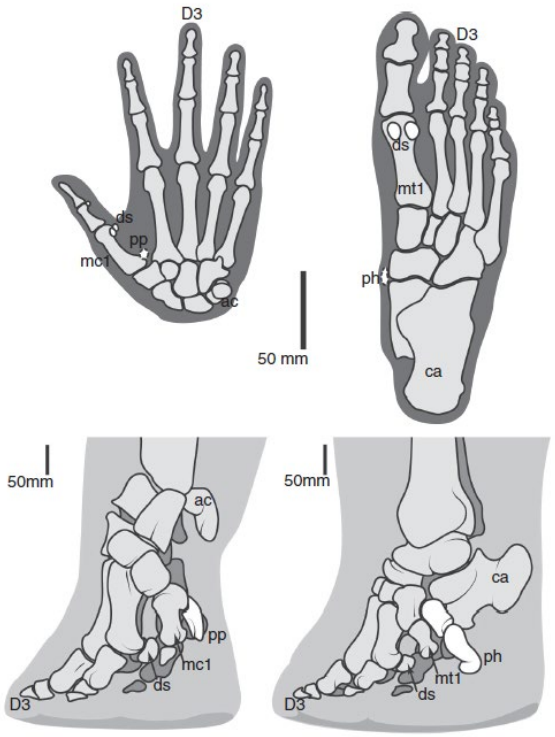

Figure 1.3 The skeletal anatomy of elephant autopodia (manus left, pes right), and demonstration of its unique posture (below), as compared to human autopodia (above, manus left, pes right). Ac = accessorium, ca = calcaneus, D3 = third digit, ds = digital sesamoids, mc1 = metacarpal 1, mt = metatarsal 1, ph = prehallux, pp = prepollex. Adapted from Hutchinson et al., (2011).

Variation in autopodial morphology based on dietary and locomotory niches is demonstrated in profound clearness by looking at the fossil ancestors of modern animals.

For example, reductions in toe number in fossil horses as they transition from forest browsing to a cursorial life in grasslands (Janis, 2007), and in dinosaurs, where several groups of bipedal carnivores transitioned first into herbivory, then into quadrupedality, resulting in bird-like feet and clawed hands evolving into elephant-like feet with fatty pads in sauropods, and hoof-like structures in hadrosaurids (Hutchinson, et al., 2011; Hamilton, et al., 2019), in beautiful demonstrations of convergent evolution with the autopodial structures of extant herbivorous quadrupeds.

Beyond the shape of the undersides of the feet, ecological niches are also reflected by the posture of the foot, with the bones and tissues of the autopodia arranged at differing positions relative to the leg and the rest of the body in order to support an organism's needs.

In general animal foot posture is divided into three main functional groups – unguligrade, digitigrade, and plantigrade. Plantigrade animals walk on their whole foot, digitigrade animals walk only on their digits, and unguligrade animals walk on the tips of their toes (their unguals). The latter posture is seen primarily in ungulates, who walk on their keratinous hoofs (Carrano, 1997). However, semi-digitigrade/subunguligrade foot postures are not uncommon, as in elephants, who walk with the support of a fatty foot pad, making them semi-digitigrade – walking on their toes but 'functionally plantigrade' (Carrano, 1997; Hutchinson et al., 2011) (see Figure 1.3).

The digitigrade ancestors of ungulates appear to have developed unguligrade posture as a means of improving their cursorial ability for greater speed (Clifford, 2010). However, for most quadrupedal mammals, foot posture appears strongly linked to an animal's size and mass. Larger mammals tend to adopt digitigrade foot postures, while plantigrade foot postures are favoured in smaller mammals (Kubo et al., 2019). Digitigrade foot posture has been associated with lower metabolic costs compared to plantigrady, and thus larger animals may have adopted the foot posture as an energy saving mechanism as demands

for food grew larger in conjunction with their body mass (Reilly et al., 2007). It should be noted that it is not clear that this is a causative relationship, and it varies between animals, eg. between a horse and a dog, with ecological roles seemingly having more influence that drivers for energy optimisation (Reilly, et al., 2007). Many exceptionally large animals, such as elephants and rhinoceroses, possess semi-digitigrade feet, seemingly as the stress of their large body masses need additional support, such as from foot pads and thicker skin (Hutchinson et al., 2011). However, it should be noted that foot pads are common in many species to absorb impact and reduce autopodial stress, albeit not to the same extent and not to the point where they effectively alter an animal's foot posture due to their size and the scope of their role (Chi and Roth, 2010).

Limb posture plays an important role in how body mass is distributed between the limbs. In general, animals with a more 'crouched' posture tend to be smaller. Small animals save little energy from the spring and inverted pendulum mechanisms used in tetrapod locomotion due to differences in stride frequency relative to animals with more erect postures. In more erect animals the energetic costs of muscle activation are more effectively recovered through pendular mechanics and inertia. While in 'crouched' animals, external joint movement is higher and moment arms are lower, leading to higher activation levels, and therefore a greater overall energy cost to the organism (Griffin et al., 2004; Reilly, et al., 2007). In more upright animals upright posture increases effective mechanical advantage of certain anti-gravity muscles (eg. m. gastrocnemius).

1.2 Studying Locomotion in Extinct Animals

Body fossils are, for the most part, purely skeletal remains. Where there are exceptions to this, e.g. skin impressions, they are rarely substantial enough, and high enough in number, to give definitive answers regarding the soft tissue makeup of extinct animals (Carpenter, 2007; Paik et al., 2017). There are of course, certain inferences that can be made from the skeletons of animals alone. However, much more context for the *in vivo* biology and biomechanics of extinct animals can be gained by studying living animals (*In vivo* herein referring to tissue as it would appear, and act, when an animal is alive).

Knowledge of the biomechanics of extant animals can, with reference to the known anatomy and ancestry of extinct animals, infer and inform the science of how extinct animals lived, and moved.

When researching extinct animal locomotion, it is important to consider which extant animals are being studied to inform analysis of the extinct animals in question. For certain studies in functional anatomy, it makes sense to consider animals with similar bone structures, posture, size, etc. to the extinct animal in question. For example, when studying an animal with a sprawling gait, it makes sense to study sprawling gaits in lizards, newts, and salamanders, to inform how such an animal may have walked (Morse et al., 2013; Kawano and Blob, 2013). When studying how sauropod dinosaurs coped with their enormous size, it makes sense to study the methods by which the largest extant land animals cope with their unusual body mass (Coombs Jr, 1975; Hutchinson et al., 2011; Jannel et al., 2019).

For other purposes, the most salient process by which to pick the extant animals that will inform an analysis of an extinct animal is that of the ‘extant phylogenetic bracket’ (Witmer, 1995). To use the extant phylogenetic bracket (EPB) is to rely on at least the first two extant outgroups of the fossil organism in question – forming a bracket around the organism’s branch on a phylogenetic tree with its two outgroups. This relies on the increased likelihood of homological structures and similar anatomical phenotype of the extant animals in comparison to the extinct animal, compared to other extant organisms, to more accurately infer the likely anatomy, functional morphology, etc., of the extinct animal. This method is a natural outgrowth of the ‘outgroup method’ used in comparative biology, wherein comparing and contrasting characteristics of outgroups can be used to estimate ancestral states for an ingroup (Maddison et al., 1984; Huey, 1987; Lyons-Weiler et al., 1998). Using the EPB when studying soft tissue structures should aid palaeobiologists in understanding and reconstructing the soft tissues in extinct animals, by approximating the ancestral state of these tissues from their closest living relatives (Witmer, 1995). In this way, osteological correlates of soft tissues in extinct animals with no soft tissue preserved can be used as proxies for these soft tissues. This technique

helps the researcher to avoid excessive leaps of logic, and to avoid further interpretations of an extinct organism's anatomy, behaviour, and evolution, based on flawed, naïve, or outright incorrect inferences (Witmer, 1995). While it is impossible to know for certain the exact soft tissue structure, behaviour, etc., of the extinct animals in question – combining this method with knowledge of appropriate modern analogues (e.g. elephants with foot pads and large size for sauropod foot comparisons), inferences are both informed, and sensible, drawing from the most likely outcomes.

1.2.1 3D Modelling of Organisms

With the use of computed tomography (CT) scans, 3D models of entire animals can be created, and segmented for research purposes. Models can also be obtained with magnetic resonance imaging (MRI) scans, or positron emission tomography (PET) scans, however, these are used less often in the study of animal biomechanics, and are expensive (Johnson et al., 1997; Watanabe et al., 1997; Zou et al., 2009; Yu et al., 2010). Alternatively, scans of the external surface of animals or animal skeletons can be obtained using laser scanning or photogrammetry (Figure 1.4), (Bates et al., 2009; Falkingham, 2012). With these models, the anatomy of animals can be studied without having the animal to hand, and can be studied from remote areas where access to the relevant facilities would be unavailable. This makes the study of these animals more feasible on a larger scale, as more people can gain access to a computer that can run 3D modelling software, than can gain access to cadavers from zoos and farms, or specimens from museums and private collections, allowing a wider potential audience of researchers (Cignoni et al., 2008; Kent, 2014; Girardeau-Montaut, 2015; Murdock, 2017). In addition, the advent of open-source repositories for 3D models facilitate wider access to these models, removing yet more barriers to research (Rowe, 2002; Boyer et al., 2016).

anatomy, and their centres of mass.

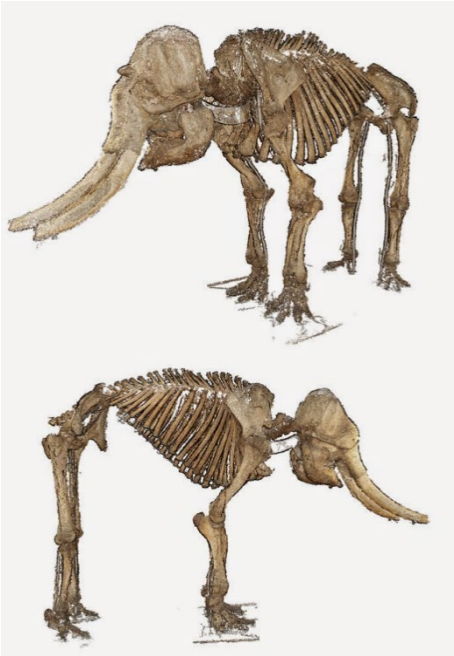

Figure 1.4 3D Point cloud of an Asian elephant (*Elephas maximus*) created using photogrammetry (Falkingham, 2012).

Whole-body 3D models of organisms can subsequently be used to calculate geometric measures such as body mass and centre of mass. Since extinct animals lack the full extent of their preserved soft tissues, their overall mass, soft tissues included, must be estimated in order to accurately estimate their *in vivo* centre of mass positions. This can be done through the creation and application of 3D volumetric models, as demonstrated by work by Sellers and Allen among others and seen in Figure 1.5 (Allen et al., 2009; Sellers et al., 2012).

The use of volumetric models, such as convex hulls to compute body mass and centre of mass has routinely been applied by palaeobiologists to track changes in centre of mass associated with evolution and phylogenetic position within clades containing extinct animals. For example, across sauropods and theropods, where changes in centre of mass position during the evolution of extremely large size (Bates et al., 2016), and across the transition from non-avian dinosaurs to birds (Allen et al., 2013), can be made respectively. Volumetric models can also be used to track changes of centre of mass during dramatic postural shifts, such as the transition from bipedalism to quadupedalism in several groups

of ornithischian dinosaurs (Maidment et al., 2014; Bates et al., 2016). In addition, alternative and perhaps more precise estimations of body mass for extinct animals than those accepted previously, can be obtained (Bates et al., 2009; 2015).

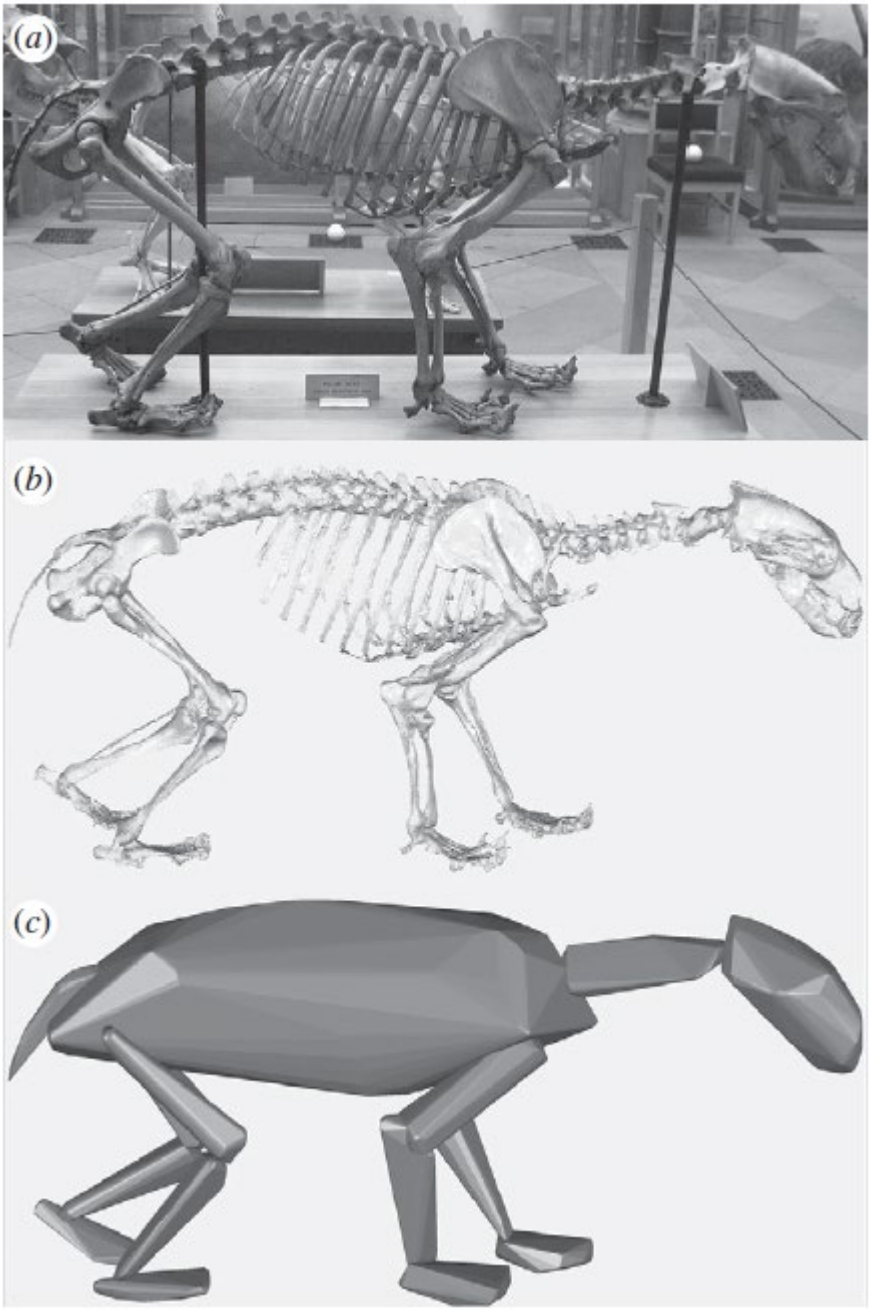

Figure 1.5 Demonstration of the digitisation and 3D convex hulling of a museum specimen – a mounted skeleton of the polar bear (*Ursus maritimus*). A = original skeleton, B = 3D point cloud derived from laser scanning, C = the completed 3D convex hulls used to compute geometric measures. From Sellers et al., (2012).

1.3 Dinosaur Footprints, Heteropody, and Extreme Heteropody

1.3.1 Ichnology and the Study of Footprints

For evidence of extinct organisms outside of body fossils, palaeontologists can draw upon trace fossils. From fossil footprints, they can infer information about animal gait and foot anatomy, such as how far apart an animal kept its feet during walking, the orientation of the feet during walking, and differences in pressure based on how deep footprints are formed within a substrate, with the caveat that pressure and depth are not necessarily always directly related, and disparate foot shape and other confounding factors can influence the relationship between these variables (Casinos, 1996; McDonald, 2007; Richmond et al., 2012; Castanera et al., 2012; Hatala et al., 2013; 2016). In addition, certain questions about the extinct animal's behaviour can be inferred, such as whether a trackmaker was an animal that travelled in herds, the composition of those herds, and whether they travelled and lived alongside species other than their own (Lockley et al., 1983; Gierlinski and Sabath, 2008; Myers and Fiorillo, 2009).

In theory, a footprint should, to some degree, reflect the underfoot contact area of its trackmaker. However, besides the basic foot anatomy of the trackmaker, the dynamics of the animal (the animal's gait, how fast it is moving, etc.), and the substrate the animal is moving on, have a significant influence on how a footprint is formed, and the resultant shape of the footprint (Baird, 1957; Padian and Olsen, 1984a; Minter et al., 2007; Falkingham, 2014). In addition to this, the taphonomy of the footprint - how it changes with the influence of the environment when it is exposed to the air, its underlying geology and how it changes over the ages, and more, can change the eventual shape of the foot that ichnologists can eventually observe and analyse (Buatois and Mángano, 2004; Razzolini et al., 2014). In this way the shape of a footprint is not an exact mirror of the underfoot anatomy of its trackmaker, often far from it, but it can tell palaeobiologists much about its trackmaker regardless, and inform their view of the anatomy of trackmakers and the makeup of their communities.

1.3.2 Heteropody and Extreme Heteropody

Heteropody is a term coined by Lockley et al., (1994a) to describe the difference in size between footprints of the manus (forefoot), and the pes (hindfoot), referring to this ratio as it pertains to underfoot contact area with the ground. It is a useful mechanism to quickly visualise the disparity of foot size in a trackway, particularly when describing trackways of sauropod dinosaurs, where 'extreme heteropody', an exceptionally large disparity between manus and pes size, is well-known (Henderson 2006; Falkingham et al., 2012). While heteropody here refers solely to autopodial size differences, it is, in the case of sauropods, accompanied by striking differences in foot shape, and posture. While heteropody itself is known across many ichnospecies, extreme heteropody is a notable feature in sauropods. Preserved trackways from these dinosaurs indicate that, rather than their foot impressions being of relatively equal area, their fore and hind feet impressions have significantly different areas (Falkingham et al., 2011;2012. In animals with extreme heteropody, size differences could indicate a correlation of foot size with centre of mass, to equalise underfoot pressure between the forefeet and hindfeet. This has the potential to reduce maximum underfoot pressure and excess internal strain in the foot (Cheung et al., 2005). It follows then, that the relative size difference between manus and pes could relate to the position of an animal's centre of mass. This is indeed found in some species of mammal (Henderson, 2006). However, how common this correlation is throughout Tetrapoda (limbed vertebrates) has yet to be fully explored.

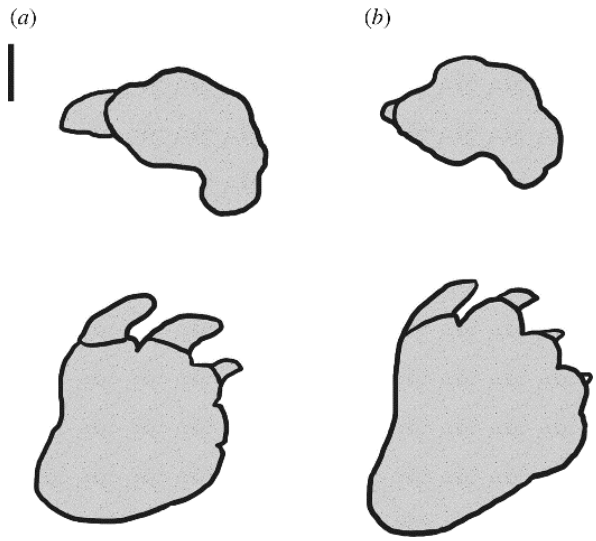

Figure 1.6 – Examples of manus versus pes underfoot contact areas in sauropod dinosaurs of two different clades A = *Diplodocus* a diplodocid, B = *Brachiosaurus,* a macronarian. The relative areas of these footprints demonstrate different degrees of heteropody between the clades, with more extreme heteropody in B, likely leading to higher manual underfoot pressures. From Falkingham et al., (2010).

Manus-only (and manus-dominated) trackways are a phenomenon found in sauropod trackways, where pes tracks are absent across the entirety of a trackway. While there are a number of potential explanations for this phenomena, one that is especially relevant to this thesis is the idea that these trackways form where only the manus makes a deep enough impression in the substrate of the trackway to be preserved. Whether manus-only trackways indicate higher pressure under the manus compared to the pes *in vivo* is still debated, but the hypothesis has not yet been comprehensively tested (Falkingham et al., 2011; 2012). The prevalence of these unusual trace fossils is dependent on the *in vivo* mass distribution under the limbs of the trackmakers. These mechanisms by which manus-only trackways may have been formed are dependent on the composition and compliance of the underlying substrate (Falkingham et al., 2011). Currently, there is no widely-accepted reason why manus-only trackways are formed, although possible links between heteropody and mass distribution in these organisms have been proposed

(Falkingham et al., 2011). Another potential explanation for this phenomenon is that it reflects locomotion in the water, whether swimming or punting, reflecting manual propulsion against a submerged substrate (Bird, 1944; Huh et al., 2003; Lee and Lee, 2006; Xing et al,. 2016a). While this hypothesis lacks substantial evidence in its favour, it is the subject of some ongoing debate (Lockley and Rice, 1990; Pittman, 1993; Lockley et al., 1994c; Henderson, 2004; Ishigaki and Matsumoto, 2009; Falkingham et al., 2010; Harter et al., 2014). A recent study of manus-only trackways by Farlow et al., (2019) offered support for differential underfoot pressures as an explanation for the manus-only trackways analysed, while not ruling out unusual locomotion.

Pes-only trackways are also known from multiple localities and ichnospecies. This phenomenon could be produced by similar mechanisms to those of manus-only trackways, or by overprinting, where a trackmaker places its pes where its manus had previously contacted the ground and left a print (Milàn and Hedegaard, 2010; Falkingham et al., 2010; Lockley et al., 2012; Xing et al., 2016a). While pes-only trackways do not necessarily indicate unusual behaviour on the part of their trackmakers, their existence does imply the presence of trackmakers for which heteropody will remain unrecorded, and therefore the diversity of heteropody in the fossil record is possibly understated, since animals walking in this manner are likely to continually overprint when walking at similar speeds/gaits, leaving scant few manus impressions (Mazzetta and Blanco, 2001; Milàn and Hedegaard, 2010).

While the existence of manus and pes only trackways are noted here as a possible consequence of heteropody in sauropods, whether they are caused by pressure differences is beyond the scope of this thesis. Instead, they are part of the inspiration for the question of whether pressure and heteropody are linked in these animals. If indeed heteropody is linked to differential underfoot pressures, it could help to inform whether it is possible that differential underfoot pressures could also be responsible for these enigmatic trackways.

In extant quadrupeds, heteropody is primarily known from animals that habitually use locomotor gaits other than walking, such as frogs and rabbits who use exceptionally large hindfeet to hop, kangaroos, who employ a similar strategy while also employing use of their tail when walking, and beavers, who use their large, webbed hind feet to paddle in the water. Sauropod dinosaurs do not appear to have had the ability to jump, and they do not appear at all specialised for semi-aquatic locomotion (Henderson, 2004; Falkingham et al., 2010; Xing et al., 2016a).

There are no extant animals with a body plan directly analogous to that of sauropods, either in terms of shape or size, to accurately use as a modern analogue. However, examination of a large number of tetrapods to determine how common correlations are between centre of mass and underfoot pressure, (especially in animals with heteropody) may expose interplay between these variables and therefore offer explanations for how and why extreme heteropody arises..

1.4 Quantifying Pressure in Living Animals

Pressure is the product of a force over an area. Heteropody then, referring to differences in underfoot area between the manus and pes of an animal, by its nature, is directly related to underfoot pressures experienced by the manus and the pes.

With current technology, it is relatively simple and easy to measure underfoot pressure using pressure mats. Pressure mats have been demonstrated to be a practical and useful tool for measuring foot pressure in humans, and many other animals (Van der Tol et al., 2003; Vereecke et al., 2003; Meijer et al., 2014).

As with many techniques in biomechanics, studies of underfoot pressure have historically been focused on human gait, and as a diagnostic tool for pathologies (Apelqvist, 2012; Kinoshita et al., 2019; Yamashita et al., 2019). Similarly, amongst studies of underfoot pressure in animals, much work has been done in veterinary diagnostics, especially in ungulates such as domestic cattle and horses, where measuring underfoot pressure can help to diagnose lameness and the overall health of a hoof (Scott, 1989; Carvalho et al., 2005; Grégoire et al., 2013).

Studies of animal gait from a functional morphology perspective using pressure mats, (Clarke et al., 2001) are commonplace. For example, comparing different modes of locomotion within a single animal such as walking versus running (Lascelles et al., 2006), or climbing versus walking in arboreal animals (Lammers et al., 2006). It is important in these experiments that subject animals are not coerced into walking when conducting locomotory experiments, as this can affect results in a way that does not resemble their natural locomotory inclinations (Leasure and Jones, 2008).

Quadrupedal mammals have been observed, in previous studies (herein citing vertical ground reaction forces to demonstrate load on the fore and hind limbs), to generally support 55-60% of their mass with their forelimbs (Reynolds, 1985a;b). Notable exceptions include primates, supporting about 30-45% of their mass with their forelimbs. Generally, cursorial mammals tend to use their forelimbs to support more weight, and cursoriality is associated with slightly anterior centre of mass positions (de Faria et al., 2015). Reptiles generally use their hindlimbs more to support their body mass, possibly due to the prevalence of long, muscular tails, and their influence on overall body mass distribution (Allen et al., 2009; Willey et al., 2004). Ecological niche can also have a profound influence on pressure differences between the manus and pes of an animal. Fossorial mammals, such as anteaters, have forelimbs of double the muscle mass of their hindlimbs, for example, with this disparity directly affecting distribution of mass along the body, and therefore the stresses experienced under each foot (Lascelles, et al., 2006; Granatosky, et al., 2018).

1.5 Extreme Heteropody as a Pressure Equalisation Mechanism?

Knowledge of relative manus-pes size is important in understanding the ways an animal can move and support its weight. In a simplified sense, as demonstrated in Figure 1.7, an animal's body can be understood as a simple beam, and its limbs the supports that hold the beam up (Alexander, 1985). In erect animals, where limbs are held under the trunk rather than to the side, the supports are directly under the beam, and thus the weight is distributed to each of its supports, relative to centre of mass location (Halliday et al.,

2013)), in a way that does not require constant force exertion and avoids the shear stresses in bones that are associated with a sprawled posture (Blob, 2000). In theory, a central load would be distributed equally between the limbs, and a load closer to one side will result in more load bearing on the side in question. If the area at the base of these supports (i.e. foot surface area) were increased on the load bearing side, the result would be equal stress on each support, despite unequal loads (Henderson, 2006). In this way, extreme heteropody, as exhibited in sauropod dinosaurs, could potentially be utilised to equalise underfoot pressures, and stabilise a front heavy, or back heavy, animal, with changes in heteropody corresponding to shifts in centre of mass (Falkingham, 2012; Falkingham et al., 2010).

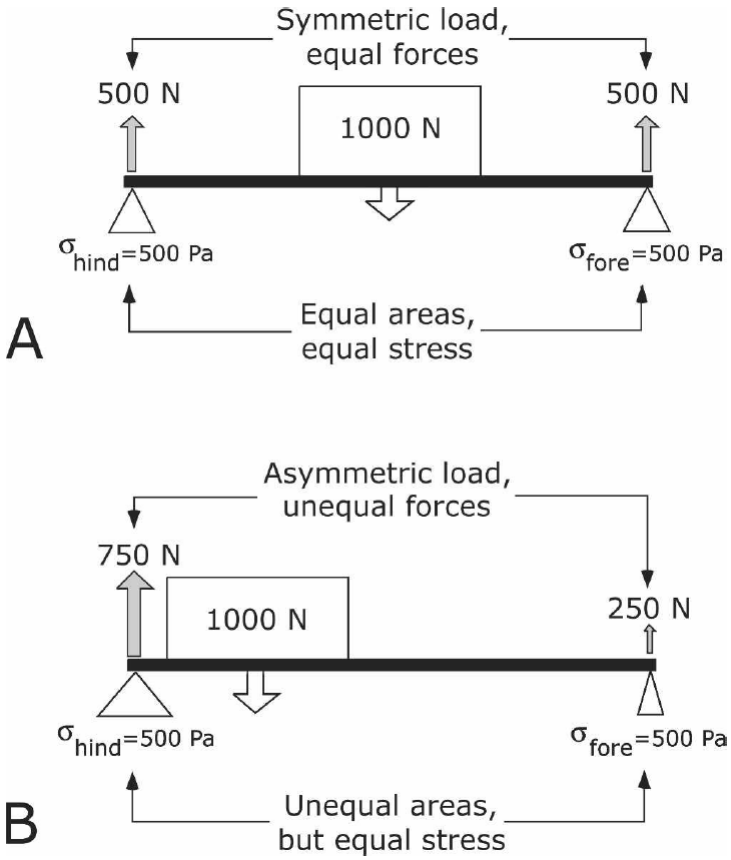

Figure 1.7 The proposed relationship between heteropody and underfoot pressure, demonstrated using a simple beam and support model. From Henderson (2006).

Ultimately it is potential disparity of pressure between manus and pes that is most pertinent to the question of how quadrupedal dinosaurs distribute their body weight. If centre of mass and foot pressure are related across quadrupedal animals, the explanation of heteropody as an equalising model (Figure 1.7) would potentially be supported. If it is unrelated, then other explanations would be necessary to understand the prevalence of extreme heteropody, and shifting heteropody, in the dinosaur fossil record. Comparing centre of mass and pressure differences in extant tetrapods should indicate whether there is a universal link between these variables. If there is not, then extreme heteropody could be a condition resulting from evolving quadrupedality from bipedal ancestors (with heteropody presumably decreasing over time as manus and pes adapt to performing similar functions), disparity in foot posture and structure between manus and pes, or due to ecological pressures or lack thereof. This thesis aims to investigate the presence or absence of heteropody and differential underfoot pressures in extant animals, and whether this presence/absence is reflective of heteropody in terms of underfoot surface area, and/or centre of mass position, to equalise pressure.

1.6 Thesis Aims

Each research chapter of this thesis attempts to answer a question that will aid in answering the larger question of whether there is a functional link between heteropody and centre of mass in tetrapods, and whether this has implications in the current understanding of extreme heteropody in dinosaurs. To do this, chapters two through five of this thesis explicitly ask the following questions:

1. Can skeletal surface area predict *in vivo* surface area (Chapter 2)
2. Is antero-posterior centre of mass correlated with heteropody in extant taxa? (Chapter 4)
3. Do underfoot forces and pressures in extant taxa indicate a pressure equalisation mechanism? (Chapter 6)
4. How do the above answers apply to extreme heteropody in dinosaurs? (Chapter 7)

By answering these questions, a greater understanding of how soft tissue and skeletal tissue interact to determine underfoot area, how underfoot area relates to centre of mass position, and whether heteropody appears to be used to equalise pressure, in terms of extant quadrupedal tetrapods should be gained, in addition to how these answers apply in context of sauropod dinosaur trackways.

Chapter 2

The contents of this chapter were published in the Journal of Anatomy.

Strickson, E.C., Hutchinson, J.R., Wilkinson, D.M. and Falkingham, P.L. (2020), Can skeletal surface area predict *in vivo* foot surface area?. J. Anat., 236: 72-84. doi:10.1111/joa.13090

Chapter 2

Can Skeletal Surface Area Predict *in vivo* Foot Surface Area?

2.1 Summary of Chapter

The surface area of feet in contact with the ground is a key morphological feature that influences animal locomotion. Underfoot pressures (and consequently stresses experienced by the foot), as well as stability of an animal during locomotion, depend on the size and shape of this area. Here, whether the area of a skeletal foot could predict *in vivo* soft tissue foot surface area was tested. Computed tomography scans of 29 extant tetrapods (covering mammals, reptiles, birds and amphibians) were used to produce models of both the soft tissues and the bones of their feet. Soft tissue models were oriented to a horizontal plane, and their outlines projected onto a surface to produce two-dimensional silhouettes. Silhouettes of skeletal models were generated either from bones in CT pose or with all autopodial bones aligned to the horizontal plane. Areas of these projections were calculated using alpha shapes (mathematical tight-fitting outline). Under-foot area of soft tissue was approximately 1.67 times that of skeletal tissue area (~2 times for manus, ~1.6 times for pes, if analyzed separately). This relationship between skeletal foot area and soft tissue area, while variable in some of this chapter's study taxa, could provide information about the size of the organisms responsible for fossil trackways, suggest what size of tracks might be expected from potential trackmakers known only from skeletal remains, and aid in soft tissue reconstruction of skeletal remains for biomechanical modelling.

2.2 Introduction

The surface area of tetrapod autopodia (feet) reflects several important biomechanical factors, including body mass (McMahon, 1975), habitat (Blackburn et al., 1999), speed (Segal et al., 2004), and bipedal or quadrupedal locomotory habits (Snyder, 1962). Foot surface area is determined by autopodial morphology and posture (Hildebrand, 1980; Full et al., 2002), and, in conjunction with the body mass and locomotory mode of an animal, determines underfoot pressure (Miller et al., 2008; Michilsens et al., 2009; Panagiotopoulou et al., 2012; Qian et al., 2013; Panagiotopoulou et al., 2016a;b).

For very large animals, such as rhinoceroses and elephants, foot surface area needs to be large, as a method of reducing underfoot pressure and avoiding injury to the foot, as well as avoiding sinking on soft ground (Falkingham et al., 2011). However, foot contact area does not appear to scale isometrically with mass. Larger animals often have smaller foot contact areas than would be expected, and the relationship between foot contact area and mass differs between unguligrade, digitigrade and plantigrade animals (Michelsens et al., 2009; Chi and Roth, 2010). Large animals must compensate for their size with other mechanisms, such as fatty footpads, in order to reduce stress (Panagiotopoulou et al., 2012). Presumably the extinct sauropod dinosaurs, many times larger than extant elephants (Bates et al., 2016) used similar compensatory adaptations (Platt and Hasiotis, 2006).

Foot surface area is also reflective of an animal's posture and limb use (Biewener, 1989), with bipedal animals requiring feet large enough to support their body weight with half as many limbs as their quadrupedal counterparts (Gatesy and Biewener, 1991), and, in the case of birds, in a huge range of environments and ecological niches with different demands (Alexander, 2004). An animal's balance (e.g. keeping the body's centre of mass (CoM) close to the centre of pressure of feet-- influenced by foot area) is also of vital importance, as the stability of an animal during locomotion is vital to its ability to catch prey, escape predators, migrate effectively, and avoid injury when overexerting itself and

when moving on unstable ground (Hodgins and Raibert, 1991; Patla, 2003; Geyer et al., 2006; Birn-Jeffery et al., 2014).

Foot surface area appears to correlate with relative speed during certain forms of locomotion. Body mass has a direct effect on maximum running speed, especially notable in large animals, as speed scales with body mass up to moderate sizes and then declines (Garland, 1983; Bejan and Marden, 2006), and the duration of foot contact with the ground also scales with body mass (Farley et al., 1993). The position and number of toes also tends to be a specialisation for terrestrial running, with a reduced number of toes present in both horses and ostriches (among other cursorial taxa; Coombs, 1978), reducing foot weight, a useful adaptation because heavier feet necessitate more energy usage to recover from a stride (Snyder, 1962; McGuigan and Wilson, 2003; Schaller, et al., 2011). Peak plantar pressure and speed are demonstrably linked in humans (Rosenbaum et al., 1994; Segal et al., 2004; Pataky et al., 2008) and ostriches (Schaller, et al., 2011); however, this link has not been fully explored in other terrestrial animals, especially quadrupeds.

Large feet have a potentially conflicting relationship with speed in that they will be more massive and thus have greater inertia, making them more difficult to swing quickly through the air (Taylor et al., 1974; Fedak et al., 1982; Kilbourne and Hoffman, 2013; Kilbourne and Carrier, 2016). Nonetheless, it is important that foot surface area and underfoot pressures evolve to allow an organism's locomotion to be energy-efficient and its posture stable, while enabling sufficient bursts of speed if necessary. In other words, the surface area of the autopodia should be subject to selective pressures in the same manner as any other part of the locomotor system.

Foot surface area is also potentially influenced by Allen's rule (Allen, 1877; Allee and Schnidt, 1937), which supposes that warm-blooded animals in cold climates will tend to have smaller feet than their relatives in warmer clines (Blackburn et al., 1999). This may or may not be due to causal links (i.e. natural selection) to either reduce surface area exposed to the cold, or be a reflection of adaptations in warmer climates to increase

surface area to promote heat dissipation. This ‘rule’ may conflict with constraints imposed by keeping pressures low (i.e. foot areas large) to avoid sinking into soft substrates such as snow or sand. Allen’s rule also potentially conflicts with the outcome of Bergmann’s rule – the contentious but broadly supported tendency for ectotherms to be larger in colder climates (Clarke, 2017). Therefore, colder conditions will tend to correlate with increased body mass, implying a larger foot surface area while simultaneously selecting for smaller feet.

Some animals exhibit notable disparity in the size of fore- and hind-feet, which is apparent in their foot surface area: a condition known as heteropody. A previous study (Henderson, 2006) demonstrated that the ratio of fore- and hind-foot surface areas, in its subject animals, could match CoM position, e.g. an elephant has 40%/60% relative fore- vs. hind-foot surface area, and a CoM of 40% of the distance from the glenoid to the acetabulum. It would seem logical to assume that animals spread their body relatively evenly over their feet, in order to reduce maximum pressure, excess tissue or substrate stress and strain (Cheung et al., 2005), and to prevent sinking when walking across compliant substrates (Falkingham et al., 2011). However, this assumption runs contrary to pressure experiments showing higher mean peak pressures in elephant forelimbs (Panagiotopoulou et al., 2012). It is therefore worth exploring a possible correlation of the relative sizes of an animal’s manus and pes, and CoM with both observations in mind, and worth considering possible implications of such a correlation across Tetrapoda.

Heteropody is a common occurrence in some extinct animals, such as sauropod dinosaurs, as indicated by trace fossil evidence (Lockley et al., 1994a; Henderson, 2006). Preserved trackways from these dinosaurs indicate that often their fore- and hind-feet impressions differ in depth (Falkingham et al., 2010; Falkingham et al., 2012), implying differential underfoot pressures. Determining foot surface area in these animals can be complex, however, and attribution of specific trackmakers to trackways is notoriously difficult (Farlow, 1992; Clack, 1997; Falkingham, 2014), partly because matching impressions of fully fleshed feet to skeletal remains would require accurate methods of

predicting skeletal to skin foot morphology, which is currently difficult and largely speculative (Jannel et al., 2019). Indeed, matching the tracks of extant animals to the correct species is often not straightforward – as illustrated by the existence of field guides produced to help fieldworkers with this problem (e.g. Bang and Dahlstrøm, 2001).

For terrestrial and arboreal fauna, the substrate underfoot can have a noticeable effect on locomotion, and the way the foot moves in a step. Both substrate and autopodial tissue will be compressible to varying degrees, slightly altering foot contact area during stance (Gatesy, et al., 1999; Gatesy, 2003; Falkingham and Gatesy, 2014; Gatesy and Falkingham, 2017).

Palaeobiologists must rely on soft tissue data from extant animals to infer many facets of the morphology of extinct animals (Witmer, 1995), because preservation of soft tissues is rare and only partial details about muscle and tendon structures can be inferred from the skeletal elements they interacted with. In this way, a study of the relationship of flesh and skeletal foot surface area should help to fill gaps in the current understanding of the anatomy of extinct animals' feet, as well as the interaction of foot structure and CoM, and would be particularly valuable for linking fossil trackways and supposed trackmakers. This chapter aims to test whether skin and skeletal surface area are correlated across Tetrapoda, and if so, if their correlation is strong enough to make it a useful tool in the study of fossils and trackways.

2.3 Materials & Methods

In order to compare skeletal and fully fleshed foot anatomy in extant animals, computed tomography (CT) scans of cadaveric autopodia from 29 species of tetrapod (one specimen of each except for *Crocodylus moreletii* and *Osteolaemus teraspis* – see supplementary material), covering amphibians, reptiles, birds, and mammals, were analysed. The sex of individuals was unknown, and all but *Crocodylus niloticus* were adults. All specimens were museum or zoo-donated specimens whose cause of death was unrelated to this study (and generally unknown).

MeVisLab (Heckel et al., 2009) was used to segment the scans into separate 3D models (OBJ format meshes) of the soft tissue and skeletal elements. The resultant meshes were then imported into Autodesk Maya 2018, where they were cleaned, aligned and re-posed to the horizontal plane (Figure 2.1). The aligned meshes were then processed using Matlab), where they were 'flattened' by setting the vertical component of each vertex to 0. This flattening produced 2D 'silhouettes' of the models, either as soft tissue of the foot or its skeleton, from which area was calculated using an alpha shape (see below).

Skin models were oriented and posed so that only areas of the feet that would touch the ground during locomotion would be used upon flattening the models, and any parts of the models that extended past this area were removed (figure 1B). The extent of the soles of the feet were, for the most part, obvious from visible anatomy. In addition, from *in vivo* biplanar fluoroscopy studies, X-ray images, and photographs *in situ,* where available, educated estimates of accurate positions for some taxa were made (Astley and Roberts, 2014; Bonnan, et al., 2016; Kambic et al., 2015; Panagiotopoulou, et al., 2016). For a more repeatable approach (Pose 2, see below), parts of the skin model extending past the functional foot area (the unguals for unguligrade animals, the digits for digitigrade animals, and the entire sole of the foot for plantigrade animals and semi-digitigrade animals, so that the full extent of fatty foot pads were accounted for) were removed where present.

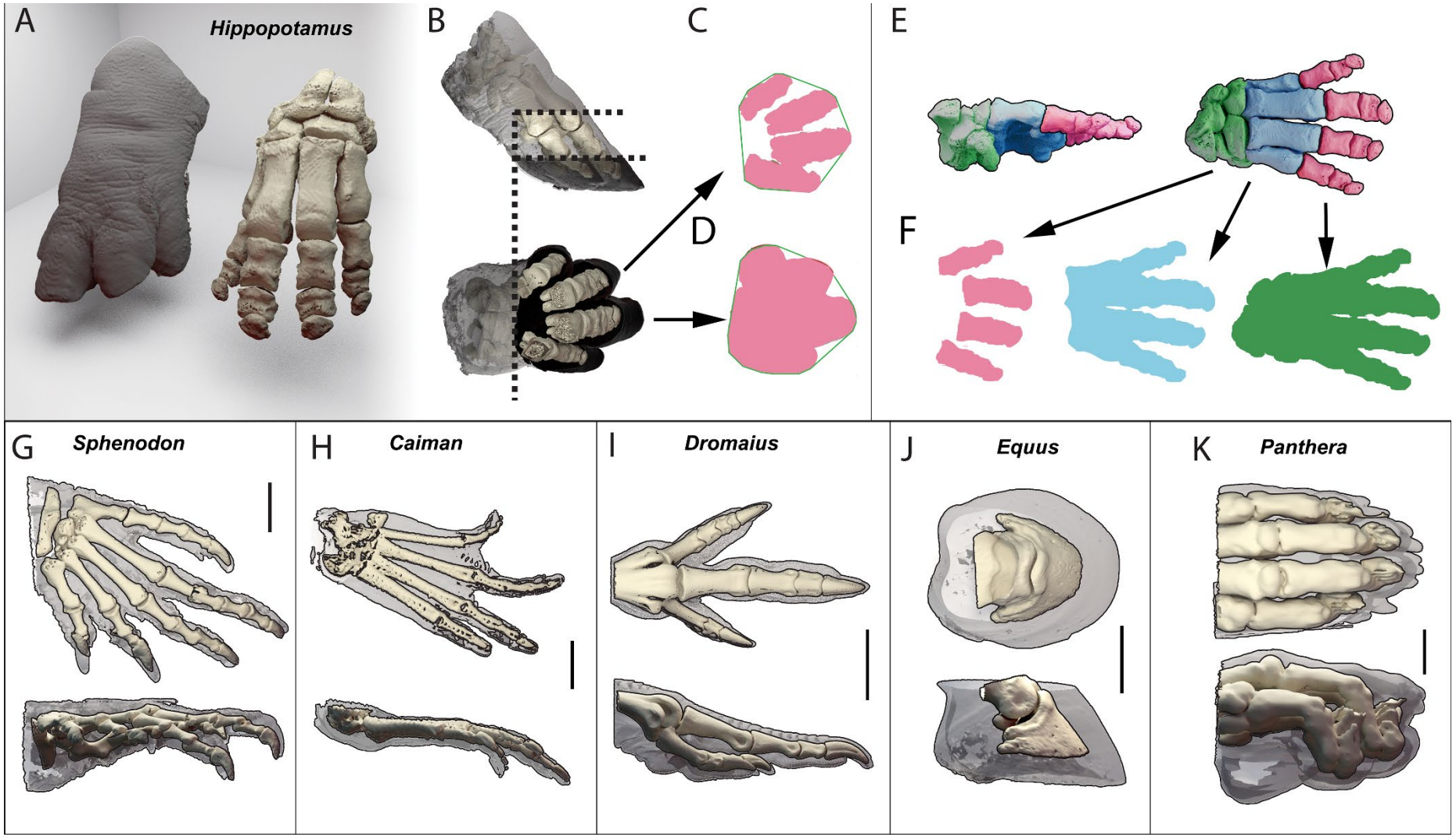
A
Hippopotamus
B
C
D
E
F
G
Sphenodon
H
Caiman
I
Dromaius
J
Equus
K
Panthera

Figure 2.1 Projected area calculated from 3D models. A) *Hippopotamus* Left forelimb, soft tissue and bones reconstructed from CT data. B) The soft tissue was cropped at a point representative of the area that would contact the ground during life. The bones were cropped based on the same posterior extent (pose 1). C) The alpha shape (pink) and the convex hull (green) were used to determine underfoot area of the bones alone and D) the soft tissue. E) Bones were laid flat for a more repeatable approach (pose 2). Where semi-digitigrade animals were treated as digitigrade (pose 2a) only bones in pink were used, where semi-digitigrade animals were treated as intermediate between digitigrade and plantigrade (pose 2b), blue and pink bones were used, and where semi-digitigrade animals were treated as plantigrade, all bones including those in green were used. F) Alpha shapes for poses 2a-c, where pink is 2a, blue is 2b, and green is 2c. G-K) Distinctive foot morphologies in the data set. Scale bar = 10cm for all but G, where scale bar = 1cm.

However, since these models were taken from CT scans, without the full weight of the animal deforming the foot underneath, the true shape of the foot during stance for many of these animals may have been slightly different, due to compliant soft tissues (Alexander, et al., 1986; Gatesy, 2003). This is especially significant for those animals with large fatty foot pads such as *Elephas* and *Ceratotherium*, and less significant for the majority of ungulates, whose hooves are stiff, and more resistant to deformation (Hinterhofer, et al., 2000; Hutchinson, et al., 2011).

Skeletal models were posed in one of two ways. Firstly (Pose 1), matching the pose of skin models (Figure 2.1B-D), secondly (Pose 2), with all bones aligned to the horizontal (Figure 2.1E-F). For the latter pose, models were cropped proximal to the digits for digitigrade animals, proximal to the unguals for unguligrade animals, proximal to the tarsals/carpals for plantigrade animals.

For large, semi-digitigrade/subunguligrade animals (*Elephas maximus, Ceratotherium simum*, and *Hippopotamus amphibius*), proximal foot elements are raised off the ground,

supported by fatty foot pads, increasing foot contact area. Therefore using only the phalanges, as for other digitigrade animals, would severely underestimate contact area. To explore this ambiguity, skeletal outlines were generated from just the digits (Pose 2a), the digits plus metatarsals (Pose 2b), and with the entire foot skeleton (Pose 2c). This analysis was designed to be more objective and repeatable in determining skin from skeletal surface area, particularly, in extinct animals, where knowledge of *in vivo* foot posture may be lacking.

Results for area where left and right forefeet or hindfeet were available were averaged (mean), as were area results for animals with multiple specimens, and *Camelus,* where both feet were unassigned as forefeet or hindfeet.

It should be noted that the 29 animals studied include 10 ungulates, possessing large, keratinous hooves, much harder and stiffer than most other tissues categorised under 'soft tissues' in this study. While ungulate hooves have properties that distinguish them from other soft tissues, and take longer to decompose than softer tissues, they are also distinct from skeletal tissue, and are rarely preserved, especially in fossils (Pollitt, 2004; Saitta, et al., 2017). In terms of comparisons between skeletal and fossil remains and the overall foot structure of living animals, hooves clearly are an important part of a living ungulate's foot structure, and their ability to locomote; thus being able to predict their size from skeletal remains is as much of a part of the goal of this study as predicting the areas of softer tissues (Warner, et al., 2013). In this sense, the term 'soft tissue' as used in this study refers to 'non-skeletal tissue', with the hardness of these tissues largely irrelevant.

Initially, 2D convex hull (a shape made by joining the outermost data points in a simplified representation of the data (see Figure 2.1C-D, in green)) of each silhouette was calculated, but it was found via pose tests using bird feet that this method was extremely sensitive to pose, particularly whether the digits were laterally spread or not (Supplementary material 1). Instead, 2D, tight-fitting alpha shapes (where the outermost data points were joined in a shape that most closely fits the silhouette's true shape (Figure 2.1C-D, in pink)) were produced for each silhouette, and the area of these alpha shapes

calculated. The alphaShape command in MatLab uses an ‘alpha value’ to determine the maximum distance between edge points to bridge (a sufficiently large ‘alpha value’ will produce a convex hull). The default alpha value for each alpha shape was used, which is calculated based on the density of vertices in the model, as this produced the tightest fitting single shape for any given set of points, adjusting for the size of each foot to enclose all points. The hole threshold was set to be extremely large (larger than the foot as a whole) to remove any holes from the interior of the alpha shape. The surface area of the skeleton’s alpha shape as a percentage of the skin’s shape was then used to compare each organism.

The dataset was then run through PGLS (phylogenetic generalised least squares) regression analyses to assess the significance of the relationship between the variables, and how much impact common ancestry between the animals studied affected the results (Blomberg et al., 2012; Felsenstein, 1985). This was accomplished using Mesquite (Maddison and Maddison, 2001) to draw three simple trees (manually compiled “consensus” phylogenies based on the most recent and broadly accepted phylogenies at the time of writing, within which the placement of Carnivora, Cetartiodactyla and Perissodactyla in relation to each other, was the only major point of contention (Gauthier et al., 1988; Nery et al., 2012; Prum et al., 2015)) connecting the organisms involved in this study. The trees were dated using first and last appearance dates taken from the paleobiology database, and PGLS ran via the Ape (Paradis et al., 2004), Geiger (Harmon et al., 2008), Nlme (Bliese, 2006) and Phytools (Revell, 2012) packages in R. Results for forefeet, hindfeet, and all feet were each tested. The influence of body mass was also tested as an external variable, in order to determine whether phylogeny, body mass, or a combination of both factors had a significant effect on the relationship between skin and skeletal foot surface area. P values <0.05 were considered significant. Body masses were taken from scan metadata where possible, or based on reported masses from the literature (e.g. Dunning Jr, 1992) where such metadata were not available (Supplementary material 1).

Skin surface area was plotted against skeletal surface area for all analyses, using the entire data set, and then broken up into smaller groups: unguligrade, digitigrade, plantigrade, terrestrial, semi-aquatic, erect posture, sprawling posture, mammals, and birds. The plots were framed in terms of the predictability of skeletal area from skin area, to emphasise potential utility for trackmaker identification from fossils. However, these data are intended to be interpretable both ways, and the prediction of *in vivo* surface area from skeletal remains is of equal utility. For the purposes of these analyses, the digitigrade (Pose 2a) and plantigrade (Pose 2c) poses of semi-digitigrade/subunguligrade (*sensu* Carrano, 1997) animals were added to their respective groups, whereas Pose 2b was used for the remaining groups, as it represents an intermediate pose. Semi-aquatic included amphibians, crocodilians and hippopotamuses, terrestrial did not include birds except for *Dromaius novaehollandiae*, and sprawling (here meaning non-erect) posture included amphibians, lepidosaurs and crocodilians, although crocodilians use a range of limb postures spanning the sprawling-to-erect continuum (Gatesy, 1991; Reilly and Elias, 1998).

2.4 Results

For the Pose 1 analysis (approximate life position), projected foot skeleton surface area as a percentage of projected fully fleshed foot surface area (Figure 2.2, above cladogram) was an average of 56% (both mean and median) for all organisms measured (three amphibians, four crocodilians, seven birds, and fourteen mammals), with means of 49% for amphibians (53% median), 47% for crocodilians (48% median), 68% for birds (67% median), and 55% for mammals (54% median) with an average standard deviation of 13%. Extremely similar results were found with bones oriented as in Pose 2. The smallest percentages of skeletal vs. fleshed surface area observed were in *Equus* species (*Equus quagga* at 34%, *Equus ferus caballus* 38%), *Giraffa camelopardalis* (38%), *Crocodylus niloticus* (38%), and *Cryptobranchus alleganiensis* (39%). However, besides *Equus* and *Giraffa*, other ungulates did not stand out as having particularly low skeletal areas relative to skin areas. Carnivorans had proportionately high skeletal calculated area. The highest

skeletal areas relative to skin areas (as seen from the underside, and in two dimensions) were *Coturnix coturnix* at 83%, followed by *Panthera leo persica* and *Ceratotherium simum*, at 81% and 73%, respectively.

Where skeletal models were set flat (Pose 2), all unguligrade animals expressed lower skeletal area compared to skin surface area, compared with Pose 1 (Figure 2.2). The zebra stood out most with just 22% skeletal representation.

Elephas, Hippopotamus, and *Ceratotherium* showed considerable variability depending on which foot bones (Pose a/b/c) were used to predict skeletal area: *Hippopotamus* (37/76/100%), *Ceratotherium* (31/74/98%), *Elephas* (17/42/68%). 100% skeletal surface area representation in the hippopotamus clearly suggests that treating these animals as plantigrade does not yield results representative of these animals' foot morphology, or indeed results that are useful for predictive purposes, especially given the steep (subvertical) angle at which these animals position their feet *in situ*.

Carnivorans, particularly cats, typically do not have their digits extended fully when walking or standing, as such relative skeletal area calculated from Pose 2 (eg. *Panthera* 93%, *Vulpes* 92%) generally produces higher relative skeletal areas than the more life-like Pose 1 (eg. *Panthera* 81%, *Vulpes* 70%).

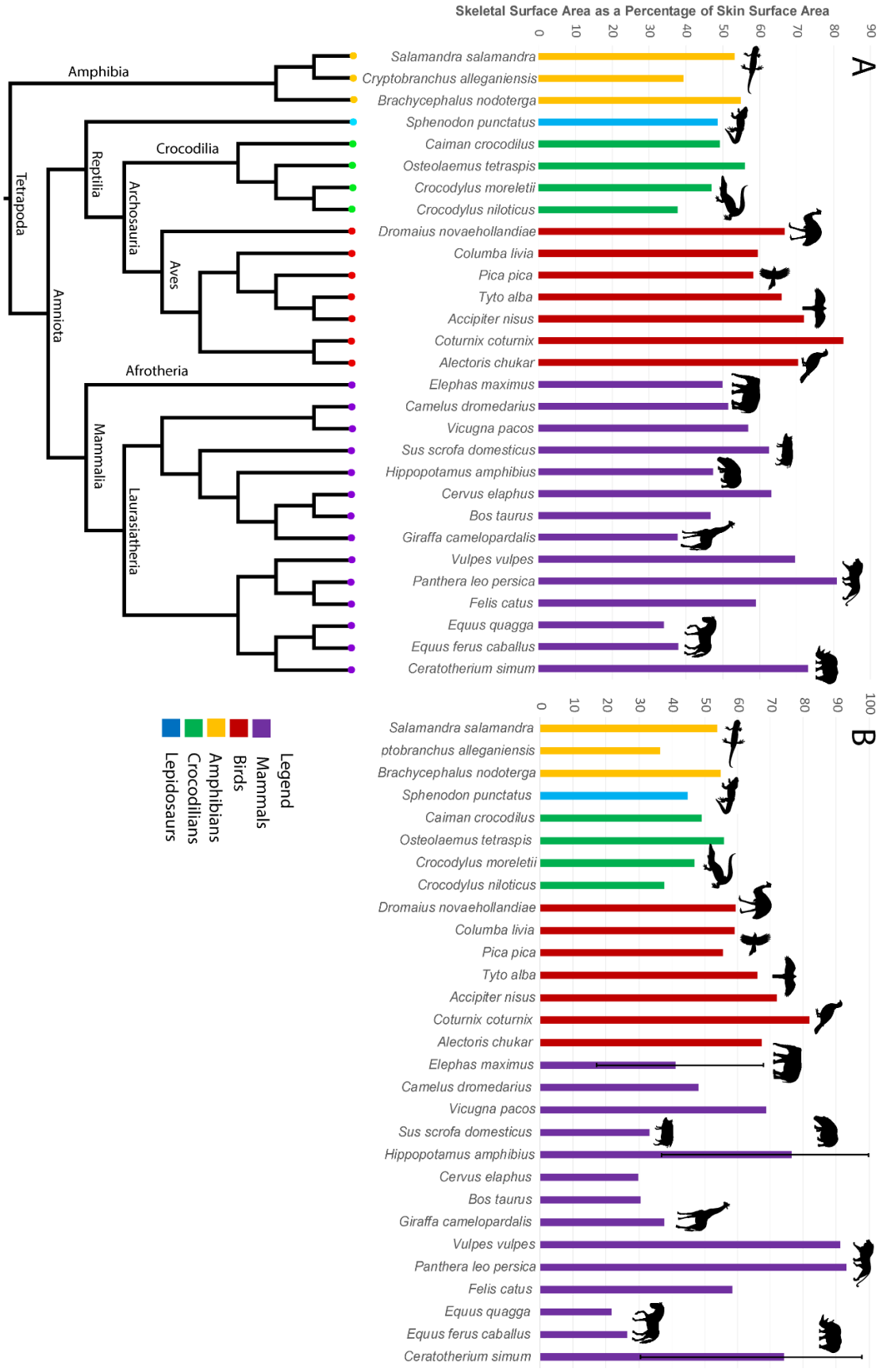
Skeletal Surface Area as a Percentage of Skin Surface Area
A
B
Amphibia
Tetrapoda
Reptilia
Crocodilia
Archosauria
Aves
Amniota
Afrotheria
Mammalia
Laurasiatheria
Salamandra salamandra
Cryptobranchus alleganiensis
Brachycephalus nodoterga
Sphenodon punctatus
Caiman crocodilus
Osteolaemus tetraspis
Crocodylus moreletii
Crocodylus niloticus
Dromaius novaehollandiae
Columba livia
Pica pica
Tyto alba
Accipiter nisus
Coturnix coturnix
Alectoris chukar
Elephas maximus
Camelus dromedarius
Vicugna pacos
Sus scrofa domesticus
Hippopotamus amphibius
Cervus elaphus
Bos taurus
Giraffa camelopardalis
Vulpes vulpes
Panthera leo persica
Felis catus
Equus quagga
Equus ferus caballus
Ceratotherium simum
ptobranchus alleganiensis
Legend
Mammals
Birds
Amphibians
Crocodilians
Lepidosaurs

Figure 2.2 Bar graph showing projected skin surface area as a percentage of projected skeletal surface area across all specimens in A) Pose 1, with phylogeny for context, and B) Pose 2 (for elephant, rhino, and hippo, main bar represents Pose 2b and additional bars show poses 2a and 2c). Silhouettes from Phylopic. Mammalia data are in purple, Aves data in red, Crocodylia data in green, Lepidosauria data in blue, and Lissamphibia in yellow.

Overall, mammalian data were highly variable (47% range from maximal to minimal values in Pose 1, over 80% range in Pose 2). Given that mammalian species dominated the study sample (then birds, then crocodilians), perhaps with more data the variability within other groups would increase to comparable levels. However, that mammalian feet have unusually high morphological disparity compared to other taxa in the sample, is reflective of their unusually high morphological disparity in terms of body size, foot anatomy, and posture compared to other groups (Kubo et al., 2019).

Bird and crocodilian data were more consistent than mammals (25% range for birds in all analyses, 18% range for crocodilians). *Dromaius*, which was morphologically and functionally distinct from the other birds in the study in terms of being large and flightless, fell neatly within the range for birds.

Raw numbers for projected skeleton and projected skin surface area, calculated from Pose 1, were plotted as a log graph, and a power trendline fitted (Figure 2.3). This plot, despite the variation seen in Figure 2.2, showed a strongly positive correlation ($R^2 = 0.99$, p value <0.05) in 'Pose 1' between skin and skeletal foot surface area. This correlation can be described with the equation $y = 0.59x^{0.99}$ (where y = skeletal foot surface area and x = foot skin surface area). This skin and skeletal foot surface area's scaling relationship was close to isometry (slope of 1.0). Soft tissue surface area may therefore be predicted, on average, as approximately 1.67 times skeletal surface area. There were very few outlying animals, indeed, *Elephas* and *Ceratotherium* were the only animals that diverged notably

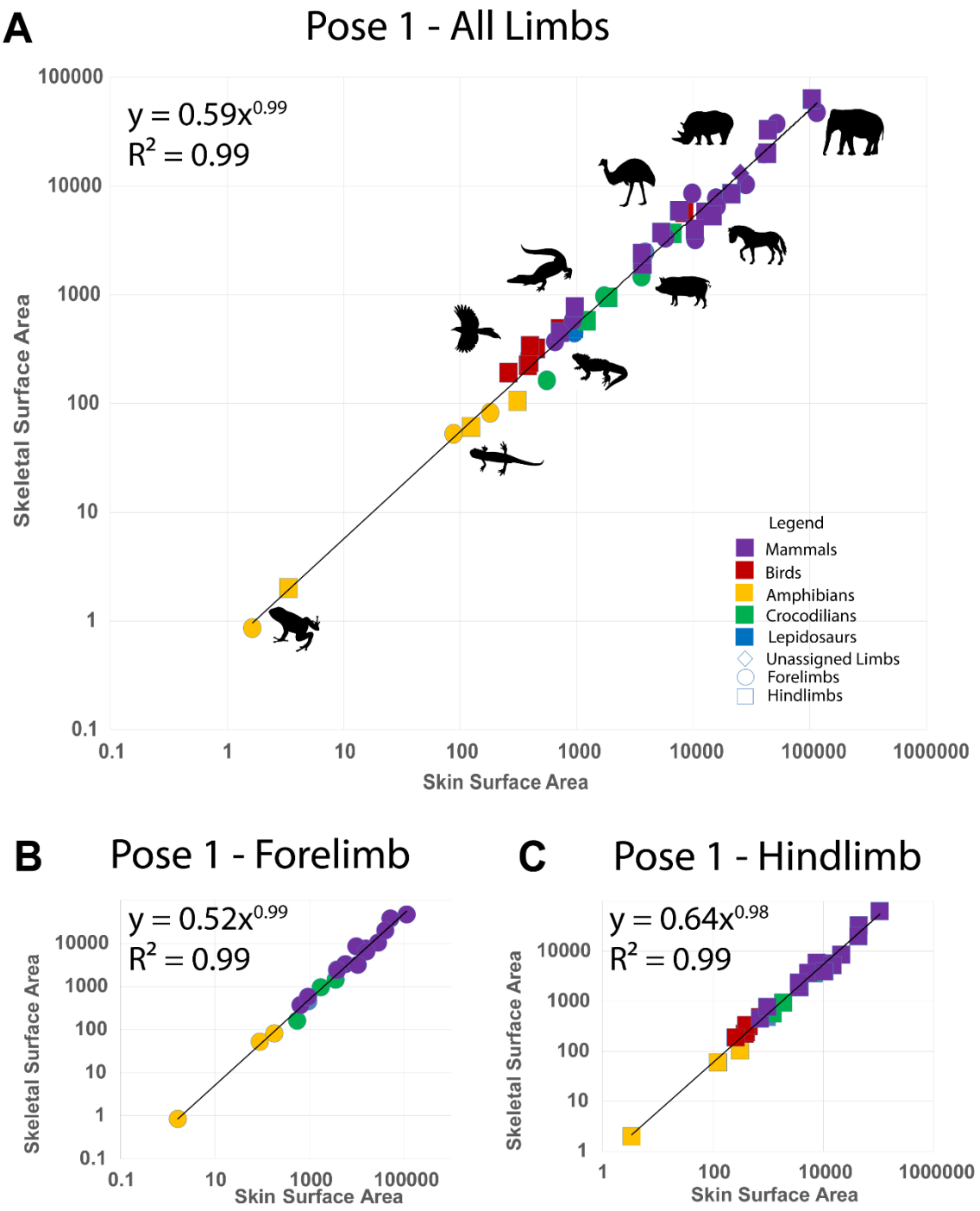

Figure 2.3 Log_{10} plots for projected skin surface area against projected skeletal surface area (mm^2) in A) Pose 1, for all limbs, B) For Pose 1, for forelimbs, C) For Pose 1, for hindlimbs, Silhouettes from Phylopic. All numbers rounded to two significant figures. Mammalia data are in purple, Aves data in red, Crocodylia data in green, Lepidosauria data in blue, and Lissamphibia in yellow.

from the linear trendline. If the three largest animals were removed from the data set, or the three smallest, the strength of the correlation was unaffected, but soft tissue area predictions from skeletal area decreased (Supplementary Material 1). If both groups were removed, the predicted value decreased further.

When the forelimb and hindlimb results were calculated separately, the equations differed noticeably ($y = 0.52x^{0.99}$ and $y = 0.64x^{0.98}$ respectively); although the difference in slope was not statistically significant, and R^2 values remained ~0.99 (Figure 2.3). However, soft tissue area was ~2 times skeletal area in the forelimb, but only ~1.56 times in the hindlimb. See Table 2.1 for full list of formulae, R^2 values, p values, and confidence intervals based on coefficient estimates and standard error, all rounded to two significant figures (and see Supplementary Material 1 for slope uncertainties for all poses, and for all limbs, forelimbs, and hindlimbs.).

Table 2.1 Regressions and Confidence Intervals for Main Analyses

Analysis	Linear Regression	Linear R^2	Log Regression	Log R^2	95% CI	P value
Pose 1 - All limbs	y = 0.51x + 146.71	R^2 = 0.94	$y = 0.59x^{0.99}$	R^2 = 0.99	1.92 ± 0.06	< 2.2E-16
Pose 1 - Forelimbs	y = 0.45x + 641.27	R^2 = 0.92	$y = 0.52x^{0.99}$	R^2 = 0.99	1.92 ± 7.89E-02	3.27E-15
Pose 1 - Hindlimbs	y = 0.59x - 292.02	R^2 = 0.97	$y = 0.64x^{0.98}$	R^2 = 0.99	1.92 ± 0.06	< 2E-16
Pose 2a -All limbs	y = 0.20x + 1303.8	R^2 = 0.82	$y = 0.87x^{0.91}$	R^2 = 0.99	3.93 ± 0.36	1.93E-11
Pose 2a -Forelimbs	y = 0.21x + 1345.4	R^2 = 0.85	$y = 0.69x^{0.93}$	R^2 = 0.97	3.96 ± 0.40	8.68E-09
Pose 2a -Hindlimbs	y = 0.19x + 1177.4	R^2 = 0.79	$y = 1.06x^{0.89}$	R^2 = 0.96	4.16 ±0.42	2.08E-10
Pose 2b - All limbs	y = 0.48x + 436.75	R^2 = 0.87	$y = 0.58x^{0.98}$	R^2 = 0.97	1.86 ± 0.12	5.98E-15
Pose 2b - Forelimbs	y = 0.52x + 410.47	R^2 = 0.89	$y = 0.47x^{0.10}$	R^2 = 0.97	1.71 ± 0.14	3.39E-10
Pose 2b - Hindlimbs	y = 0.44x + 535.85	R^2 = 0.89	$y = 0.71x^{0.96}$	R^2 = 0.97	2.03 ± 0.14	4.83E-14
Pose 2c - All limbs	y = 0.74x - 700.51	R^2 = 0.93	$y = 0.49x^{1.00}$	R^2 = 0.97	1.28 ± 6.23E-02	< 2.2E-16
Pose 2c - Forelimbs	y = 0.79x - 1120.2	R^2 = 0.95	$y = 0.40x^{1.02}$	R^2 = 0.97	1.21 ± 6.47E-02	3.03E-13
Pose 2c - Hindlimbs	y = 0.69x - 228.13	R^2 = 0.92	$y = 0.57x^{0.99}$	R^2 = 0.97	1.33 ± 7.68E-02	8.04E-16

For all flat pose analyses (Pose 2), heavier animals remained the outliers, with *Elephas, Hippopotamus,* and *Ceratotherium* diverging most from the trendline (Figure 2.4). Similar to the Pose 1 analysis, Pose 2b suggested high predictability, with soft tissue as approximately 1.67 times skeletal surface area. Regressions for Pose 1 and Pose 2b were

statistically similar. The analysis treating semi-digitigrade/sub-unguligrade as plantigrade (Pose 2c) suggested soft tissue as approximately 2.04 times skeletal surface area, and semi-digitigrade as digitigrade (Pose 2a) resulted in soft tissue as 1.05 times skeletal surface area. Interestingly, the hindlimbs-only regression for Pose 2b was significantly different from its equivalent with both fore- and hindlimbs and forelimbs-only (Table 2.1).

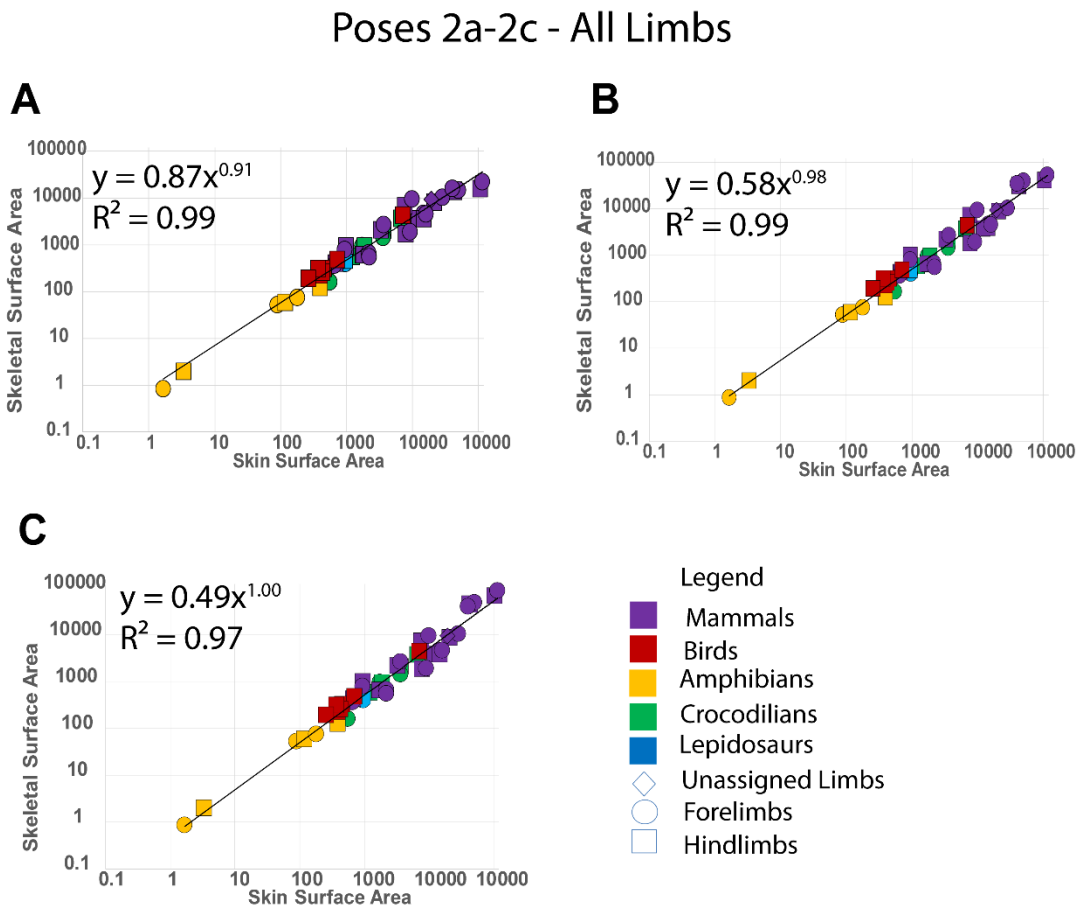

Figure 2.4 Log_{10} plots for projected skin surface area against projected skeletal surface area (mm^2) for A) Pose 2a, all limbs, B) Pose 2b, all limbs, and C) For Pose 2c, all limbs. Silhouettes from Phylopic. Mammalia data are in purple, Aves data in red, Crocodylia data in green, Lepidosauria data in blue, and Lissamphibia in yellow. All numbers rounded to two significant figures.

PGLS results (e.g. for all feet, in ‘Pose 1’, with Carnivora and Perissodactyla in a single clade) produced a Pagel’s lambda value ~1. Similar results were found when running the same tests on fore-and hind-feet separately, with the other two phylogenetic tree arrangements. When skeletal elements were laid flat Pagel’s lambda remained ~1, (Supplementary material 1). However, p values were ~0 which seems to contradict this, with mixed results for p value suggesting no clear answer on whether body mass is a significant driver either. These results are not sufficient to suggest whether phylogeny or body mass are significant drivers of the correlations found.

Separate regressions for unguligrade, digitigrade, plantigrade, terrestrial, semi-aquatic, erect posture, sprawling posture, birds and mammals, all showed strong correlations (Table 2.2, Supplementary material 1 and 2). Equations for all the analyses varied, with opposing regressions (e.g. sprawling versus erect posture, or terrestrial versus semi-aquatic) statistically different from each other (Table 2.2, equations and R^2 values rounded to two significant figures). Although R^2 values suggest high correlations for these regressions, the lack of data points in each of them (particularly those with the highest R^2 values) suggests their predictive value is relatively low at present. There are potentially functional reasons why, for example, sprawling animals, semi-aquatic animals, and birds would have stronger correlations and more predictable foot morphologies, but the lower scores in groups with more data points suggests high correlation in groups with few data points may be an artefact, and should be viewed with caution.

Table 2.2 Regressions and Confidence Intervals for Analysis Subgroups

Analysis	Linear Regression	Linear R^2	Log Regression	Log R^2	95% CI	P value
Unguligrade	y = 0.36x - 593.56	R^2 = 0.95	y = 0.27x1.01	R^2 = 0.97	2.61 ± 0.29	0.00
Digitigrade	y = 0.19x + 1823.1	R^2 = 0.83	y = 2.02x0.84	R^2 = 0.97	4.34 ± 0.54	2.02E-06
Plantigrade	y = 0.74x + 1128.3	R^2 = 0.96	y = 0.35x1.06	R^2 = 0.99	1.30 ± 0.09	1.25E-07
Terrestrial	y = 0.45x + 491.99	R^2 = 0.91	y = 0.68x0.96	R^2 = 0.91	2.00 ± 0.18	4.25E-08
Semi-aquatic	y = 0.77x + 408.03	R^2 = 1.00	y = 0.42x1.02	R^2 = 0.99	1.30 ± 0.02	4.26E-09
Erect	y = 0.48x + 588.49	R^2 = 0.89	y = 0.94x0.93	R^2 = 0.95	1.85 ± 0.15	1.37E-10
Sprawling	y = 0.51x - 19.70	R^2 = 0.99	y = 0.50x0.99	R^2 = 1.00	1.96 ± 0.07	1.13E-07
Birds	y = 0.59x + 32.25	R^2 = 1.00	y = 0.87x0.96	R^2 = 0.99	1.69 ± 0.02	1.59E-09
Mammals	y = 0.48x + 903.78	R^2 = 0.87	y = 0.57x0.98	R^2 = 0.91	1.84 ± 0.20	9.87E-07

2.5 Discussion

Projected skeletal surface area as a percentage of projected skin surface area varied between the organisms studied, most notably in mammals, which yielded both the lowest and second highest values (Figure 2.2). Bird feet are all similarly digitigrade in their posture and are largely made up of skeleton (with three major digits and consistent phalangeal numbers), skin, and connective tissue, so their more consistent percentages are not surprising considering that some of the mammals in this dataset had hooves, fatty footpads, and a wide range of foot anatomies and postures (from plantigrade to unguligrade). PGLS results suggested that the correlation between skin and skeletal foot surface area in all poses, as well as being very strong, still held with phylogeny taken into account. This suggestion was supported by Figures 2.3 and 2.4.

Equus and *Giraffa* stood out in this dataset for having an especially low relative skeletal surface area. All extant horses have one toe with a large, keratinous hoof (Bowker et al., 1998), so this was perhaps to be expected. Giraffes also have relatively small feet and gracile legs compared to other animals of similar size, and a combination of high body mass and high running speeds, which contribute to an overall unique morphology (van Sittert et al., 2015). Pose 2 resulted in a lower relative skeletal area across unguligrade

animals, though none as extreme as either *Equus* species. By focusing on ungual bones, it became clear that the keratinous sheath that forms the hoof dominates the 'silhouettes', with skeletal tissue only represented by the very tip of the toe, so this is to be expected. Non-unguligrade ungulates: *Ceratotherium, Hippopotamus*, *Camelus dromedaries, and Vicugna pacos*, did not yield similar results to unguligrade ungulates, and varied significantly from this group, as well as from each other.

For *Crocodylus niloticus*, the fact that Crocodylia have relatively thin, long, digital bones, somewhat similar to human phalanges, that converge to form a surprisingly robust foot, could have some effect (Ferraro and Binetti, 2014). Furthermore, joint range of motion studies have suggested an unusual wrist function and resultant manus posture in crocodilians favouring rigidity, which could affect potential foot contact area (Hutson and Hutson, 2014). This rigidity could potentially aid in swimming, with the stiff foot acting in a flipper-like fashion to push through water efficiently, which smaller crocodilians tend to rely upon (Seebacher, et al., 2003). Furthermore, the *Crocodylus niloticus* specimen used was the only juvenile in this study, and its phalanges were small and spaced far apart in some cases, so this result could be an artefact of ontogeny, or the quality of the models used. Further studies on the effect of ontogeny on skeleton to skin surface area ratio could elucidate this further. Indeed, in future studies consideration should be given to levels of ossification of manus and pes bones. For example, this chapter's *Cryptobranchus* CT scan was missing wrist bones on all feet when segmented because these elements were cartilaginous in the specimen scanned, and were indistinguishable from soft tissue. Such ossification is likely to vary across species, and across ontogeny.

At the other extreme, where skeletal surface area was high (most closely approaching projected skin surface area), several birds (most notably *Coturnix*, *Accipiter nisus*, and *Alectoris chukar*) along with carnivorans and *Ceratotherium* (as well as *Hippopotamus* in Pose 2b and 2c) stood out the most. For birds, this is understandable considering their relative lack of musculature and fat in their feet. For carnivorans this could be explained by their claws, extending beyond the main body of the foot, by the resting position of their

digits *in vivo,* and by their footpads, for which stiffness scales directly with body mass, while foot contact area lags behind (Chi and Roth, 2010). This scaling allows carnivorans to maintain relatively small feet that are light enough to be moved quickly (Kilbourne and Carrier, 2016; Kilbourne and Hoffman, 2013).

Body mass seemed to have little general effect on the relationship between skin and skeletal foot surface area. Previous studies have found a scaling relationship between body mass and foot contact area not significantly different from isometry (Michilsens et al., 2009), implying that the ratio of skeleton to soft tissue in the foot was not affected by this scaling effect. The scaling relationship between the ratio of skin to skeletal foot surface area was at best trivially different from isometry– a sensible result given that the variables are two facets of the same structure (i.e. the manus or pes), and therefore their structure and development are intrinsically linked. Despite this result, the largest animals in the dataset were the most outlying (much less so when plotted logarithmically (Figure 3)). It is notable that these largest animals, namely, *Elephas, Ceratotherium,* and *Hippopotamus*, were also the only semi-digitigrade/subunguligrade animals in this chapter's data. These animals both had the largest feet in the study and possess fatty foot pads to reduce loads on their individual toes and spread out underfoot pressure due to their large body masses (Hutchinson et al., 2011; Regnault et al., 2013). The divergence of these data appears to be influenced by their foot posture as well as their large size, with the adaptation of a semi-digitigrade posture potentially occurring specifically to support their large body weights.

It may be worth considering that beyond a certain weight threshold, specialised foot morphologies are necessary for weight support and locomotion, and thus successively heavier animals may have more disparate soft tissue structure and foot posture adaptations to cope with increased load (Hutchinson, et al., 2011). This has implications for the inherent predictability of this study's methods for very large extinct animals, such as sauropod dinosaurs, especially where foot posture is loosely inferred and little information about soft tissue structure is available. Follow-up studies on semi-digitigrade

foot postures and how they support loads differently to other foot postures, as well as similar studies to this, using additional heavy and semi-digitigrade animals, would increase understanding of this variation of foot form and function. Contrary to the semi-digitigrade animals in this study, the giraffe, an unguligrade animal, was the largest other tetrapod (<1500kg vs. 3000+kg in larger individuals of the semi-unguligrade taxa), and deviated little from trendlines.

The strength of the correlation between skin and skeletal foot surface area, despite variations seen in Figure 2.2, implied sufficient reliability to predict one from the other (Figure 3). Despite this, birds only appeared above the trendline (Figure 3). Perhaps a more accurate correlation could be achieved for birds alone with a larger avian dataset (with a wider range of foot sizes), which would allow more accurate predictions of bird foot surface area, and of foot surface area for animals with similar pedal anatomy to birds (such as non-avian theropod dinosaurs). Although this study's main results could be refined with a much larger tetrapod data set, it appears that foot surface area can be predicted from foot skeletal surface area, with soft tissue generally predictable as approximately 1.67 times skeletal foot surface area, as demonstrated in Poses 1 and 2b. However, when analyzed separately, manus and pes presented differing ratios, with soft tissue surface area of the former being predicted as ~2 times skeletal area, but just ~1.56 times for the pes. This correlation could potentially be used to estimate skeletal foot surface area of animals from their footprints, and its inverse used to predict skin-on-foot surface area of extinct animals from their skeletons, and even of cadavers from skeletons, with potential forensic applications.

For Pose 2, *Elephas, Ceratotherium,* and *Hippopotamus* were tested in three different poses. Their foot anatomy is unusual in that they have a foot posture with most foot elements far off the ground, but also have fatty pads which give them a large foot surface area. With this in mind, all foot elements being in line with the horizontal plane, as in Pose 2c, is highly unrealistic. Pose 2a is perhaps more realistic than 2c, but assumes fewer foot elements are supportive during stance than is accurate *in vivo*. The most representative

position for semi-digitigrade would arguably be Pose 1, as this did not force these animals into an unrealistic foot posture. However, both Pose 1, and Pose 2b both result in the same 1.67 times skeletal surface area value, and Pose 2b's intermediate nature tests a pose in between digitigrade and plantigrade. Pose 2b then, is perhaps the best repeatable method. If, despite this, this chapter's other methods were chosen to predict foot surface area, skin surface area would be equal to 1.05 times skeletal surface area for Pose 2a, and 2.04 times skeletal surface area for Pose 2c. The variability in these analyses does reveal that altering the results of the largest animals in the study alters the equation used. Larger animals have have unique selective pressures on foot structure and locomotion, specializing more for bearing large loads, and less for speed and maneuverability, resulting in reduced locomotor performance and therefore smaller percentages of their body weight being borne on a single foot at any one time (Iriarte-Diaz, 2002). Therefore, perhaps this method would be best applied to smaller and non-semi-digitigrade animals. However, variation in area results is to be expected when fundamentally changing the number of skeletal elements in an analysis.

Where data were divided into smaller groups for analysis, strong correlations were found in results for plantigrade animals, semi-aquatic animals, sprawling posture, and birds (Table 2.2). Selective pressures potentially could drive a need for similar foot anatomy across these groups, and therefore predictable foot structures, such as adaptations for perching, swimming, and supporting body weight when feet are not directly under the body. Yet considering that these groups were also the groups with the fewest data points, definitive conclusions cannot be drawn from these results.

In terms of methods used, it was found that convex hulls are highly sensitive to foot pose, such as the size of inter-digital angles (Supplementary material 1), a result consistent with previous findings (Cholewo and Love, 1999). This could be the cause of wide error margins if these hulls were used for predictive purposes. This is especially relevant in re-posed foot models, where inter-digital angles are manipulated to resemble *in vivo* arrangements, and in animals that have long, thin digits, such as crocodilians. Alpha

shapes produced more consistent, ‘tight-fitting’ outlines for area calculation, a much more accurate measure of the real scope of foot surface area for these models.

Inevitably, models derived from CT scans, such as those used in this study, ignore certain *in vivo* factors such as foot deformation during contact with the ground. While in this study an attempt was made to stick closely to the *in situ* positions of feet (Pose 1), and aimed for a more objective iteration of this study’s analysis by laying bones flat to remove subjectivity (Pose 2), deformation is a very difficult issue to control for. Collection of the data needed to account for this would require advanced *in vivo* imaging techniques such as biplanar fluoroscopy (i.e. “XROMM”; Brainerd et al., 2010; Gatesy et al., 2010); however, such techniques remain limited in the size of potential subjects (e.g. Panagiotopoulou et al., 2016) and can be expensive and time-consuming to conduct. Despite this issue, deformation of the foot should generally not be significant enough that it should diminish the usefulness of this study or the predictability of the methods employed here, as even in soft footpads, foot contact area does not maintain constant stress with body mass, and larger body mass can lead to increased foot stiffness (Chi and Roth, 2010). Combining this methodology with XROMM data for elephants and other animals with large, fatty foot pads, however, would be advantageous in determining the overall effect of deformation on the predictability of these methods and on foot surface area in general, as this particular aspect of foot anatomy is the most prone to deformation with body weight, due to its high compliance (Hutchinson, et al., 2011). Overall, CT scans are a reliable resource for studies like these, and their utility in determining foot surface area could potentially contribute to future studies on animal locomotion and posture if used in conjunction with *in vivo* loading, centre of mass and pressure data. However, as in this study, where quality of the models varied, results could potentially be limited by the fidelity of the scans available, and therefore, more scans available for each animal to have the option to pick and choose the most complete and highest quality, as well as more computing power and high-end software, would be a boon to future studies.

Most studies concerning underfoot areas and pressures have focused on humans and other primates. Adaptations for arboreal locomotion have resulted in large functional differences between the forelimb and hindlimb in primates (Schmitt and Hanna, 2004). Such differences would make them an interesting subject for a follow-up study.

Assigning specific trackmakers to fossilised trackways is a difficult task (Falkingham and Gatesy, 2014). It is intended that these results could be used to constrain potential trackmaker identity. However, as an extrapolation from a bivariate plot, with a number of variables unaccounted for such as soft tissue and substrate compliance, the applications of figure 3 and its predictions are currently limited, and such identifications of trackmakers must be undertaken cautiously.

When predicting the skeletal surface area of the feet of extinct animals, and identifying trackmakers, the many complexities of footprint formation must be taken into account. The shape of footprints is determined not only by foot anatomy, but also dynamics of the limbs, and substrate consistency (Falkingham, 2014; Minter et al., 2007; Padian and Olsen, 1984a). Underfoot pressures (Hatala et al., 2013), centre of mass position (Castanera et al., 2013), and style of locomotion (Hatala et al., 2016) all contribute to variations in limb dynamics, and consequently the morphology of a track. Given that foot size and shape is the focus of this study, the findings herein concern matters of critical importance to footprint formation and trackmaker identification, relating as they do to both anatomy and dynamics.

When trying to model footprint formation and dynamics of extinct animals, centre of mass and underfoot pressures of the animals in question are determining factors. When considering these factors, the difference between manus and pes size and pressure is of great importance. Disparity between the cranial and caudal parts of the body is especially notable as previous biomechanical models have often underestimated mass in the cranial half of the body (See discussion in Allen et al., 2009). Simply put, taking into account the differences between soft tissue area in manus and pes could make a notable difference in estimations of underfoot pressures and simulations of footprint formation. As an example,

when the skeletal remains of *Plateosaurus engelhardti* feet were laid flat, and their skin areas predicted from alpha hulls, estimated manus skin area was 32% of pes area when using the 1.67 multiplier from combined analyses, and 40% of pes area using the separate multipliers (2 for manus, 1.6 for pes). Using body mass and centre of mass calculations from Allen et al. (2013), these results predicted manus underfoot pressure of 80% pes pressure when combined, and 64% when separate (Supplementary Material 1). This effect should also be considered in the inverse when considering trackmaker anatomy from fossil footprints. In this way, this method is a useful tool to consider in digital reconstruction and trackmaker identification.

2.6 Conclusions

The surface areas of the skin of the foot *in situ* and of the foot's skeletal components are strongly correlated and thus should be predictable in terrestrial tetrapods. Skin surface area was approximately 1.67 times that of skeletal surface area (~2 times for manus, ~1.6 times for pes, if analysed separately). This trend was not affected by body mass and showed little evidence of being strongly affected by phylogeny. This predictability has potential in aiding with estimating the size and possible species of trackmakers in the fossil record, both by estimating the size of skeletal feet using footprints, and by estimating foot size, and therefore potential footprint size, from fossil feet.

Chapter 3

Foot Shape Tests

3.1 Purpose

When analysing fossil footprints, most publications approximate area and area differences between manus and pes using 'heteropody index' (HI) (HI=[(manus length x manus width)/(pes length x pes width)]*100) (Equation 1), a simple length x width proxy (Riga and Calvo, 2009). This is useful as a quick and easy method of generating area estimates, but in reality, footprints rarely resemble regular polygons, and on occasion the differences in shape of the manus and pes are so stark that approximating them as both the same shape could potentially be more misleading than helpful (Falkingham, 2010). This chapter set out to investigate how foot shape and size affects calculations of area and heteropody based on simple area proxies, to determine how much, error can be expected when this technique is employed. From this data, it should be more apparent whether this is a useful measure to employ in the next few chapters, and how well its use in future chapters will approximate area of animal feet to determine whether there is a functional link between heteropody and centre of mass for the purpose of pressure equalisation.

3.2 Methods

This series of tests pitted the area estimates of length x width (area of a square and other regular quadrilaterals), and pi x radius squared (area of a circle), against the true area for three basic shapes, and how using these area proxies would affect calculations of heteropody index for combinations of these shapes (i.e. square 'manus' as a % of circle 'pes) compared to heteropody index calculated using their true areas. The shapes tested were: equilateral triangle, square, and circle (height 10mm, width 10mm).

The difference between the true area and the proxy area was recorded in the form of raw numbers and percentage difference. Then, to test how different shaped feet affect heteropody in animals, two shapes at a time were compared using the formula for heteropody index (Equation 1), to simulate how heteropody index changes when an animal has a manus and pes of different sizes and shape. Heteropody index was calculated using area values for true area, and area proxies, to see how accurate proxies were at estimating area difference between manus and pes, versus true difference in area, again using raw difference and percentage difference. All shapes were combined in all possible combinations, and for all combinations of shapes, size was tested for where one shape – the 'manus' is 25%, 50%, 75% and 100% size, to test whether size of these shapes, as well as the different shapes themselves, affected HI predictions for different methods.

Following this, the same protocol was used to test area proxy accuracy and accuracy of proxies for calculating heteropody, using animal foot outlines. The animal foot outlines in question were derived from CT scans, using the same custom Matlab script described in Chapter 2, where true area is known and calculated using alpha hulls. For all of these except the cow, horse, and elephant, a new metric (besides length x width, pi x radius squared, and true area), length x 'carpal width' was calculated, replacing overall width with the width of the foot at the most proximal point where the toes touch the ground, aiming representing an estimation of the minimum width of the foot, not reliant on how toes are splayed to determine width. Since for ungulates and elephants, only the tip of the foot bones touch the ground, an estimate for this would be tricky with foot outlines, and so they were not calculated for these animals. Following this, combinations of animal feet (one manus, one pes, as before) were carried out using the same methods employed for basic shapes above, comparing all methods to true area, with manus as four different sizes compared to pes. Animal feet included *Dromaius*, *Brachycephalus, Osteolaemus, Sphenodon, Bos, Equus, Elephas,* and *Panthera*, as described in Chapter 2. A two-way ANOVA was then performed to test if there was a significant difference in HI estimates using the 3 methods, for all animals where all 3 methods could be applied.

The manus and pes outlines for *Plateosaurus* used in Chapter 2 where then repurposed to calculate how their area estimates would compare, comparing the methods tested in this chapter to area estimates from skeleton models, and with the skin area estimates established in Chapter 2 to demonstrate the most accurate method for determining foot area and heteropody in a dinosaur.

3.3 Test Outcomes

3.3.1 Basic Shapes

Area calculations revealed LxW to be a better estimate for shapes in general than PiR2 overall, with the latter being a better estimate for the circle (as it give the true area of a circle) (Table 3.1). When shapes were combined the same pattern was not found, with LxW HI estimates resulting in an average 7.81% difference from true area across all combinations, with PiR2 resulting in 2.89% difference (Table 3.2). However, this will change based on which basic shapes are tested and is not necessarily a general rule.

Table 3.1 Area proxies compared to true area for basic shapes (mm2)

	MEASUREMENTS OF AREA IN SHAPES (mm2)			AREA PROXIES VERSUS TRUE AREA			
	AREA PROXIES			RAW ERROR (mm2)		% DIFFERENCE	
Shapes	Length*Width	Pi*Radius Squared	True Area	LxW	PiR2	LxW	PiR2
Eq Triangle	86.60	104.59	43.30	43.30	61.29	100.00	141.55
Square	100.00	157.08	100.00	0.00	57.08	0.00	57.08
Circle	100.00	78.54	78.54	21.46	0.00	27.32	0.00
				Average % Difference		42.44	66.21

Table 3.2 Combinations for basic shapes to test estimates for area differences between manus and pes (HI = manus as % of pes)

BASIC SHAPES		Heteropody Index (HI) with Manus (M) as % of Pes				
Difference from True Area	Area Proxy	HI M=25%	HI M=50%	HI M=75%	HI M=100%	Overall
Raw Error	LxW	-3.12	-6.25	-9.37	-12.50	-7.81
Raw Error	PiR2	-1.16	-2.31	-3.47	-4.62	-2.89
Raw Error	LxCW					
% Difference	LxW	8.51	8.51	8.51	8.51	8.51
% Difference	PiR2	13.61	13.61	13.61	13.61	13.61
% Difference	LxCW					

3.3.2 Animal Foot Outlines

In terms of raw area calculations for individual animal feet, LxW was much more accurate as an area proxy compared to PiR2, except for in ungulates, where the more rounded shape of the keratinous hoof appeared to prove well-suited to estimating foot area based on circle area. Where LxCW was used as an area proxy, it proved much more accurate than either LxW or PiR2, at -6.55% difference compared to 71.44% and 123.39% respectively. It should be noted that for ungulates, both LxCW and PiR2 area estimates were more accurate than for other animals, which only reached similar levels of accuracy with LxCW methods (Table 3.3). With ungulates removed from the data, efficacy of LxW as an estimate decreased.

When employing these proxies in combinations of feet - testing how this affects heteropody calculations (including at 4 different sizes), a similar result was found, with LxCW combinations averaging 3.72% difference from true area estimates, compared to LxW at 5.56% and PiR2 at 34.32% (Figure 3.1, Table 3.4). It appears then, that the lessons learned from area estimation accuracy can be carried through to manus and pes ratios, such as heteropody index.

Despite this, ANOVA tests for percentage difference for all animals for which LxCW was available as a measure, resulted in a significant difference only between LxCW-based estimates and PiR2-based estimates (Table 3.5).

Table 3.3 Area proxies compared to true area for animal foot outlines (mm2)

ANIMAL FOOT	RAW MEASUREMENTS (mm2)				ERROR TRUE VS PROXY (mm2)			% DIFFERENCE TRUE VS PROXY		
Taxon/Autopodium	LxW	PiR2	LxCW	True Foot Area	LxW	PiR2	LxCW	LxW	PiR2	LxCW
Dromaius Pes	18700.00	22698.01	8500.00	8524.23	10175.77	14173.77	-24.23	**119.37**	**166.28**	**-0.28**
Brachycephalus Manus	2.96	5.60	1.47	1.65	1.31	3.95	-0.18	**79.46**	**239.03**	**-11.08**
Brachycephalus Pes	5.88	12.57	3.40	3.39	2.49	9.18	0.01	**73.45**	**270.68**	**0.29**
Osteolaemus Manus	3520.00	5026.55	1600.00	1733.12	1786.88	3293.43	-133.12	**103.10**	**190.03**	**-7.68**
Osteolaemus Pes	4753.00	7389.81	2910.00	3678.33	1074.67	3711.48	-768.33	**29.22**	**100.90**	**-20.89**
Sphenodon Manus	1816.41	1842.69	522.16	962.97	853.44	879.73	-440.81	**88.63**	**91.36**	**-45.78**
Sphenodon Pes	2250.00	2827.43	1020.00	960.43	1289.57	1867.00	59.57	**134.27**	**194.39**	**6.20**
Salamandra Manus	145.00	122.72	82.50	88.94	56.06	33.78	-6.44	**63.04**	**37.99**	**-7.24**
Salamandra Pes	258.75	336.54	129.38	124.89	133.86	211.65	4.49	**107.18**	**169.47**	**3.59**
Bos Manus	17589.00	16060.61		15663.52	1925.48	397.09		**12.29**	**2.54**	**0.00**
Bos Pes	15180.00	14957.12		12729.92	2450.08	2227.20		**19.25**	**17.50**	**0.00**
Equus Manus	19250.00	18626.50		16103.96	3146.04	2522.54		**19.54**	**15.66**	**0.00**
Equus Pes	19712.00	18626.50		14886.19	4825.81	3740.31		**32.42**	**25.13**	**0.00**
Elephas Manus	150000.00	125663.71		115297.70	34702.30	10366.01		**30.10**	**8.99**	**0.00**
Elephas Pes	144892.19	191083.89		106205.00	38687.19	84878.89		**36.43**	**79.92**	**0.00**
Panthera Manus	13750.00	12271.85	9625.00	9849.39	3900.61	2422.46	-224.39	**39.60**	**24.60**	**-2.28**
Panthera Pes	9605.00	10028.75	8701.00	7690.17	1914.83	2338.58	1010.83	**24.90**	**30.41**	**13.14**

Table 3.4 Combination comparisons for all animal print outlines to test estimates for area differences between manus and pes (HI = manus as % of pes) for varying foot sizes.

ALL FOOT OUTLINES		HI M=25%	HI M=50%	HI M-75%	HI M=100%	Overall
Raw Error	**LxW**	-6155.08	-12310.15	-18465.23	-24620.30	-15387.69
Raw Error	**PiR2**	-14626.77	-29253.53	-43880.21	-58507.06	-36566.89
Raw Error	**LxCW**	420.85	841.69	1262.54	1683.38	1052.11
% Difference	**LxW**	5.56	5.56	5.56	5.56	5.56
% Difference	**PiR2**	19.62	19.62	78.44	19.62	34.32
% Difference	**LxCW**	3.72	3.72	3.72	3.72	3.72

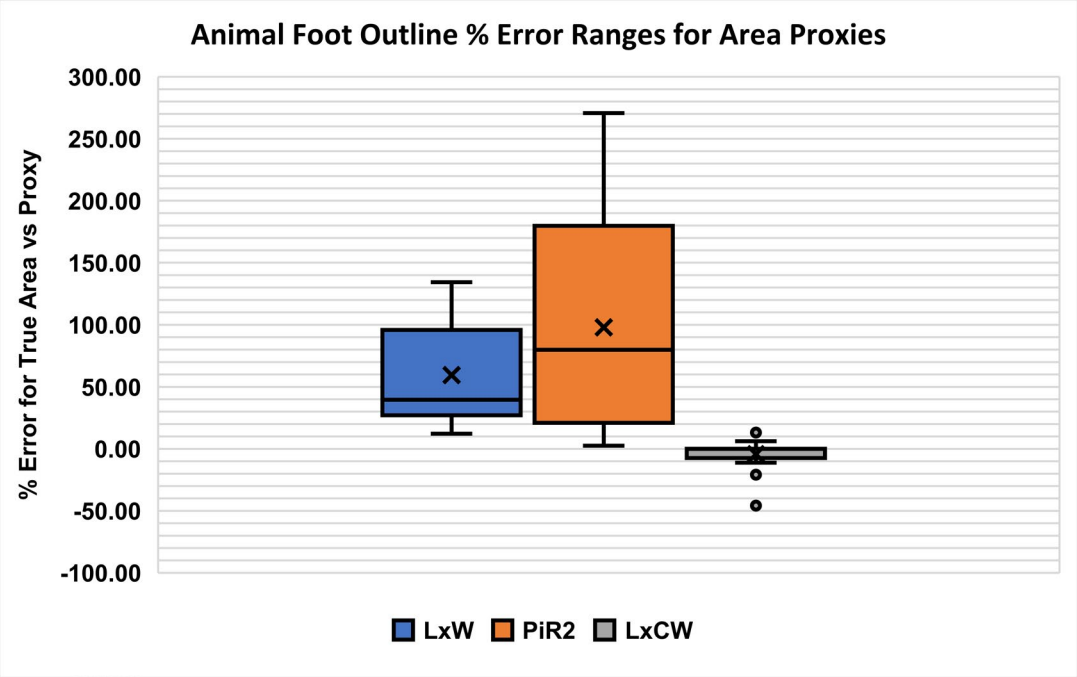

Figure 3.1 Box and whisker plot to show % error in estimating accurate heteropody values from animal foot area, for all animals and all sizes, for all area proxies, compared to true area.

Table 3.5 ANOVA results for animal foot outlines where all measurements were available for comparison

ANOVA: LxW Vs	Degrees of Freedom	Sum of Squares	Mean of Squares	F Value	P Value
PiR2	1	4907	4907	5.43	0.05
LxCW	1	3	3	0	0.96
PiR2:LxCW	1	2154	2154	2.38	0.17

3.3.3 Dinosauria Predictions

Applying the techniques used above and the lessons learned therein to extinct animals, where *Plateosaurus* was tested, estimates for skin area from Chapter 2 were very close to those predicted by LxCW area proxies, particularly for the pes, and closer when using separate forelimb and hindlimb predictions as outlined in Chapter 2. LxCW predictions lead to less close results, with PiR2 the furthest from Chapter 2 estimates (Table 3.6). If possible, this method of foot area estimation appears likely to be more accurate than

simply calculating length x width, for animals in general, where the proximal extent of the foot touching the ground is able to be estimated accurately. Based on this, calculations of area estimates and heteropody index for several dinosaurs based on measurements from the literature is given in Table 3.7.

Table 3.6 Area proxies compared to estimated true area in *Plateosaurus* based on skeletal remains and estimates of underfoot skin surface area as predicted in Chapter 2.

ANIMAL FOOT	RAW MEASUREMENTS				RAW ERROR TRUE VS PROXY			% DIFFERENCE TRUE VS PROXY		
Taxon/Autopodium	LxW	PiR2	LxCW	True Foot Area	LxW	PiR2	LxCW	LxW	PiR2	LxCW
***Plateosaurus* Manus**	0.05	0.05	0.03	0.02	0.03	0.03	0.01	150.62	173.67	67.53
***Plateosaurus* Pes**	0.11	0.18	0.10	0.06	0.05	0.12	0.04	82.48	199.10	58.68
***Plateosaurus* Manus Skin Estimate with Limbs Together**	0.05	0.05	0.03	0.03	0.02	0.02	0.00	50.07	63.88	0.31
***Plateosaurus* Pes Skin Estimate with Limbs Together**	0.11	0.18	0.10	0.10	0.01	0.08	-0.01	9.27	79.10	-4.98
***Plateosaurus* Manus Skin Estimate with Limbs Separate**	0.05	0.05	0.03	0.04	0.01	0.01	-0.01	25.31	36.84	-16.24
***Plateosaurus* PesSkin Estimate with Limbs Separate**	0.11	0.18	0.10	0.10	0.01	0.08	0.00	14.05	86.94	-0.83

Table 3.7 Area estimations based on LxCW for dinosaur measurements from the literature (mm2) and their predicted manus and pes ratios (HI)

Taxon	Source	Digit L*CW Manus	Digit L*CW Pes	Heteropody Index
Plateosaurus	The Complete Dinosaur	24800	14300	173.4266
Apatosaurus	The Complete Dinosaur	134400	373333.33	36
Plateosaurus	The Dinosauria	24201.39	68750	35.20202
Riojasaurus	The Dinosauria	5866.667	36100	16.25115
Yunnanosaurus	The Dinosauria	7744.444	8243.8017	93.94263
Anchisaurus	The Dinosauria	1787.5	23100	7.738095
Shunosaurus	The Dinosauria	97500	48442.907	201.2679
Lufengosaurus	Young 1941a and b	26624	103360	25.75851
Camarasaurus	Schopp, 2015	58500	62900	93.00477

3.4 Conclusions

The findings of these tests suggest that where possible, the width of the most proximal part of the foot touching the ground should be used in place of general width for area estimations where possible. It also established that in general LxW is a better proxy for area in most animals than PiR2, except in animals with close to circular foot shape, as is the case in some ungulates. However, for those animals where LxW is a better estimate

than PiR2, LxCW is more accurate. These trends work for both estimating area of a foot, and for estimating heteropody index – a manus to pes area ratio. In addition, by combining the findings of these tests with those of Chapter 2, foot area estimations for dinosaurs can be estimated to a more accurate degree using LxCW, to find an area close to estimates for soft tissue area. Where possible in future works, this method should be employed to find accurate underfoot areas and heteropody.

Chapter 4

Are Heteropody and Centre of Mass Position Linked in Skeletons of Extant Tetrapods?

4.1 Summary of Chapter

To investigate a possible correlation of different sized manus and pes (heteropody) with centre of mass, 57 extant, quadrupedal, digitised animal skeletons (representing mammals, crocodiles, and lepidosaurs) were compiled. The digital skeletons consisted of freely available laser scans, CT scans, and specimens from the Liverpool World Museum digitised using photogrammetry. Several foot measurements were recorded from these animals and used to calculate heteropody. Convex hulls of the skeletons were then used to calculate centre of mass positions for each. The data were used to attempt to answer the question of whether centre of mass position was correlated with heteropody in extant animals. Most animals clustered around a centre of mass of ~50-70% gleno-acetabular distance in front of the hip, and a heteropody index of ~60-140% (manus is 0.6 to 1.4 times pes size).The lizards studied had CoM of less than 25% gleno-acetabular distance in front of the hip. The majority of semi-aquatic species exhibited extreme heteropody. Semi-aquatic animals (excluding lizards) were the only sub-group to show a strong correlation, with higher heteropody ratios associated with a more anterior centre of mass. This indicates that differential foot size and centre of mass may be linked in certain groups but not as a general rule across Tetrapoda.

4.2 Introduction

Heteropody, as defined by Lockley, et al (1994a), refers to the ratio of manus to pes area (specifically foot contact area). It is commonly used in reference to footprints, particularly fossil trackways of large dinosaurs such as sauropods, for whom this ratio is often more exaggerated compared to other, especially extant, animals. As well as 'extreme heteropody', sauropod dinosaurs have been associated with large numbers of 'manus-only' and 'manus-dominated' sauropod trackways, a possible explanation for which involves the forelimbs, carrying a disproportionate amount of the animal's body weight on a smaller area, sinking deeper into compliant substrate than the hindlimbs, potentially implying large differences in underfoot pressure as well as area (Lee and Lee, 2006).

Sauropods, and some ornithischian dinosaurs, are also notable for having evolved from a bipedal ancestor into quadrupeds. Since no extant vertebrates share this evolutionary history, palaeobiologists can only test how their unique ancestry impacted their forelimb and hindlimb pressures through simulations, extrapolation of known anatomy, and biomechanical principles. This has become less of an obstruction to science in recent years, as computational methods are becoming increasingly sophisticated, and through this, reconstructions of the musculoskeletal systems for sauropods (Sellers et al., 2013), and other dinosaurs (Hutchinson and Gatesy, 2000; Carrano and Hutchinson, 2002; Hutchinson and Gatesy, 2006; Sellers et al., 2009; Maidment and Barrett, 2011), have been made and their capabilities inferred.

In simplified terms, a quadrupedal animal's relationship to its centre of mass can be explained with the trunk as a beam, and the limbs as its supports (Alexander, 1985), as demonstrated in Figure 1.7. In erect animals, limbs are held under the trunk rather than to the side - directly under the beam, and therefore directly supporting the animal. Weight is distributed to each of the beam's supports, relative to centre of mass location (Halliday et al., 2013; Blob, 2000). In theory, a central load would be distributed equally between the limbs, and a load closer to the forelimbs or hindlimbs will result in more load bearing on the side in question. If the area at the base of these supports (i.e. foot surface area, for

example, of forefeet compared to hindfeet) were increased on the load bearing side, the result would be equal stress on each support, despite unequal loads (Henderson, 2006). In this way, by having larger hindfeet for example, where centre of mass is closer to the tail, extreme heteropody, as exhibited in some sauropod dinosaurs, could potentially result in equalisation of underfoot pressures, and could stabilise an otherwise front heavy, or back heavy, animal (Falkingham, 2012; Falkingham et al., 2010). Inversely, reduced heteropody would imply less extreme centre of mass positions, as demands to compensate for limb loads on one side of the body decrease, allowing for more uniform underfoot areas for equal pressure under both manus and pes.

4.2.1 Mechanical Roles of the Forelimb and Hindlimb

Going beyond the beam and supports model, forelimbs and hindlimbs have important roles in locomotion, with hindlimbs providing the majority of the propulsive power of the animal, and forelimbs the braking (Demes et al., 1994). These roles appear to be linked to CoM position, relative to limb contact points with the ground/substrate (Granatosky et al., 2018). In addition, the beam and supports model can only explain so much, and quadrupedal animals have bodies that are complicated, perform a variety of functions, and can be adapted for multiple behaviours and traits that add confounding factors that can not be accounted for by the model as it is. As a result, it is important to consider the positions of the CoM, manus, and pes, as a dynamic system, and recognise the limitations of the insights that can be gained from static, simplified models.

The degree to which an animal is upright, or ‘crouched’, (for example, the columnar limbs of an elephant versus those of a mouse), could also affect the distribution of its mass. In these cases, gleno-acetabular distance would, on the occasion the limbs are not held directly under the hip and shoulder joints, not equal manus-pes distance. In this instance the metaphor of simple columns supporting a beam would lose a little of its explanatory power. Perhaps crouched animals, then, do not equalise stress in the same way as their upright counterparts.

Heteropody could also be influenced by ecological niche and locomotory mode. Fossorial animals require muscular forelimbs for efficient digging (Lehmann, 1963), and in extreme cases lose their hindlimbs completely (Sakata and Hikida, 2003). Arboreal animals often require manual adaptations for grasping (Cartmill, 1974). Semi-aquatic animals may use large pedes for more efficient swimming (Grasse, 1951; Hershkovitz, 1971), although such animals often also make use of enlarged musculature and increased propulsion from their tails, as seen in beavers (De Muizon and McDonald, 1995; Reynolds, 1993) and crocodilians (Gatesy, 1990; Willey et al., 2004). Digitigrady in animals, as well as plantigrady, unguligrady, and intermediate foot postures, may also play a role in determining heteropody, although it does not necessarily follow that having a certain foot posture is a precursor to heteropody or otherwise.

CoM position changes during locomotion (Biewener, 2006), but when an animal is standing still its CoM should be relatively stable in comparison (preventing tipping and falling) (Ting et al., 1994), and therefore easier to estimate, at least in extinct species where *in vivo* movement cannot be tracked (Eames et al., 1999; Henderson, 1999). The CoM should, in the case of the beam and supports model mentioned above, lie along the beam somewhere between the two supports, namely the glenoid (shoulder joint) and acetabulum (hip joint) in quadrupeds, preventing tipping and allowing the animal to stay stable while still (Henderson, 2006). In crouched and sprawling animals, the position of the manus and pes may extend beyond the glenoid or acetabulum, granting additional manoeuvrability, but increasing the intensity of muscle and bone stress on the limbs (Biewener, 1983a; Schmitt, 1994).

If, as theorised above, uneven loads in the body are offset by differences in the surface area of the manus and pes affected (i.e. a front-heavy animal benefits from having relatively large manus in comparison to its pedes), CoM position would be expected to correlate with heteropody, and animals with extreme heteropody would be expected to also demonstrate unusually offset CoM positions.

4.3 Materials & Methods

4.3.1 3D Models and Hulls

A database of 57 digitised animal skeletons was gathered using photogrammetry performed on the zoology collections at the Liverpool World Museum, previously published data (Sellers et al., 2012), and from CT scans from Crocbase (Hutchinson, 2016). These skeletons were manipulated so that their necks and tails were straight and aligned with the X axis, and that their limbs were straight and parallel to the Z axis, in line with the standard ‘neutral posture’ of previous studies (Allen et al., 2009; Bates et al., 2016, 2015) (example in Figure 4.1). Reposing the skeletons in this way ensured that the pose of the skeleton would not be responsible for variation in results, for example, curvature of the trunk and tail, or upright posture of the neck.

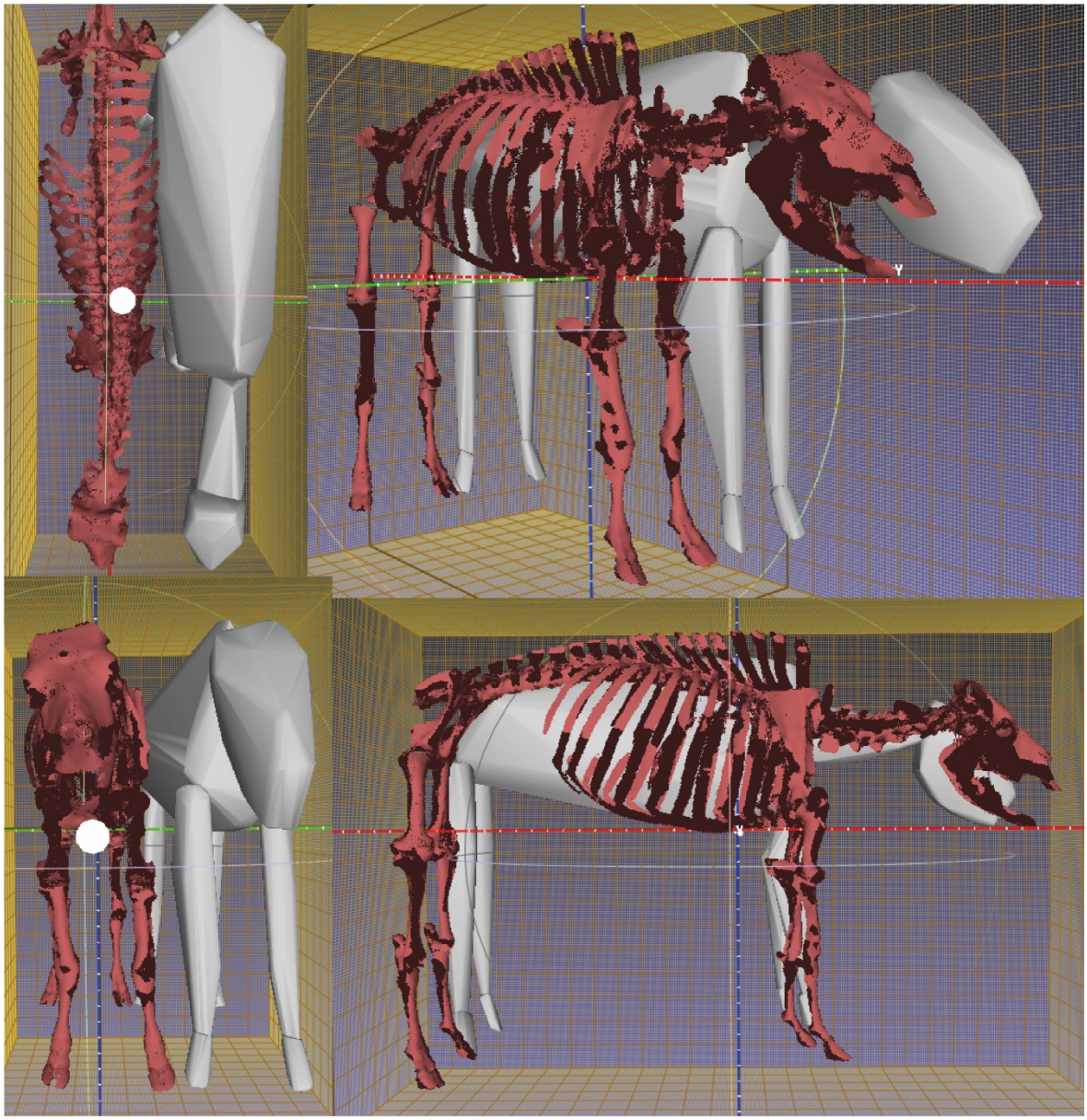

Figure 4.1 Example of convex hulls beside the *Bos taurus* skeleton they are derived from, at multiple angles, with legs, neck, and spine in neutral pose.

Horns, tusks, and antlers -where present- were deleted from the digitised skeletons, leaving only the main body of the animal to be used in calculations, following the protocol of Sellers et al. (2012). Keratin sheaths, i.e. on claws and hooves, were not present in most taxa. In the reindeer, *Rangifer*, however, the keratin of the hoof was obviously present, and its point cloud could not be removed without removing the entire foot. Even in this instance, however, assuming keratin on the manus and pes decayed at the same rate, the ratio of manus to pes size should still be reflective of the same ratio in the skeleton, especially as skin and skeletal surface area appear to be correlated (previous

chapter). Foot length, for the purposes of this study includes claw length, since claws serve a functional use in the locomotion of some taxa, for example, the giant anteater, *Myrmecophaga* (de Faria et al., 2015).

Each digitised skeleton was divided into its functional components (usually consisting of head, neck, trunk, tail, fore and hind feet, and upper and lower limb) (Sellers et al., 2012), for each of which a 3D minimum convex hull was calculated in Meshlab (Cignoni et al., 2008). These individual hulls were merged into a single mesh and, again in Meshlab, its CoM co-ordinates calculated, along with its mass (mesh volume*893.36, the total bulk density of horses in kg/m^3 (Buchner et al., 1997)). In previous studies, lung volume was also calculated to account for its density difference compared to the rest of the body. Assuming isometric scaling of lung density (at % volume per unit volume of animal), the lack of modelled lungs should not affect the spread of data, if isometric scaling is an invalid model, this could potentially be a source of error. It should still be noted, due to this, that the CoMs and masses calculated herein are estimates, and true CoM positions for this chapter's taxa would perhaps be positioned more anteriorly. In the same vein, if tail hulls were to underestimate tail size and mass, true CoM positions would be more posterior. Other animals would vary throughout their life cycle, i.e. seasonal growth and loss of antlers in deer. It should be noted here that while this is unlikely to affect lung volume, gut volume can vary significantly in mammals depending on diet (Clauss, et al., 2016).

CoM, in terms of % length from the acetabulum to the glenoid (gleno-acetabular distance) of each animal, was calculated by importing the CoM co-ordinates for each model (see above) into Autodesk Maya, and determining the relative co-ordinates of the centre of the glenoid and acetabulum. With these co-ordinates, the distance on the x-axis between the acetabulum and the glenoid, and the acetabulum and the CoM were used to calculate percentage gleno-acetabular distance.

4.3.2 Anatomical Measurements

In order to compare foot size between taxa, several anatomical measurements of the manus and pes were taken for each, using CloudCompare for point clouds (Girardeau-Montaut, 2015) or Maya for meshes constructed from CT data. Measurements recorded were: ungual length, digit length, whole foot length, posed width (width of the extent of the foot in pose), and carpal width, representing the maximal length of each facet (see Figure 4.2). Whole foot length included all bones up to and including the most proximal wristbones (manus) or calcaneum (pes), i.e. every bone more distal than the radius and ulna, or tibia and fibula (Figure 4.2C).

To calculate ‘functional foot lengths’ (where ‘functional foot’ is the extent of the foot that interacts with the ground during walking), it was necessary to outline the foot posture of each taxa. Foot posture in tetrapods is generally split into three groups: plantigrade, digitigrade, and unguligrade, based on which parts of the foot are in contact with the ground during standing and locomotion (Carrano, 1997). Intermediate stages exist, such as semi-digitigrade, however, in this study the definition outlined in Kubo, et al. (2019) was used, separating the animals in this analysis into these three functional groups based on whether their tarso-metatarsal joints, and metatarso-phalangeal joints, are clearly off the ground. This determines how semi-digitigrade ‘functional foot length’ was measured, while semi-digitigrade animals themselves were still considered a separate subset of data.

Each animal’s ‘Functional foot length’ was determined based on its foot posture: ungual length for unguligrade animals, digit length for digitigrade animals, and whole foot length for plantigrade animals. For semi-digitigrade animals, digit length was used rather than an intermediate measurement for the purposes of this study, as their tarso-metatarsal joints are clearly off the ground (Kubo et al., 2019).

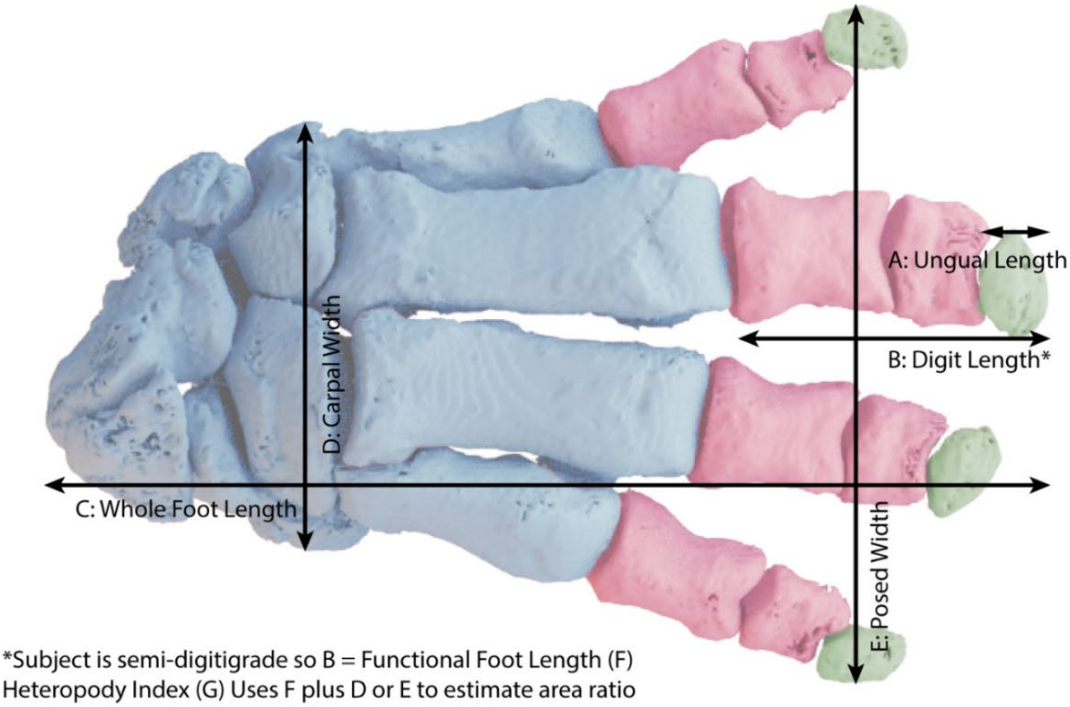

*Subject is semi-digitigrade so B = Functional Foot Length (F)
Heteropody Index (G) Uses F plus D or E to estimate area ratio
eg. G = ((Manus B * Manus D) / (Pes B * Pes D)) * 100

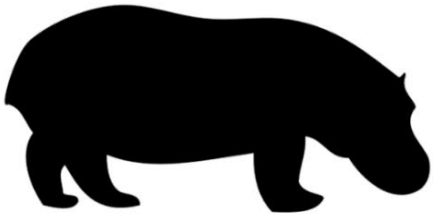

Manus Size as % of Pes Size	Pes	Manus
Heteropody Index = 50		
Heteropody Index = 100		
Heteropody Index = 150		

Figure 4.2 Foot measurements used for analysis and demonstration of Heteropody Index methods displayed on a skeletal *Hippopotamus* foot.

For animals with one set of plantigrade feet and one set of digitigrade feet, their functional foot lengths were derived from different measurements for manus and pes. For the purposes of this study, carpal width and posed width were multiplied by 'functional foot length' to generate proxies for foot area. Carpal length was assumed to be more reliable, as foot pose in mounted skeletons is arbitrary, while carpal width was approximately equal to the width of the foot with all toes adducted (Figure 4.2).

Heteropody measures were calculated for all foot measurements by comparing them between manus and pes for each specimen, along with functional foot length multiplied by posed width, functional foot length multiplied by carpal width, and heteropody index for functional foot with posed width, and with carpal width. Heteropody Index is a ratio of manus to pes area (Equation 1) used to represent and compare heteropody in fossil footprints (Riga and Calvo, 2009).

$$HI=[(\text{manus length} \times \text{manus width})/(\text{pes length} \times \text{pes width})]*100 \quad [\textbf{Equation 1}]$$

A Heteropody Index of 100 represents an equal sized manus and pes, HI = 50 represents a manus half the size of the pes, and HI = 150 represents a pes half the size of the manus (Figure 4.2).

4.3.3 Analysis

The different measurements of heteropody were then plotted against CoM position. All taxa were examined via linear regression, along with several subgroups: namely unguligrade, digitigrade, semi-digitigrade, plantigrade, erect posture, semi-aquatic, and terrestrial. For the purposes of this study, semi-aquatic animals are any animals that spend a significant part of their life in water. For the taxa included here, this consisted of crocodiles, tapirs, beavers, hippos, polar bears, capybaras, otters, and water monitors.

The results of this analysis were then run through phylogenetic comparative methods (Cooper et al., 2016) phylogenetic generalised least squares (PGLS) tests, to statistically

analyse the effects of phylogeny (based on Brownian Motion, Ornstein-Uhlenbeck, and Pagel's Lambda models, and dated using first appearance dates reported on Paleodb (Uhen, et al., 2013), and then analysed with body mass as a discrete predictor, using mass estimates from the literature (Supplementary material)), on the spread of data.

4.4 Results

Calculated CoMs were generally around 50-70% GA distance in front of the hip, with anteaters, beavers, the wolverine, *Gulo,* and the civet, *Civettictis* being slightly lower (Figure 4.3). Lowest of all were the lizards, at less than 25% distance, largely due to the length of their tails. Despite their outlying CoM result, they were within the range of heteropody values of the remaining taxa, which (using carpal width and functional foot length to derive a heteropody index) clustered around 60 -140% heteropody (manus is 0.6 to 1.4 times pes size), although they fell into the lower range of the cluster at 63 and 76% heteropody for the green iguana, *Iguana* and Asian water monitor, *Varanus* respectively (Figure 4.4).

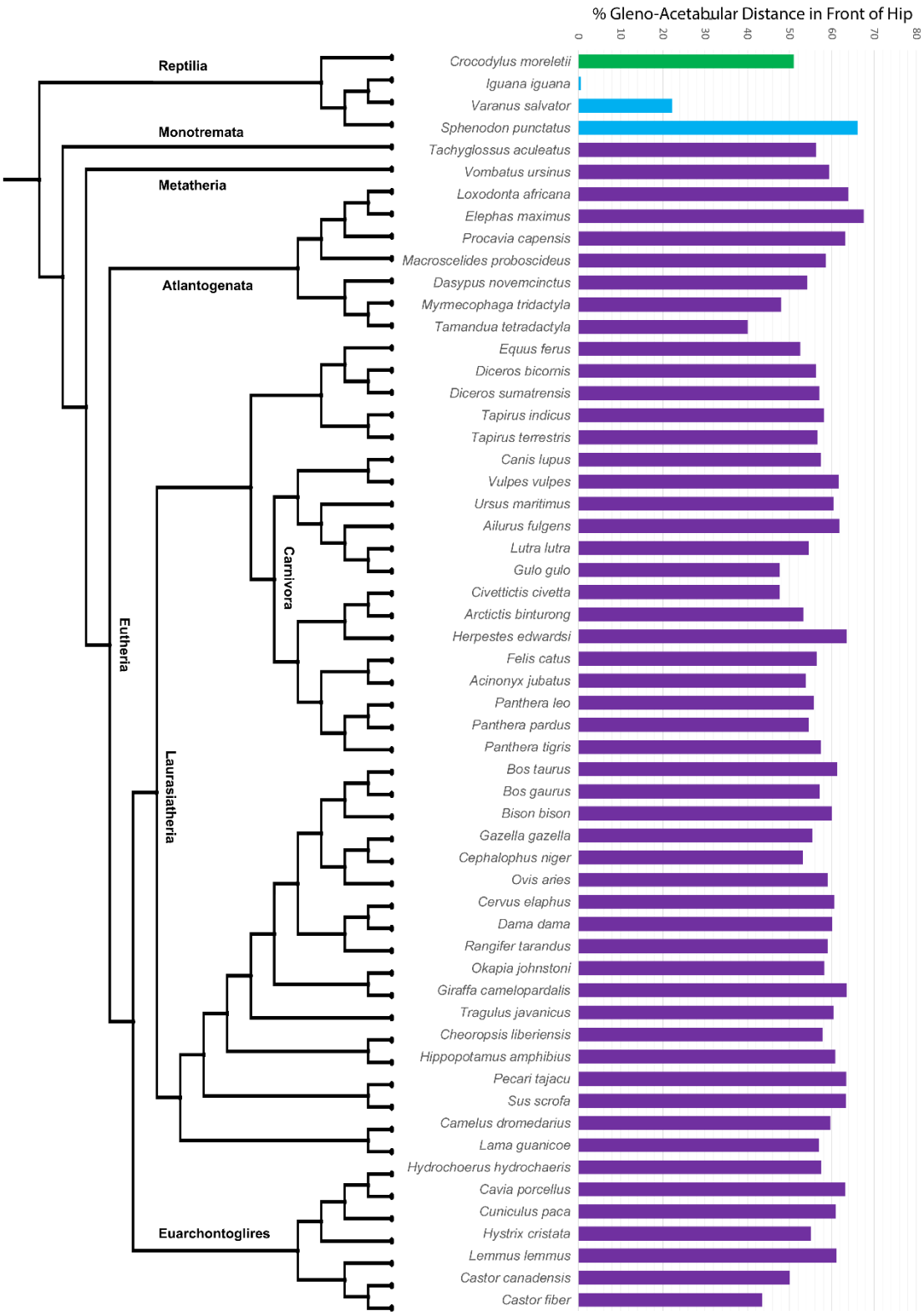

Figure 4.3 Range of centre of mass results for the taxa studied, arranged by phylogeny. Purple data points are mammals, blue are lepidosaurs, and green are crocodiles.

There were some examples of extreme heteropody in this chapter's data set, primarily in the beavers and crocodiles. In fact, most semi-aquatic animals had a much larger pes than manus. Heteropody in favour of pes size was mainly an artefact of functional foot differences, where one foot is digitigrade, and one is plantigrade, as in the bearcat, *Arctictis* and the hyrax, *Procavia*. The African elephant, *Loxodonta* also displayed notable manus dominance, but only about 10% more than the main cluster of the data. In fact, all large semi-digitigrade animals were slightly manus dominant, making up a large part of the high end of the cluster (both elephants and rhinos, as well as *Hippopotamus*, with the pygmy hippo, *Choeropsis* the lowest, at 118% HI).

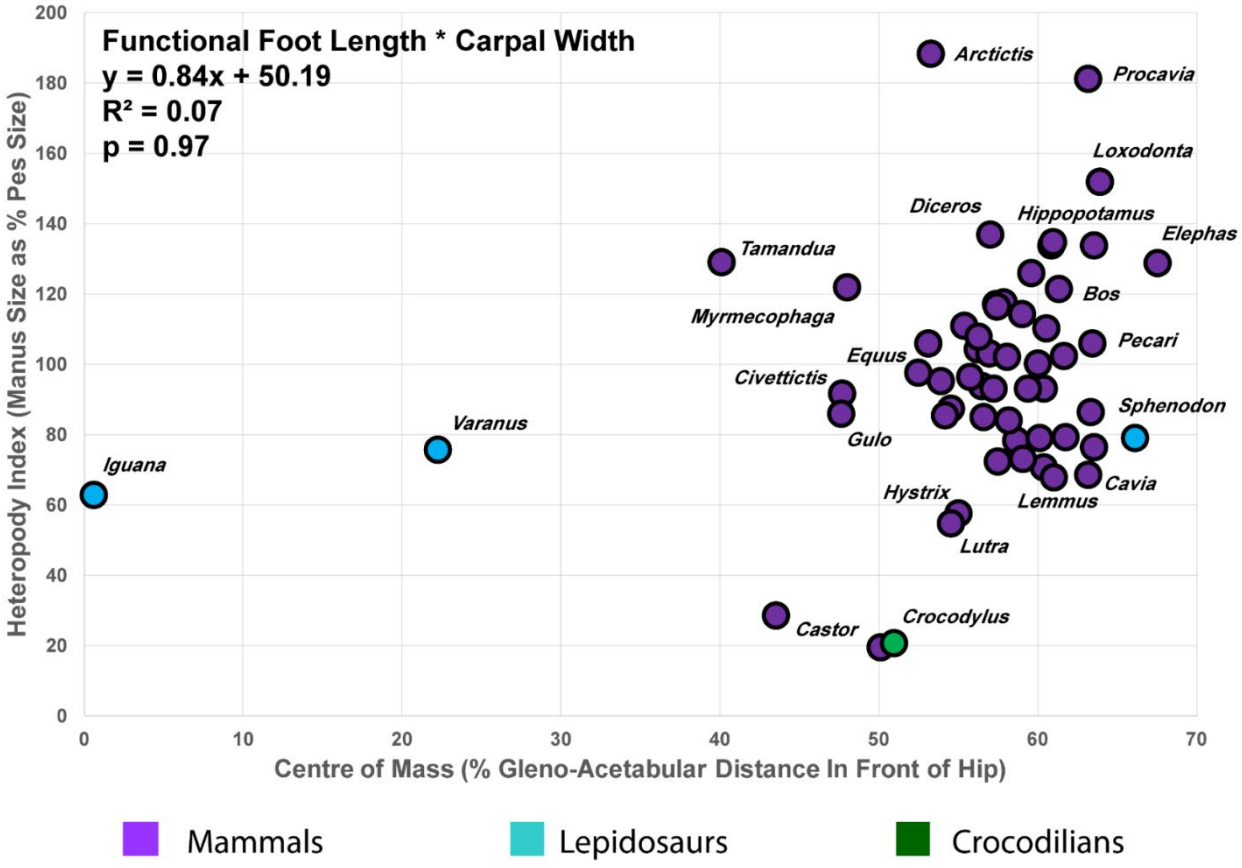

Figure 4.4 Plot of heteropody vs, centre of mass (percentage GAD in front of hip) of linear regression models for all taxa using heteropody index (manus size as percentage of pes size), for functional foot length multipled by carpal width. Purple data points are mammals, blue are lepidosaurs, and green are crocodilians.

Table 4.1 Table showing linear model regression, correlation, confidence based on coefficients and standard error, and p value, for the different heteropody versus centre of mass position analyses plotted in Figures 4.4 and 4.5

Analysis vs CoM	Linear Regression	Linear R^2	95% CI	P Value
Functional Foot Length	y=-0.01x+1.67	0.11	-12.88±39.29	0.74
Ungual Length	y=-0.00x+1.28	0.01	19.59±7.46	0.01
Digit Length	y=-0.00x+1.60	0.09	-29.25±11.89	0.02
Whole Foot Length	y=-0.00x+1.51	0	2.36±4.44	0.6
Carpal Width	y=-0.00x+1.32	0.01	2.088±38.12	0.96
Heteropody Index (using FFL*CW)	y=0.84x+50.19	0.07	0.01±0.17	0.97
Heteropody Index (using FFL*PW)	y=0.68x+56.27	0.04	-0.04±0.086	0.68

Table 4.2 Table showing linear model regression, correlation, confidence based on coefficients and standard error, and p value, for the different data subgroups of the heteropody versus centre of mass position analyses (based on heteropody index for functional foot length multiplied by carpal width as a proxy for underfoot area) plotted in Figure 4.6

Analysis (Heteropody Index (FFL*CW) vs CoM)	Linear Regression	Linear R^2	95% CI	P Value
Terrestrial	y=0.69x+62.53	0.02	0.03±0.03	0.42
Semi-Aquatic	y=6.46x-282.83	0.73	0.11±0.02	0
Erect	y=1.18x-0.99	0.09	0.05±0.03	0.14
Unguligrade	y=0.54x+67.38	0.01	0.02±0.05	0.72
Digitigrade	y=1.10x+35.26	0.06	0.06±0.06	0.37
Semi-Digitigrade	y=4.09x-131.8	0.31	0.08±0.04	0.1
Plantigrade	y=0.14x+67.15	0.01	0.04±0.14	0.79

There was no clear universal correlation between CoM and heteropody for any of the foot measurement methods used (maximum R^2 was 0.1, for functional foot length ratio), with the majority of the animals, particularly the mammals (in purple), clustering around a central point where CoM is around 60% and manus and pes size is roughly equal.

This remained true no matter which anatomical measure is used, even while individual taxa results varied between methods (Figure 4.4). Similar results were achieved with smaller analyses: for erect animals, unguligrade, semi-digitigrade, digitigrade, and

plantigrade animals, semi-aquatic and terrestrial animals (Figure 4.5). Semi-digitigrade animals achieved an R^2 of 0.3, which is only notable for being an order of magnitude higher than other functional subgroups of the data. The only analysis performed which showed positive correlation was for semi-aquatic animals, when *Varanus,* a clear outlier, was excluded (0.73 R^2). For that analysis, higher heteropody ratios (larger manus compared to pes size), were associated with a more anterior CoM.

Despite this, the fact that cursorial mammals clustered around a similar CoM and relative homopody is arguably a positive result, with these animals having the lack of heteropody that would be expected for a relatively mid-trunk centre of mass position if heteropody and CoM were correlated. As such, while there is not enough data to say for certain that this is representative of a wider pattern, and indeed other animals do not seem to fit this trend, pressure equalisation could indeed be the reason for lack of heteropody in these animals.

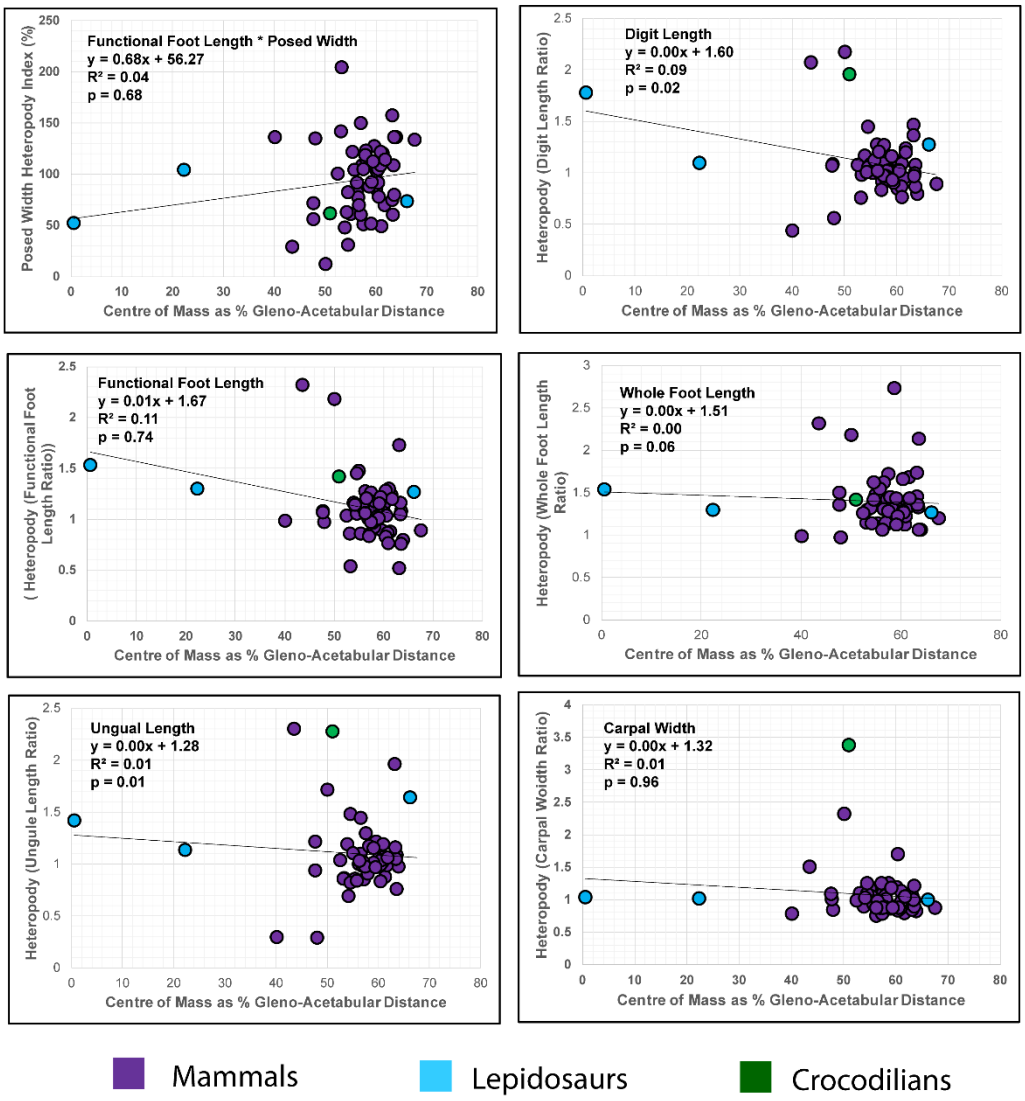

Figure 4.5 Plots of heteropody vs, centre of mass (percentage GAD in front of hip) of linear regression models for all taxa using various foot measurements (Heteropody Index with posed width, Functional foot length, Ungual length, Digit length, Whole foot length, Carpal width). Purple data points are mammals, blue are lepidosaurs, and green are crocodilians.

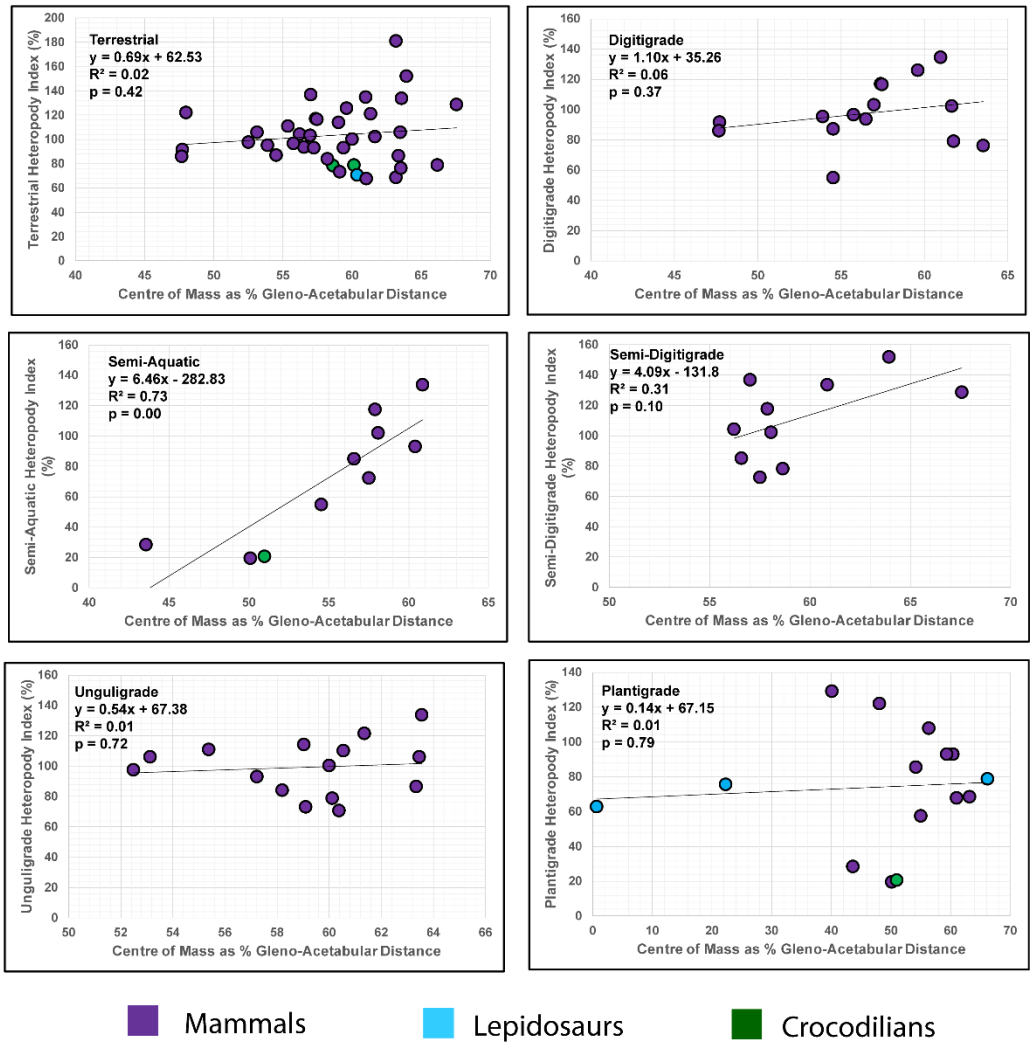

Figure 4.6 Graphs showing centre of mass (percentage GAD in front of hip) and heteropody (manus size as percentage of pes size, for functional foot length multipled by carpal width), for all taxa for subgroups of taxa (B: Taxa with erect posture, C: Terrestrial taxa, D: Semi-aquatic taxa (excluding *Varanus salvator*), E: Unguligrade taxa, F: Digitigrade taxa, G: Semi-digitigrade taxa, H: Plantigrade taxa). Purple data points are mammals, blue are lepidosaurs, and green are crocodilians.

In phylogenetic comparative tests (Supplementary Table 3.S1), it was made clear that phylogeny had no effect (PIC, Brownian model PGLS) to a negative effect (OU model PGLS). Body mass was also shown to have no effect. In addition, T-tests demonstrated

no significant difference between left and right feet for this analysis (Supplementary Table 4.S2).

4.5 Discussion

The focus of this study was the question of whether centre of mass and heteropody may be linked. While the results of this study might be surprising based on this premise, the clustering of CoM data within a narrow range is rather typical. CoM position for mammals is generally in the 50-70% range produced by this chapter's analysis (Henderson, 2006; Lammers et al., 2006). For other animals with long fleshy tails the CoM will typically be affected. In fact, removing the tail from a crocodilian model may result in a ~40% anterior shift in CoM position, as demonstrated with *Alligator mississipiensis* (Willey et al., 2004). That this typical CoM position also clusters around equal manus and pes sizes implies that animals with roughly equal fore and hind feet have CoM positions in the expected range. However, animals with high or low heteropody did not necessarily have unusual CoM positions to match, with the exception of anteaters and beavers (Figure 4.4). This may suggest that pressure equalisation is a factor in the relatively equal manus and pes size of cursorial mammals, while not being a universal factor across tetrapod species. It should be noted here that cursorial mammals do not, for the most part, require any degree of heteropody for foraging or locomotion, compared to fossorial animals, or animals which swim primarily with their hind legs and tail, such as beavers.

The correlation between semi-aquatic animal CoM and heteropody (excluding *Varanus*) is interesting, as these animals have a range of ~20-~140% heteropody index, ranging from the large-footed beavers, then the river otter, *Lutra*, *Hydrochoerus*, tapirs, the polar bear, *Ursus maritimus*, and hippos at the top. The high position of the hippos is possibly connected to their semi-digitigrade foot posture, as elephants, also semi-digitigrade, showed notably high heteropody indices. Some of these animals, beavers most notably, could be described as displaying extreme heteropody. Using this case as an example then, certain groups of animals may show a link between CoM and heteropody, as is the case here. Perhaps semi-aquatic animals lack the evolutionary pressures of terrestrial

mammals to maintain a relatively even manus-pes ratio. The unique anatomy of certain dinosaur groups could make them susceptible to evolutionary pressures to equalise underfoot pressure. Follow-up studies should consider this line of inquiry. It is notable that larger semi-aquatic animals appeared to be more manus-dominant (with the exception of the Morelet's crocodile, *Crocodylus moreletii),* with the hippos, then the tapirs and *Ursus maritimus* being the top five points, then *Hydrochoerus* below, followed by *Lutra*, the beavers, and *Crocodylus moreletii.* The larger mammals, listed above, have very small tails compared to crocodiles, beavers and otters, and thus the utility of the tail and hind legs for propulsion in swimming would be why the smaller semi-aquatic animals are pes-dominant, whereas hippos, tapirs, and polar bears, use all four limbs for paddling, which, while less efficient, does not require a large tail or full body oscillation (Fish, 1996).

It is notable that this work was based on skeletons, and that using heteropody figures based on *in vivo* functional foot length, width, and/or area, may have produced variable results, especially in animals with a large non-bony component to their feet such as elephants with their fatty foot pads (Hutchinson et al., 2011), and horses with their large, keratinous hooves (Casanova and Oosterlinck, 2012).

It should be acknowledged at this point that there are quite stark limitations of the explanatory power of unexpanded convex hulls for which no density information is available. Whereas it might make sense to process a large amount of data in a short time to presume that all animals will suffer a uniform amount of error due to lack of density information, this may only truly apply to animals with similar body plans and diets. While herbivorous mammals have similar gut volumes, for example, these volumes can differ significantly compared to animals with different diets (Clauss, et al., 2016). In addition, long tails and necks could potentially pull estimated centre of masses into extreme positions when not split into small sections and hulled separately, as a single hull for, for example, a lizard tail, could overestimate the volume of the tail considerably due to its length and relatively gracile structure not being conducive to the same hulling process as, for example, a thigh. This could explain the difference between the *Iguana* and *Sphenodon* CoM measurements (~5 and ~65% respectively), despite their relatively

similar body plans. In addition, when comparing, for example, *Elephas* CoM values from the literature (58.03% GAD (Henderson, 2006), compared to 67.54% in this study), results vary from what one would expect by about 10%. Therefore, these CoM values should not be taken as realistic CoM values for the animals as they would be in life, but as estimates to compare to each other.

While the idea that extreme heteropody in animals could be linked to CoM position in a potential pressure equalisation mechanism does not appear to be supported by this study, outside of promising signs in cursorial mammals, it is important to note that the majority of the animals in this study did not exhibit extreme heteropody. Those that did were only a few points in the data set. Furthermore, the classic examples of extreme heteropody, sauropod dinosaurs, are long extinct, and there are no extant analogues for animals their size and shape. Arguably, their closest modern analogues are elephants (Coombs Jr, 1975), which in this study do indeed sit on the higher end of the range of heteropody, as well as the higher end of the ranges of centres of mass.

While this study does not support a universal pressure equalisation role linking tetrapod CoM and heteropody (Falkingham, 2012; Falkingham et al., 2010), it is possible that no living animal has similar enough foot anatomy to sauropod dinosaurs to truly test whether pressure equalisation is a factor in these animals through studies of extant tetrapods such as this. It does not necessarily follow, after all, that multiple lineages of large tetrapods reached the same solutions to the problem of managing unequal stresses on the limbs. Still, the question of how much of the extreme heteropody and variations in heteropody in sauropods seen in the fossil record is due to preservational bias, substrate compliance, or a result of the anatomy of sauropod feet *in situ,* should be considered. It remains the case that there are no fully preserved, mummified sauropod feet with which to accurately model their exact soft tissue anatomy. Hence it is not known how adaptations for large size, such as fatty foot pads seen in elephant feet (Hutchinson et al., 2011), could affect the shape of their foot contact areas in ways that may not be able to accurately accounted for by inferring shape from skeletons. Using Figure 4.1, and its variant adjusted for skin (Supplementary Figure 4.S1), it will be possible to compare heteropody in extant animals

to that of sauropod dinosaurs using heteropody index and CoM data from trackways, of which there is a wealth, to evaluate whether they are a truly exceptional group in this regard, or if they follow the lack of pattern seen in the rest of terrestrial Tetrapoda.

The fact that a specific subgroup of this chapter's data showed a correlation, while the rest did not, suggests that while heteropody may not universally reflect CoM position, extreme heteropody may evolve as a result of unequal underfoot pressures in groups without strong evolutionary pressures to keep manus and pes area relatively equal. Terrestrial, cursorial tetrapods, which tend to have more uniform manus and pes sizes (Lull, 1904), would be most restricted in this way, requiring forefoot and hindfoot parity for effective propulsion and braking at speed, and this bears out in this study's data. Semi-aquatic animals, armoured animals, and animals too large to run would be capable of functional foot size disparity, whether for stability, pressure equalisation, or for behavioural purposes.

Chapter 5

Calibration Tests for Footscan Pressure Mat

5.1 Purpose

The pressure mat data being gathered for this thesis from live animals, by necessity cannot be calibrated to each individual animal. Due to time constraints, and lack of data gathered by Blackpool Zoo, weight and shoe size of each animal was not available prior to data gathering, and data was gathered based on which animals were available at the zoo at the time. As such, the pressure mat was calibrated to a human, the writer of this thesis.

Since this is not an ideal scenario, it is necessary to test whether calibrations that do not match the subject being observed significantly impact pressure mat readings. In particular, it is important to determine whether manus vs pes load remains consistent across trials, despite any potential inconsistencies in raw pressure data.

5.2 Methods

For these tests of the 1m Footscan pressure mat, a 135x245x390mm plastic tub (553g), filled with varying weights of ‘The Big B’ builder’s sand (each time made level with the tub rim to avoid bias) was used, with four table leg raisers supporting the sand-filled tub (90x90x90x90 contacting the tub, 120x120x120x120 contacting the pressure mat, with 95x95x95x95 sides, at an acute angle, and 135g each) to act as stand-ins for subject animal legs, placed 10mm back from the most distal short end of the tub on both sides. The base set up of the tub with all raiser ‘legs’ and no sand weighed 1095g. The set up with and without sand (pre-flattening) is demonstrated in Figure 5.1.

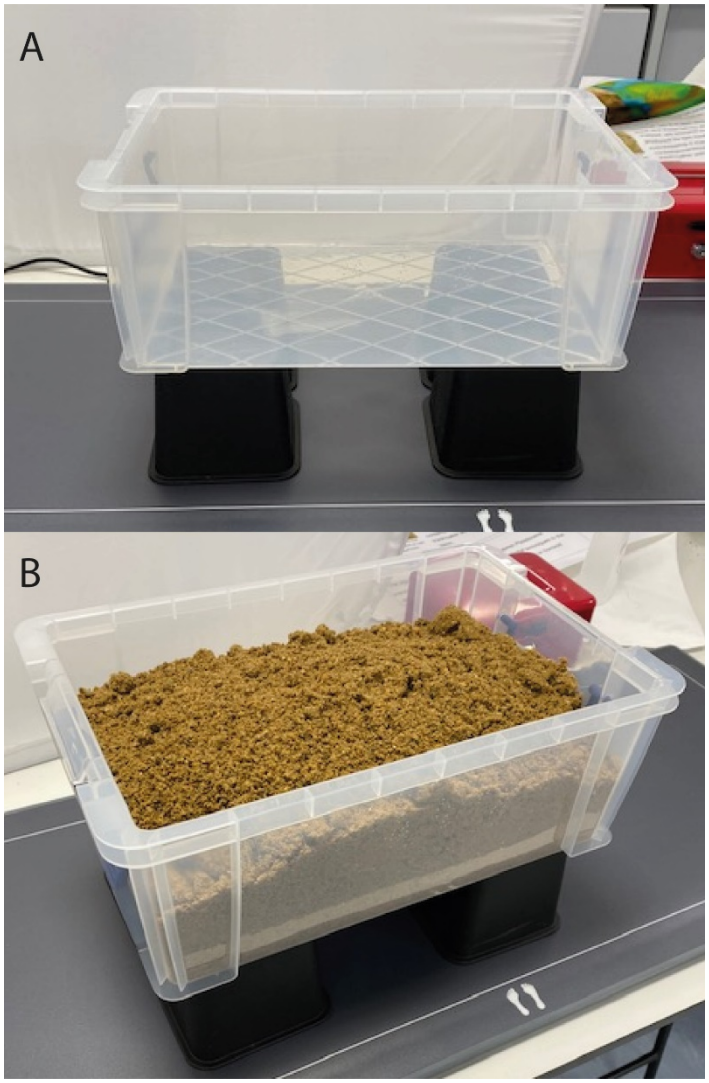

Figure 5.1 Calibration test set up using Tupperware tub and table leg risers with (B) and without (A) sand to simulate a quadruped of varying weights for different calibration settings.

To record pressure data via the Footscan 1m pressure mat, the pressure mat must be calibrated to a specific weight and shoe size (given in UK shoe sizes or length in mm). For data collected from Blackpool Zoo this necessitated using a human subject for calibration, as foot dimensions and weight of animals was not provided prior to live animal tests.

To test how calibration of the pressure mat affects pressure results and comparative load between manus and pes read by the mat, a series of 10 different calibration trials were set up: one calibrated to humans (the writer of this thesis), and 9 using the sand box with legs (3 trials calibrated accurately with 5kg, 10kg, and 15kg sand with accurate shoe size for

table leg riser feet, 3 with half foot length of riser feet at same weights, and 3 with double foot length of riser feet at same weights). For each of these calibration tests, the tub filled with 5kg, 10kg, and 15kg of sand were measured for load on each 'foot' and pressure on each 'foot. In this way we were able to test the effect of inaccurate calibration versus accurate calibration on pressure mat readings, for both different weights and shoe sizes for the same 'animal', but also for when a subject animal's data is collected while the pressure mat is calibrated to human weight and shoe size.

Since an empty tub is not heavy enough to detect pressure from all table leg riser 'feet', empty box tests were not performed. However, for potential interest, the results for an empty tub are presented in Table 5.1, with the caveat that the results given are dubious and their accuracy hard to discern.

For the purposes of these tests, legs on the left side of the pressure mat were considered forelegs, and legs on the right considered hindlegs.

These trials were tabulated in Table 5.1, and the average error of each trial in terms of manus vs pes load and maximum pressure recorded, compared to accurate calibrations, tabulated in Tables 5.2 and 5.3 respectively.

Following this, paired T-tests were performed to test whether there was a significant difference in manus versus pes load readings for each tub test across all 10 calibrations. If there was no significant difference, this would lend support to the idea that despite any difference to pressure readings in terms of raw numbers, manus versus pes load percentages would remain objective and accurate, thereby validating the reliability of the Blackpool Zoo data despite the setbacks.

5.3 Test Outcomes

5.3.1 Human Calibration

While results varied across all calibrations (Table 5.1), tub tests examined while calibrated to humans produced high degrees of error, overestimating manus load by about 10%

(Table 5.1), and maximum pressure by -161.1 n/cm2 (Table 5.2), the highest error margin in terms of maximum pressure readings, and in the mid-range for percentage load error. This degree of error was most apparent on human calibration with 5kg sand, with error decreasing as weight was added to the tubs, a fact consistent across different calibration methods. This indicates that lighter loads are perhaps less accurately read, or that the closer the calibrated weight is to the actual weight, the more accurate the results.

Table 5.1 Percentage load and error results for different trials at different calibrations

% Load Error		**Actual Subject of Trial**			[redacted]
Calibrated to	**Shoe Size (mm)**	**5kg Box**	**10kg Box**	**15kg Box**	**Avg Error**
Human	**280**	13.9	8.3	7.3	9.83
5kg Box	**120**	[redacted]	7.5	7.7	7.6
10kg Box	**120**	-6	[redacted]	0.5	-2.75
15kg Box	**120**	-16.1	-1.9	[redacted]	-9
5kg Box	**240**	-16.5	-10.5	-10.6	-12.53
10kg Box	**240**	-16.1	-4.6	-3.5	-8.07
15kg Box	**240**	-16.1	-1.9	0	-6
5kg Box	**60**	-24.7	-8.9	-3.6	-12.4
10kg Box	**60**	-20.1	-2.2	-4	-8.77
15kg Box	**60**	-23.9	-10.4	-9.5	-14.6

Table 5.2 Max pressure and error results for different trials at different calibrations

Calibrated to	Shoe Size (mm)	5kg Box	10kg Box	15kg Box	Avg Error
Human	280	-78.5	-106.8	-298	-161.1
5kg Box	120		42.8	-101	-29.1
10kg Box	120	4.4		-82.2	-38.9
15kg Box	120	15.8	88.2		52
5kg Box	240	-4.1	-24.4	-236.7	-88.4
10kg Box	240	-38.7	-30.5	-217.4	-95.53
15kg Box	240	15.8	88.2	0	34.67
5kg Box	60	-14.9	-16.2	-216.5	-82.53
10kg Box	60	-36.6	-64.6	-233.5	-111.57
15kg Box	60	-20.1	-9.4	-184.4	-71.3

5.3.2 Weight and Shoe Size Calibration

Calibrating the tub to alternate weights produced equivalent to greater error compared to human calibration in 5kg trials, with less impact on 10 and 15kg, with the same pattern when shoe size calibrations were changed, supporting the conclusions of the previous paragraph.

5.3.3 T-tests

T-test results revealed significant difference between manus and pes results when comparing all calibrations, for all trials. This proves that manus versus pes loads will be affected by calibrations, and therefore cannot be considered objective despite differences in raw pressure readings (Table 5.3).

In light of these results, extra attention should be given to the differences highlighted by tests on calibrating with human measurements, as guidelines on the likely errors to be encountered when testing animals without prior knowledge of their foot and mass dimensions, relying on calibration by humans of known weight and shoe size.

Following this, caution must be urged regarding recording pressure results for animals without prior knowledge of the subjects, and their body mass and foot size. This makes it difficult to gain lots of data quickly, as processing whatever animals are to hand on a certain day at a zoo or farm will result in skipping the step of recording the necessary data to calibrate the pressure mat accurately and gain an accurate picture of underfoot pressure and area in these animals.

Table 5.3 T-test results for all calibrations for all trials to test consistency in manus and pes result disparity across different weights and calibration methods

T Tests	**5kg**	**10kg**	**15kg**
T value	2.97	3.5	2.72
DFs	9	9	9
p-value	0.02	0.01	0.02
95% CI upper	5.37	5.2	1.77
95% CI lower	39.59	24.16	19.15
mean differences	22.48	14.68	10.46

5.4 Conclusions

There will be significant differences between the readings gathered for the purpose of this study, and those that would have been gathered if all calibrations were accurate and had enough preparation time. As a result, data from live animals gathered for this study must be considered in this context, with a high margin for error. Data gathered from the literature for this study should not have this same problem, as the studies referenced for the most part focused on a single subject animal, with the time and resources needed to accurately calibrate their equipment for the subject.

Chapter 6

Are Underfoot Pressures Reflective of Heteropody and Centre of Mass Position?

6.1 Summary of Chapter

Heteropody is the phenomenon in which the manus and pes of quadrupedal animals differ substantially in size and shape. The term is most often used in reference to the extreme heteropody present in fossils and trackways of some non-avian dinosaurs, particularly sauropods. Previous studies have asserted the possibility that extreme heteropody developed in these animals as a mechanism to equalise underfoot pressure, compensating for unusually anterior/posterior centre of mass positions. To investigate this possibility, pressure data were collected from extant taxa, and supplemented from the scientific literature, to establish whether centre of mass position reflects heteropody. Data for cursorial mammals tended to cluster around centre of mass 52-64% (% gleno-acetabular distance from hip) with area, vertical force, and pressure under the manus ~100-140% that of the pes. Data collected as part of this thesis was combined with data from the literature (3 crocodilians, 25 mammals - of which 7 were primates and 8 were ungulates). In newly collected data, correlations of more anterior CoM positions with increased manus area, increased manus underfoot vertical forces, and slightly negative manus underfoot pressures, compared to those of the pes were found, but with only 5 data points (R^2 between 0.7 and 0.85). When these data were combined with data from the literature, the correlation was much weaker (R^2 between 0.26 and 0.32). These results do not offer substantial support to the hypothesis that heteropody equalises underfoot pressure.

6.2 Introduction

Heteropody, as discussed in previous chapters, is a phenomenon in which manus and pes size are observably distinct (Lockley et al., 1994a). Work by Falkingham (2012) suggested extreme heteropody in quadrupeds arises as a result of selective pressures to equalise underfoot pressures, in correspondence with centre of mass (CoM) position (i.e. where a CoM is far enough anterior or posterior that an animal's mass is disproportionately supported by two of its four limbs). This idea arose as a way of explaining extreme heteropody in sauropod dinosaurs (Falkingham et al., 2010; 2012), as seen in their body fossils and footprints, where foot contact area of the manus and pes can be vastly different. This extreme heteropody has been linked to the trace fossil phenomenon of 'manus-only trackways', often attributed to derived sauropod dinosaurs (Lee and Lee, 2006). In combination with increasingly anterior CoM positions, hypothetically, unusually small manus impressions in sauropod trackways would produce greater underfoot pressures. Subsequently, deeper tracks would be produced under the manus than the pes.

Foot size has a direct and observable effect on foot pressure, whether this hypothesis is ultimately accepted or rejected, since pressure equals force divided by area. Even with a centre of mass exactly halfway between the shoulder (glenoid) and hip joints (acetabulum), a smaller manus will exert greater underfoot pressure, whereas a larger foot will exert less pressure, as the force of the animal's weight is allowed a larger area to disperse. The same logic should hold true across varied centre of mass positions. In this way it is also important to emphasise the role of foot shape on *in situ* foot pressure exertions and how this feeds into a more complex interaction between an animal and its underfoot forces than the simplified model illustrated in Henderson (2006) and chapter 1 might suggest (Falkingham, 2014). *In vivo*, differing foot postures (digitigrady, plantigrady, etc.), and foot support mechanisms such as fatty foot pads, can influence foot angle, size, and shape in a way that is not accounted for in a simple plank and struts model, since

structural support mechanisms may act in a pressure-saving manner beyond simply foot contact area, absorbing some of the pressure cost with thick layers of soft tissues, for example (Carrano, 1997; Hutchinson et al., 2011).

Much of the literature around underfoot pressure has centered primate gait and pathological studies (Kinoshita et al., 2019; Yamashita et al., 2019; Apelqvist, 2012), with a number of non-human animal studies also focused on veterinary diagnostics rather than locomotory biomechanics in healthy animals, mostly concerned with lameness and hoof health (Scott, 1989; Grégoire et al., 2013; Carvalho et al,. 2005). However, a lot of important work has been done on underfoot pressure across the animal kingdom, particularly regarding pressure scaling (Michilsens, et al., 2009; Panagiotopoulou, et al., 2012). Because foot pressure has a history as a human and animal diagnostic tool, there is a variety of tools available for measuring foot pressure, such as pressure mats (Xu et al., 2017; Franklyn-Miller et al., 2014). Despite being designed primarily for human use, this equipment has been demonstrated on many occasions to be an appropriate and useful tool for measuring underfoot pressures and locomotion in non-human, and notably for this study, quadrupedal, animals (Meijer et al., 2014; Van der Tol et al., 2003; Vereecke et al., 2003).

Pressure differences between manus and pes have previously been measured in multiple extant animals. Generally, quadrupedal mammals have been found to support 55-60% of their body weight on their forelimbs (Reynolds, 1985a). Elephants, as an example of the typical quadrupedal pattern, support around 60% of their weight with their forelimbs when standing or walking (Henderson, 2006; Panagiotopoulou et al., 2016). In primates this number tends to be lower, around 30-45%, and reptiles, which tend to have longer and more muscular tails than mammals, generally support more weight still with their hindlimbs (Allen et al., 2009; Willey et al., 2004). Cursorial animals tend to use their forelimbs to support more weight, and additionally have centres of mass closer to their forelimbs (de Faria et al., 2015).

6.3 Materials & Methods

To examine differences in forefoot and hindfoot foot pressure and area, data both newly collected, and from the scientific literature were gathered.

Data from the literature where any variables of interest (centre of mass, foot surface area, peak pressure, and peak vertical force) were recorded and made available were collected into a database for analysis. The aforementioned literature data used in this chapter were derived from the following papers: (Henderson, 2006; Panagiotopoulou et al., 2012; 2016; Warner et al., 2013; Willey et al., 2004; Allen et al., 2009; Kubo, 2011; McElroy et al., 2014; Reynolds, 1985b; Raichlen, 2004; Schmitt and Hanna, 2004; Schmitt, 2003; de Faria et al., 2015; Agostinho et al., 2012; Scott, 1989; Verdugo et al., 2013; Lascelles et al., 2006; Lascelles et al., 2007; Lammers, 2007; Walter and Carrier, 2007; Clarke, 1995; Howard et al., 2000; Clarke et al., 2001; Ueda et al., 1981; Oosterlinck et al., 2011; Panagiotopoulou et al., 2019). While most of these studies were on mammals, data for crocodilians, lizards, and turtles were used where possible. These data were recorded, compared, and kept for comparison with newly collected data. Especially of interest were data recorded for animals for which previously estimated centre of mass data from skeletons existed (Chapter 4). It should be made clear at this point that peak pressure and force in this case refer to the highest pressure or force of the footfall overall, collected over the course of the footfall, and not the highest pressure or force detected in any part of the foot, as is the case in Figures 6.2 and 6.3, and in the previous chapter.

New data, consisting of underfoot pressure, area, and vertical force were collected from five animals (dog, alpaca, goat, pony, and tapir – *Canis, Vicugna, Capra, Equus, and Tapirus,* in latin) using a 1m (1068mm x 418 mm x 12 mm) Footscan pressure mat (up to 200Hz for recording), Footscan 9 software, and a high speed camera (1000 fps, 1280x720 resolution, Slowmo camera company) to film subject animals during data collection to aid in identifying footprints.

Dog data were collected at Liverpool John Moores University. Ethical approval was given for all live animal studies. The subject animal was a male adult husky weighing 44kg.

Data for the remaining subject animals were collected at Blackpool Zoo, where the subjects were a male tapir weighing 153kg, a male goat weighing 11.8kg, and a male alpaca and male pony, weights unknown. During trials, the pressure mat was covered in a protective mat (PedalPro – 180x70x0.6cm, shock resistant PVC) to prevent damage from hooves and claws. The subject animals were guided over the pressure mat by their respective handlers, as the animals for the most part avoided the pressure mat altogether without guidance, and only with encouragement from trainers would walk over the mat enough times to collect sufficient data.

Figure 6.1 Still image from high-speed camera footage of subject animal (goat/*Capra aegagrus herpus*) walking across the pressure mat, covered by the protective mat, guided by its handler.

Raw data from Footscan 9 were exported and then analysed using a custom Matlab script (https://github.com/pfalkingham/matlabPressureAnalysis). This script identified the total underfoot surface area of each foot as well as peak and median temporal vertical force and pressure for each recorded footfall (where median represents the vertical force or pressure halfway through the time the foot produces a readable input (inputs begin when any sensor is triggered)). Recorded footfalls were identified as forefeet or hindfeet, and left or right, using a combination of the dynamic recordings in Footscan 9, and high speed camera footage. Once extracted, these data were tabulated and plotted into box plots, comparing manus and pes for each animal.

Manus and pes data for each subject animal were then subjected to paired T-tests to determine whether manus and pes were significantly different across the relevant variables, for each subject animal, i.e. to establish whether there is statistical support for heteropody, or significantly different underfoot pressures. In addition paired T-tests were performed to investigate whether there was a significant difference between left and right feet for each animal.

Newly collected data were then combined with literature data, and previously calculated area values (from Chapter 2, (Strickson et al., 2019)). This combined data set was plotted to examine heteropody and differential forces and pressures across multiple species, and to determine whether any trend exists between manus/pes differences in area, vertical force, and pressure, and estimated centre of mass. CoM values for each animal can be found in table 6.S4. Since CoM estimates from convex hull analysis were combined with those from the literature, it is worth noting that the methods by which CoM were derived in different studies, and therefore, any associated error or bias, were somewhat inconsistent. CoM estimates from convex hulls did not adjust for lung volume and other air-filled organs, which can have a significant effect on body mass estimation but affects CoM calculations much more on the ventral-dorsal axis than the anterior-posterior axis (Allen et al., 2009; Sellers et al., 2009; Bates et al., 2009). Since only the latter axis is used in this study's CoM measures this effect should be minimal, but it is acknowledged that a small amount of error may be present.

Beyond this, the same limitations apply as in Chapter 4, regarding convex hulls without density information, and without calculating each body segment separately and carefully. This is especially relevant when looking at animals with long tails and necks, where a small error could make a body segment seem much larger, and therefore move the centre of mass considerably.

6.3.1 Pressure Mat Use

Calibrating the pressure mat required a subject of known weight and shoe size. These were entered for the author of this thesis, and the pressure mat calibrated prior to each experiment.

The Footscan pressure mat is designed primarily for experiments on humans. This presents a potential issue with the size of the sensors within the mat. Each sensor in the Footscan 9 pressure mat is 7.62mm x 5.08mm. The size and shape of these sensors is much less noticeable in the feet of large animals (such as humans, or for the purposes of this study, tapir, equids, large dogs), but could potentially affect area and pressure estimates for smaller animals, where the size of the sensors compared to the size of their feet results in a ‘blocky’ estimate of foot shape, which distorts the true shape of the foot compared to that of animals with larger feet. This variation can be seen visually in Figure 6.4.

As mentioned above, a protective mat (PedalPro – 180x70x0.6cm, shock resistant PVC) was used for all animal tests to protect the pressure mat from damage from hooves and claws. When testing the mat with the author of this thesis as subject (figure 6.2), reduced pressures were detected when using the protective mat, versus without, but a greater area of the foot was detected with the mat, and differences in pressure between foot regions were lessened. These tests imply that peak values for pressure and vertical force may be underestimated with use of the protective mat.

In addition to this, the calibration tests outlined in the previous chapter, indicate that inaccurate calibration can affect manus and pes ratios as well as overall pressure detected. Since it is necessary for this experiment to calibrate the pressure mat to humans rather than each animal individually, this should be noted and considered carefully before making conclusions from the live animal data collected. The same issues should not be present in the data collected from the literature.

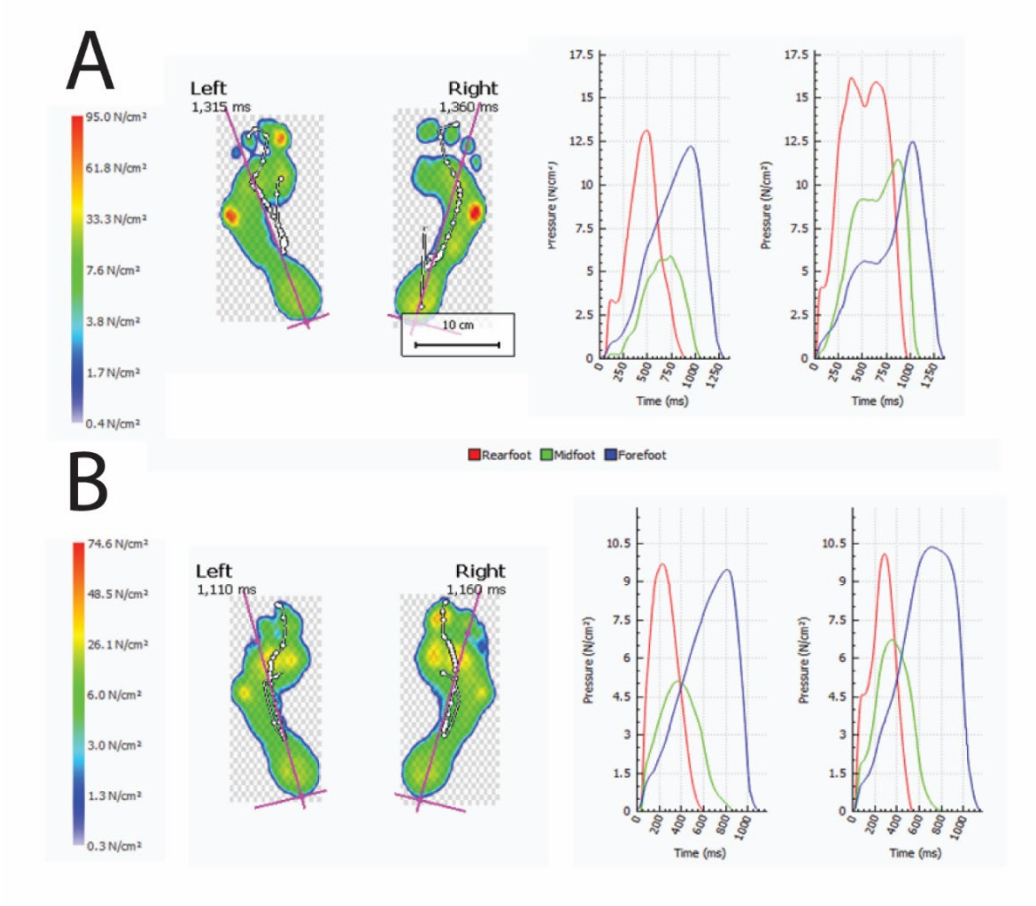

Figure 6.2 Pressure mat test results with a human subject, showing differences in detected pressures across the left and right foot with A) no protective mat, and B) with a protective mat. Foot impressions are representative samples, and speed of footfall varied for each individual footfall.

6.4 Results

Pressure mat analyses conducted for this study showed an overlap between manus and pes area, peak/median vertical forces, and peak/median pressures, for the majority of animals, although this was not without exceptions, and ranges of results for each foot varied. (See Table 6.1, see Figure 6.3.)

Table 6.1 Table showing linear model regression, correlation coefficients, confidence intervals (based on coefficients and standard error), and p value, for area, peak pressure, and peak vertical force vs CoM for newly-collected data, and newly-collected data combined with data from the literature, as plotted in Figure 6.5.

Newly Collected Data	Linear Regression	Linear R^2	95% CI	P Value
Area	y=6.05x-229.17	0.70	-0.35±0.70	0.71
Peak Vertical Force	y=10.70x-466.76	0.75	0.24±0.46	0.69
Peak Pressure	y=3.11x-53.64	0.85	0.29±0.44	0.74
Combined Data	**Linear Regression**	**Linear R^2**	**95% CI**	**P Value**
Area	y=1.50x+23.63	0.32	1.74±0.12	0.12
Peak Vertical Force	y=2.44x-18.33	0.27	-1.20±0.26	0.26
Peak Pressure	y=-1.74x+216.71	0.28	-0.27±0.54	0.54

Area results for combined data ranged from manus area as 92-140% of pes area. Manus peak vertical force ranged from 101-184% pes peak vertical force (always higher than pes peak vertical force). Manus peak pressure ranged from 111-134% pes peak pressure (always higher than pes peak pressure). Of these animals, the *Vicugna, Canis,* and *Tapirus* consistently fell within the middle of this range (Table 6.1), as well as having similar estimated centres of mass (all ~57% gleno-acetabular distance, from the hip). *Equus* consistently demonstrated the lowest manus dominance out of all newly-tested animals, across all variables, with the lowest manus pressure, area, and vertical force. Inversely, *Capra* consistently represented the highest value in each range, demonstrating the highest level of manus dominance for each variable. *Equus* and *Capra* as the highest and lowest in the range is consistent to their estimated centres of mass, with the estimated CoM of *Equus* at 52% G-A distance from the hip, and of *Capra* at 59%. Although the range of CoMs and manus-dominance was somewhat narrow, centre of mass position was a reliable predictor of a subject animal's degree of heteropody, and vertical force distribution. In fact, linear models of each of these values against estimated CoM results in a strong correlation between CoM and heteropody for area, peak vertical force, where manus is larger, or produces more vertical force, the more anterior the estimated CoM. The slope of these models is notably shallow, however, but this may be

because all subject animals occupied a narrow range of centre of mass positions. Despite this pattern, there was still some overlap in ranges between forefeet and hindfeet for some variables for all animals (Figure 6.4).

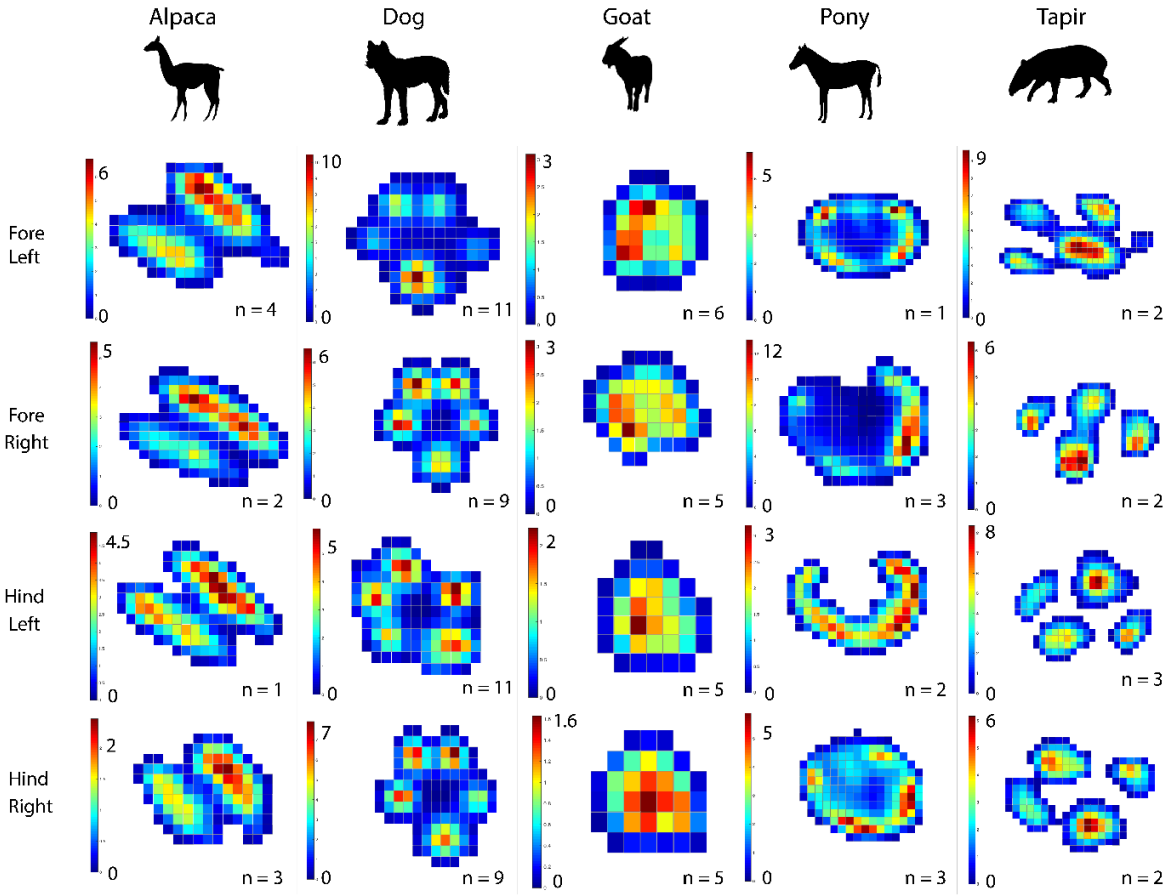

Figure 6.3 Examples of heat maps for pressure (N/cm²) for newly-collected data, with one example for each foot, along with number of whole footprints recorded (partials were discarded). Pressures recorded here are fore different foot regions, not representative of the data presented in the rest of this study, which tracks pressure for the entire foot across a footfall.

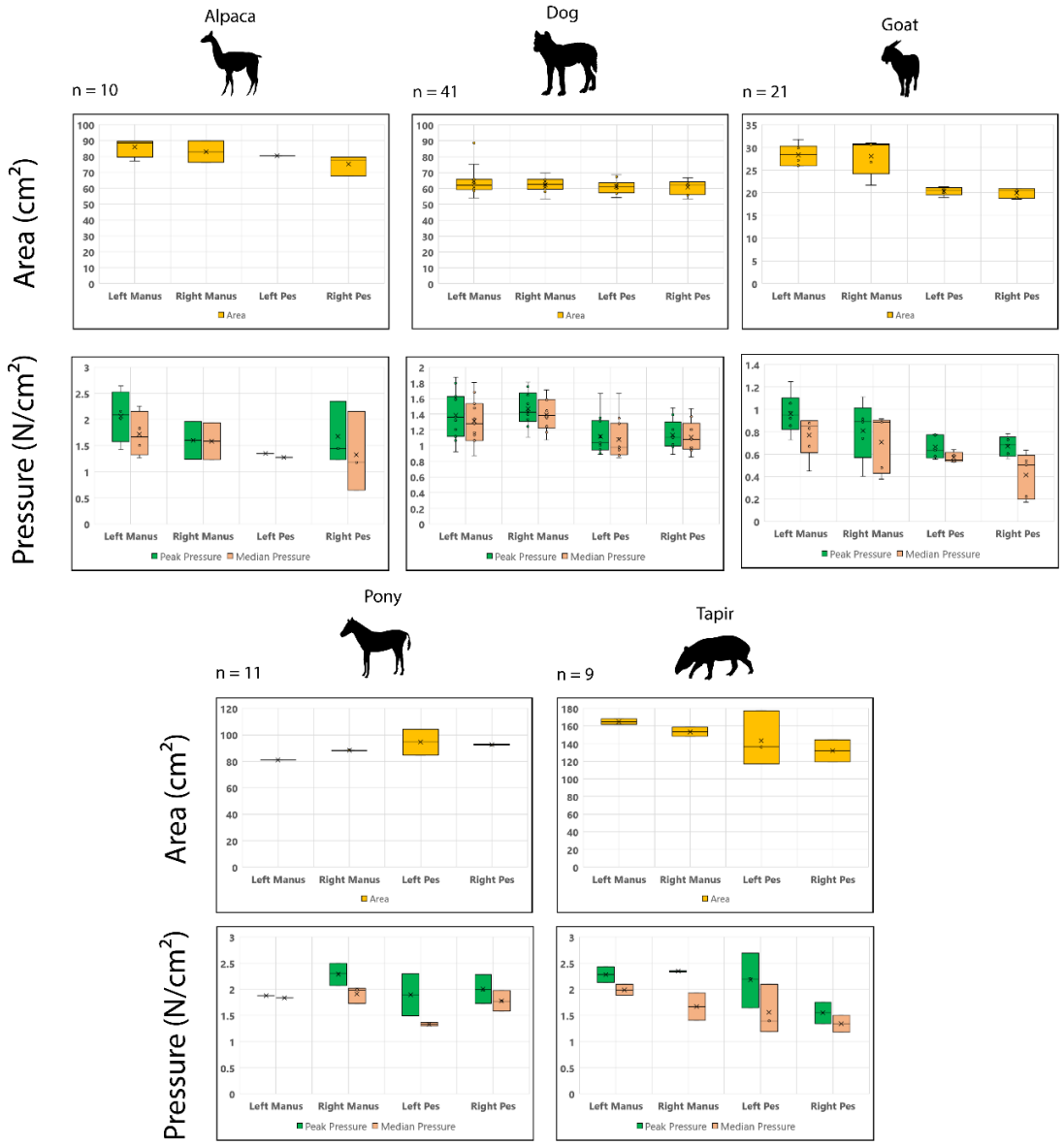

Figure 6.4 Box plots comparing results for area (cm²), peak pressure (N/cm²), and median pressure (N/cm²), for all four feet of each subject animal, along with total number of footprints collected.

Paired T-tests assessed whether the difference in manus and pes values (for all variables) for each animal were significant, and those testing pressure in left versus right feet were not significant (Table S6.2 and S6.3). *Capra* manus and pes values were significantly different for all variables ($p < 0.05$ for all, $p < 0.01$ for all except peak and median pressure). *Canis* manus and pes values were significantly different ($p < 0.01$) for all

variables except area. *Tapirus* manus and pes values were significantly different for peak vertical force ($p < 0.05$), and for area ($p < 0.01$), and not significant for pressure. *Vicugna* manus and pes values were largely not significantly different (median vertical force $p < 0.01$, other variables non-significant). *Equus* manus and pes values were not significantly different for area, pressure, or vertical force. It should be noted that the animals with the largest number of footsteps sampled, *Canis* and the *Capra* ($n = 41$ and $n = 21$, respectively) displayed the most significant differences between their respective manus and pes. It is perhaps possible that with equal sample sizes, manus and pes differences across all animals would be more significant.

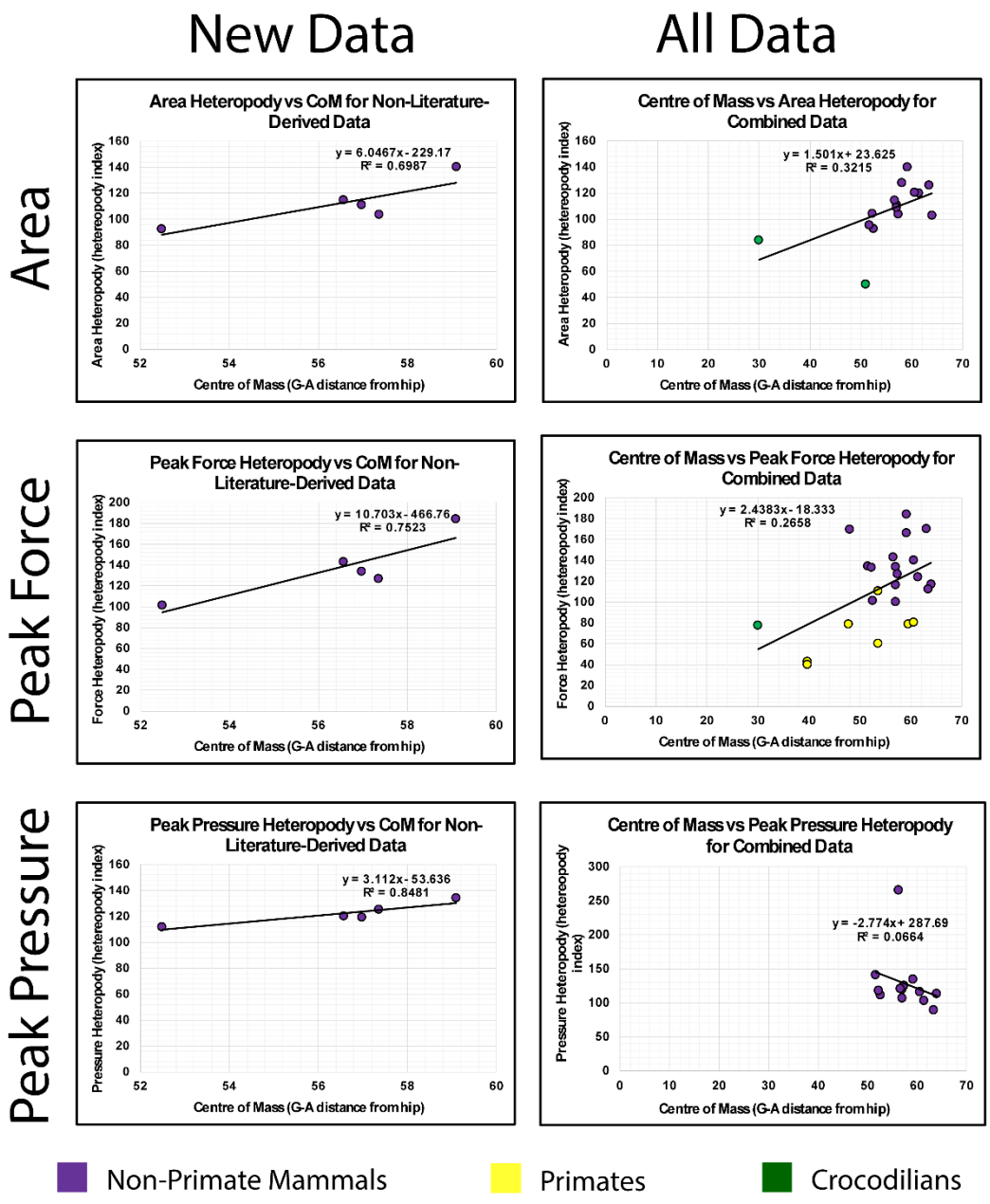

Figure 6.5 Linear plots showing data for centre of mass against area, peak vertical force, and peak pressure, for newly-collected data, and newly-collected data combined with data from the literature.

Data from the literature showed a range of manus area as 38-135% pes area. Both the low and high extremes of this range were lizards (*Pogona* and *Furcifer* respectively). No

mammal displayed heteropody less than 100% (manus smaller than pes) based on data from the literature alone. However, using calculated areas based on CT scans (Chapter 2) domestic cat data showed a mammalian low of 95%. Scores below 100% were common for reptiles, representing the majority of crocodile, lizard, and turtle data compiled. Peak manus vertical force data from the literature ranged from 39-170% of pes peak vertical force. The low end of the peak vertical force range mainly represented reptiles and primates, with the high end almost entirely composed of cursorial mammals. Very few peak pressure data were extracted from the literature. What data were available was entirely made up of cursorial mammals and ranged from 89-265% manus peak pressure as a percentage of pes peak pressure. However, the 265% figure belonging to *Ceratotherium*, is a significant outlier, and without it the range would be 89-140% *with Sus* and *Felis* at the low and high ends, respectively. It might be expected that *Ceratotherium's* large, horned head would make it a special case, not representative of general trends across Tetrapoda or Mammalia, however, its calculated centre of mass is not equally extreme, at 56% G-A distance from the hip. Given these findings, *Ceratotherium* was excluded from further analysis.

Analyses using combined literature and new data displayed no discernible correlation between area and peak pressure manus-pes distribution, but a weak correlation between area and peak vertical force distribution, where comparatively greater underfoot peak vertical force in the manus was associated with a larger manus area relative to pes area (Figure 6.5). In general, more anterior centre of mass was associated with greater manus area and manus peak vertical force, compared to pes area and peak vertical force, with the inverse true in terms of pressure. This would imply that as anterior vertical force increases and CoM moves anteriorly, manus area increases relative to pes area, which results in reduced peak underfoot pressures. However, the correlations associated with these trends were weak and non-significant (Figure 6.5), and newly collected data was not calibrated in a way that makes them reliable as an indicator of overall trends. Correlation increased with removal of certain outliers, but not to a point where it rose to moderate or strong. This effect could possibly be strengthened with greater sample size.

6.5 Discussion

Across all analyses, most animals maintained manus area, peak vertical force, and peak pressure, as 100-140% that of pes area, peak vertical force, and peak pressure. This range is consistent with CoM positions of 52-64% G-A distance in front of the hip. Given the sheer number of animals in this range, this appears to be a relatively consistent state for quadrupedal mammals, especially for cursorial mammals, which make up most of the data in this cluster (Figure 6.5). Animals with CoM >52% that do not fit in this range include anteaters, goats, sheep, possums, and the outlying *Ceratotherium* (Figure 6.5 excludes *Ceratotherium* as an outlier).

In the same way that animals with CoM <52% (and pes dominance in terms of area and peak vertical force) were largely animals with muscular tails used for non-terrestrial locomotion, i.e. crocodilians and new world monkeys (Lemelin, 1995; Seebacher et al., 2003), outlying animals with CoM >52% may have possessed anatomical features that prevented them from achieving the otherwise standard 100-140% manus dominance. The most obvious of these is the clear outlier, *Ceratotherium,* with its large head and horns. Large skulls with ornamentation have been suggested to influence CoM position in ceratopsian dinosaurs (Maidment et al., 2014).

As seen in Figure 6.5, more anterior centres of mass appear associated with more anterior peak vertical forces, and larger manus surface areas compared to pes surface areas. Since most literature sources presented data for only force or area, and very few gave data for pressure, less data was available for pressure analysis. However, the data collected resulted in a shallow, negative slope, indicating that manus pressure compared to pes pressure decreased with more anterior centre of mass positions.

While this could be construed as an argument for the model of pressure equalisation (Henderson, 2006), correlations were much lower with the combined data set. As well as this, the high p values of associated linear models, and the shallow slope of the newly-collected data deserve careful consideration. Why the findings of this chapter conflict slightly with those of chapter 4 could potentially relate to the findings of chapter 2 of this

thesis, wherein underfoot soft tissue extent was greater in the manus than the pes compared to skeletal tissue extent. Following the logic of chapter 2's findings, analysis of osteology alone would underestimate heteropody, and *in vivo* analysis would reveal greater disparity between manus and pes underfoot areas.

One reason why a weakened correlation may be present in the combined data set (Figure 6.5) is the morphological disparity, and the varying sample sizes for each morphology, present in the data. CoM values <50% G-A distance (closer to the hip) are limited to reptiles, new world monkeys, *Myrmecophaga,* and *Cercopithecus.* The remainder of the data, which are entirely mammalian, has CoM values between 50 and 64%. The distinction in this difference appears to be the presence or absence of a robust tail, as present in Crocodilia (Willey et al., 2004; Seebacher et al., 2003), and new world monkeys, who possess prehensile tails (Lemelin, 1995). Many mammals in this study (notably, ungulates) have short tails (Siegfried, 1990; Stankowich, 2008). Unfortunately, most data available on centre of mass, underfoot forces, pressure, and area, are mammalian, and thus the data are primarily distributed around the typically mammalian CoM position of ~50-70% G-A distance from the hip, across a wide range of morphologies and ecologies (Reynolds 1985b). In this case the 50-64% CoM range includes all ungulates, carnivores, anteaters, elephants, rhinos, and most primates. This results in a situation where the more anterior CoM positions have a much wider range of taxa represented, and thus have more disparate results. However, the fact remains that there are too many issues with the new data collected to use them to argue that more data would result in more desirable results.

The main outliers in the 50-64% CoM range possess adaptations that could affect heteropody and relative underfoot vertical forces. For example, rhinos, which were by far the most outlying, have large keratinous horns, large heads, and are protected by a thick layer of skin that reduces its investment in adaptations for cursoriality compared, for example, to horses or gazelles (Berger and Cunningham, 1998; Shadwick et al., 1992). Giant anteaters have large claws on their manus which aid in digging, an adaptation also seen in their arboreal relatives, the tamandua and the sloths, and does not seem to be

advantageous to terrestrial locomotion (Coombs, 1983; Naples, 1999; de Faria et al., 2015). Possums are arboreal marsupials (Lammers et al., 2006), goats and sheep possess horns of bone and keratin (although cows and deer also possess these features and are non-outlying) (Zhang et al., 2018). These adaptations could reduce selective pressures to maintain equalised underfoot pressures for balanced posture during terrestrial locomotion. Yet these adaptations are still potentially important to survival and ability to compete for mates. In this way pressure equalisation via heteropody could potentially act as a default mechanism for maintaining stability during terrestrial locomotion, with outliers emerging when outside selective pressures are prioritised.

The correlation is much stronger with only the five animals directly measured as a part of this study. However, it is not advisable to draw conclusions from graphs with only five data points, and there were several issues present in the data collection due to inability to calibrate accurately for each animal. Still, since the five animals involved are all cursorial mammals (although tapirs are also semi-aquatic and removing them does not change the relationship) (Stein and Casinos, 1997; Endo et al., 2019), their stronger correlation could lend support to the above postulation, wherein heteropody is employed to equalise pressure in the absence of obstructive selective pressures. The same relationship remains when *Capra*, and *Tapirus*, are removed. However, it does not hold when *Capra* and *Equus* (the animals with the most posterior and anterior CoM positions) are both removed. With the remaining three animals, area and peak vertical force values are lower on the manus with more anterior CoM positions, with R^2s of 0.96 and 0.99 respectively. Therefore, any support for the idea of heteropody as a pressure equalisation mechanism from this subsection of the data remains speculative and unjustified. The hypothesis that heteropody functions as a pressure equalisation mechanism then, is not supported.

With the above in mind, it should be noted that a lack of definitive correlation between CoM position and heteropody corresponds with the findings of the previous chapter, albeit with an increased signal. When using length and width of skeletal feet to determine area, CoM position did not seem to have any correlation with heteropody, except in semi-aquatic animals. However, almost all the skeletons used for that analysis were of cursorial

mammals. Of the four non-mammals in that analysis, only *Sphenodon* fell within the range of the cursorial mammals, with both lizards and *Crocodylus* as clear outliers. In fact, the two lizards are in a position relative to the rest of the data that would put them on the trendline seen in this study for heteropody (area) vs CoM position (Figure 6.5). In addition, the skeletal data's most outlying mammals were non-cursorial, for example: beavers, anteaters, bearcats, hyraxes, and otters (Stein and Casinos, 1997). Animals with large heads and/or horns/tusks, such as elephants, rhinos, and hippos were at the high end of the range, with *Loxodonta* outlying. In this chapter, there were more animals present that were not cursorial mammals, such as fully arboreal primates, and additional crocodilians. With a dataset with equal representation across different clades and modes of life, especially non-mammalian clades, it is possible that skeletal data would show a clear correlation, and that a stronger correlation would be seen in this study. A more representative dataset would ideally contain more crocodilians, large lizards (varanids, iguanas), tortoises, giant salamanders, as well as specialised hopping, fossorial, semi-aquatic, and arboreal mammals.

It is also possible that skeletal data produced different results due to determination of heteropody data from skeletal anatomy rather than *in vivo* foot dimensions. As determined in chapter 2, forelimbs and hindlimbs tend to have different ratios of skeletal tissue to soft tissue, with pes underfoot surface area lower relative to skeletal underfoot surface area than that of the manus. In this way, heteropody could be underestimated in studies reliant solely on skeletal data. In addition, the analysis of heteropody using static skeletons, rather than measuring the total area of the foot that contacts the ground in a footfall *in vivo,* makes assumptions about how much of the foot area to count in heteropody assessments, and, by necessity, requires value judgements of which parts of the foot to count in measurements, using simplified categories (Carrano, 1997).

Despite the results of this chapter, it is still possible that with their unique body plan and extreme heteropody, sauropod dinosaurs utilised heteropody as a pressure equalisation mechanism while other animals do not. As with several other animals in this study, centre of mass for sauropodomorph dinosaurs underwent anterior shifts in relation to adaptations

in the head and neck, first in association with the origin of quadrupedality (associated with increased neck lengths), and second in titanosauriformes who possess more upright necks and long forelimbs relative to their hindlimbs (Bates et al., 2016). In addition, previous studies have suggested that some sauropods may have possessed fatty foot pads on their feet (Paik et al., 2017; Jannel et al., 2019), a technique used by heavier mammals such as elephants and rhinos (Hutchinson et al., 2011; Panagiotopoulou et al., 2019). Titanosauriformes, unlike elephants and rhinos, possessed a fleshy tail, affecting requirements for foot posture, and had bird-like air cavities in their vertebrae (Lambertz et al., 2018; Zurriaguz and Cerda, 2017). The front feet in these animals would experience high pressures due to their long necks (although relatively longer necks are found in other sauropods), and anterior CoM. Vertical forces experienced by the forelimbs would also be more severe in titanosauriformes due to more anterior CoM positions (Bates et al., 2016; Klinkhamer et al., 2019).

The unusual body plan of sauropods is potentially an unsolvable problem for studies of this kind. Their sheer size as a terrestrial animal, and their unusual body plan – with their long necks and tails, are unmatched by any extant analogues. These animals however, can only be studied with the tools, and modern analogues, available. How they can be biomechanically analysed with their unique biology is a perhaps useful test for how reliably the anatomy and mechanics of extinct animals in general can be understood (Currie, 2018).

The hypothesis of heteropody as a pressure equalisation mechanism then, is not supported based on extant data. Even if it is employed within certain functional groups or clades not studied here, it is not a universal mechanism.

Chapter 7

Does the Fossil Record of Dinosauria Suggest the Use of Extreme Heteropody as an Underfoot Pressure Equalisation Mechanism?

7.1 Summary of Chapter

This chapter sought to investigate a possible link between centre of mass position and heteropody in non-avian dinosaurs, particularly sauropodomorphs. No link was found between centre of mass position and heteropody across Dinosauria through osteological analysis using skeletons, a finding consistent with previous chapters. However, the necessarily small sample size does not lend itself towards a definitive conclusion. There was also no marked shift in the presence of heteropody in the body fossil record through geological time.

Fossil trackways demonstrated two spikes in heteropody in sauropodomorph dinosaurs, as would be expected if heteropody and centre of mass position were functionally linked. However, these spikes are associated with spikes in fossil trackway sampling, rather than with anterior shifts in centre of mass position during sauropodomorph evolution as described in (Bates et al., 2016) and are, notably, 40-50 million years removed from the two CoM shifts, making a link between CoM shifts and heteropody spikes very unlikely.

7.2 Background for Heteropody and Pressure Equalisation in Palaeobiology

Heteropody, the ratio of manus to pes underfoot area (Lockley et al., 1994a), is a useful metric to the study of fossil trackways, as the size and shape of a footprint should, in theory, reflect the ground contact area of the underside of an animal's foot. However, footprint size and shape is not a pure reflection of a trackmaker's anatomy (Padian and Olsen, 1984a; Minter et al., 2007; Falkingham, 2014). Typically, and herein, heteropody is measured using 'heteropody index': manus foot contact area as a percentage of pes foot contact area (Riga and Calvo, 2009) (Equation 1).

Pressure equalisation is an important factor to consider in the stability and biomechanical structure of animals. The weight of an animal during standing, or during locomotion, exerts pressures on the limbs, and especially the feet, that can lead to long term damage over time, particularly in animals with large masses, such as elephants and rhinoceroses (Michilsens et al., 2009; Panagiotopoulou et al., 2016; Panagiotopoulou et al., 2019). To counter this stress, animals can evolve mechanisms to offset, or spread out pressure, evening out loads across the foot, as demonstrated by the presence of foot pads in many animals (Chi and Schmitt, 2005; Chi and Roth, 2010; Barbera et al., 2019), and the larger and more elaborate fatty foot pads present in elephants (Hutchinson et al., 2011). In dinosaurs, although the presence of pneumaticity within the bones might somewhat reduce mass (Zurriaguz and Cerda, 2017), the large size of many of these animals makes it likely that mechanisms to reduce excess pressures underfoot would have evolved to cope with these pressures and prevent damage over time. These adaptations include theorised fatty foot pads in sauropod dinosaurs (Jannel et al., 2019), and their upright posture, compared to other diapsids such as lizards (Kubo and Benton, 2007).

Previous explanations for the phenomenon of extreme heteropody have posited its potential as a mechanism to equalise pressure, offsetting potential excess stress caused by unusually anterior centre of mass positions in some sauropod species (Henderson, 2006; Falkingham et al., 2012). These explanations hypothesise that a condition of equal sized autopodia is beneficial in animals with centre of mass positions around the centre of the trunk. Inversely, where mass is distributed more anteriorly, or posteriorly, along the trunk, a larger manus or pes, respectively, is beneficial, resulting in more equal pressure under each foot despite an offset centre of mass. It is possible that this is the reason for the extreme heteropody found in many sauropod trackways (Falkingham, et al., 2012). This could be demonstrated by observing a clear link between heteropody and underfoot pressure or CoM in these dinosaurs, for example, CoM positions closer to the hip in the most extreme cases of extreme heteropody – indicating a trend towards pressure equalisation. This hypothesis is complicated by the possibility that manus-only sauropod trackways could have been formed by sauropods with high underfoot pressure under the

manus compared to the pes (Falkingham et al., 2010; Falkingham et al., 2012). Pes-only trackways may have been formed in a similar way, but could also have been formed by overprinting (Milàn and Hedegaard, 2010; Falkingham et al., 2010; Lockley et al., 2012; Xing et al., 2016a). Alternatively, manus-only trackways could have been formed while swimming or punting against a submerged substrate (Bird, 1944; Huh et al., 2003; Lee and Lee, 2006). Both explanations are disputed, and the subject of ongoing debate. If high underfoot pressure under the manus is the main driver of manus-only trackway creation, it is unlikely that pressure equalisation via changes in heteropody is happening in these organisms, or at least that it is happening to the point that it makes a noticeable difference to differential underfoot pressures between manus and pes.

7.2.1 Factors in Footprint Formation

Footprints are traces that act as reflections of the gait of an animal, interacting with a substrate at a particular point in time. Studying how the feet of extant animals interact with substrates of different mechanical compositions *in situ* (Brand, 1996; Padian and Olsen, 1984a;b; Hatala et al., 2013), as well as in simulations (Margetts et al., 2006; Bates et al., 2013; Falkingham and Gatesy, 2014), can provide a useful model of how fossil trackways were formed. Importantly, composition of geological formations can inform the type of substrate underfoot during trackway formation. Knowledge of these factors improves understanding of the confounding factors leading to the eventual shape of a fossil footprint, and how it both reflects and distorts the underfoot anatomy of its trackmaker (Buatois and Mángano, 2004; Razzolini et al., 2014).

According to (Minter et al., 2007), building on work by (Baird, 1957; Padian and Olsen, 1984a), trace fossil formation is driven by three influences: behaviour, producer, and substrate, which can be represented as a Venn diagram, with the interactions between these three influences (eg. substrate and behaviour = sediment mechanics), leading to the myriad of differences between trace fossils, and how they are formed and preserved. This concept was reinterpreted in (Falkingham, 2014), as a three dimensional graph, with anatomy, dynamics, and substrate as the three primary drivers of track morphology. In

this model, if a substrate is consistent across a number of track traces, track morphology varies based on the disparate anatomy or dynamics of the trackmaker, with similar inferences for consistency across the other two axes (Figure 7.1).

This is important to note, as it is tempting when looking at ichnofossils from a biologist's perspective to assume a one to one relationship between the shape of a trackmaker's foot and the resultant footprint, and from a sedimentologist's perspective to overstate the role of the underlying substrate, when anatomy, and gait dynamics, are equally crucial factors (Hatala et al., 2013; Gatesy and Falkingham, 2017).

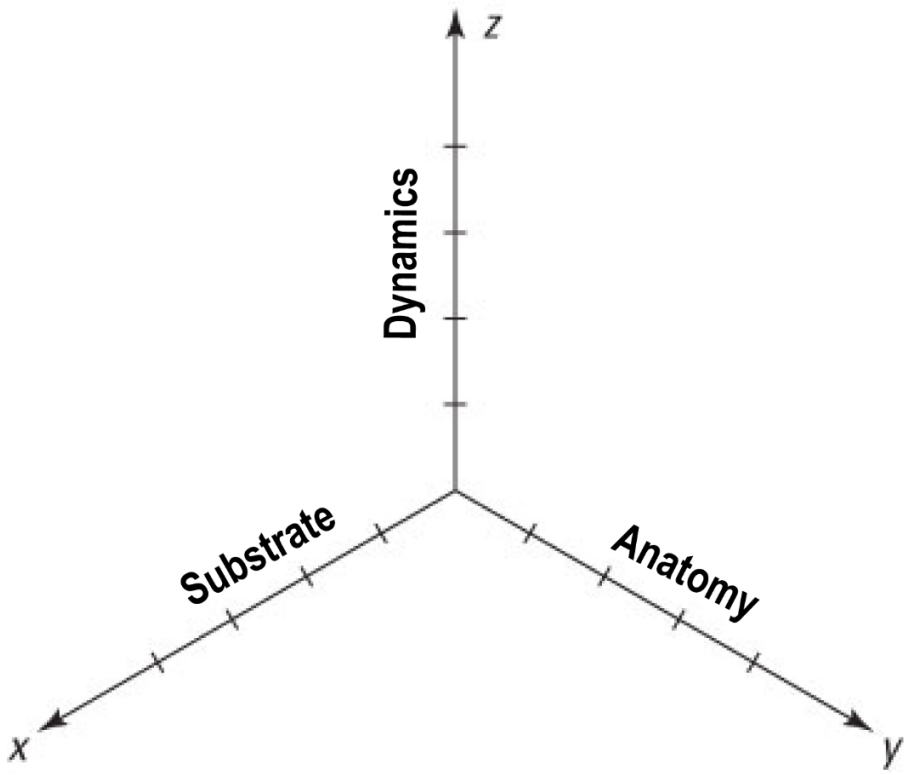

Figure 7.1 A visual representation of the three-dimensional graph proposed by Falkingham (2014) to demonstrate the three fundamental factors in footprint formation.

7.2.2 Extreme Heteropody and Manus-Only Trackways as Phenomena

Extreme forms of heteropody are relatively rare in extant, quadrupedal taxa, especially among cursorial animals (as demonstrated in chapters 4 and 6). Extant animals with pronounced heteropody are most often animals that specialise in non-cursorial forms of locomotion, with heteropody often accompanied by differences in posture - i.e. frogs, rabbits and kangaroos, specialised for hopping, and beavers, for swimming (see chapter 4). Extreme heteropody is perhaps more common in the fossil record, with sauropod dinosaurs being an example of a group in which extreme heteropody is common, and one where all species appear fully terrestrial and ill-suited for hopping or digging.

Manus-dominated trackways have been attributed to both wide- and narrow-gauge trackmakers (they are preserved where only the manus exerts enough pressure to leave an impression in substrate). It has been hypothesised the formation of these trackways may be related to more anterior centre of mass positions in their trackmakers (Vila et al., 2005; Falkingham et al., 2010).

Wide gauge trackways are most often attributed to derived macronarian sauropods, many of them titanosauriforms, the only sauropod group to survive up until the K-Pg mass extinction event 66 million years ago (Lee and Lee, 2006; Castanera et al., 2011; Mannion and Upchurch, 2011; Vila et al., 2012).

7.2.3 Centre of Mass and Convex Hulls

Many previous studies have focused on producing centre of mass data for non-avian dinosaurs, with the aim of giving context to postural transitions, such as reversions to quadrupedality in ornithischian dinosaurs (Maidment et al., 2014), and shifts towards avian posture in derived theropods (Allen et al. 2013), and to investigate locomotory ability (Henderson, 2004; Alexander, 2006). The findings of Bates et al. (2016) are important to consider for the context of this chapter, finding two significant shifts in centre of mass across sauropodomorph evolution, with the evolution of quadrupedalism, and the evolution of titanosauriforms, both associated with elongation of the neck. If heteropody and CoM position are functionally linked, there could be similar shifts occurring in

sauropod heteropody to match – namely shifts away from extreme heteropody, towards more even sized manus and pes, which would presumably be observable in fossil trackway evidence.

7.2.4 Aims

This chapter aims to identify potential links between heteropody and CoM position in sauropod dinosaurs using the fossil record. This is attempted in two ways: by examining heteropody in sauropodomorph trace fossils, and how it compares to known trends in CoM position in this clade, and by examining preserved manus/pes pairs in dinosaur body fossils where CoM position estimates are available. If, as previously hypothesised, shifts in heteropody in sauropod dinosaurs are reflections of a pressure equalisation mechanism, their trackway data should indicate two major shifts away from heteropody. This would be consistent with the CoM positions shifts demonstrated in Bates et al. (2016). Such a trend could also be expected from body fossil evidence. If this were the case however, its signal would likely be muted due to manus-pes differences in soft tissue extent, as demonstrated in Chapters 2 and 6.

7.3 Methods for Examining Heteropody and Its Implications in the Fossil Record

Since all quadrupedal members of the clade Dinosauria are extinct, no *in vivo* data can be gathered to test differences in manus and pes pressures, vertical forces, or contact areas, during locomotion, nor heteropody in a static position. Nor are sufficient soft tissue remains available to aid in estimations of centre of mass data. Despite this, there is a wealth of literature describing the anatomy of dinosaur body fossils in detail, along with comprehensive descriptions of trace fossils. These data partly reflect the behaviour and biomechanics of extinct organisms, such as dinosaurs, *in vivo.* Unfortunately, finding articulated manus and pes for any dinosaur is a rare occurrence (Bonnan, 2003; 2005; Bedell Jr. and Trexler, 2005). Therefore the body fossil dataset for this study is small. Fossil trackways containing preserved manus and pes prints from dinosaurs are much more common, and a useful resource for observing heteropody. However, assigning trackmakers to fossil trackways is a difficult task (Lockley et al., 1994b; Smith and Farlow,

2003; Castanera et al., 2013). To keep the trackway analysis portion of this study less dependent on the distinctions between trackmakers, only heteropody measures from sauropodomorph trackways were collected, with distinctions made only between macronarian and diplodocid trackmakers.

7.3.1 Methods Involving Body Fossils

To examine any possible correlation between heteropody and centre of mass position in non-avian dinosaurs, a similar technique as employed in chapter 3 was used. In that chapter, manus and pes underfoot area was estimated by multiplying the maximum width of the foot at the carpals/tarsals (the wrist/ankle joint) with 'functional foot length', corresponding to the foot posture of the animal in question. In the case of Dinosauria, the current evidence points to the majority of non-avian dinosaurs being functionally digitigrade (Carrano, 1997; Sereno, 1997). The possible exception to this rule is derived sauropod dinosaurs, who most likely possessed a semi-digitigrade pes with a fatty foot pad to help deal with excessive stress. Similar structures are found in the foot anatomy of modern elephants, which, in terms of their interactions with substrate, are functionally plantigrade, despite their osteology (Hutchinson et al., 2011; Jannel et al., 2019).

The lengths and widths of the skeletal elements of the manus and pes of dinosaurs with both sets of autopodia preserved were taken, and the length of the longest digit in each, where both elements were preserved, was multiplied by the maximum width at the carpals/tarsals. Of the available data, 7 were sauropodomorphs (5 of which were sauropods), 3 were thyreophorans, and 3 were ornithopods. The sample size was small due to lack of preserved, articulated manus and pes for quadrupedal dinosaurs, outside of composites.

Digit length was obtained through figures, photographs, and diagrams from the literature for each specimen, from sources from the literature are outlined in Table 7.1.

Heteropody index was then calculated (manus underfoot area, as a percentage of pes underfoot area) (Riga and Calvo, 2009). In chapter 4, no correlation was found between heteropody and centre of mass position using these methods, except for in semi-aquatic

animals. However, despite the terrestriality of non-avian dinosaurs, evidence from fossil trackways suggests a higher prevalence in extreme heteropody among dinosaurs than in the extant taxa tested in chapter 4, in which case they might prove to show correlation, as semi-aquatic animals did. It may also highlight differences between foot contact area with the ground, and underfoot area of the foot as measured osteologically.

Centre of mass data was also gathered using sources from the literature (Table 7.1) (Henderson, 2006; Allen et al., 2013; Maidment et al., 2014; Bates et al., 2016). In addition to these sources, centre of mass values for *Iguanodon, Edmontosaurus, and Tenontosaurus* were calculated as in chapter 3, using laser scans retrieved from a previous study (Sellers et al., 2012), reposed into a neutral position, and combined whole-body convex hulls. It is important to consider that collating CoM values derived using three different methods is potentially dubious, especially considering some of the surprising findings of Maidment et al., regarding thyreophoran CoMs. However, this study is limited by the scope of the data available, while any findings as a result of this collation of methods should be interpreted with extra scepticism.

Table 7.1 Osteological data for dinosaurs where whole body CoM and manus/pes lengths were available, with references.

Taxon	CoM (% G-A Distance from hip)	HI (manus as % of pes)	CoM Value Reference	Manus/Pes Dimensions Reference
Lufengosaurus	31.20	25.76	(Bates et al., 2016)	(Young, 1941; 1947)
Plateosaurus	11.30	173.43	(Henderson, 2006)	(Farlow and Brett-Surman, 1999)
Apatosaurus	30.40	36.00	(Henderson, 2006)	(Farlow and Brett-Surman, 1999)
Brachiosaurus	37.40	28.43	(Henderson, 2006)	(Falkingham, 2010)
Diplodocus	11.50	45.80	(Henderson, 2006)	(Falkingham, 2010)
Camarasaurus	30.90	93.00	(Henderson, 2006)	(Tschopp et al., 2015)
Shunosaurus	27.40	201.27	(Henderson, 2006)	(Weishampel et al., 2007)
Edmontosaurus	26.80	43.03	Original Calculation	(Farlow and Brett-Surman, 1999)
Iguanodon	29.92	11.48	Original Calculation	(Farlow and Brett-Surman, 1999)
Tenontosaurus	21.95	118.11	Original Calculation	(Farlow and Brett-Surman, 1999)
Scelidosaurus	21.00	42.75	(Maidment et al., 2014)	Photo Reference
Euoplocephalus	19.00	127.91	(Maidment et al., 2014)	(Coombs Jr, 1986)
Stegosaurus	4.00	78.34	(Maidment et al., 2014)	(Weishampel, et al., 2007)

Where both heteropody and centre of mass values could be derived using the above methods, centre of mass was plotted against heteropody for 18 taxa, with heteropody index recorded for 31 taxa. Articulated manus and pes non-avian dinosaur fossils are rarely found for the same specimen, so a small sample size was to be expected. Age data for the taxa in question were gathered using Paleodb (Uhen et al., 2013).

7.3.2 Methods Involving Trace Fossils

To examine heteropody in fossil footprints, papers published on sauropod fossil trackways where both manus and pes imprints were preserved were collected to determine heteropody over geological time, for sauropodomorphs, macronarian sauropodomorphs, and diplodocid sauropodomorphs. These data were not compatible with collected centre of mass data due to difficulties assigning tracks to trackmakers. However, by tracking heteropody in fossil trackways through time, it should be possible to observe whether there are major shifts in heteropody in sauropods concurrent with shifts in sauropod CoM position, as observed in Bates et al. (2016), (Figure 7.2) which would suggest heteropody and CoM position are functionally linked. In addition, it is possible to observe heteropody in quadrupedal sauropodomorphs across temporal and, to some extent, phenotypic, distance from their bipedal ancestors. If this is the case, in data for all sauropodomorphs, there should be a shift in heteropody with the evolution of, and proliferation of, quadrupedal sauropods, and a second shift should be visible in data for all sauropodomorphs, and in data for macronarians, which is absent in data for diplodocids, as it is associated with the evolution of, and proliferation of, titanosauriforms.

Manus and pes data for individual trackways were collected, and the average manus length and width per trackway was used to determine heteropody index, as described above, in section 7.2.1. Age data for each trackway was gathered from the individual papers describing the trackways and their sites and were binned into time units of 5 million years each.

Since manus and pes data are both necessary for this analysis, this data does not account for the presence of manus-only, or pes-only trackways. While this may result in

some obfuscation of the true range of heteropody in Sauropodomorpha, manus-only trackways do not necessarily indicate extreme heteropody in and of themselves, since many manus-dominated trackways with faint pes impressions have relatively even manus/pes area (Lee and Huh, 2002; Falkingham et al., 2012).

A database of 136 sauropodomorph trackways was assembled, where manus and pes data for the trackway were available with which to calculate heteropody index, representing a spread of disparate geological eras and sauropod ichnotaxa, of which 93 were identified as macronarians, and 32 as diplodocids. These data were collected using the studies outlined in Table 7.2

These results were plotted alone as well as against those of Bates et al. (2016), both raw taxon values and ancestral states estimations, to compare and contrast how CoM and heteropody changed in sauropodomorphs over time (Figure 7.2).

To account for potential sampling bias, diversity curves for sauropod dinosaurs and the ichnotaxa analysed in this study alone were created using data from Paleodb (Uhen, et al., 2013) (Figure 7.5). In addition, heteropody results for sauropod trackways were plotted alongside number of trackways sampled and range of results to make the diversity of results, and effect of sampling, transparent (Figure 7.6).

Table 7.2 Trackways used for analysis in this chapter, with their assigned ichnotax, age in millions of years, heteropody index (manus area as percentage pes area), and their reference from the literature.

Ichnotaxon	Age (Ma)	HI (Manus as % Pes)	Reference
Polyonyx	142	41.07	(Fernández-Baldor et al., 2015)
Polyonyx	142	40.34	(Fernández-Baldor et al., 2015)
Misc. Sauropod	168.5	15.44	(Barnes and Lockley, 1994)
Breviparopus	167.2	25.25	(dePolo et al., 2018)
Misc. Titanosaurid	72.1	39.67	(Bates et al., 2008)
Misc. Titanosaurid	72.1	47.82	(Bates et al., 2008)
Misc. Titanosaurid	72.1	41.27	(Bates et al., 2008)
Misc. Sauropod	119	29.17	(Casanovas et al., 1997)
Sauropodichnus giganteus	142	40.23	(Castanera et al., 2011)
Sauropodichnus giganteus	142	43.18	(Castanera et al., 2011)
Sauropodichnus giganteus	142	33.54	(Castanera et al., 2011)

Sauropodichnus giganteus	142	44.25	(Castanera et al., 2011)
Misc. Sauropod	142.4	31.84	(Castanera et al., 2012)
Misc. Sauropod	142.4	27.89	(Castanera et al., 2012)
Brontopodus pentadactylus	106.75	61.07	(Kim and Lockley, 2012)
Brontopodus pentadactylus	106.75	66.10	(Kim and Lockley, 2012)
Misc. Titanosaurid	69.05	39.30	(Lockley et al., 2002)
Brontopodus	154.7	32.17	(Marty et al., 2010)
Parabrontopodus	154.7	17.07	(Marty et al., 2010)
Misc. Sauropod	154.7	31.49	(Marty et al., 2010)
Misc. Sauropod	154.7	48.36	(Marty et al., 2010)
Breviparopus taghbaloutensis	157.8	16.79	(Marty et al., 2010)
Breviparopus taghbaloutensis	157.8	19.82	(Marty et al., 2010)
Titanopodus mendozensis	72.1	32.36	(Riga and Calvo, 2009)
Brontopodus	112.75	18.63	(Xing et al., 2014)
Brontopodus	112.75	42.83	(Xing et al., 2014)
Brontopodus	112.75	40.15	(Xing et al., 2014)
Brontopodus	112.75	44.36	(Xing et al., 2014)
Brontopodus	112.75	32.99	(Xing et al., 2014)
Brontopodus	112.75	35.19	(Xing et al., 2014)
Brontopodus	112.75	25.25	(Xing et al., 2015a)
Liujianpus shunan	187.7	35.88	(Xing et al., 2016c)
Liujianpus shunan	187.7	43.18	(Xing et al., 2016c)
Brontopodus	187.7	38.55	(Xing et al., 2016c)
Parabrontopodus	106.75	43.80	(Xing et al., 2017)
Misc. Sauropod	187.7	25.25	(Xing et al., 2016d)
Misc. Sauropod	187.7	30.67	(Xing et al., 2016d)
Misc. Non-Titanosauriform Macronarian	142.4	31.84	(Arribas et al., 2008)
Misc. Prosauropod	186.75	30.87	(Avanzini et al., 2001)
Lavinipes cheminii	199.3	35.63	(Avanzini et al., 2003)
Misc. Macronarian	66	23.88	(Diaz-Martinez et al., 2018)
Elephantopoides	152.4	32.62	(Diedrich, 2011)
Elephantopoides	152.4	42.03	(Diedrich, 2011)
Elephantopoides	152.4	33.22	(Diedrich, 2011)
Elephantopoides	152.4	33.17	(Diedrich, 2011)
Elephantopoides	152.4	39.02	(Diedrich, 2011)
Elephantopoides	152.4	18.42	(Diedrich, 2011)
Elephantopoides	152.4	39.93	(Diedrich, 2011)
Elephantopoides	152.4	18.77	(Diedrich, 2011)
Titanopodus mendozensis	72.1	40.35	(Riga et al., 2015)
Titanopodus mendozensis	72.1	31.58	(Riga et al., 2015)
Misc. Brachiosaurid	112.75	96.34	(Hwang et al., 2004)
Misc. Brachiosaurid	112.75	66.11	(Hwang et al., 2004)
Misc. Brachiosaurid	112.75	69.59	(Hwang et al., 2004)
Misc. Brachiosaurid	112.75	66.04	(Hwang et al., 2004)
Misc. Brachiosaurid	112.75	71.04	(Hwang et al., 2004)
Misc. Brachiosaurid	112.75	55.98	(Hwang et al., 2004)
Misc. Brachiosaurid	112.75	66.96	(Hwang et al., 2004)
Misc. Brachiosaurid	112.75	57.36	(Hwang et al., 2004)
Misc. Brachiosaurid	112.75	50.59	(Hwang et al., 2004)
Misc. Brachiosaurid	112.75	68.41	(Hwang et al., 2004)
Parabrontopodus	148.55	45.31	(Le Lœuff et al., 2006)

Parabrontopodus	148.55	37.42	(Le Lœuff et al., 2006)
Parabrontopodus	148.55	26.03	(Le Lœuff et al., 2006)
Parabrontopodus	148.55	37.56	(Le Lœuff et al., 2006)
Parabrontopodus	148.55	42.22	(Le Lœuff et al., 2006)
Parabrontopodus	148.55	40.68	(Le Lœuff et al., 2006)
Misc. Titanosaurid	93.9	58.09	(Martin et al., 2017)
Misc. Sauropod	93.9	29.71	(Martin et al., 2017)
Parabrontopodus	150.275	28.17	(Marty et al., 2013)
Parabrontopodus	150.275	31.49	(Marty et al., 2013)
Brontopodus plagnensis	150.275	47.10	(Mazin et al., 2017)
Parabrontopodus	157	28.20	(Mazin et al., 2016)
Brontopodus	157	48.77	(Mazin et al., 2016)
Misc. Sauropod	157	38.96	(Mazin et al., 2016)
Brontopodus	157	59.58	(Mazin et al., 2016)
Misc. Sauropod	157	22.11	(Mazin et al., 2016)
Parabrontopodus/Breviparopus	157	25.75	(Mazin et al., 2016)
Misc. Sauropod	157	56.93	(Mazin et al., 2016)
Misc. Sauropod	157	36.00	(Mazin et al., 2016)
Misc. Sauropod	157	26.13	(Mazin et al., 2016)
Misc. Sauropod	157	58.84	(Mazin et al., 2016)
Misc. Sauropod	157	30.43	(Mazin et al., 2016)
Misc. Sauropod	157	52.67	(Mazin et al., 2016)
Misc. Sauropod	157	46.70	(Mazin et al., 2016)
Parabrontopodus/Breviparopus	157	23.80	(Mazin et al., 2016)
Misc. Sauropod	157	51.71	(Mazin et al., 2016)
Misc. Sauropod	157	46.60	(Mazin et al., 2016)
Brontopodus	89.8	45.37	(Mezga et al., 2006)
Brontopodus	89.8	18.72	(Mezga et al., 2006)
Brontopodus	146.775	30.41	(Mezga et al., 2007)
Parabrontopodus	106.75	20.61	(Moratalla, 1994)
Titanopodus	72.1	38.87	(Riga and Tomaselli, 2019)
Titanopodus	72.1	32.11	(Riga and Tomaselli, 2019)
Titanopodus	72.1	42.91	(Riga and Tomaselli, 2019)
Misc. Sauropod	106.75	27.27	(Santos et al., 2015)
Misc. Sauropod	168.3	24.27	(Wagensommer et al., 2012)
Brontopodus	113	52.59	(Xing et al., 2013)
Parabrontopodus	113	58.95	(Xing et al., 2013)
Brontopodus	100.5	58.95	(Xing et al., 2015b)
Brontopodus	100.5	58.34	(Xing et al., 2015b)
Brontopodus	100.5	29.08	(Xing et al., 2015b)
Parabrontopodus	122.75	25.69	(Xing et al., 2015c)
Parabrontopodus	122.75	23.30	(Xing et al., 2015c)
Brontopodus	112.5	61.22	(Xing et al., 2015b)
Parabrontopodus	145.5	41.12	(Xing et al., 2015d)
Misc. Titanosaurid	145.5	39.68	(Xing et al., 2015d)
Misc. Titanosaurid	145.5	49.91	(Xing et al., 2015d)
Misc. Titanosaurid	113	31.33	(Xing et al., 2015e)
Brontopodus	112.5	41.89	(Xing et al., 2016e)
Brontopodus	159.55	33.94	(Xing et al., 2016b)
Brontopodus	159.55	45.65	(Xing et al., 2016b)
Misc. Titanosauriform	113	41.97	(Xing et al., 2016f)

Misc. Titanosauriform	113	58.20	(Xing et al., 2016f)
Misc. Titanosauriform	113	39.50	(Xing et al., 2016f)
Parabrontopodus-like	106.75	43.80	(Xing et al., 2017a)
Brontopodus	187.7	35.32	(Xing et al., 2019a)
Parabrontopodus	105	18.62	(Xing et al., 2018)
Parabrontopodus	105	22.71	(Xing et al., 2018)
Brontopodus	105	68.00	(Xing et al., 2018)
Brontopodus	105	48.37	(Xing et al., 2019b)
Brontopodus	105	32.96	(Xing et al., 2019b)
Brontopodus	90.1	37.57	(Xing et al., 2019c)
Brontopodus	90.1	43.66	(Xing et al., 2019c)
Brontopodus	90.1	31.93	(Xing et al., 2019c)
Brontopodus	90.1	36.46	(Xing et al., 2019c)
Brontopodus	90.1	36.90	(Xing et al., 2019c)
Brontopodus	90.1	42.85	(Xing et al., 2019c)
Brontopodus	122.25	34.03	(Zhang et al., 2006)
Sauropodichnus giganteus	119	34.48	(Meyer et al., 2018)
Brontopodus	125	45.45	(Meyer et al., 2018)
c.f. Brontopodus	69.05	33.33	(Meyer et al., 2018)
Rotundichnus	154.6	27.78	(Meyer et al., 2018)
Rotundichnus	142.4	29.41	(Meyer et al., 2018)
Brontopodus	125	41.67	(Meyer et al., 2018)
Calorckosauripus	69.05	54.05	(Meyer et al., 2018)

7.4 Results

7.4.1 Trace Fossil Analysis

Analysis of sauropodomorph trackways demonstrated a great deal of diversity in heteropody, particularly in trackways assigned to macronarian trackmakers, ranging from almost equal sized manus and pes, to manus of ~15% pes size (with diplodocid-assigned trackmakers showing a range of ~17-60% manus size as % pes size) (Table 7.1).

Data did not appear to closely match that of Bates et al (2016), either with ancestral states estimations, or with raw taxon data. Despite two apparent peaks in heteropody reduction in the dinosaur track data, these peaks were greatly temporally offset from the anterior CoM shifts found by Bates et al, are linked with known sampling bias, and do not show any indication that these two variables are linked (Figure 7.2).

Figure 7.2 Estimated centre of mass trends (gleno-acetabular distance in front of the hip) over geological time in sauropodomorphs (and outgroups), showing major CoM shifts across sauropodomorph evolution, based on centre of mass estimates from 3D convex hulls of mounted skeletons (from Bates et al., 2016), overlaid with sauropodomorph trackway data collected in this chapter (green dots). Above – Estimated evolutionary patterns based on taxon data and calculated ancestral states versus trackway data. Below – Raw taxon values versus trackway data.

Linear models of heteropody over time for individual trackways showed R^2 = 0.05 for all sauropodomorpha, 0.02 for macronarian-assigned ichnotaxa, and 0 for diplodocid assigned taxa (Figure 7.3). The linear model for individual trackways for all sauropodomorphs was significant, where no other analyses were (Figures 7.3 and 7.4). Taking the mean of heteropody results for time bins of 5Ma (from 66Ma backwards) as linear models resulted in R^2 = 0.15 for all sauropodomorpha, 0.16 for macronarians, and 0.05 for diplodocids. These results imply no overall increase or decrease in heteropody over time, as might be expected if heteropody decreased or increased with phylogenetic and temporal distance from the bipedal ancestors of sauropodomorphs. Instead, increases in diversity of heteropody results, accompanied by peaks in heteropody index results are observable at ~160 and ~110 Ma, indicating lowering heteropody at these points. However, the periods in which these peaks occur are coincide with the largest number of samples per time bin, both in terms of those trackways analysed in this study, and fossil trackway samples in general (Figures 7.5 and 7.6). Since the timing of these sampling and heteropody peaks are so similar, sampling error is likely the reason for these apparent peaks, and not the anterior shifts in CoM found in Bates et al (2016), which are offset by millions of years.

Peaks at ~160 and ~110 Ma are most prominent in macronarian-assigned taxa, at averages of ~42 and ~57% manus as % pes size, compared to ~38 and ~47% for all sauropodomorphs. This pattern is less clear in diplodocid-assigned ichnotaxa, where,

aside from one trackway from (Xing et al., 2013), which was obviously outlying at almost 60% manus size as % pes size, heteropody index remained between around 20-40%.

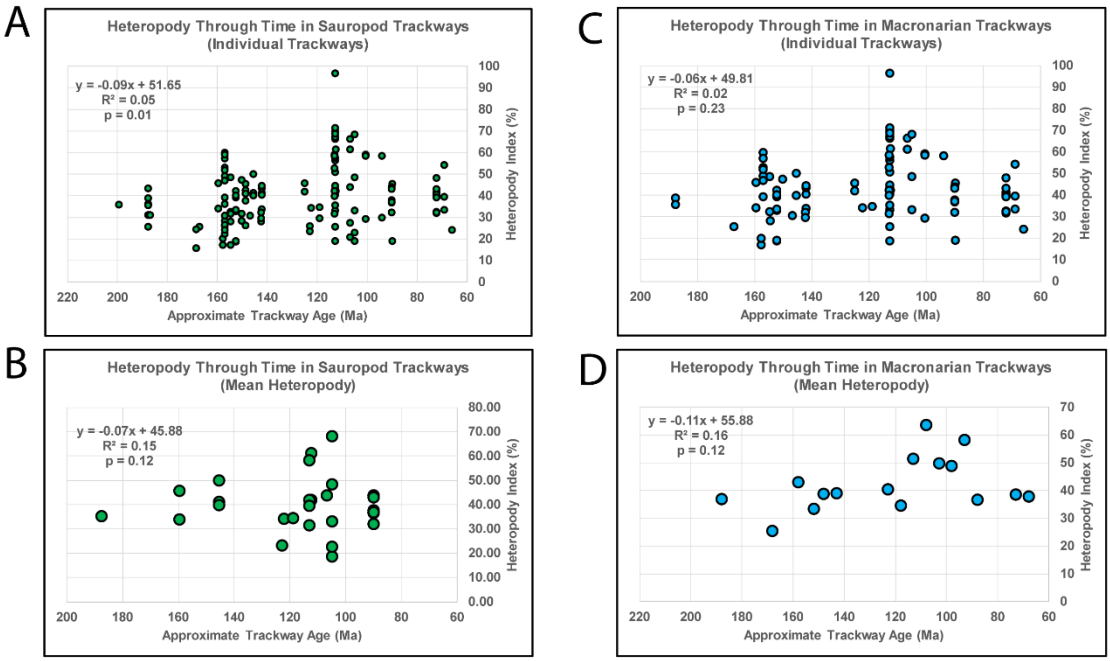

Figure 7.3 Trackway analysis results for sauropodomorphs. A – all individual trackways and linear model. B – trackways averaged by 5 Ma time bins and linear model data. C – individual trackways and linear model for macronarians. D – trackways averaged by 5 Ma time bins and linear model data for macronarians.

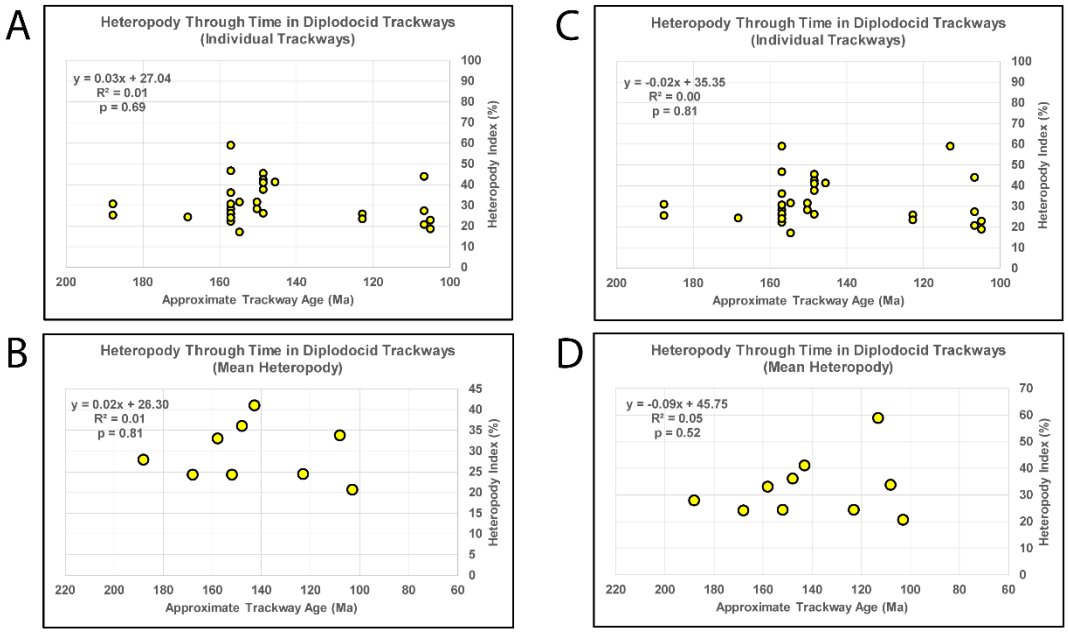

Figure 7.4 Trackway analysis results for diplodocid sauropodomorphs (A and B excluding Xing, et al., 2013). A and C – all individual trackways and linear model. B and D – trackways averaged by 5 Ma time bins and linear model data.

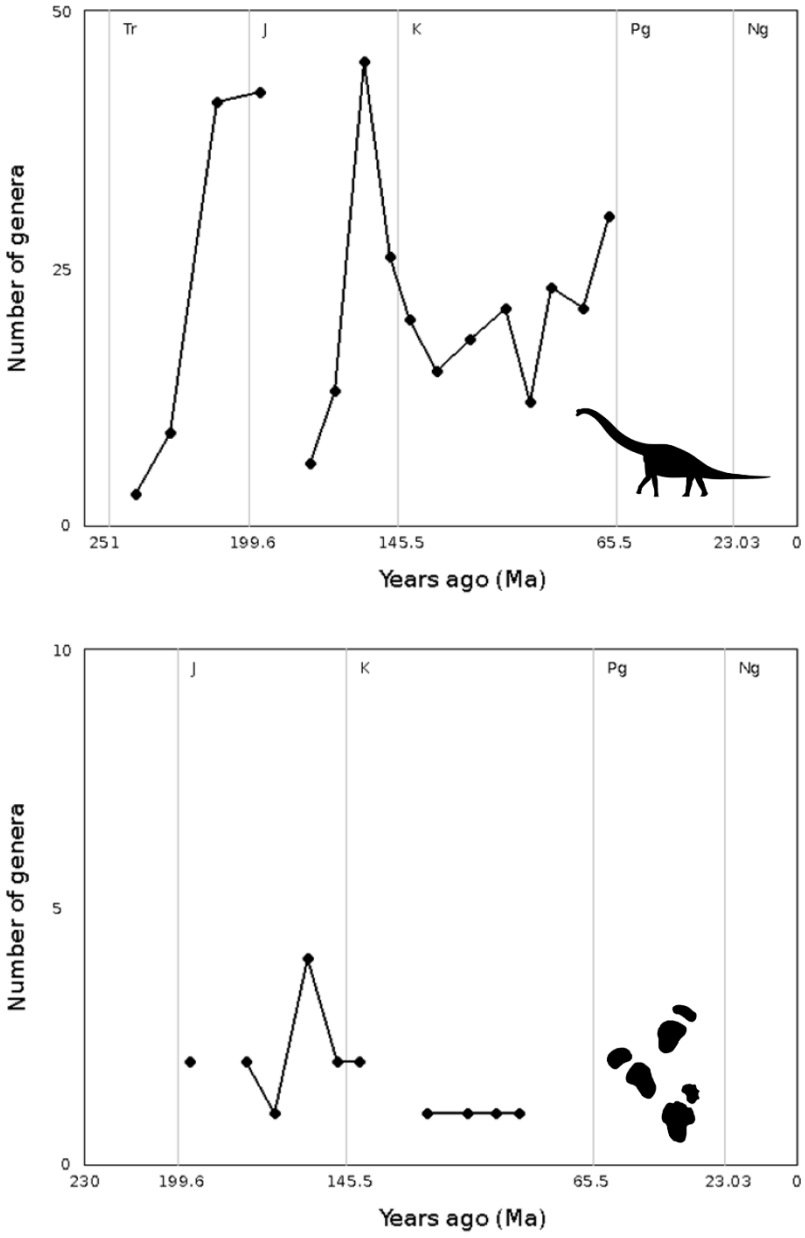

Figure 7.5 Taxa diversity in sauropodomorphs over time from total sauropod fossil diversity (above), and diversity of the ichnotaxa analysed in this chapter (below) to highlight possible sampling bias in the fossil footprint literature.

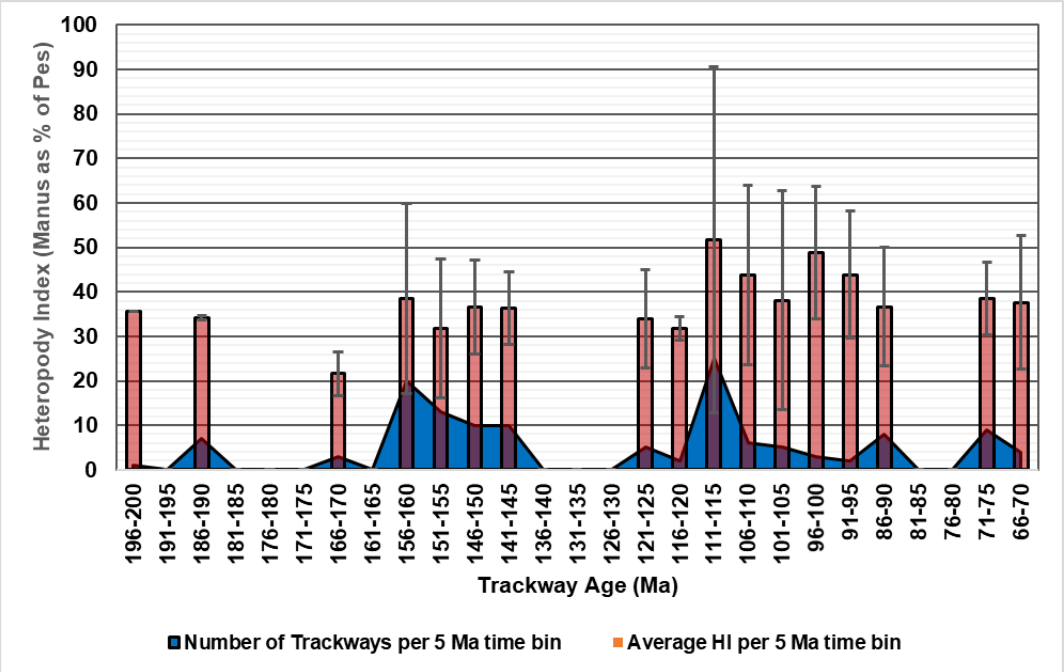

Figure 7.6 Heteropody in sauropodomorph trackways over time, plotted with number of samples per 5Ma time bin and error bars for range of heteropody values for each 5Ma time bin.

7.4.2 Body Fossil Analysis

For osteological analyses, weak correlations between centre of mass position and heteropody index were found for both quadrupedal dinosaurs in general, and sauropodormophs (R^2 = 0.11 and 0.14 including *Shunosaurus,* and 0.27 and 0.36 without *Shunosaurus,* respectively, none of which had p value <0.05) (Figure 7.7). From these correlations, ~10% of the data fits the hypothesis quadrupedal dinosaurs, especially sauropods, have a smaller manus compared to their pes associated with more anterior centre of mass positions. If the hypothesis were true, it would theoretically mean higher pressure in the manus is associated with more anterior CoM, which would rule out any universal pressure equalisation mechanisms at work. However, given the small sample size present, allowing for human error in measuring the feet, and the fact that this method only accounts for skeletal underfoot surface area, and not the entire *in vivo* extent of the foot, along with the weak correlations found, there are many reasons to doubt this result. In addition, the range of CoM positions seen across these data is small. In context of the

diversity of CoM positions in tetrapods, as seen in previous chapters, and not plotted as linear models, these results might not appear as unusual. This result could possibly become more pronounced, or the opposite, with more data, and more fossil discoveries. However, articulated manus and pes fossils are rare finds.

Of the manus and pes pairs used for this analysis, only 6 belonged to sauropodomorphs, and 5 to members of Sauropoda. Most notably, there were no titanosaurs with both manus and pes to analyse, (outside of composites of multiple specimens) which, in this analysis underrepresents the spread of extreme heteropody in the clade, as demonstrated by the trace fossil analysis in 7.4.1. In addition, *Shunosaurus* as an outlier in the data is noteworthy, given it possesses a shorter neck than many other sauropods as a plesiomorphic trait (Zheng, 1996; Henderson, 2013), and that changes in neck size were found to be associated with CoM position changes in sauropodomorphs in (Bates et al., 2016).

Figure 7.7 Scatter graphs showing linear model regressions for ost6ological analysis, with heteropody index against centre of mass position as a percentage of gleno-acetabular distance in front of the hip (excluding *Shunosaurus*). A – analysis with sauropodomorphs and ornithischians. B – analysis with ornithischians alone. C – analysis with sauropodomorphs alone.

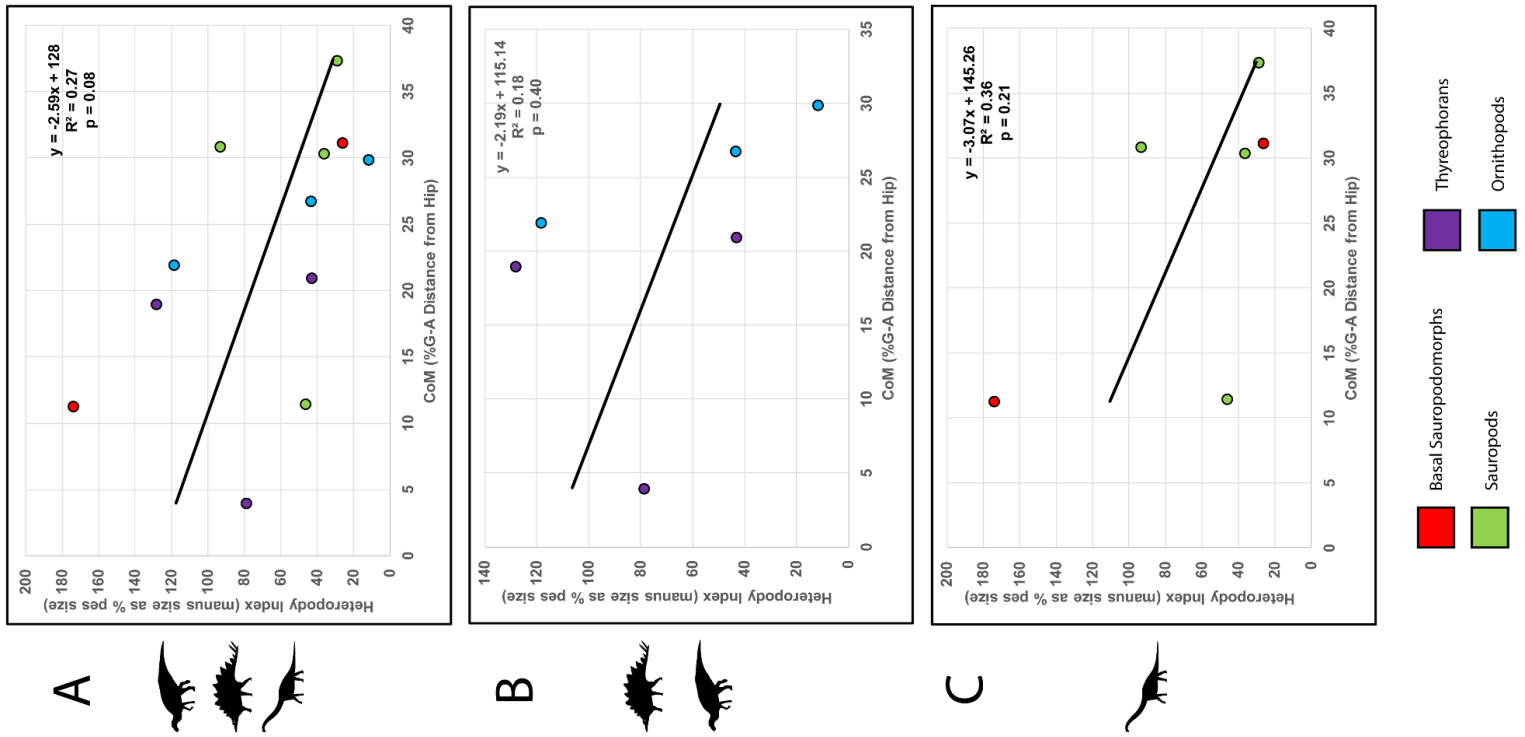

7.5 Discussion, Implications and Explanations of Dinosaur Analysis

The above evidence suggests no definitive trend between centre of mass position and heteropody in the osteology of Dinosauria. This makes sense given the findings of chapter 4, where tetrapods in general, showed no universal trend between these variables when looking at osteology. It is possible that a larger sample size, with representative numbers for different sauropodomorph clades would produce more compelling results. However, that is speculative, and previous chapters seem to suggest a more likely explanation, wherein osteological heteropody shows no clear link with centre of mass, with more of an effect visible from analyses that take account of soft tissue. In this way, the trackway analysis in this chapter could have potentially offered a more promising result in terms of establishing the presence/absence of a functional link between heteropody and centre of mass position. However, this does not appear to have borne out in the data, with no clear evidence for a functional link even in trackway data.

The result that two peaks in heteropody over geological time were found in this chapter's trackway analysis may at first suggest a result reflective of centre of mass shifts reported in Sauropodomorpha over time, in which two significant centre of mass shifts were recorded, coinciding with the onset of quadrupedality in sauropodomorphs, and the evolution of titanosauromorphs, with both shifts associated with increases in neck length (Bates et al., 2016). There is, however, 40-50 Ma between the reported shifts in CoM position in sauropodomorphs, and the two potential peaks in heteropody index found in this chapter. This could reflect on the time it took for quadrupedal sauropodomorphs, and titanosaurs, to proliferate enough in terms of numbers, diversity, and cosmopolitanism to leave more fossil trackways than other sauropodomorphs. However, there were enough body fossils being left for them to be known in the fossil record throughout this time. The peaks more likely reflects a preservation bias, supported by the diversity plots in Figure 7.5, and the close association between spikes in number of samples and heteropody shown in Figure 7.6. This sample biasing could potentially be exacerbated by the geographic distribution of titanosaurs versus other sauropodomorphs. Since it has previously been proposed that titanosaurs lived in inland, mountainous regions, compared

to a more coastal distribution for other sauropods (Mannion and Upchurch, 2010; 2011). Where these animals lived, and had potential to fossilise, could be influencing the strength of their signal in these data. However, poor preservation in mountainous regions also applies to osteology.

7.5.1 Potential Trackway Issues

Manus-only fossil trackways have been described by multiple teams, at multiple sites (Vila et al., 2005; Falkingham et al., 2010; Farlow et al., 2019). While their necessary absence from this study potentially downplays the diversity of manus track size in the fossil record, since the formation of these trackways is influenced by substrate, it can be assumed that these trackmakers have left other trackways in different substrates that are reflected in the data (Falkingham et al., 2010).

Pes-only trackways are necessarily absent from the data for the same reasons. However, since these trackways are potentially formed by animals overprinting on the manus with the pes (a behaviour recorded in extant animals when filming them with high speed cameras in previous chapters), animals that exhibit this behaviour regularly would possibly lack definitive preserved manus and pes prints in the fossil record, and therefore are perhaps less likely to be represented in the data than animals forming manus-only trackways (Zhang et al., 2006; Falkingham et al., 2010; Milàn and Hedegaard, 2010; Lockley et al., 2012; Xing, Li, Falkingham, et al. 2016).

In addition, since what is counted definitively as a manus or a pes print is dependent on assignments by individuals, there is a risk of manus and pes sizes being impacted by proximity, wherein a previous print may be distorted by the formation of the new one and the movement of the relevant substrate (Lockley et al., 2002; Schumacher and Lockley, 2014). This problem would also be more common in more compliant substrates, and as such can vary from trackway to trackway (Jackson et al., 2010; Razzolini, 2017).

7.5.2 Sauropod Foot Posture

It is worth noting that, while all dinosaurs were counted as digitigrade in the osteological potion of this study, the true foot posture of the sauropod pes is likely semi-digitigrade, with the existence of a fatty foot pad underneath the toes restricting movements, akin to that found in elephants (Platt and Hasiotis, 2006; Foster and Hunt-Foster, 2011; Hutchinson et al., 2011; Paik et al., 2017; Jannel et al., 2019).

This posture would render the sauropod pes 'functionally plantigrade'. However, since the extra support comes in the form of unpreserved soft tissue, rather than bone, using osteology to estimate foot size would not give an accurate estimate of sauropod foot size. At the same time, 'functionally plantigrade', and plantigrade, are rather different concepts, and not interchangeable. Since sauropods with this foot posture would still be walking on their digits, with added functional support, they were considered digitigrade, and measured as such (Carrano, 1997). Based on the research done in chapter 2 however, it appears that measuring heteropody via osteology underestimates heteropody, with the underfoot surface area of the manus *in vivo* larger than the underfoot surface area of the pes that would be expected based on osteology alone. In addition, *in vivo* analysis of heteropody showed more possibility of a functional link with centre of mass position than found looking at osteology alone. It is also likely that, as with the semi-digitigrade animals studied in Chapter 2, estimates of sauropod foot size would vary wildly with how the foot is posed. In this way, footprint evidence is vital to understanding the true surface area of sauropod feet. While using the formulae from Chapter 2 may produce a more accurate estimate of heteropody in this way, by adjusting for differences in soft tissue, it does not change the weakness of correlations found and thus an adjusted osteology results graph was not included in this chapter.

7.5.3 Cursoriality

In chapters 4 and 6, the tendency of cursorial mammals to retain largely equal-sized manus and pes, with associated centre of masses just anterior of the centre of the trunk was postulated, and evidence found to support this.

While bipedal dinosaurs, and therefore the ancestors of quadrupedal dinosaurs, were largely cursorial, quadrupedal dinosaurs retained few adaptations for cursoriality, and were more likely graviportal or mediportal (Coombs Jr, 1978; Carrano, 1999). Many of these dinosaurs retained a centre of mass position much closer to the hip than would be expected for a large, quadrupedal animal (Maidment et al., 2014).

In chapter 4, it was postulated that cursoriality prevents the ability of an animal to effectively utilise heteropody to equalise pressure in quadrupeds, as it would potentially be more advantageous to maintain relatively equal sized fore and hindfeet, potentially to keep propulsive/braking capabilities of the feet even, or for balance purposes. Cursorial animals tend to have digitigrade foot postures and reduced numbers of digits, as well as potentially fusing/reducing the bones of the wrist/ankle, which could serve to further restrict morphological disparity (Lull, 1904). This was not to say that any non-cursorial quadrupeds would equalise pressure in this way, rather that they would be freer from potential selective pressures not to do so. Sauropodomorpha as a clade would presumably have had greater selective pressures to equalise their underfoot pressures, due to their unprecedented body size and mass. However, this is not borne out in the data, suggesting that these animals found other solutions to this problem, perhaps reflected in their very different manus and pes foot postures, the effects of which, and how they evolved from bipedal hands and feet, will be a fruitful source of follow-up research to this thesis.

7.5.4 What Can Be Gleaned from Osteological Analyses

The lack of a definitive effect of CoM on heteropody seen in analyses of osteology, suggests several possibilities. First, this effect was small. Second, that the phenomenon of extreme heteropody is largely due to soft tissue differences between the manus and pes of these dinosaurs. Third, that there were other factors involved in influencing the disparity between manus and pes sizes, and spread of centre of masses found in the clade, outside of a biomechanical link between heteropody and centre of mass for pressure equalisation purposes. Fourth, some combination of the above.

If the lack of correlation between heteropody and centre of mass position were to remain the case with more evidence to hand, this would support the idea that dinosaurs do not use extreme heteropody as a pressure equalisation mechanism. In this case, there would be little selective pressure preventing the manus-pes underfoot pressure differences that would produce manus-only, and pes-only trackways naturally on land. This does not necessarily disprove the idea that these trackways were caused by swimming, or punting, sauropods, but would instead make the presupposition of aquatic locomotory habits less necessary for explaining the presence of these trackways. This would potentially be an interesting result, but is somewhat contradicted by the results of the trackway analysis in this chapter.

With more fossil discoveries, a link between CoM position and heteropody could potentially be found using the same methods as this chapter. This possibility is given validity by the absence of a representative sample of sauropods in the osteological analysis, in particular a complete absence of data representing Titanosauria. In this way, the weak correlations found here may be suggestive of a possible correlation between heteropody and centre of mass across the clade in the ancient past, and a snapshot of the real trend. However, it is possible that the presence of extreme heteropody in Dinosauria is more a product of soft tissue distribution between manus and pes than a phenomenon easily visible in osteology, as has been suggested is the case in extant animals in previous chapters.

7.5.5 Soft Tissue Implications

As with the analysis of heteropody in extant quadrupedal tetrapods (chapters 4 and 6), the true picture of heteropody is incomplete without *in vivo* evidence, or at least, evidence of the extent of soft tissue under the foot, for both manus and pes. In this chapter, an analysis of fossil trackways was performed to provide information about the extent of soft tissue heteropody in sauropodomorphs where both manus and pes tracks were preserved. However, fossil tracks are by no means a perfect representation of *in vivo* foot anatomy, and rely on its interactions between the substrate, and the dynamics of the

trackmaker (Baird, 1957; Padian and Olsen, 1984a; Minter et al., 2007; Razzolini et al., 2014).

Based on the analysis of soft tissue and skeletal differences in underfoot surface area from chapter 2, it is likely that the *in vivo* foot surface areas of these animals would be defined by greater surface area taken up by soft tissue in the manus, compared to the pes. In this case heteropody results found in the body fossil analysis herein would change. However, this effect may be offset by the presence of fatty foot pads in most sauropod pes (Jannel et al., 2019), and the vast size, and unique morphology of the clade, which is unlike anything covered in chapter 2.

7.5.6 Centre of Mass Diversity, and Explanations for Extreme Heteropody

The bipedal ancestry of all quadrupedal dinosaurs (VanBuren and Bonnan, 2013; Maidment et al., 2014) means that ancestral centre of mass positions for these animals are much more posteriorly positioned than would be expected for, for example, a quadrupedal mammal (Warner, et al., 2013) or even past the range of lizards (Clemente, et al., 2008). In ornithischian dinosaurs, centre of mass position can be close to the hips, as in *Stegosaurus,* or more anterior, as seen in *Chasmosaurus* (associated with an enlarged and elongated skull of substantial mass) (Maidment et al., 2014). In sauropodomorphs, significant anterior shifts in centre of mass position have been found at two pivotal points in their evolution, during the shift to quadrupedality, and the evolution of titanosauriforms, both associated with shifts in neck size (Bates et al., 2016).

In chapters 4 and 6, it was proposed that extreme heteropody in sauropod dinosaurs might be a product of phylogenetic inertia, an ‘evolutionary hangover’ from their bipedal ancestry. Support for this postulation was not found in the results of the analysis herein, largely because this is hard to test for without macroevolutionary analyses. However, based on the lack of positive results for a link between CoM and heteropody here, and the different foot postures found in sauropod manus and pes, this will be the subject of further study.

It is also possible that the extreme heteropody seen in sauropod trackways, is a function of the evolution of a fatty foot pad to support the pes (Jannel et al., 2019). Since fatty foot pads act to prevent excess pressures underfoot, this is not necessarily an argument against the use of heteropody as a pressure equalisation mechanism. Rather, it is further evidence that pressure reduction strategies were necessary in sauropods, and were selected for, due to their large size and mass. These adaptations could theoretically work in tandem (Chi and Roth, 2010; Hutchinson et al., 2011; Jannel et al., 2019). The analyses in this chapter however, do not lend sufficient support to support this case. No clear evidence was found for a functional link between heteropody and centre of mass position in sauropod dinosaurs.

Chapter 8
Discussion

8.1 Summary of Preceding Chapters and Wider Implications

The preceding major chapters (chapters 2, 4, 6, and 7), along with the ancillary test chapters (chapters 3 and 5), represent four parts of an investigation into whether the phenomenon of extreme heteropody, seen in sauropod dinosaurs, was correlated with unusually anterior/posterior centre of mass positions in quadrupedal tetrapods. If this were the case, heteropody in tetrapods could act as an underfoot pressure equalisation mechanism. Chapter 2 explored how the underfoot surface area differs between the results for live, and skeletons of, extant tetrapods, which is necessary for understanding how the latter chapters relate to each other, and how to interpret data from the fossil record in comparison to living species. Chapters 4, 6, and 7 directly attempt to address a possible correlation between heteropody and centre of mass (CoM), through investigations of live, and skeletons of, extant animals, as well as evidence from the fossil record. In summary, to answer the question of whether extreme heteropody is functionally linked to unusual antero-posterior CoM positions in extant tetrapods, the following questions were proposed and answered:

1. Can skeletal surface area predict *in vivo* foot surface area?
2. Is antero-posterior CoM position correlated with heteropody?
3. Do underfoot forces and pressures indicate the presence of a pressure equalisation mechanism?
4. Is there evidence in the fossil record for a link between CoM position and heteropody variation in dinosaurs?

The findings of each of this thesis' research chapters, in which these questions were answered, are summarised in the following sections:

8.1.1 Predictability of *in vivo* from Skeletal Foot Contact Area

In chapter 2, CT scans of the feet of 29 extant tetrapods were segmented and reposed so that alpha shape 'footprints' of the skeletal tissue and soft tissue could be created. From there underfoot surface area was calculated for each and how predictable one was from the other was tested. Analyses in both an approximated 'life pose' and with bones laid flat against the plane both determined that *in vivo* surface area was highly predictable at approximately 1.67 times skeletal surface area, with phylogeny and body mass not significantly affecting this relationship. Interestingly, when analysing manus and pes separately, soft tissue area was approximately 2 times skeletal surface area in the manus, and 1.6 times skeletal surface area in the pes. This study outlined a new method for predicting approximate *in vivo* foot size for extinct animals based on fossil specimens, with applications for narrowing down potential fossil trackmakers. This study highlights the importance in considering differential soft tissue amounts between the manus and pes, which is directly considered in later chapters as a possible explanation for extreme heteropody in sauropod dinosaurs.

8.1.2 Pressure Measurements and their Utility

There are multiple ways of measuring underfoot pressure, mean pressure over time, maximum pressure during a footfall, pressure at median footfall time, pressure across time intervals, etc (Duckworth, et al., 1985; Bus, 2016). This thesis put more emphasis on maximum and median pressure during a footfall, but there are merits and downsides to any method of pressure measurement. For the purposes of this thesis, maximum pressure over the course of a footfall was a useful measurement as it coincided with the point at which the subject animal's entire foot was placed upon the ground. In addition, the studies where literature data was pulled from recorded peak pressure data, and so recording peak pressure in the new data made comparing these data more comparable with the literature. Median pressure values tended to be close to, or identical to, peak values. As well as this, since one of the major aims of this thesis was to decipher how weight distributed across

the feet was connected to foot area, it was beneficial to analyse the maximum load a foot regularly deals with during walking, so loads under each foot were not underestimated. While measuring underfoot pressure this way makes sense in studies like this where multiple animals are being compared and maximum load on each foot is relevant, for instance, when studying a single animal's locomotion in depth, it would be beneficial to be extensive, analysing total pressure over each footfall, and collecting means (panagiotopoulou, et al. 2016). Stationary animals, or animals performing alternative gaits such as galloping, hopping, or running would have additional considerations. During rapid locomotion, such as running or hopping, CoM movement is the inverse of its movements during walking, as such, forefoot/hindfoot pressure recorded during such gaits would not be reflective of walking (Zhang, et al., 2017). However, these measurements should be considered carefully based on each individual circumstance. For example, measuring mean pressure across a footfall could potentially be beneficial for comparing animals with very different footfall speeds, or gaits, where maximum load under each foot is more relative.

For these instances, however, more considerations need to be taken, as changing gait, stance time, or duty factors in the forelimbs or hindlimbs can be used to reduce pressure equalisation in ways not directly related to foot anatomy (Biewener, 1983b; Assaf, et al., 2019). In addition, heteropody, as it refers to differences in foot contact area under the manus and the pes, can be changed in real time in these cases, by changing foot posture for different gaits, to cope with the mechanical challenges of different speeds, terrain, or overall gait (Young, et al., 1992). In addition, pressure reduction techniques are not the exclusive purview of the area of the foot touching the ground, and foot posture, leg posture and structure, and anatomical gait restrictions can affect how pressure under the foot is managed in ways that may not be obvious from the anatomy of foot contact area (Biewener, 1983b; Biewener and Patek, 2018). These factors, both anatomical and non-anatomical, will inevitably change how pressure is recorded. Maximum pressure will vary across different gaits, so studying pressure over time, and taking the mean, could be a more useful metric. This measure becomes less useful in instances of changing duty

factor, where time on each foot is adjusted. Running animals may reduce both foot contact area and contact time, and measures of heteropody would not reflect the foot contact area of walking gaits. As might be expected, consulting similar studies in the literature is advised for optimising data collection in this regard, and avoiding error.

8.1.3 Linking Centre of Mass Position and Heteropody In Extant Tetrapod Skeletons

In chapter 4, the possibility of a functional link between CoM position and underfoot surface area in extant tetrapods was examined using foot measurements and whole-body convex hulls of 57 skeletons. This followed the shape analysis in chapter 3, which established length x 'carpal width' (minimum width on most proximal area of foot in contact with the ground) as the most accurate area proxy. No correlation between heteropody and CoM position was found, except arguably in cursorial mammals. Cursorial mammals were found to cluster together with slightly anterior centres of mass and roughly equal foot sizes. There was also a strong correlation between heteropody and CoM position in semi-aquatic animals (excluding the Asian water monitor, *Varanus salvator*), with relatively larger manus areas associated with a more anterior centre of mass. This study did not support the hypothesis that heteropody and centre of mass are functionally linked in a mechanism to equalise underfoot pressure. However, it did not rule out certain groups exhibiting this correlation, as in semi-aquatic animals, and the clustering of cursorial animals together in a narrow range could potentially indicate an equalisation effect. These chapters established the usefulness of different foot area proxies for determining foot area from footprints and the likelihood for cursorial mammals to retain a relatively central CoM position.

8.1.4 Manus-Pes Disparity During Locomotion in Pressure, Area and Vertical Force

Chapter 6 sought to test whether centre of mass was correlated with relative differences between underfoot area, vertical force, and pressure, of the manus and pes of extant animals, using footfall data from animals walking on pressure mats, both new and from

the literature. Cursorial mammals showed a similar pattern to chapter 4 for all three underfoot measurements. However, contrary to the findings in chapter 4, overall data showed a slight association between more anterior CoM positions and relatively greater manus area/peak vertical force, as well as very slightly lower manus pressure. The correlations associated with these trends were weak when applied to the entire data set. There was a strong and significant correlation when using only the newly collected taxa, but this was limited to only 5 data points. However, the pressure mat tests carried out in chapter 5 suggest that these data are not reliable on their own due to issues with calibration of the plate using humans as a baseline. These results, therefore were not convincing enough to support the hypothesis that CoM position could act as a pressure equalisation mechanism in extant tetrapods during movement. In addition, these results further indicated the importance of accounting for soft tissue, as indicated by differential soft tissue coverage in the manus and pes in chapter 2. The differences between the results of this chapter and those of chapter 4 indicate that an analysis of heteropody data from non-avian dinosaurs from osteology alone would potentially underestimate correlations between heteropody and CoM position. Since there is little direct evidence of full soft tissue extents in the manus and pes of non-avian dinosaurs, it follows that evidence for foot contact area of dinosaurs *in vivo* should ideally be analysed based on fossil footprints, which are more frequently preserved than dinosaur soft tissue. But difficulty linking tracks and trackmakers makes this very difficult in practice. These chapters established a lack of overall trend between CoM position and heteropody/pressure distribution in extant animals.

8.1.5 Heteropody and Centre of Mass Trends in Quadrupedal Dinosaurs

The data for extant animals, analysed in chapters 2, 3, 4 and 6, indicated no relationship between CoM and heteropody index. However, sauropod dinosaurs exhibit extremes of size well beyond modern terrestrial taxa, and may have been under stronger selection pressures to reduce underfoot pressures. Chapter 7 attempted to examine the case for a functional link between CoM and heteropody in quadrupedal dinosaurs. By examining both osteological and trackway evidence, this chapter aimed to establish whether

evidence for a link was inconclusive, or underestimated with osteological data only, as demonstrated in the contrast between chapters 4 and 6.

A database of 136 sauropodormorph trackways, with data for trackway age and heteropody index, was gathered from the literature to establish trends in heteropody over geological time within the clade. In addition, heteropody and centre of mass data for 13 dinosaurs where articulated manus and pes were available was gathered to compare using the same methods as chapter 4. Osteological data showed no clear trend between CoM position and heteropody in dinosaurs. Data from fossil trackways suggested what could be two peaks in heteropody reflecting increased manus area compared to pes area in sauropodomorph dinosaurs throughout geological time. While two major peaks in centre of mass were previously detected across geological time for the same clade (Bates et al., 2016), the peaks in heteropody as observed in trackways occurred 40-50 million years after the observed anterior shifts in CoM position, and are very unlikely to be connected. Analysing sampling of fossil footprints revealed these peaks to most likely be an artefact of preservation/publishing bias. This chapter determined the lack of a clear link between heteropody and CoM position in sauropod dinosaurs.

8.2 Wider Implications of This Work

Through the synthesis of the findings of the previous chapters, several points stand out as having implications beyond the scope of the individual chapters, and this thesis, themselves.

8.2.1 Heteropody as a Potential Equalisation Mechanism

This thesis set out to investigate the potential of heteropody as a potential mechanism to equalise underfoot pressure. This possibility was previously asserted as an explanation for disparity in heteropody in sauropod dinosaurs (Falkingham et al., 2012; Falkingham et al., 2010), but was never tested. Chapters 4, 6, and 7 took different approaches to answering this question directly. Clustering of cursorial mammal data in chapters 4 and 6,

might indicate that such a mechanism is utilised by certain groups. However, this thesis found little evidence that this mechanism of pressure reduction occurs universally across quadrupedal animals. An interesting follow-up study to this would focus on cursorial mammals, looking at how CoM and heteropody interact with them, along with comparative anatomy of the hoof, and relative speed, in order to build a clearer picture of the factors at play in this investigation.

It remains possible that more extreme heteropody is applied as a pressure equalisation mechanism within certain groups, where manus and pes anatomy, and centre of mass position, are not constrained by adaptations to terrestrial running. Sauropod dinosaurs could potentially have benefitted from this mechanism if this is the case, as they could rely on their large size as a defence mechanism, and likely could not run at speed (Sellers et al., 2013). The trackway analysis in chapter 7, however, does not support this. Compared with two anterior shifts in CoM position (Bates et al., 2016), the two apparent peaks in heteropody found in sauropod trackways were temporally separated from the CoM shifts by 40-50Ma, and lined up with peaks in fossil sampling.

The absence of this mechanism in dinosaurs then raises the question of what the reasons are behind extreme heteropody in sauropod dinosaurs. Future work will try and answer this question by focusing on the disparities between manus and pes foot structures and posture, and whether the manus and pes evolved at different speeds, combining comparative biomechanics and phylogenetic comparative methods.

8.2.2 Implications of Soft Tissue Disparity and Heteropody

The results of chapter 2 suggest that soft tissue makes up a greater percentage of underfoot surface area in forelimbs than hindlimbs in tetrapods. This could potentially explain why there is more signal found for a possible link between heteropody and CoM position overall in chapter 6, compared to chapter 4, since the former analysed soft tissue extent while chapter 4 compared estimates of skeletal underfoot surface area exclusively. When forelimb underfoot surface area is underestimated/hindlimb underfoot surface area is overestimated, the true ratio of forefoot to hindfoot surface area is not communicated.

Furthermore, since most pressure-reducing structures in the feet of tetrapods, such as foot pads and hooves, are composed entirely of soft tissue (Chi and Roth, 2010; Chi and Schmitt, 2005; Hutchinson et al., 2011; Warner et al., 2013), it follows that the true picture of how underfoot pressures are potentially equalised using heteropody would be obscured by analysing osteology alone.

With that said, the studies with a further focus on soft tissue extents do not offer any further support to the hypothesis that heteropody acts as a pressure equalisation mechanism in its relationship to centre of mass. If anything, their further lack of support indicates that such a mechanism being universal to tetrapods is extremely unlikely.

The presence of more soft tissue underfoot in the manus than the pes, that would be expected from osteology alone has implications for the study of fossil trackways, and the possible identity of fossil trackmakers. If the results from chapter 2 are indicative of manus versus pes underfoot soft tissue surface area in dinosaurs and other extinct animals, the degree of heteropody displayed by trackways would be unlikely to be directly reflected in osteological remains of candidate species. This would add a further obstacle in the process of identifying potential trackmakers, an already difficult task. It is, however, possible that some extinct animals would not follow this trend, as it was established using extant animals. In addition, sauropod dinosaurs, have no modern analogues of their vast size and unusual body plan. In addition sauropods have a unique (for an obligate quadruped) disparity in structure and posture between their manus and pes (Falkingham, 2010). By combining trackway data with structural information from osteological correlates for soft tissue structures, a more clear picture of sauropod soft tissue extent and disparity between manus and pes could be established.

8.2.3 Body Plans of Taxonomic Groups and Heteropody

As discussed above, the possibility of heteropody as a pressure equalisation mechanism used universally across tetrapods appears unlikely to be true. This thesis did, however, note some interesting results from individual tetrapod clades that highlight how the

diversity of body plans in tetrapods is reflected in their degrees of heteropody and general underfoot anatomy.

In chapters 4 and 6, cursorial mammals clustered around relatively equal forefoot and hindfoot size, and slightly anterior CoM positions, where animals with other locomotory modes, body plans, and specialised limbs were more likely to have results outside of these clusters. Cursorial mammals are specialised for running, so a relatively central CoM position and relatively equal foot size makes a certain amount of sense. Cursorial mammals tend to be digitigrade, increasing the functional length of their limbs, with rigid spines to reduce stress from oscillations (Hildebrand, 1962). They have relatively even underfoot area and CoM positions, and must be able to run at speed and accelerate quickly when needed to evade predators (Stein and Casinos, 1997). Uneven foot sizes and unusually antero-posterior CoM positions could potentially reduce their ability to do this efficiently, changing how these animals are balanced, by potentially resulting in unequal underfoot pressures and how weight is distributed among the limbs so one set dominates, and changing how propulsive and braking forces of the forelimbs and hindlimbs translate into underfoot pressures (Demes and Günther, 1989; Demes et al. 1994; Henderson, 2006; Granatosky et al., 2018). Heteropody in extant mammals is more common among hopping mammals such as rabbits and kangaroos, and semi-aquatic mammals, such as beavers.

In chapter 4, heteropody and CoM position were strongly correlated in semi-aquatic animals. By not having to rely exclusively on terrestrial cursoriality, it is possible that in non-cursorial, or partly cursorial animals, adaptations for heteropody are more selected for. In other words, selective pressures to keep relatively even-sized manus and pes reduces with reduced terrestrial cursoriality. In this way, beavers, for example, would be free to adapt their hindfeet for paddling more as they relied on aquatic locomotion more than terrestrial locomotion. Results for primates in chapter 6 also largely exist outside of the cluster of results for cursorial mammals, suggesting that this clustering of cursorial mammals around relatively even foot areas and slightly anterior CoM positions is related to their locomotory mode, and possibly selected for.

8.2.4 Why Have Extreme Heteropody?

If extreme heteropody is not used as a pressure equalisation mechanism, as the inconclusive nature of the above results hint at, why might this phenomenon otherwise occur?

In some animals, heteropody clearly occurs for a functional purpose, for example, to aid with locomotion in rabbits, hares, and kangaroos (Alexander and Vernon, 1975; Farley et al., 1993), or in some semi-aquatic animals (Reynolds, 1993). Sauropod dinosaurs, however, were too large to be able to hop, and the idea that sauropods spent a substantial amount of their life swimming is largely unsupported (Coombs Jr, 1975; Henderson, 2004).

Previous chapters speculated that extreme heteropody in sauropod dinosaurs could have occurred as a result of their evolution from a bipedal ancestor. No extant quadruped is known to be descended from bipeds, so this assertion would be difficult to test through extant analogues. However, more data to support this could be gathered from osteological correlates, phylogenetic comparative methods, and comparative anatomy of the manus and pes in different sauropod clades, compared with a more expansive trackway analysis.

Heteropody may also be reflective of methods of stress reduction, and other functional adaptations, in soft tissue and posture. Fatty foot pads, as seen in elephants and other large animals (Hutchinson et al., 2011), do seem likely to be have been present in sauropod dinosaurs, and, as with elephants, seem likely to have adopted a semi-digitigrade foot posture (Carrano, 1997; Hutchinson et al., 2011). These structures appear to be more prominent on the pes compared to the vertically posed manus, which would be reflected by extreme heteropody in trackways. Following the logic of chapter 2, these adaptations, which would have resulted in underfoot area extents largely being determined by fatty foot pads, could have resulted in unusually different manus and pes sizes, in conjunction with different foot postures. Presumably too, without selective pressures for cursoriality, there is less of a mechanical need to equalise underfoot pressure in these animals.

With future studies in foot anatomy and centre of mass, these possibilities may be able to be explored and their validity tested. A universal mechanism for pressure equalisation through heteropody appears unlikely to be found, even with more data. However, for certain functional groups, further studies with additional data could potentially support or disprove currently speculative possible links.

8.3 Potential Future Studies

8.3.1 Larger/More Focused Data Sets

Data sets with more animals, especially reptiles, amphibians, and non-cursorial mammals, could potentially produce results with clearer conclusions for the methods employed in chapters 4 and 6. The same applies for the dinosaur analysis in chapter 7, in regards to osteological evidence, as well as the problems presented by sampling bias hindering the chapter's trackway analyis. Dinosaur analyses, as with many palaeobiological studies, would be aided by the collection of more, and more diverse, body fossils with articulated manus and pes, and fossils complete enough to be able to employ convex hulling to estimate whole-body CoM. In addition, a wider range of sauropod track fossils, both in terms of samples, localities, and trackway ages, would be able to give a clearer picture of heteropody trends in these creatures.

In addition, studies focusing on individual functional or phylogenetic groups would be ideal follow-ups to this research. Birds stood out in chapter 2 as having different soft tissue compared to skeletal tissue underfoot, which could have potential implications for trackmaker identification in theropod and ornithopod dinosaurs. Chapters 4 and 6 suffered slightly for having cursorial mammals make up the bulk of the data points, at the expense of reptiles or animals that employ alternate means of locomotion. (Studies on terrestrial locomotion are quite likely to favour cursorial mammals, so future literature-based studies on locomotion will likely face the same issues.) However, studying cursorial mammals in terms of heteropody, CoM position, and comparative foot anatomy would be an interesting avenue in which to take this research, and one that will be considered for future work. Chapter 3 indicated a potential link between CoM position in heteropody in semi-aquatic

animals, and chapter 4 indicated that the relationship between CoM position and heteropody is different in primates compared to other animals. Both findings would be interesting and potentially fruitful to explore, with a large dataset limited to these groups.

8.3.2 Foot Posture

Variation in foot posture and its relationship with underfoot area and heteropody in the context of mass distribution could be an interesting avenue with which to continue this field of inquiry. In chapter 4, osteological remains were binned by foot posture to calculate their 'functional foot area' in the context of examining a possible universal link between heteropody and CoM. However, how the underfoot areas and pressures of animals with different foot postures differ, and are influenced by mass distribution, as well as their soft tissue versus skeletal tissue distribution underfoot, could be examined in a similar manner with large and comparable sample sizes for underfoot pressure and area of each foot posture gathered using pressure mats, and CT scans.

The potential effect of foot posture on extreme heteropody in sauropod dinosaurs would also be interesting to examine, especially given the morphological transitions in the evolution of sauropod dinosaurs from digitigrade, cursorial bipeds, to extremely large, potentially semi-digitigrade quadrupeds. Studies of this nature should consider differential soft tissue distribution between the manus and pes, especially if reconstructing manual and pedal soft tissue based on osteological correlates. Ideally manus and pes comparisons on an anatomical level would be made for different species, representative of different clades, and paired with evolutionary rates analyses to investigate if manus and pes evolved at different speeds, and how they diverged on an anatomical and mechanical level.

8.3.3 Manus Versus Pes Underfoot Soft Tissue Distribution

Future studies could examine further the distinction between manus and pes underfoot surface area of soft and skeletal tissue found in chapter 2. How universally this distinction applies, and how it presents in different clades and functionally similar groups using larger

datasets could be interesting avenues to explore. Analyses of this type would likely involve large numbers of CT scans, or dissections, to gather enough data.

8.4 Conclusions

1. Underfoot surface area *in vivo* is highly predictable from skeletal surface area

2. Soft tissue underfoot surface area in the manus is proportionately higher than soft tissue area in the pes compared to skeletal underfoot surface area.

3. Length x minimal width at most proximal end of foot touching the ground, or ‘carpal width’, is a more accurate predictor of foot area than either length x width, or pi x radius squared, with length x width being the second most accurate.

3. Antero-posterior CoM position and heteropody are not universally correlated in tetrapods. Heteropody is therefore unlikely to have been employed universally as a pressure equalisation mechanism.

4. Cursorial mammals retain relatively similar CoM and heteropody values, whereas animals with differing locomotory modes, and non-mammals are less likely to.

5. More signal for a link between CoM position and heteropody was present using *in vivo* data compared to results relying on osteology alone, but no link was present. This disparity of results may be related to manus-pes soft tissue differences underfoot.

6 Sauropod dinosaurs do not appear to have employed heteropody as a pressure equalisation mechanism, with a more likely explanation for variation in heteropody in these animals being disparities in morphology and posture between manus and pes, resulting from bipedal ancestry.

References

Agostinho, F.S., Rahal, S.C., Araújo, F.A., Conceição, R.T., Hussni, C.A., El-Warrak, A.O. and Monteiro, F.O., 2012. Gait analysis in clinically healthy sheep from three different age groups using a pressure-sensitive walkway. *BMC veterinary research*, *8*(1), p.87.

Alexander, R.M. and Vernon, A., 1975. The mechanics of hopping by kangaroos (Macropodidae). *Journal of Zoology*, *177*(2), pp.265-303.

Alexander, R.M., 1985. Mechanics of posture and gait of some large dinosaurs. *Zoological journal of the linnean society*, *83*(1), pp.1-25.

Alexander, R. M. (2003). *Principles of animal locomotion*. Princeton University Press.

Alexander, R.M., 2004. Bipedal animals, and their differences from humans. *Journal of anatomy*, *204*(5), pp.321-330.

Alexander, R.M., 2006. Dinosaur biomechanics. *Proceedings of the Royal Society B: Biological Sciences*, *273*(1596), pp.1849-1855.

Alexander, R.M., Bennett, M.B. and Ker, R.F., 1986. Mechanical properties and function of the paw pads of some mammals. *Journal of Zoology*, *209*(3), pp.405-419.

Allee, W.C. and Schmidt, K.P., 1951. *Ecological animal geography* (Vol. 72, No. 6, p. 479). LWW.

Allen, J.A., 1877. The influence of physical conditions in the genesis of species. *Radical review*, *1*, pp.108-140.

Allen, V., Bates, K.T., Li, Z. and Hutchinson, J.R., 2013. Linking the evolution of body shape and locomotor biomechanics in bird-line archosaurs. *Nature*, *497*(7447), p.104.

Allen, V., Paxton, H. and Hutchinson, J.R., 2009. Variation in center of mass estimates for extant sauropsids and its importance for reconstructing inertial properties of extinct archosaurs. *The Anatomical Record: Advances in Integrative Anatomy and*

Evolutionary Biology: Advances in Integrative Anatomy and Evolutionary Biology, *292*(9), pp.1442-1461.

Apelqvist, J., 2012. Diagnostics and treatment of the diabetic foot. *Endocrine*, *41*(3), pp.384-397.

Arribas, C.P., Medrano, N.H., Macarrón, P.L. and Pérez, E.S., 2008. Estudio de un rastro de huellas de saurópodo del yacimiento de las Cuestas I (Santa Cruz de Yanguas, Soria, España). Implicaciones taxonómicas. *Studia geologica salmanticensia*, *44*(1), pp.13-40.

Assaf, N. D., Rahal, S. C., Mesquita, L. R., Kano, W. T., and Abibe, R. B. Evaluation of parameters obtained from two systems of gait analysis. *Australian Veterinary Journal,* 97(10), 137-171.

Astley, H.C. and Roberts, T.J., 2014. The mechanics of elastic loading and recoil in anuran jumping. *Journal of Experimental Biology*, *217*(24), pp.4372-4378.

Avanzini, M., Leonardi, G. and Mietto, P., 2003. *Lavinipes cheminii ichnogen., ichnosp. nov.,* a possible sauropodomorph track from the Lower Jurassic of the Italian Alps. *Ichnos*, *10*(2-4), pp.179-193.

Avanzini, M., Leonardi, G., Tomasoni, R. and Campolongo, M., 2001. Enigmatic dinosaur trackways from the Lower Jurassic (Pliensbachian) of the Sarca valley, Northeast Italy. *Ichnos: An International Journal of Plant & Animal*, *8*(3-4), pp.235-242.

Baird, D., 1957. *Triassic reptile footprint faunules from Milford, New Jersey*.

Bang, P., Dahlstrøm, P. and Walters, M., 2001. *Animal tracks and signs*. Oxford university press.

Barbera, A.M., Delaunay, M.G., Dougill, G. and Grant, R.A., 2019. Paw Morphology in the Domestic Guinea Pig (*Cavia porcellus*) and Brown Rat (*Rattus norvegicus*). *The Anatomical Record*, *302*(12), pp.2300-2310.

Barnes, F.A. and Lockley, M.G., 1994. Trackway evidence for social sauropods from the Morrison Formation, Eastern Utah (USA). *Gaia*, *10*, pp.37-42.

Bates, K.T., Falkingham, P.L., Macaulay, S., Brassey, C. and Maidment, S.C., 2015. Downsizing a giant: re-evaluating *Dreadnoughtus* body mass. *Biology letters*, *11*(6), p.20150215.

Bates, K.T., Manning, P.L., Hodgetts, D. and Sellers, W.I., 2009. Estimating mass properties of dinosaurs using laser imaging and 3D computer modelling. *PloS one*, *4*(2), p.e4532.

Bates, K.T., Manning, P.L., Vila, B. and Hodgetts, D., 2008. Three-Dimensional Modelling and Analysis of Dinosaur Trackways. *Palaeontology*, *51*(4), pp.999-1010.

Bates, K.T., Mannion, P.D., Falkingham, P.L., Brusatte, S.L., Hutchinson, J.R., Otero, A., Sellers, W.I., Sullivan, C., Stevens, K.A. and Allen, V., 2016. Temporal and phylogenetic evolution of the sauropod dinosaur body plan. *Royal Society Open Science*, *3*(3), p.150636..

Bates, K.T., Savage, R., Pataky, T.C., Morse, S.A., Webster, E., Falkingham, P.L., Ren, L., Qian, Z., Collins, D., Bennett, M.R. and McClymont, J., 2013. Does footprint depth correlate with foot motion and pressure? *Journal of the Royal Society Interface*, *10*(83), p.20130009.

Bedell, M.W.J., Trexler, D.L., Tidwell, V. and Carpenter, K., 2005. First articulated manus of *Diplodocus carnegii*. Thunder-lizards: the Sauropodomorph dinosaurs.

Bejan, A. and Marden, J.H., 2006. Unifying constructal theory for scale effects in running, swimming and flying. *Journal of Experimental Biology*, *209*(2), pp.238-248.

Berger, J. and Cunningham, C., 1998. Natural variation in horn size and social dominance and their importance to the conservation of black rhinoceros. *Conservation Biology*, *12*(3), pp.708-711.

Biewener, A.A., 1983a. Locomotory stresses in the limb bones of two small mammals: the ground squirrel and chipmunk. *Journal of Experimental Biology*, *103*(1), pp.131-154.

Biewener, A.A., 1983b. Allometry of quadrupedal locomotion: the scaling of duty factor, bone curvature and limb orientation to body size. *Journal of Experimental Biology,* 105 (1), 147-171.

Biewener, A.A., 1989. Mammalian terrestrial locomotion and size. *Bioscience*, *39*(11), pp.776-783.

Biewener, A.A., 2005. Biomechanical consequences of scaling. *Journal of Experimental Biology*, *208*(9), pp.1665-1676.

Biewener, A.A., 2006. Patterns of mechanical energy change in tetrapod gait: pendula, springs and work. *Journal of Experimental Zoology Part A: Comparative Experimental Biology*, *305*(11), pp.899-911.

Biewener, A. A., 2018. Animal Locomotion. *Oxford University Press.*

Bird, R.T., 1944. Did *Brontosaurus* ever walk on land? *Natural History*, *53*, pp.60-70.

Birn-Jeffery, A.V., Hubicki, C.M., Blum, Y., Renjewski, D., Hurst, J.W. and Daley, M.A., 2014. Don't break a leg: running birds from quail to ostrich prioritise leg safety and economy on uneven terrain. *Journal of Experimental Biology*, *217*(21), pp.3786-3796.

Blackburn, T.M., Gaston, K.J. and Loder, N., 1999. Geographic gradients in body size: a clarification of Bergmann's rule. *Diversity and distributions*, *5*(4), pp.165-174.

Bliese, P., 2006. Multilevel Modeling in R (2.2)–A Brief Introduction to R, the multilevel package and the nlme package.

Blob, R.W., 2000. Interspecific scaling of the hindlimb skeleton in lizards, crocodilians, felids and canids: does limb bone shape correlate with limb posture?. *Journal of Zoology*, *250*(4), pp.507-531.

Blomberg, S.P., Lefevre, J.G., Wells, J.A. and Waterhouse, M., 2012. Independent contrasts and PGLS regression estimators are equivalent. *Systematic Biology*, *61*(3), pp.382-391.

Bonnan, M.F., 2003. The evolution of manus shape in sauropod dinosaurs: implications for functional morphology, forelimb orientation, and phylogeny. *Journal of Vertebrate Paleontology*, *23*(3), pp.595-613.

Bonnan, M.F., 2005. Pes anatomy in sauropod dinosaurs: implications for functional morphology, evolution, and phylogeny. *Thunder-Lizards: The Sauropodomorph Dinosaurs. Indiana University Press, Bloomington*, pp.346-380.

Bonnan, M.F., Shulman, J., Varadharajan, R., Gilbert, C., Wilkes, M., Horner, A. and Brainerd, E., 2016. Forelimb kinematics of rats using XROMM, with implications for small eutherians and their fossil relatives. *PloS one*, *11*(3), p.e0149377.

Bowker, R.M., Van, K.W., Springer, S.E. and Linder, K.E., 1998. Functional anatomy of the cartilage of the distal phalanx and digital cushion in the equine foot and a hemodynamic flow hypothesis of energy dissipation. *American journal of veterinary research*, *59*(8), pp.961-968.

Boyer, D.M., Gunnell, G.F., Kaufman, S. and McGeary, T.M., 2016. Morphosource: Archiving and sharing 3-d digital specimen data. *The Paleontological Society Papers*, *22*, pp.157-181.

Brainerd, E.L., Baier, D.B., Gatesy, S.M., Hedrick, T.L., Metzger, K.A., Gilbert, S.L. and Crisco, J.J., 2010. X-ray reconstruction of moving morphology (XROMM): precision, accuracy and applications in comparative biomechanics research. *Journal of Experimental Zoology Part A: Ecological Genetics and Physiology*, *313*(5), pp.262-279.

Brand, L.R., 1996. Variations in salamander trackways resulting from substrate differences. *Journal of Paleontology*, *70*(6), pp.1004-1010.

Buatois, L.A. and Mángano, M.G., 2004. Animal-substrate interactions in freshwater environments: applications of ichnology in facies and sequence stratigraphic analysis of fluvio-lacustrine successions. *Geological Society, London, Special Publications*, *228*(1), pp.311-333.

Buchner, H.H.F., Obermüller, S. and Scheidl, M., 2000. Body centre of mass movement in the sound horse. *The Veterinary Journal*, *160*(3), pp.225-234.

Buchner, H.H.F., Savelberg, H.H.C.M., Schamhardt, H.C. and Barneveld, A., 1997. Inertial properties of Dutch Warmblood horses. *Journal of biomechanics*, *30*(6), pp.653-658.

Bus, S. A., 2016. Innovations in plantar pressure and foot temperature measurements in diabetes. *Diabetes/Metabolism Research and Reviews,* 32, 221-226.

Butler, R.J., Upchurch, P. and Norman, D.B., 2008. The phylogeny of the ornithischian dinosaurs. *Journal of Systematic Palaeontology*, *6*(1), pp.1-40.

Carpenter, K., 2007. How to make a fossil: Part 2—Dinosaur mummies and other soft tissue. *The Journal of Paleontological Science*, *7*, pp.1-23.

Carrano, M.T. and Hutchinson, J.R., 2002. Pelvic and hindlimb musculature of *Tyrannosaurus rex* (Dinosauria: Theropoda). *Journal of Morphology*, *253*(3), pp.207-228.

Carrano, M.T., 1997. Morphological indicators of foot posture in mammals: a statistical and biomechanical analysis. *Zoological Journal of the Linnean Society*, *121*(1), pp.77-104.

Carrano, M.T., 1999. What, if anything, is a cursor? Categories versus continua for determining locomotor habit in mammals and dinosaurs. *Journal of Zoology*, *247*(1), pp.29-42.

Cartmill, M., 1974. Pads and claws in arboreal locomotion. *Primate locomotion*, pp.45-83.

Carvalho, V.R.C., Bucklin, R.A., Shearer, J.K. and Shearer, L., 2005. Effects of trimming on dairy cattle hoof weight bearing and pressure distributions during the stance phase. *Transactions of the ASAE*, *48*(4), pp.1653-1659.

Casanova, P.M.P. and Oosterlinck, M., 2012. Hoof size and symmetry in young Catalan Pyrenean horses reared under semi-extensive conditions. *Journal of equine veterinary science*, *32*(4), pp.231-234.

Casanovas, M., Fernández, A., Pérez-Lorente, F. and Santafé, J.V., 1997. Sauropod trackways from site el sobaquillo (Munilla, La Rioja, Spain) indicate amble walking. *Ichnos: An International Journal of Plant & Animal*, *5*(2), pp.101-107.

Casinos, A., 1996. Bipedalism and quadrupedalism in *Megatheriurn*: an attempt at biomechanical reconstruction. *Lethaia*, *29*(1), pp.87-96.

Castanera, D., Barco, J.L., Díaz-Martínez, I., Gascón, J.H., Pérez-Lorente, F. and Canudo, J.I., 2011. New evidence of a herd of titanosauriform sauropods from the lower Berriasian of the Iberian range (Spain). *Palaeogeography, Palaeoclimatology, Palaeoecology*, *310*(3-4), pp.227-237.

Castanera, D., Pascual, C., Canudo, J.I., Hernandez, N. and Barco, J.L., 2012. Ethological variations in gauge in sauropod trackways from the Berriasian of Spain. *Lethaia*, *45*(4), pp.476-489.

Castanera, D., Pascual, C., Razzolini, N.L., Vila, B., Barco, J.L. and Canudo, J.I., 2013. Discriminating between medium-sized tridactyl trackmakers: tracking ornithopod tracks in the base of the Cretaceous (Berriasian, Spain). *PloS one*, *8*(11), p.e81830.

Castanera, D., Vila, B., Razzolini, N.L., Falkingham, P.L., Canudo, J.I., Manning, P.L. and Galobart, À., 2013. Manus track preservation bias as a key factor for assessing trackmaker identity and quadrupedalism in basal ornithopods. *PloS one*, *8*(1), p.e54177.

Cheung, J.T.M., Zhang, M., Leung, A.K.L. and Fan, Y.B., 2005. Three-dimensional finite element analysis of the foot during standing—a material sensitivity study. *Journal of biomechanics*, *38*(5), pp.1045-1054.

Chi, K.J. and Louise Roth, V., 2010. Scaling and mechanics of carnivoran footpads reveal the principles of footpad design. *Journal of the Royal Society Interface*, *7*(49), pp.1145-1155.

Chi, K.J. and Schmitt, D., 2005. Mechanical energy and effective foot mass during impact loading of walking and running. *Journal of biomechanics*, *38*(7), pp.1387-1395.

Cho, D.J., Kim, J.H. and Gweon, D.G., 1995. Optimal turning gait of a quadruped walking robot. *Robotica*, *13*(6), pp.559-564.

Cholewo, T.J. and Love, S., 1999, January. Gamut boundary determination using alpha-shapes. In *Color and Imaging Conference* (Vol. 1999, No. 1, pp. 200-204). Society for Imaging Science and Technology.

Cignoni, P., Callieri, M., Corsini, M., Dellepiane, M., Ganovelli, F. and Ranzuglia, G., 2008, July. Meshlab: an open-source mesh processing tool. In *Eurographics Italian chapter conference* (Vol. 2008, pp. 129-136).

Clack, J.A., 1997. Devonian tetrapod trackways and trackmakers; a review of the fossils and footprints. *Palaeogeography, Palaeoclimatology, Palaeoecology*, *130*(1-4), pp.227-250.

Clarke, A., 2017. *Principles of thermal ecology: Temperature, energy and life*. Oxford University Press.

Clarke, K.A., 1995. Differential fore-and hindpaw force transmission in the walking rat. *Physiology & behavior*, *58*(3), pp.415-419.

Clarke, K.A., Smart, L. and Still, J., 2001. Ground reaction force and spatiotemporal measurements of the gait of the mouse. *Behavior Research Methods, Instruments, & Computers*, *33*(3), pp.422-426.

Clifford, A.B., 2010. The evolution of the unguligrade manus in artiodactyls. *Journal of Vertebrate Paleontology*, *30*(6), pp.1827-1839.

Coombs Jr, W.P., 1975. Sauropod habits and habitats. *Palaeogeography, Palaeoclimatology, Palaeoecology*, *17*(1), pp.1-33.

Coombs Jr, W.P., 1978. Theoretical aspects of cursorial adaptations in dinosaurs. *The Quarterly Review of Biology*, *53*(4), pp.393-418.

Coombs Jr, W.P., 1986. A juvenile ankylosaur referable to the genus *Euoplocephalus* (Reptilia, Ornithischia). *Journal of Vertebrate Paleontology*, *6*(2), pp.162-173.

Coombs, M.C., 1983. Large mammalian clawed herbivores: a comparative study. *Transactions of the American Philosophical Society*, *73*(7), pp.1-96.

Cooper, N., Thomas, G.H. and FitzJohn, R.G., 2016. Shedding light on the ‘dark side’of phylogenetic comparative methods. *Methods in ecology and evolution*, *7*(6), pp.693-699.

Cuff, A.R., Goswami, A. and Hutchinson, J.R., 2017. Reconstruction of the musculoskeletal system in an extinct lion. *Palaeontologia Electronica*, *20*(2), pp.1-25.

Currie, A., 2018. *Rock, bone, and ruin: An optimist's guide to the historical sciences*. MIT Press.

de Faria, L.G., Rahal, S.C., dos Reis Mesquita, L., Agostinho, F.S., Kano, W.T., Teixeira, C.R. and Monteiro, F.O.B., 2015. Gait analysis in giant anteater (*Myrmecophaga tridactyla*) with the use of a pressure-sensitive walkway. *Journal of Zoo and Wildlife Medicine*, *46*(2), pp.286-290.

De Muizon, C. and McDonald, H.G., 1995. An aquatic sloth from the Pliocene of Peru. *Nature*, *375*(6528), p.224.

Demes, B. and Günther, M.M., 1989. Biomechanics and allometric scaling in primate locomotion and morphology. *Folia Primatologica*, *53*(1-4), pp.125-141.

Demes, B., Larson, S.G., Stern Jr, J.T., Jungers, W.L., Biknevicius, A.R. and Schmitt, D., 1994. The kinetics of primate quadrupedalism: "hindlimb drive" reconsidered. *Journal of Human Evolution*, *26*(5-6), pp.353-374.

dePolo, P.E., Brusatte, S.L., Challands, T.J., Foffa, D., Ross, D.A., Wilkinson, M. and Yi, H.Y., 2018. A sauropod-dominated tracksite from Rubha nam Brathairean (Brothers' Point), Isle of Skye, Scotland. *Scottish Journal of Geology*, *54*(1), pp.1-12.

Diaz-Martinez, I., de Valais, S. and Cónsole-Gonella, C., 2018. New sauropod tracks from the Yacoraite Formation (Maastrichtian–Danian), Valle del Tonco tracksite, Salta, northwestern Argentina. *Journal of Iberian Geology*, *44*(1), pp.113-127.

Diedrich, C., 2011. Upper Jurassic tidal flat megatracksites of Germany—coastal dinosaur migration highways between European islands, and a review of the dinosaur footprints. *Palaeobiodiversity and Palaeoenvironments*, *91*(2), pp.129-155.

Duckworth, T., Boulton, A. J., Betts, R. P., Franks, C. I., and Ward, J. D. Plantar pressure measurements and the prevention of ulceration in the diabetic foot. *The Journal of Bone and Joint Surgery,* 67(1), 79-85.

Dunning Jr, J.B., 2007. *CRC handbook of avian body masses*. CRC press.

Eames, M.H.A., Cosgrove, A. and Baker, R., 1999. Comparing methods of estimating the total body centre of mass in three-dimensions in normal and pathological gaits. *Human movement science*, *18*(5), pp.637-646.

Endo, H., Yoshida, M., Nguyen, T.S., Akiba, Y., Takeda, M. and Kudo, K., 2019. Three-dimensional CT examination of the forefoot and hindfoot of the hippopotamus and tapir during a semiaquatic walking. *Anatomia, histologia, embryologia*, *48*(1), pp.3-11.

Eng, J.J. and Winter, D.A., 1993. Estimations of the horizontal displacement of the total body centre of mass: considerations during standing activities. *Gait & Posture*, *1*(3), pp.141-144.

Falkingham, P.L., 2010. Computer simulation of dinosaur tracks.

Falkingham, P.L., 2012. Acquisition of high resolution three-dimensional models using free, open-source, photogrammetric software. *Palaeontologia electronica*, *15*(1), pp.1-15.

Falkingham, P.L., 2014. Interpreting ecology and behaviour from the vertebrate fossil track record. *Journal of Zoology*, *292*(4), pp.222-228.

Falkingham, P.L. and Gatesy, S.M., 2014. The birth of a dinosaur footprint: subsurface 3D motion reconstruction and discrete element simulation reveal track ontogeny. *Proceedings of the National Academy of Sciences*, *111*(51), pp.18279-18284.

Falkingham, P.L., Bates, K.T. and Mannion, P.D., 2012. Temporal and palaeoenvironmental distribution of manus-and pes-dominated sauropod trackways. *Journal of the Geological Society*, *169*(4), pp.365-370.

Falkingham, P.L., Bates, K.T., Margetts, L. and Manning, P.L., 2010. Simulating sauropod manus-only trackway formation using finite-element analysis. *Biology Letters*, *7*(1), pp.142-145.

Falkingham, P.L., Bates, K.T., Margetts, L. and Manning, P.L., 2011. The 'Goldilocks' effect: preservation bias in vertebrate track assemblages. *Journal of the Royal Society Interface*, *8*(61), pp.1142-1154.

Farley, C.T., Glasheen, J. and McMahon, T.A., 1993. Running springs: speed and animal size. *Journal of experimental Biology*, *185*(1), pp.71-86.

Farlow, J.O. and Brett-Surman, M.K. eds., 1999. *The complete dinosaur*. Indiana University Press.

Farlow, J.O., 1992. Sauropod tracks and trackmakers integrating the ichnological and skeletal records. *Zubia*, (10), pp.89-138.

Farlow, J.O., Bakker, R.T., Dattilo, B.F., Everett Deschner, E., Falkingham, P.L., Harter, C., Solis, R., Temple, D. and Ward, W., 2019. Thunder lizard handstands: Manus-only sauropod trackways from the Glen Rose Formation (Lower Cretaceous, Kendall County, Texas). *Ichnos*, pp.1-33.

Fedak, M.A., Heglund, N.C. and Taylor, C.R., 1982. Energetics and mechanics of terrestrial locomotion. II. Kinetic energy changes of the limbs and body as a function of speed and body size in birds and mammals. *Journal of Experimental Biology*, *97*(1), pp.23-40.

Felsenstein, J., 1985. Phylogenies and the comparative method. *The American Naturalist*, *125*(1), pp.1-15.

Ferraro, J.V. and Binetti, K.M., 2014. American alligator proximal pedal phalanges resemble human finger bones: Diagnostic criteria for forensic investigators. *Forensic science international*, *240*, pp.151-e1.

Fish, F.E., 1996. Transitions from drag-based to lift-based propulsion in mammalian swimming. *American Zoologist*, *36*(6), pp.628-641.

Foster, J.R. and Hunt-Foster, R.K., 2011. New occurrences of dinosaur skin of two types (Sauropoda? and *Dinosauria indet.*) from the Late Jurassic of North America (Mygatt-Moore Quarry, Morrison Formation). *Journal of Vertebrate Paleontology*, *31*(3), pp.717-721.

Franklyn-Miller, A., Bilzon, J., Wilson, C. and McCrory, P., 2014. Can RSScan footscan® D3D™ software predict injury in a military population following plantar pressure assessment? A prospective cohort study. *The Foot*, *24*(1), pp.6-10.

Full, R.J., Kubow, T., Schmitt, J., Holmes, P. and Koditschek, D., 2002. Quantifying dynamic stability and maneuverability in legged locomotion. *Integrative and comparative biology*, *42*(1), pp.149-157.

Garland, T., 1983. The relation between maximal running speed and body mass in terrestrial mammals. *Journal of Zoology*, *199*(2), pp.157-170.

Gatesy, S.M. and Biewener, A.A., 1991. Bipedal locomotion: effects of speed, size and limb posture in birds and humans. *Journal of Zoology*, *224*(1), pp.127-147.

Gatesy, S.M. and Falkingham, P.L., 2017. Neither bones nor feet: track morphological variation and 'preservation quality'. *Journal of Vertebrate Paleontology*, *37*(3), p.e1314298.

Gatesy, S.M., 1990. Caudofemoral musculature and the evolution of theropod locomotion. *Paleobiology*, *16*(2), pp.170-186.

Gatesy, S.M., 1991. Hind limb movements of the American alligator (*Alligator mississippiensis*) and postural grades. *Journal of Zoology*, *224*(4), pp.577-588.

Gatesy, S.M., 2003. Direct and indirect track features: What sediment did a dinosaur touch?. *Ichnos*, *10*(2-4), pp.91-98.

Gatesy, S.M., Baier, D.B., Jenkins, F.A. and Dial, K.P., 2010. Scientific rotoscoping: a morphology-based method of 3-D motion analysis and visualization. *Journal of Experimental Zoology Part A: Ecological Genetics and Physiology*, *313*(5), pp.244-261.

Gatesy, S.M., Middleton, K.M., Jenkins Jr, F.A. and Shubin, N.H., 1999. Three-dimensional preservation of foot movements in Triassic theropod dinosaurs. *Nature*, *399*(6732), p.141.

Gauthier, J., Kluge, A.G. and Rowe, T., 1988. Amniote phylogeny and the importance of fossils. *Cladistics*, *4*(2), pp.105-209.

Geyer, H., Seyfarth, A. and Blickhan, R., 2006. Compliant leg behaviour explains basic dynamics of walking and running. *Proceedings of the Royal Society B: Biological Sciences*, *273*(1603), pp.2861-2867.

Gierlinski, G.D. and Sabath, K., 2008. Stegosaurian footprints from the Morrison Formation of Utah and their implications for interpreting other ornithischian tracks. *Oryctos*, *8*, pp.29-46.

Girardeau-Montaut, D., 2015. Cloud compare—3d point cloud and mesh processing software. *Open Source Project*.

Grafen, A., 1989. The phylogenetic regression. *Philosophical Transactions of the Royal Society of London. B, Biological Sciences*, *326*(1233), pp.119-157.

Granatosky, M.C., Fitzsimons, A., Zeininger, A. and Schmitt, D., 2018. Mechanisms for the functional differentiation of the propulsive and braking roles of the forelimbs and hindlimbs during quadrupedal walking in primates and felines. *Journal of Experimental Biology*, *221*(2), p.jeb162917.

Grasse, J.E., 1951. Beaver ecology and management in the Rockies. *Journal of Forestry*, *49*(1), pp.3-6.

Gray, J., 1944. Studies in the mechanics of the tetrapod skeleton. *Journal of Experimental Biology*, *20*(2), pp.88-116.

Grégoire, J., Bergeron, R., d'Allaire, S., Meunier-Salaün, M.C. and Devillers, N., 2013. Assessment of lameness in sows using gait, footprints, postural behaviour and foot lesion analysis. *Animal*, *7*(7), pp.1163-1173.

Griffin, T.M., Main, R.P. and Farley, C.T., 2004. Biomechanics of quadrupedal walking: how do four-legged animals achieve inverted pendulum-like movements? *Journal of Experimental Biology*, *207*(20), pp.3545-3558.

Halliday, D., Resnick, R. and Walker, J., 2013. *Fundamentals of physics*. John Wiley & Sons.

Hamilton, Samantha M., Yan-yin Wang, Michael J. Ryan, and Corwin Sullivan., 2019. "Structure and articular relationships of the partially ossified sternum in hadrosaurid dinosaurs." In *7th Annual Meeting Canadian Society of Vertebrate Palaeontology May 10-13, 2019 Grande Prairie, Alberta*, 23.

Harmon, L.J., Weir, J.T., Brock, C.D., Glor, R.E. and Challenger, W., 2007. GEIGER: investigating evolutionary radiations. *Bioinformatics*, *24*(1), pp.129-131.

Harter, C., Dattilo, B., Farlow, J.O., Deschner, E. and Solis, R., 2014, October. Bottoms up: a sedimentological analysis of the manus-only coffee hollow sauropod tracks. In *2014 GSA Annual Meeting in Vancouver, British Columbia*.

Hatala, K.G., Dingwall, H.L., Wunderlich, R.E. and Richmond, B.G., 2013. The relationship between plantar pressure and footprint shape. *Journal of human evolution*, *65*(1), pp.21-28.

Hatala, K.G., Wunderlich, R.E., Dingwall, H.L. and Richmond, B.G., 2016. Interpreting locomotor biomechanics from the morphology of human footprints. *Journal of human evolution*, *90*, pp.38-48.

Heckel, F., Schwier, M. and Peitgen, H.O., 2009. Object-oriented application development with MeVisLab and Python. *GI Jahrestagung*, *154*, pp.1338-51.

Henderson, D.M., 1999. Estimating the masses and centers of mass of extinct animals by 3-D mathematical slicing. *Paleobiology*, *25*(1), pp.88-106.

Henderson, D.M., 2004. Tipsy punters: sauropod dinosaur pneumaticity, buoyancy and aquatic habits. *Proceedings of the Royal Society of London. Series B: Biological Sciences*, *271*(4), pp.180-183.

Henderson, D.M., 2006. Burly gaits: centers of mass, stability, and the trackways of sauropod dinosaurs. *Journal of Vertebrate Paleontology*, *26*(4), pp.907-921.

Henderson, D.M., 2013. Sauropod necks: are they really for heat loss?. *PloS one*, *8*(10), p.e77108.

Hershkovitz, P., 1971. A new rice rat of the *Oryzomys palustris* group (Cricetinae, Muridae) from northwestern Colombia, with remarks on distribution. *Journal of Mammalogy*, *52*(4), pp.700-709.

Hildebrand, M., 1962. Walking, running, and jumping. *American Zoologist*, pp.151-155.

Hildebrand, M., 1965. Symmetrical gaits of horses. *Science*, *150*(3697), pp.701-708.

Hildebrand, M., 1980. The adaptive significance of tetrapod gait selection. *American Zoologist*, *20*(1), pp.255-267.

Hinterhofer, C.H., Stanek, C.H. and Haider, H., 2000. The effect of flat horseshoes, raised heels and lowered heels on the biomechanics of the equine hoof assessed by finite element analysis (FEA). *Journal of Veterinary Medicine Series A*, *47*(2), pp.73-82.

Hodgins, J.K. and Raibert, M.N., 1991. Adjusting step length for rough terrain locomotion. *IEEE Transactions on Robotics and Automation*, *7*(3), pp.289-298.

Howard, C.S., Blakeney, D.C., Medige, J., Moy, O.J. and Peimer, C.A., 2000. Functional assessment in the rat by ground reaction forces. *Journal of biomechanics*, *33*(6), pp.751-757.

Huey, R.B., 1987. Phylogeny, history, and the comparative method. *New directions in ecological physiology*, pp.76-98.

Huh, M., Hwang, K.G., Paik, I.S., Chung, C.H. and Kim, B.S., 2003. Dinosaur tracks from the Cretaceous of South Korea: Distribution, occurrences and paleobiological significance. *Island Arc*, *12*(2), pp.132-144.

Huson, A., 1991. Functional anatomy of the foot. *Disorders of the foot and ankle*, *1*, 409-31.

Hutchinson, J.R. and Gatesy, S.M., 2000. Adductors, abductors, and the evolution of archosaur locomotion. *Paleobiology*, *26*(4), pp.734-751.

Hutchinson, J.R. and Gatesy, S.M., 2006. Dinosaur locomotion: beyond the bones. *Nature*, *440*(7082), p.292.

Hutchinson, J.R., 2016. CrocBase: DOI 10.17605/OSF.IO/X38NH.

Hutchinson, J.R., Delmer, C., Miller, C.E., Hildebrandt, T., Pitsillides, A.A. and Boyde, A., 2011. From flat foot to fat foot: structure, ontogeny, function, and evolution of elephant “sixth toes”. *Science*, *334*(6063), pp.1699-1703.

Hutson, J.D. and Hutson, K.N., 2014. A repeated-measures analysis of the effects of soft tissues on wrist range of motion in the extant phylogenetic bracket of dinosaurs: Implications for the functional origins of an automatic wrist folding mechanism in crocodilia. *The Anatomical Record*, *297*(7), pp.1228-1249.

Hwang, K.G., Huh, M. and Paik, I.S., 2004. Sauropod trackways from the Cretaceous Jindong formation at Docheon-ri, Changnyeon-gun, Gyeongsangnam-do, Korea. *Gosaengmul Hag-hoeji: Journal of the Paleontological Society of Korea*, *40*(2), pp.145-159.

Iriarte-Díaz, J. (2002). Differential scaling of locomotor performance in small and large terrestrial mammals. *Journal of Experimental Biology*, *205*(18), 2897-2908.

Ishigaki, S. and Matsumoto, Y., 2009. Re-examination of manus-only and manus-dominated sauropod trackways from Morocco. *Geological Quarterly*, *53*(4), pp.441-448.

Jackson, S.J., Whyte, M.A. and Romano, M., 2009. Laboratory-controlled simulations of dinosaur footprints in sand: a key to understanding vertebrate track formation and preservation. *Palaios*, *24*(4), pp.222-238.

Jackson, S.J., Whyte, M.A. and Romano, M., 2010. Range of experimental dinosaur (*Hypsilophodon foxii*) footprints due to variation in sand consistency: how wet was the track? *Ichnos*, *17*(3), pp.197-214.

Janis, C. M., 2007. "The horse series." *Icons of evolution*, pp. 257-280.

Jannel, A., Nair, J.P., Panagiotopoulou, O., Romilio, A. and Salisbury, S.W., 2019. “Keep your feet on the ground”: Simulated range of motion and hind foot posture of the Middle Jurassic sauropod *Rhoetosaurus brownei* and its implications for sauropod biology. *Journal of morphology*, *280*(6), pp.849-878.

Johnson, C.A., Seidel, J., Carson, R.E., Gandler, W.R., Sofer, A., Green, M.V. and Daube-Witherspoon, M.E., 1997. Evaluation of 3D reconstruction algorithms for a small animal PET camera. *IEEE Transactions on Nuclear Science*, *44*(3), pp.1303-1308.

Kawano, S.M. and Blob, R.W., 2013. Propulsive forces of mudskipper fins and salamander limbs during terrestrial locomotion: implications for the invasion of land. *Integrative and comparative biology*, *53*(2), pp.283-294.

Kent, B.R., 2014. *3D scientific visualization with blender*. Morgan & Claypool Publishers.

Kilbourne, B.M. and Hoffman, L.C., 2013. Scale effects between body size and limb design in quadrupedal mammals. *PLoS One*, *8*(11), p.e78392.

Kim, J.Y. and Lockley, M.G., 2012. New sauropod tracks (*Brontopodus pentadactylus ichnosp. nov.*) from the Early Cretaceous Haman Formation of Jinju area, Korea: implications for sauropods manus morphology. *Ichnos*, *19*(1-2), pp.84-92.

Kimura, T., 1979. Kinesiological characteristics of primate walking. *Environment, behavior, and morphol-ogy: Dynamic interactions in primates*, pp.297-311.

Kinoshita, K., Okada, K., Saito, I., Saito, A., Takahashi, Y., Kimoto, M. and Wakasa, M., 2019. Alignment of the rearfoot and foot pressure patterns of individuals with medial tibial stress syndrome: A cross-sectional study. *Physical Therapy in Sport*, *38*, pp.132-138.

Klinkhamer, A.J., Mallison, H., Poropat, S.F., Sloan, T. and Wroe, S., 2019. Comparative Three-Dimensional Moment Arm Analysis of the Sauropod Forelimb: Implications for the Transition to a Wide-Gauge Stance in Titanosaurs. *The Anatomical Record*, *302*(5), pp.794-817.

Knaust, D. and Hauschke, N., 2004. Trace fossils versus pseudofossils in Lower Triassic playa deposits, Germany. *Palaeogeography, Palaeoclimatology, Palaeoecology*, *215*(1-2), pp.87-97.

Kubo, T. and Benton, M.J., 2007. Evolution of hindlimb posture in archosaurs: limb stresses in extinct vertebrates. *Palaeontology*, *50*(6), pp.1519-1529.

Kubo, T., 2011. Estimating body weight from footprints: application to pterosaurs. *Palaeogeography, Palaeoclimatology, Palaeoecology*, *299*(1-2), pp.197-199.

Kubo, T., Sakamoto, M., Meade, A. and Venditti, C., 2019. Transitions between foot postures are associated with elevated rates of body size evolution in mammals. *Proceedings of the National Academy of Sciences*, *116*(7), pp.2618-2623.

Lambertz, M., Bertozzo, F. and Sander, P.M., 2018. Bone histological correlates for air sacs and their implications for understanding the origin of the dinosaurian respiratory system. *Biology letters*, *14*(1), p.20170514.

Lammers, A.R., 2007. Locomotor kinetics on sloped arboreal and terrestrial substrates in a small quadrupedal mammal. *Zoology*, *110*(2), pp.93-103.

Lammers, A.R., Earls, K.D. and Biknevicius, A.R., 2006. Locomotor kinetics and kinematics on inclines and declines in the gray short-tailed opossum *Monodelphis domestica*. *Journal of Experimental Biology*, *209*(20), pp.4154-4166.

Lascelles, B.D.X., Findley, K., Correa, M., Marcellin-Little, D. and Roe, S., 2007. Kinetic evaluation of normal walking and jumping in cats, using a pressure-sensitive walkway. *Veterinary Record*, *160*(15), pp.512-516.

Lascelles, B.D.X., Roe, S.C., Smith, E., Reynolds, L., Markham, J., Marcellin-Little, D., Bergh, M.S. and Budsberg, S.C., 2006. Evaluation of a pressure walkway system for measurement of vertical limb forces in clinically normal dogs. *American journal of veterinary research*, *67*(2), pp.277-282.

Le Lœuff, J., Gourrat, C., Landry, P., Hautier, L., Liard, R., Souillat, C., Buffetaut, E. and Enay, R., 2006. A Late Jurassic sauropod tracksite from southern Jura (France). *Comptes Rendus Palevol*, *5*(5), pp.705-709.

Leasure, J.L. and Jones, M., 2008. Forced and voluntary exercise differentially affect brain and behavior. *Neuroscience*, *156*(3), pp.456-465.

Lee, D.V., Stakebake, E.F., Walter, R.M. and Carrier, D.R., 2004. Effects of mass distribution on the mechanics of level trotting in dogs. *Journal of Experimental Biology*, *207*(10), pp.1715-1728.

Lee, T.T., Liao, C.M. and Chen, T.K., 1988. On the stability properties of hexapod tripod gait. *IEEE Journal on Robotics and Automation*, *4*(4), pp.427-434.

Lee, Y.N. and Huh, M., 2002. Manus-only sauropod tracks in the Uhangri Formation (Upper Cretaceous), Korea and their paleobiological implications. *Journal of Paleontology*, *76*(3), pp.558-564.

Lee, Y.N. and Lee, H.J., 2006. A sauropod trackway in Donghae-Myeon, Goseong county, south Gyeongsang province, Korea and its palaeobiological implications of Uhangri manus-only sauropod tracks. *Journal of the Paleontological Society of Korea*, *22*(1), pp.1-14.

Lehmann, W.H., 1963. The forelimb architecture of some fossorial rodents. *Journal of Morphology*, *113*(1), pp.59-76.

Lemelin, P., 1995. Comparative and functional myology of the prehensile tail in New World monkeys. *Journal of Morphology*, *224*(3), pp.351-368.

Li, R., Lockley, M.G., Makovicky, P.J., Matsukawa, M., Norell, M.A., Harris, J.D. and Liu, M., 2008. Behavioral and faunal implications of Early Cretaceous deinonychosaur trackways from China. *Naturwissenschaften*, *95*(3), pp.185-191.

Lockley, M., Schulp, A.S., Meyer, C.A., Leonardi, G. and Mamani, D.K., 2002. Titanosaurid trackways from the Upper Cretaceous of Bolivia: evidence for large manus, wide-gauge locomotion and gregarious behaviour. *Cretaceous Research*, *23*(3), pp.383-400.

Lockley, M.G. and Rice, A., 1990. Did "*Brontosaurus*"; ever swim out to sea?: Evidence from brontosaur and other dinosaur footprints. *Ichnos: An International Journal of Plant & Animal*, *1*(2), pp.81-90.

Lockley, M.G. and Xing, L., 2015. Flattened fossil footprints: implications for paleobiology. *Palaeogeography, Palaeoclimatology, Palaeoecology*, *426*, pp.85-94.

Lockley, M.G., Farlow, J.O. and Meyer, C.A., 1994. *Brontopodus* and *Parabrontopodus ichnogen. nov*. and the significance of wide-and narrow-gauge sauropod trackways. *Gaia*, *10*, pp.135-145.

Lockley, M.G., Huh, M. and Kim, B.S., 2012. *Ornithopodichnus* and pes-only sauropod trackways from the Hwasun tracksite, Cretaceous of Korea. *Ichnos*, *19*(1-2), pp.93-100.

Lockley, M.G., Meyer, C.A., Hunt, A.P. and Lucas, S.G., 1994. The distribution of sauropod tracks and trackmakers. *Gaia*, *10*, pp.233-248.

Lockley, M.G., Nadon, G. and Currie, P.J., 2004. A diverse dinosaur-bird footprint assemblage from the Lance Formation, Upper Cretaceous, eastern Wyoming: implications for ichnotaxonomy. *Ichnos*, *11*(3-4), pp.229-249.

Lockley, M.G., Pittman, J.G., Meyer, C.A. and Santos, V.D., 1994. On the common occurrence of manus-dominated sauropod trackways in Mesozoic carbonates. *Gaia*, *10*(119), p.24.

Lockley, M.G., Young, B.H. and Carpenter, K., 1983. Hadrosaur locomotion and herding behavior: evidence from footprints in the Mesaverde Formation, Grand Mesa Coal Field, Colorado. *The Mountain Geologist*.

Lull, R.S., 1904. Adaptations to aquatic, arboreal, fossorial and cursorial habits in mammals. IV. Cursorial adaptations. *The American Naturalist*, *38*(445), pp.1-11.

Lyons-Weiler, J., Hoelzer, G.A. and Tausch, R.J., 1998. Optimal outgroup analysis. *Biological Journal of the Linnean Society*, *64*(4), pp.493-511.

Maddison, W. and Maddison, D., 2001. Mesquite: a modular system for evolutionary analysis (Mesquite Project).

Maddison, W.P., Donoghue, M.J. and Maddison, D.R., 1984. Outgroup analysis and parsimony. *Systematic biology*, *33*(1), pp.83-103.

Maidment, S.C. and Barrett, P.M., 2011. The locomotor musculature of basal ornithischian dinosaurs. *Journal of Vertebrate Paleontology*, *31*(6), pp.1265-1291.

Maidment, S.C., Henderson, D.M. and Barrett, P.M., 2014. What drove reversions to quadrupedality in ornithischian dinosaurs? Testing hypotheses using centre of mass modelling. *Naturwissenschaften*, *101*(11), pp.989-1001.

Mannion, P.D. and Upchurch, P., 2010. A quantitative analysis of environmental associations in sauropod dinosaurs. *Paleobiology*, *36*(2), pp.253-282.

Mannion, P.D. and Upchurch, P., 2011. A re-evaluation of the 'mid-Cretaceous sauropod hiatus' and the impact of uneven sampling of the fossil record on patterns of regional dinosaur extinction. *Palaeogeography, Palaeoclimatology, Palaeoecology*, *299*(3-4), pp.529-540.

Manter, J.T., 1938. The dynamics of quadrupedal walking. *Journal of Experimental Biology*, *15*(4), pp.522-540.

Margetts, L., Smith, I.M., Leng, J. and Manning, P.L., 2006. Parallel three-dimensional finite element analysis of dinosaur trackway formation. *Numerical methods in geotechnical engineering*, pp.743-749.

Martin, J.E., Menkem, E.F., Djomeni, A., Fowe, P.G. and Ntamak-Nida, M.J., 2017. Dinosaur trackways from the early Late Cretaceous of western Cameroon. *Journal of African Earth Sciences*, *134*, pp.213-221.

Marty, D., Belvedere, M., Meyer, C.A., Mietto, P., Paratte, G., Lovis, C. and Thüring, B., 2010. Comparative analysis of Late Jurassic sauropod trackways from the Jura Mountains (NW Switzerland) and the central High Atlas Mountains (Morocco): implications for sauropod ichnotaxonomy. *Historical Biology*, *22*(1-3), pp.109-133.

Marty, D., Meyer, C.A., Belvedere, M., Ayer, J. and Schafer, K.L., 2013. Rochefort-Les Grattes: an early Tithonian dinosaur tracksite from the Canton Neuchatel, Switzerland. *Revue de Paléobiologie*, *32*, pp.373-384.

Marty, D., Strasser, A. and Meyer, C.A., 2009. Formation and taphonomy of human footprints in microbial mats of present-day tidal-flat environments: implications for the study of fossil footprints. *Ichnos*, *16*(1-2), pp.127-142.

Mazin, J.M., Hantzpergue, P. and Olivier, N., 2017. The dinosaur tracksite of Plagne (early Tithonian, Late Jurassic; Jura Mountains, France): the longest known sauropod trackway. *Geobios*, *50*(4), pp.279-301.

Mazin, J.M., Hantzpergue, P. and Pouech, J., 2016. The dinosaur tracksite of Loulle (early Kimmeridgian; Jura, France). *Geobios*, *49*(3), pp.211-228.

Mazzetta, G.V. and Blanco, R.E., 2001. Speeds of dinosaurs from the Albian-Cenomanian of Patagonia and sauropod stance and gait. *Acta Palaeontologica Polonica*, *46*(2).

McDonald, G. H. 2007. Biomechanical Inferences of Locomotion in Ground Sloths: Integrating Morphological and Track Data. *Cenozoic Vertebrate Tracks and Traces: Bulletin 42,* 42, p.201.

McElroy, E.J., Wilson, R., Biknevicius, A.R. and Reilly, S.M., 2014. A comparative study of single-leg ground reaction forces in running lizards. *Journal of Experimental Biology*, *217*(5), pp.735-742.

McGhee, R. B., & Frank, A. A., 1968. On the stability properties of quadruped creeping gaits. *Mathematical Biosciences*, *3*, 331-351.

McGuigan, M.P. and Wilson, A.M., 2003. The effect of gait and digital flexor muscle activation on limb compliance in the forelimb of the horse *Equus caballus. Journal of Experimental Biology*, *206*(8), pp.1325-1336.

McMahon, T.A., 1975. Using body size to understand the structural design of animals: quadrupedal locomotion. *Journal of Applied Physiology*, *39*(4), pp.619-627.

Meijer, E., Bertholle, C.P., Oosterlinck, M., van der Staay, F.J., Back, W. and van Nes, A., 2014. Pressure mat analysis of the longitudinal development of pig locomotion in growing pigs after weaning. *BMC veterinary research*, *10*(1), p.37.

Meyer, C.A., Marty, D. and Belvedere, M., 2018, December. Titanosaur trackways from the Late Cretaceous El Molino Formation of Bolivia (Cal Orck'o, Sucre). In *Annales Societatis Geologorum Poloniae* (Vol. 88, No. 2, pp. 223-241).

Mezga, A., Meyer, C.A., Tešović, B.C., Bajraktarević, Z. and Gušić, I., 2006. The first record of dinosaurs in the Dalmatian part (Croatia) of the Adriatic-Dinaric carbonate platform (ADCP). *Cretaceous research*, *27*(6), pp.735-742.

Mezga, A., Tešović, B.C. and Bajraktarević, Z., 2007. First record of dinosaurs in the Late Jurassic of the Adriatic-Dinaridic carbonate platform (Croatia). *Palaios*, *22*(2), pp.188-199.

Michilsens, F., Aerts, P., Van Damme, R. and D'Août, K., 2009. Scaling of plantar pressures in mammals. *Journal of Zoology*, *279*(3), pp.236-242.

Milàn, J. and Hedegaard, R., 2010. Interspecific variation in tracks and trackways from extant crocodylians. *New Mexico Museum of Natural History and Science Bulletin*, *51*, pp.15-29.

Miller, C.E., Basu, C., Fritsch, G., Hildebrandt, T. and Hutchinson, J.R., 2007. Ontogenetic scaling of foot musculoskeletal anatomy in elephants. *Journal of The Royal Society Interface*, *5*(21), pp.465-475.

Minter, N.J., Braddy, S.J. and Davis, R.B., 2007. Between a rock and a hard place: arthropod trackways and ichnotaxonomy. *Lethaia*, *40*(4), pp.365-375.

Moore, J., 2010. General biomechanics: the horse as a biological machine. *Journal of equine veterinary science*, *30*(7), pp.379-383.

Moratalla, J.J., 1994. *Sauropod trackways from the Lower Cretaceous of Spain*.

Morse, S.A., Bennett, M.R., Liutkus-Pierce, C., Thackeray, F., McClymont, J., Savage, R. and Crompton, R.H., 2013. Holocene footprints in Namibia: the influence of substrate on footprint variability. *American Journal of Physical Anthropology*, *151*(2), pp.265-279.

Murdock, K., 2017. *Autodesk Maya 2019 Basics Guide*. SDC Publications.

Myers, T.S. and Fiorillo, A.R., 2009. Evidence for gregarious behavior and age segregation in sauropod dinosaurs. *Palaeogeography, Palaeoclimatology, Palaeoecology*, *274*(1-2), pp.96-104.

Naples, V.L., 1999. Morphology, evolution and function of feeding in the giant anteater (*Myrmecophaga tridactyla*). *Journal of Zoology*, *249*(1), pp.19-41.

Nery, M.F., González, D.J., Hoffmann, F.G. and Opazo, J.C., 2012. Resolution of the laurasiatherian phylogeny: evidence from genomic data. *Molecular phylogenetics and evolution*, *64*(3), pp.685-689.

Oosterlinck, M., Pille, F., Back, W., Dewulf, J. and Gasthuys, F., 2011. A pressure plate study on fore and hindlimb loading and the association with hoof contact area in sound ponies at the walk and trot. *The Veterinary Journal*, *190*(1), pp.71-76.

Osburn, R.C., 1903. Adaptation to aquatic, arboreal, fossorial and cursorial habits in mammals. I. Aquatic adaptations. *The American Naturalist*, *37*(442), pp.651-665.

Padian, K. and Olsen, P.E., 1984a. Footprints of the Komodo monitor and the trackways of fossil reptiles. *Copeia*, pp.662-671.

Padian, K. and Olsen, P.E., 1984b. The fossil trackway *Pteraichnus*: not pterosaurian, but crocodilian. *Journal of Paleontology*, *58*(1), pp.178-184.

Paik, I.S., Kim, H.J., Lee, H. and Kim, S., 2017. A large and distinct skin impression on the cast of a sauropod dinosaur footprint from Early Cretaceous floodplain deposits, Korea. *Scientific reports*, *7*(1), p.16339.

Panagiotopoulou, O., Pataky, T.C. and Hutchinson, J.R., 2019. Foot pressure distribution in White Rhinoceroses (*Ceratotherium simum*) during walking. *PeerJ*, *7*, p.e6881.

Panagiotopoulou, O., Pataky, T.C., Day, M., Hensman, M.C., Hensman, S., Hutchinson, J.R. and Clemente, C.J., 2016. Foot pressure distributions during walking in African elephants (*Loxodonta africana*). *Royal Society open science*, *3*(10), p.160203.

Panagiotopoulou, O., Pataky, T.C., Hill, Z. and Hutchinson, J.R., 2012. Statistical parametric mapping of the regional distribution and ontogenetic scaling of foot pressures during walking in Asian elephants (*Elephas maximus*). *Journal of Experimental Biology*, *215*(9), pp.1584-1593.

Panagiotopoulou, O., Rankin, J.W., Gatesy, S.M. and Hutchinson, J.R., 2016. A preliminary case study of the effect of shoe-wearing on the biomechanics of a horse's foot. *PeerJ*, *4*, p.e2164.

Paradis, E., Claude, J. and Strimmer, K., 2004. APE: analyses of phylogenetics and evolution in R language. *Bioinformatics*, *20*(2), pp.289-290.

Pataky, T.C., Caravaggi, P., Savage, R., Parker, D., Goulermas, J.Y., Sellers, W.I. and Crompton, R.H., 2008. New insights into the plantar pressure correlates of walking speed using pedobarographic statistical parametric mapping (pSPM). *Journal of biomechanics*, *41*(9), pp.1987-1994.

Patel, B.A., Wallace, I.J., Boyer, D.M., Granatosky, M.C., Larson, S.G. and Stern Jr, J.T., 2015. Distinct functional roles of primate grasping hands and feet during arboreal quadrupedal locomotion. *Journal of human evolution*, *88*, pp.79-84.

Patla, A.E., 2003. Strategies for dynamic stability during adaptive human locomotion. *IEEE Engineering in Medicine and Biology Magazine*, *22*(2), pp.48-52.

Pfau, T., Witte, T.H. and Wilson, A.M., 2006. Centre of mass movement and mechanical energy fluctuation during gallop locomotion in the Thoroughbred racehorse. *Journal of Experimental Biology*, *209*(19), pp.3742-3757.

Pittman, J.G., 1993. Stratigraphy and vertebrate ichnology of the Glen Rose Formation, western Gulf Basin, United States.

Platt, B.F. and Hasiotis, S.T., 2006. Newly discovered sauropod dinosaur tracks with skin and foot-pad impressions from the Upper Jurassic Morrison Formation, Bighorn Basin, Wyoming, USA. *Palaios*, *21*(3), pp.249-261.

Pollitt, C.C., 2004. Anatomy and physiology of the inner hoof wall. *Clinical techniques in equine practice*, *3*(1), pp.3-21.

Prum, R.O., Berv, J.S., Dornburg, A., Field, D.J., Townsend, J.P., Lemmon, E.M. and Lemmon, A.R., 2015. A comprehensive phylogeny of birds (Aves) using targeted next-generation DNA sequencing. *Nature*, *526*(7574), p.569.

Qian, Z., Ren, L., Ding, Y., Hutchinson, J.R. and Ren, L., 2013. A dynamic finite element analysis of human foot complex in the sagittal plane during level walking. *PLoS One*, *8*(11), p.e79424.

Raichlen, D.A., 2004. Convergence of forelimb and hindlimb Natural Pendular Period in baboons (*Papio cynocephalus*) and its implication for the evolution of primate quadrupedalism. *Journal of Human Evolution*, *46*(6), pp.719-738.

Razzolini, N., 2017. Morphological variation and ichnotaxonomy of dinosaur tracks: linking footprint shapes to substrate and trackmaker's anatomy and locomotion.

Razzolini, N.L., Vila, B., Castanera, D., Falkingham, P.L., Barco, J.L., Canudo, J.I., Manning, P.L. and Galobart, A., 2014. Intra-trackway morphological variations due to substrate consistency: the El Frontal dinosaur tracksite (Lower Cretaceous, Spain). *PloS one*, *9*(4), p.e93708.

Regnault, S., Hermes, R., Hildebrandt, T., Hutchinson, J. and Weller, R., 2013. Osteopathology in the feet of rhinoceroses: lesion type and distribution. *Journal of Zoo and Wildlife Medicine*, *44*(4), pp.918-927.

Reilly, S.M. and Elias, J.A., 1998. Locomotion in *Alligator mississippiensis*: kinematic effects of speed and posture and their relevance to the sprawling-to-erect paradigm. *Journal of Experimental Biology*, *201*(18), pp.2559-2574.

Reilly, S.M., McElroy, E.J. and Biknevicius, A.R., 2007. Posture, gait and the ecological relevance of locomotor costs and energy-saving mechanisms in tetrapods. *Zoology*, *110*(4), pp.271-289.

Revell, L.J., 2012. phytools: an R package for phylogenetic comparative biology (and other things). *Methods in Ecology and Evolution*, *3*(2), pp.217-223.

Reynolds, P.S., 1993. Size, shape, and surface area of beaver, *Castor canadensis*, a semiaquatic mammal. *Canadian Journal of Zoology*, *71*(5), pp.876-882.

Reynolds, T.R., 1985a. Mechanics of increased support of weight by the hindlimbs in primates. *American Journal of Physical Anthropology*, *67*(4), pp.335-349.

Reynolds, T.R., 1985b. Stresses on the limbs of quadrupedal primates. *American Journal of Physical Anthropology*, *67*(4), pp.351-362.

Richmond, B.G., Hatala, K.G., Dingwall, H.L. and Wunderlich, R.E., 2012. Using modern taxa to understand biomechanical variables: interpreting function from fossil footprints. *Am. J. Phys. Anthropol. S*, *54*, p.249.

Riga, B.J.G. and Tomaselli, M.B., 2019. Different trackway patterns in titanosaur sauropods: Analysis of new *Titanopodus* tracks from the Upper Cretaceous of Mendoza, Neuquén Basin, Argentina. *Cretaceous Research*, *93*, pp.49-59.

Riga, B.J.G., Calvo, J.O., 2009. A New Wide-Gauge Sauropod Track Site from the Late Cretaceous of Mendoza, Neuquén Basin, Argentina. *Palaeontology* 52(3), pp.631–640.

Riga, B.J.G., David, L.D.O., Tomaselli, M.B., dos Anjos Candeiro, C.R., Coria, J.P. and Prámparo, M., 2015. Sauropod and theropod dinosaur tracks from the Upper Cretaceous of Mendoza (Argentina): trackmakers and anatomical evidences. *Journal of South American Earth Sciences*, *61*, pp.134-141.

Rosenbaum, D., Hautmann, S., Gold, M. and Claes, L., 1994. Effects of walking speed on plantar pressure patterns and hindfoot angular motion. *Gait & posture*, *2*(3), pp.191-197.

Rowe, T., 2002. Digimorph: A National Science Foundation Digital Library at the University of Texas at Austin. http://*digimorph.org*.

Saitta, E.T., Rogers, C., Brooker, R.A., Abbott, G.D., Kumar, S., O'Reilly, S.S., Donohoe, P., Dutta, S., Summons, R.E. and Vinther, J., 2017. Low fossilization potential of

keratin protein revealed by experimental taphonomy. *Palaeontology*, *60*(4), pp.547-556.

Sakata, S. and Hikida, T., 2003. A Fossorial Lizard with Forelimbs Only. *Current herpetology*, *22*(1), pp.9-15.

Sander, P.M., Christian, A., Clauss, M., Fechner, R., Gee, C.T., Griebeler, E.M., Gunga, H.C., Hummel, J., Mallison, H., Perry, S.F. and Preuschoft, H., 2011. Biology of the sauropod dinosaurs: the evolution of gigantism. *Biological Reviews*, *86*(1), pp.117-155.

Santos, V.D., Callapez, P.M., Castanera, D., Barroso-Barcenilla, F., Rodrigues, N.P.C. and Cupeto, C.A., 2015. Dinosaur tracks from the Early Cretaceous of Parede tracksite (Cascais, Portugal): New implications on the sauropod palaeobiology of the Iberian Peninsula.

Schaller, N.U., D'Août, K., Villa, R., Herkner, B. and Aerts, P., 2011. Toe function and dynamic pressure distribution in ostrich locomotion. *Journal of Experimental Biology*, *214*(7), pp.1123-1130.

Schmitt, D. and Hanna, J.B., 2004. Substrate alters forelimb to hindlimb peak force ratios in primates. *Journal of Human Evolution*, *46*(3), pp.237-252.

Schmitt, D., 1994. Forelimb mechanics as a function of substrate type during quadrupedalism in two anthropoid primates. *Journal of Human Evolution*, *26*(5-6), pp.441-457.

Schmitt, D., 2003. Insights into the evolution of human bipedalism from experimental studies of humans and other primates. *Journal of Experimental Biology*, *206*(9), pp.1437-1448.

Schumacher, B. and Lockley, M.G., 2014. Newly documented trackways at “dinosaur lake”, the Purgatoire Valley dinosaur tracksite. *New Mexico Museum of Natural History and Science Bulletin*, *62*, pp.261-267.

Scott, G.B., 1989. Changes in limb loading with lameness for a number of Friesian cattle. *British Veterinary Journal*, *145*(1), pp.28-38.

Seebacher, F., Elsworth, P.G. and Franklin, C.E., 2003. Ontogenetic changes of swimming kinematics in a semi-aquatic reptile (*Crocodylus porosus*). *Australian Journal of Zoology*, *51*(1), pp.15-24.

Segal, A., Rohr, E., Orendurff, M., Shofer, J., O'Brien, M. and Sangeorzan, B., 2004. The effect of walking speed on peak plantar pressure. *Foot & Ankle International*, *25*(12), pp.926-933.

Sellers, W.I., Hepworth-Bell, J., Falkingham, P.L., Bates, K.T., Brassey, C.A., Egerton, V.M. and Manning, P.L., 2012. Minimum convex hull mass estimations of complete mounted skeletons. *Biology Letters*, *8*(5), pp.842-845.

Sellers, W.I., Manning, P.L., Lyson, T., Stevens, K. and Margetts, L., 2009. Virtual palaeontology: gait reconstruction of extinct vertebrates using high performance computing. *Palaeontologia Electronica*, *12*(3), p.11A.

Sellers, W.I., Margetts, L., Coria, R.A. and Manning, P.L., 2013. March of the titans: the locomotor capabilities of sauropod dinosaurs. *PloS one*, *8*(10), p.e78733.

Sereno, P.C., 1997. The origin and evolution of dinosaurs. *Annual Review of Earth and Planetary Sciences*, *25*(1), pp.435-489.

Shadwick, R.E., Russell, A.P. and Lauff, R.F., 1992. The structure and mechanical design of rhinoceros dermal armour. *Philosophical Transactions of the Royal Society of London. Series B: Biological Sciences*, *337*(1282), pp.419-428.

Shimer, H.W., 1903. Adaptations to aquatic, arboreal, fossorial and cursorial habits in mammals. III. Fossorial adaptations. *The American Naturalist*, *37*(444), pp.819-825.

Siegfried, W.R., 1990. Tail length and biting insects of ungulates. *Journal of Mammalogy*, *71*(1), pp.75-78.

Smith, J.B. and Farlow, J.O., 2003. Osteometric Approaches to Trackmaker Assignment for the Newark Supergroup. *The Great Rift Valleys of Pangea in Eastern North America: Sedimentology, Stratigraphy, and Paleontology*, *2*, p.273.

Snyder, R.C., 1952. Quadrupedal and bipedal locomotion of lizards. *Copeia*, *1952*(2), pp.64-70.

Stankowich, T., 2008. Tail-flicking, tail-flagging, and tail position in ungulates with special reference to black-tailed deer. *Ethology*, *114*(9), pp.875-885.

Starke, S.D., Robilliard, J.J., Weller, R., Wilson, A.M. and Pfau, T., 2008. Walk–run classification of symmetrical gaits in the horse: a multidimensional approach. *Journal of the Royal Society Interface*, *6*(33), pp.335-342.

Stein, B.R. and Casinos, A., 1997. What is a cursorial mammal?. *Journal of Zoology*, *242*(1), pp.185-192.

Strickson, E.C., Hutchinson, J.R., Wilkinson, D.M. and Falkingham, P.L., 2020. Can skeletal surface area predict in vivo foot surface area? *Journal of anatomy*, *236*(1), pp.72-84.

Taylor, C.R., Shkolnik, A.M., Dmi'el, R.A., Baharav, D. and Borut, A.R., 1974. Running in cheetahs, gazelles, and goats: energy cost and limb configuration. *American Journal of Physiology-Legacy Content*, *227*(4), pp.848-850.

Ting, L.H., Blickhan, R. and Full, R.J., 1994. Dynamic and static stability in hexapedal runners. *Journal of Experimental Biology*, *197*(1), pp.251-269.

Torcida Fernández Baldor, F., Díaz Martínez, I., Contreras, R., Huerta, P., Montero, D. and Urién, V., 2015. Unusual sauropod tracks in the Jurassic-Cretaceous interval: Cameros Basin (Burgos, Spain).

Tschopp, E., Wings, O., Frauenfelder, T. and Brinkmann, W., 2015. Articulated bone sets of manus and pedes of *Camarasaurus* (Sauropoda, Dinosauria). *Palaeontologia Electronica*, *18*(2), pp.1-65.

Ueda, Y., Niki, Y., Yoshida, K. and Masumitsu, H., 1981. Force Plate Study of Equine Biomechanics. *Bulletin of Equine Research Institute*, *1981*(18), pp.28-41.

Uhen, M.D., Barnosky, A.D., Bills, B., Blois, J., Carrano, M.T., Carrasco, M.A., Erickson, G.M., Eronen, J.T., Fortelius, M., Graham, R.W. and Grimm, E.C., 2013. From card catalogs to computers: databases in vertebrate paleontology. *Journal of Vertebrate Paleontology*, *33*(1), pp.13-28.

Upchurch, P., 1995. The evolutionary history of sauropod dinosaurs. *Philosophical Transactions of the Royal Society of London. Series B: Biological Sciences*, *349*(1330), pp.365-390.

Van der Tol, P.P.J., Metz, J.H.M., Noordhuizen-Stassen, E.N., Back, W., Braam, C.R. and Weijs, W.A., 2003. The vertical ground reaction force and the pressure distribution on the claws of dairy cows while walking on a flat substrate. *Journal of dairy science*, *86*(9), pp.2875-2883.

van Sittert, S., Skinner, J. and Mitchell, G., 2015. Scaling of the appendicular skeleton of the giraffe (*Giraffa camelopardalis*). *Journal of morphology*, *276*(5), pp.503-516.

VanBuren, C.S. and Bonnan, M., 2013. Forearm posture and mobility in quadrupedal dinosaurs. *PloS one*, *8*(9), p.e74842.

Verdugo, M.R., Rahal, S.C., Agostinho, F.S., Govoni, V.M., Mamprim, M.J. and Monteiro, F.O., 2013. Kinetic and temporospatial parameters in male and female cats walking over a pressure sensing walkway. *BMC veterinary research*, *9*(1), p.129.

Vereecke, E., D'Août, K., De Clercq, D., Van Elsacker, L. and Aerts, P., 2003. Dynamic plantar pressure distribution during terrestrial locomotion of bonobos (*Pan paniscus*). *American Journal of Physical Anthropology: The Official Publication of the American Association of Physical Anthropologists*, *120*(4), pp.373-383.

Vila, B., Galobart, À., Canudo, J.I., Le Loeuff, J., Dinarès-Turell, J., Riera, V., Oms, O., Tortosa, T. and Gaete, R., 2012. The diversity of sauropod dinosaurs and their first taxonomic succession from the latest Cretaceous of southwestern Europe: clues to demise and extinction. *Palaeogeography, Palaeoclimatology, Palaeoecology*, *350*, pp.19-38.

Vila, B., Oms, O. and Galobart, À., 2005. Manus-only titanosaurid trackway from Fumanya (Maastrichtian, Pyrenees): further evidence for an underprint origin. *Lethaia*, *38*(3), pp.211-218.

Wagensommer, A., Latiano, M., Leroux, G., Cassano, G. and Porchetti, S.D.O., 2012. New dinosaur tracksites from the Middle Jurassic of Madagascar:

Ichnotaxonomical, behavioural and palaeoenvironmental implications. *Palaeontology*, *55*(1), pp.109-126.

Walter, R.M. and Carrier, D.R., 2007. Ground forces applied by galloping dogs. *Journal of Experimental Biology*, *210*(2), pp.208-216.

Warner, S.E., Pickering, P., Panagiotopoulou, O., Pfau, T., Ren, L. and Hutchinson, J.R., 2013. Size-related changes in foot impact mechanics in hoofed mammals. *PloS one*, *8*(1), p.e54784.

Watanabe, M., Okada, H., Shimizu, K., Omura, T., Yoshikawa, E., Kosugi, T., Mori, S. and Yamashita, T., 1997. A high resolution animal PET scanner using compact PS-PMT detectors. *IEEE Transactions on Nuclear Science*, *44*(3), pp.1277-1282.

Weishampel, D.B., Dodson, P. and Osmólska, H. eds., 2007. *The Dinosauria*. Univ of California Press.

Willey, J.S., Biknevicius, A.R., Reilly, S.M. and Earls, K.D., 2004. The tale of the tail: limb function and locomotor mechanics in *Alligator mississippiensis*. *Journal of experimental biology*, *207*(3), pp.553-563.

Wilson, J., 2002. Sauropod dinosaur phylogeny: critique and cladistic analysis. *Zoological Journal of the Linnean Society*, *136*(2), pp.215-275.

Witmer, L.M. 1995. The extant phylogenetic bracket and the importance of reconstructing soft tissues in fossils. *Functional morphology in vertebrate paleontology*, *1*, pp.19-33.

Wright, W. G., Ivanenko, Y. P., & Gurfinkel, V. S., 2012. Foot anatomy specialization for postural sensation and control. *Journal of neurophysiology*, *107*(5), 1513-1521.

Xing, L., Li, D., Falkingham, P.L., Lockley, M.G., Benton, M.J., Klein, H., Zhang, J., Ran, H., Persons IV, W.S. and Dai, H., 2016a. Digit-only sauropod pes trackways from China–evidence of swimming or a preservational phenomenon?. *Scientific reports*, *6*, p.21138.

Xing, L., Liu, Y., Marty, D., Kuang, H., Klein, H., Persons IV, W.S. and Lyu, Y., 2017a. Sauropod trackway reflecting an unusual walking pattern from the Early Cretaceous of Shandong Province, China. *Ichnos*, *24*(1), pp.27-36.

Xing, L., Lockley, M.G., Marty, D., He, J., Hu, X., Dai, H., Matsukawa, M., Peng, G., Ye, Y., Klein, H. and Zhang, J., 2016d. Wide-gauge sauropod trackways from the Early Jurassic of Sichuan, China: oldest sauropod trackways from Asia with special emphasis on a specimen showing a narrow turn. *Swiss Journal of Geosciences*, *109*(3), pp.415-428.

Xing, L., Lockley, M.G., Marty, D., Klein, H., Buckley, L.G., McCrea, R.T., Zhang, J., Gierliński, G.D., Divay, J.D. and Wu, Q., 2013. Diverse dinosaur ichnoassemblages from the lower Cretaceous Dasheng Group in the Yishu fault zone, Shandong Province, China. *Cretaceous Research*, *45*, pp.114-134.

Xing, L., Lockley, M.G., Marty, D., Pinuela, L., Klein, H., Zhang, J. and Persons, W.S., 2015. Re-description of the partially collapsed Early Cretaceous Zhaojue dinosaur tracksite (Sichuan Province, China) by using previously registered video coverage. *Cretaceous Research*, *52*, pp.138-152.

Xing, L., Lockley, M.G., Matsukawa, M., Klein, H., Zhang, J., Wang, T., IV, W.S.P., Hu, J., Dai, H. and Hu, H., 2019c. Review and Detailed Description of Sauropod-Dominated Trackways from the Upper Cretaceous Jiangdihe Formation of Yunnan, China. *Ichnos*, *26*(2), pp.108-118.

Xing, L., Lockley, M.G., Romilio, A., Klein, H., Zhang, J., Chen, H., Zhang, J., Burns, M.E. and Wang, X., 2018. Diverse sauropod-theropod-dominated track assemblage from the Lower Cretaceous Dasheng Group of Eastern China: Testing the use of drones in footprint documentation. *Cretaceous Research*, *84*, pp.588-599.

Xing, L., Lockley, M.G., Yang, G., Cao, J., McCrea, R.T., Klein, H., Zhang, J., Persons IV, W.S. and Dai, H., 2016f. A diversified vertebrate ichnite fauna from the Feitianshan Formation (Lower Cretaceous) of southwestern Sichuan, China. *Cretaceous Research*, *57*, pp.79-89.

Xing, L., Lockley, M.G., Yang, G., Mayor, A., Klein, H., Persons IV, W.S., Chen, Y., Peng, G., Ye, Y. and Ebi, J., 2015a. Tracking a legend: an early Cretaceous sauropod trackway from Zhaojue County, Sichuan Province, southwestern China. *Ichnos*, *22*(1), pp.22-28.

Xing, L., Lockley, M.G., Zhang, J., Klein, H., Li, D., Miyashita, T., Li, Z. and Kümmell, S.B., 2016c. A new sauropodomorph ichnogenus from the Lower Jurassic of Sichuan, China fills a gap in the track record. *Historical Biology*, *28*(7), pp.881-895.

Xing, L., Lockley, M.G., Zhang, J., Klein, H., Persons IV, W.S. and Dai, H., 2014. Diverse sauropod-, theropod-, and ornithopod-track assemblages and a new ichnotaxon *Siamopodus xui ichnosp. nov.* from the Feitianshan Formation, Lower Cretaceous of Sichuan Province, southwest China. *Palaeogeography, Palaeoclimatology, Palaeoecology*, *414*, pp.79-97.

Xing, L., Lockley, M.G., Zhang, J., Romilio, A., Klein, H., Wang, Y., Tang, Y., Burns, M.E. and Wang, X., 2019b. A diversified vertebrate ichnite fauna from the Dasheng Group (Lower Cretaceous) of southeast Shandong Province, China. *Historical Biology*, *31*(3), pp.353-362.

Xing, L., Lockley, M.G., Zhang, L., Klein, H., Zheng, Y., Peng, G., Jiang, S., Dai, L. and Burns, M.E., 2019a. First Jurassic dinosaur tracksite from Guizhou Province, China: morphology, trackmaker and paleoecology. *Historical Biology*, *31*(10), pp.1423-1432.

Xing, L., Marty, D., Wang, K., Lockley, M.G., Chen, S., Xu, X., Liu, Y., Kuang, H., Zhang, J., Ran, H. and Persons IV, W.S., 2015c. An unusual sauropod turning trackway from the Early Cretaceous of Shandong Province, China. *Palaeogeography, palaeoclimatology, palaeoecology*, *437*, pp.74-84.

Xing, L., Peng, G., Lockley, M.G., Ye, Y., Klein, H., McCrea, R.T., Zhang, J. and Persons IV, W.S., 2016e. Saurischian (theropod–sauropod) track assemblages from the Jiaguan Formation in the Sichuan Basin, Southwest China: ichnology and indications to differential track preservation. *Historical Biology*, *28*(8), pp.1003-1013.

Xing, L., Yang, G., Cao, J., Lockley, M.G., Klein, H., Zhang, J., Persons IV, W.S., Hu, H., Shen, H., Zheng, X. and Qin, Y., 2015d. Cretaceous saurischian tracksites from southwest Sichuan Province and overview of Late Cretaceous dinosaur track assemblages of China. *Cretaceous Research*, *56*, pp.458-469.

Xing, L., Zhang, J., Lockley, M.G., McCrea, R.T., Klein, H., Alcalá, L., Buckley, L.G., Burns, M.E., Kümmell, S.B. and He, Q., 2015e. Hints of the early Jehol Biota: important dinosaur footprint assemblages from the Jurassic-Cretaceous Boundary Tuchengzi Formation in Beijing, China. *PloS one*, *10*(4), p.e0122715.

Xing, L.D., Lockley, M.G., Zhang, J.P., Klein, H., Wang, T., Kümmell, S.B. and Burns, M.E., 2016b. A theropod–sauropod track assemblage from the Middle–Upper Jurassic Shedian Formation at Shuangbai, Yunnan Province, China, reflecting different sizes of trackmakers: Review and new observations. *Palaeoworld*, *25*(1), pp.84-94.

Xing, L.D., Peng, G.Z., Lockley, M.G., Ye, Y., Klein, H., Zhang, J.P. and Persons IV, W.S., 2015b. Early Cretaceous sauropod and ornithopod trackways from a stream course in Sichuan Basin, Southwest China. *New Mex Mus Nat Hist Sci Bull*, *68*, pp.319-325.

Xu, C., Wen, X.X., Huang, L.Y., Shang, L., Cheng, X.X., Yan, Y.B. and Lei, W., 2017. Normal foot loading parameters and repeatability of the Footscan® platform system. *Journal of foot and ankle research*, *10*(1), p.30.

Yamashita, T., Yamashita, K., Rinoie, C., Takase, Y., Sato, M., Yamada, K. and Sawa, Y., 2019. Improvements in lower-limb muscle strength and foot pressure distribution with foot care in frail elderly adults: a randomized controlled trial from Japan. *BMC geriatrics*, *19*(1), p.83.

Young, C.C., 1941. *A Complete Osteology of Lufengosaurus Heunei Young (gen. et Sp. Nov.) from Lufeng, Yunnan, China*. Geol. Survey of China.

Young, C.C., 1947. *On Lufengosaurus magnus Young (sp. nov.) and additional finds of Lufengosaurus huenei Young*. Geol. Survey of China.

Young, M. J., Cavanagh, P. R., Thomas, G., Johnson, M. M., Murray, H., and Boulton, A. J. M., The effect of callus removal on dynamic plantar foot pressures in diabetic patients. *Diabetic Medicine 9,* 1, 55-57.

Yu, X., Wang, S., Chen, D.Y., Dodd, S., Goloshevsky, A. and Koretsky, A.P., 2010. 3D mapping of somatotopic reorganization with small animal functional MRI. *Neuroimage*, *49*(2), pp.1667-1676.

Zhang, J., Li, D., Li, M., Lockley, M.G. and Bai, Z., 2006. Diverse dinosaur-, pterosaur-, and bird-track assemblages from the Hakou Formation, Lower Cretaceous of Gansu Province, northwest China. *Cretaceous Research*, *27*(1), pp.44-55.

Zhang, Y., Huang, W., Hayashi, C., Gatesy, J. and McKittrick, J., 2018. Microstructure and mechanical properties of different keratinous horns. *Journal of the Royal Society Interface*, *15*(143), p.20180093.

Zhang, R., Han, D., Ma, S., Luo, G., Ji, Q., Xue, S., Yang, M., and Li, J., 2017. Plantar pressure distribution of ostrich during locomotion on loose sand and solid ground. *PeerJ,* 5, e3613.

Zheng, Z., 1996. *Cranial anatomy of Shunosaurus and Camarasaurus (Dinosauria: Sauropoda) and the phylogeny of the Sauropoda* (Doctoral dissertation, Texas Tech University).

Zou, J., Poe, D., Bjelke, B. and Pyykkö, I., 2009. Visualization of inner ear disorders with MRI in vivo: from animal models to human application. *Acta Oto-Laryngologica*, *129*(560), pp.22-31.

Zurriaguz, V.L. and Cerda, I.A., 2017. Caudal pneumaticity in derived titanosaurs (Dinosauria: Sauropoda). *Cretaceous Research*, *73*, pp.14-24.

Supplementary Material

Chapter 2 Supplementary Material

The following supplementary material contains the following:

1. Supplementary tables, showing phylogenetic comparative methods tests, alongside body mass tests – using generalised least squares to establish the roles of phylogeny and body mass in determining the correlations found in Chapter 2,

tables with raw data and their regressions, tables with latin and common names for taxa, and tables showing data for regressions for large and small animals, as well as the fossil test using *Plateosaurus engelhardti.*

2. Supplementary graphs showing Chapter 2 data for different poses, as well as data for subgroups based on foot posture, overall posture, ecology, and phylogeny.
3. Outlines for the foot alpha shapes generated via matlab, for each animal.

Supplementary Tables

Supplementary Table S2.1 – Phylogenetic and Body Mass Comparative GLS Tests for All Limbs

		PIC			PGLS	
Analysis	Correlation at Intercept	CI	SE	T value	P Value	Lambda
Pose 1	-0.15	1.693	0.094	18.02	0	1.027319
Pose 2	-0.05	1.294	0.099	13.02	0	1.030825

Analysis	Correlation at Intercept	CI	SE	T value	P Value
Pose 1 with Body Mass	0.35	0	0	0.37	0.72
Pose 2 with Body Mass	0.42	0	0	3.15	0

Supplementary Table S2.2 – Area (mm2) Measurements for All Animals and Proportions of Skeleton to Skin Surface Area (%)

Pose 1

Specimen	Fore/Hind Foot	Skin SA	Skel SA	Skeleton as % of Skin
Salamandra salamandra	Forefoot	88.93501	52.14457	58.6322122
Salamandra salamandra	Hindfoot	124.8898	59.64688	47.75962093
Cryptobranchus alleganiensis	Forefoot	181.4453	82.04254	45.21613433
Cryptobranchus alleganiensis	Hindfoot	311.3837	103.9794	33.39268462
Brachycephlus nodoterga	Forefoot	1.6515	0.852027	51.59112909
Brachycephlus nodoterga	Hindfoot	3.39012	1.973128	58.20229633
Sphenodon punctatus	Forefoot	962.9668	447.0096	46.42004335
Sphenodon punctatus	Hindfoot	960.4319	487.3412	50.74188493
Crocodylus niloticus	Forefoot	553.7884	162.1849	29.28643561
Crocodylus niloticus	Hindfoot	1228.612	566.4358	46.10373211
Osteolaemus teraspis	Forefoot	1733.117	962.1605	55.51618621
Osteolaemus teraspis	Hindfoot	3678.328	2070.685	56.29419196
Caiman crocodilus	Hindfoot	1902.971	935.316	49.15029816
Crocodylus moreletii	Forefoot	3619.647	1447.981	40.00337567
Crocodylus moreletii	Hindfoot	6721.266	3618.094	53.83053494
Alectoris chukar	Hindfoot	451.7428	318.1106	70.4185217
Tyto alba	Hindfoot	721.4122	475.5846	65.92411232
Pica pica	Hindfoot	382.6398	222.9701	58.2715291
Columba livia	Hindfoot	397.7637	236.5437	59.46839319
Coturnix coturnix	Hindfoot	404.1557	334.2137	82.69428892
Accipiter nisus	Hindfoot	262.7824	189.0737	71.95065971
Dromaius novaehollandiae	Hindfoot	8524.232	5689.942	66.75019735
Bos taurus	Forefoot	15663.52	7659.069	48.8974879
Bos taurus	Hindfoot	12739.92	5669.063	44.49841375
Elephas maximus	Forefoot	115297.7	47094.3	40.84583773
Elephas maximus	Hindfoot	106205	62562.12	58.90696806
Ceratotherium simum	Forefoot	52322.45	37586.9	71.8370514
Ceratotherium simum	Hindfoot	43938.84	32640.53	74.28627909
Vicugna pacos	Forefoot	3879.717	2447.911	63.09507459
Vicugna pacos	Hindfoot	3737.41	1889.661	50.56071099
Giraffa camelopardalis	Forefoot	28591.02	10324.47	36.11087691
Giraffa camelopardalis	Hindfoot	21393.04	8422.208	39.36892218
Panthera leo persica	Forefoot	9849.389	8485.304	86.15055843
Panthera leo persica	Hindfoot	7690.173	5819.748	75.6777249
Felis catus	Forefoot	651.6308	367.1313	56.34038863
Felis catus	Hindfoot	724.9928	446.6624	61.6092115

Equus ferus caballus	Forefoot	16103.96	6521.98	40.49922225
Equus ferus caballus	Hindfoot	14886.19	5258.705	35.32606867
Sus scrofa	Forefoot	5833.796	3301.937	56.60015442
Sus scrofa	Hindfoot	5410.751	3703.087	68.43944159
Cervus elaphus	Forefoot	3876.212	2398.473	61.87673137
Cervus elaphus	Hindfoot	3644.912	2343.958	64.30766863
Equus quagga	Forefoot	10510.49	3188.5	30.33636481
Equus quagga	Hindfoot	10438.59	3927.968	37.62927945
Camelus dromedarius	Unassigned	25222.78	12990.49	51.50299004
Vulpes vulpes	Forefoot	939.0155	575.1637	61.25178197
Vulpes vulpes	Hindfoot	974.4242	759.2161	77.91433447
Hippopotamus amphibius	Forefoot	40556.15	19879.08	49.01619162
Hippopotamus amphibius	Hindfoot	43485.7	19909.79	45.78468328
Pose 2				
Salamandra salamandra	Forefoot	88.93501	52.14457	58.6322122
Salamandra salamandra	Hindfoot	118.7929	58.1717	48.9690014
Cryptobranchus alleganiensis	Forefoot	179.4845	75.75179	42.2052092
Cryptobranchus alleganiensis	Hindfoot	398.9009	121.8758	30.55289108
Brachycephlus nodoterga	Forefoot	1.6515	0.852027	51.59112909
Brachycephlus nodoterga	Hindfoot	3.39012	1.973128	58.20229633
Sphenodon punctatus	Forefoot	962.9668	394.6228	40.97989334
Sphenodon punctatus	Hindfoot	960.432	467.5052	48.67655561
Crocodylus niloticus	Forefoot	553.7884	162.1849	29.28643561
Crocodylus niloticus	Hindfoot	1228.612	566.4358	46.10373211
Osteolaemus teraspis	Forefoot	1733.117	962.1605	55.51618621
Osteolaemus teraspis	Hindfoot	3678.328	2070.685	56.29419196
Caiman crocodilus	Hindfoot	1902.971	935.316	49.15029816
Crocodylus moreletii	Forefoot	3619.647	1447.981	40.00337567
Crocodylus moreletii	Hindfoot	6721.266	3618.094	53.83053494
Alectoris chukar	Hindfoot	463.5517	312.3395	67.37963874
Tyto alba	Hindfoot	721.4122	475.5846	65.92411232
Pica pica	Hindfoot	398.4393	221.1307	55.49920666
Columba livia	Hindfoot	430.617	254.0651	59.00024677
Coturnix coturnix	Hindfoot	374.0761	306.0736	81.82121905
Accipiter nisus	Hindfoot	262.7824	189.0737	71.95065971
Dromaius novaehollandiae	Hindfoot	7189.013	4273.903	59.45048029
Bos taurus	Forefoot	14860.38	4672.811	31.44475656
Bos taurus	Hindfoot	12400.11	3656.876	29.49067084
Elephas maximus	Forefoot pose 2a	115297.7	21888.71	18.98452046
Elephas maximus	Hindfoot pose 2a	106205	16361.32	15.40542458
Elephas maximus	Forefoot pose 2b	115297.7	53085.99	46.04255484

Elephas maximus	Hindfoot pose 2b	106205	39665.72	37.34827271
Elephas maximus	Forefoot pose 2c	115297.7	85872.49	74.47894594
Elephas maximus	Hindfoot pose 2c	106205	64990.32	61.19330515
Ceratotherium simum	Forefoot pose 2a	40263.47	15929.85	39.56403613
Ceratotherium simum	Hindfoot pose 2a	43571.67	14885.36	34.1629407
Ceratotherium simum	Forefoot pose 2b	50319.26	38994.05	77.49327689
Ceratotherium simum	Hindfoot pose 2b	43938.84	31147.23	70.88768228
Ceratotherium simum	Forefoot pose 2c	40263.47	40068.14	99.51486813
Ceratotherium simum	Hindfoot pose 2c	43571.67	43695.43	100.2840375
Vicugna pacos	Forefoot	3651.553	2680.183	73.39842765
Vicugna pacos	Hindfoot	3349.815	2141.799	63.93783478
Giraffa camelopardalis	Forefoot	28591.02	10324.47	36.11087691
Giraffa camelopardalis	Hindfoot	21393.04	8422.208	39.36892218
Panthera leo persica	Forefoot	9849.389	9416.026	95.60010391
Panthera leo persica	Hindfoot	7690.173	6969.753	90.63193541
Felis catus	Forefoot	651.6308	367.1313	56.34038863
Felis catus	Hindfoot	680.9717	412.0175	60.50435475
Equus ferus caballus	Forefoot	16103.96	4560.854	28.3213136
Equus ferus caballus	Hindfoot	14886.19	3679.188	24.71545112
Sus scrofa	Forefoot	2182.029	665.3783	30.49356342
Sus scrofa	Hindfoot	1730.437	621.656	35.92479041
Cervus elaphus	Forefoot	2213.147	556.7199	25.15511885
Cervus elaphus	Hindfoot	1835.489	631.2443	34.39107695
Equus quagga	Forefoot	9146.338	1911.856	20.902962
Equus quagga	Hindfoot	7881.42	1775.487	22.5275036
Camelus dromedarius	Unassigned	19383.7	9322.263	48.09331236
Vulpes vulpes	Forefoot	939.0155	789.1365	84.03871265
Vulpes vulpes	Hindfoot	974.4242	958.9808	98.41512652
Hippopotamus amphibius	Forefoot pose 2a	40263.47	15929.85	39.56403613
Hippopotamus amphibius	Hindfoot pose 2a	43571.67	14885.36	34.1629407
Hippopotamus amphibius	Forefoot pose 2b	40263.47	34742	86.28665173
Hippopotamus amphibius	Hindfoot pose 2b	43571.67	29026.14	66.61700047
Hippopotamus amphibius	Forefoot pose 2c	40263.47	40068.14	99.51486813
Hippopotamus amphibius	Hindfoot pose 2c	43571.67	43695.43	100.2840375

Supplementary Table S2.3 - Body Mass for Each Subject Animal and Source of Data

Species	Body Mass (g)	Source
Salamandra salamandra	19.1	Encyclopedia of Life

Cryptobranchus alleganiensis	358	Encyclopedia of Life
Brachycephalus nodoterga	1	Pires Jr et al, 2005 (Toxicon, vol. 45, issue 1, 73-79)
Sphenodon punctatus	700	Animal Diversity Web
Caiman crocodilus	2174	Hutchinson metadata (Crocbase)
Osteolaemus tetraspis	7820	Hutchinson metadata (Cocbase)
Crocodylus moreletii	14150	Hutchinson metadata (Crocbase)
Crocodylus niloticus	1336	Hutchinson metadata (Crocbase)
Dromaius novaehollandiae	34200	CRC Handbook of Avian Body Masses
Columba livia	358.7	Encyclopedia of Life
Pica pica	151.3865	Encyclopedia of Life
Tyto alba	520	Animal Diversity Web
Accipiter nisus	237.5	CRC Handbook of Avian Body Masses
Coturnix coturnix	112.5	Encyclopedia of Life
Alectoris chukar	503.5	CRC Handbook of Avian Body Masses
Elephas maximus	3269794.34	Pantheria
Camelus dromedarius	492714.47	Pantheria
Vicugna pacos	64900	Pantheria
Sus scrofa domesticus	84471.54	Pantheria
Hippopotamus amphibius	1536310.4	Pantheria
Cervus elaphus	240867.13	Pantheria
Bos taurus	618642.42	Pantheria
Giraffa camelopardalis	964654.73	Pantheria
Vulpes vulpes	4820.36	Pantheria
Panthera leo persica	158623.93	Pantheria
Felis catus	2884.8	Pantheria
Equus quagga	400000	Pantheria
Equus ferus caballus	403598.53	Pantheria
Ceratotherium simum	2285939.43	Pantheria

Supplementary Table S2.4 – Slope Uncertainties for all Poses and Combinations of Limbs

	All Limbs 1	Forelimbs 1	Hindlimbs 1	All Limbs 2a	Forelimbs 2a	Hindlimbs 2a
Slope	1.83	2.05	1.66	3.82	3.74	4.08
Uncertainty (Slope)	0.07	0.14	0.05	0.28	0.42	0.42
Correlation Coefficient (R^2)	0.94	0.92	0.97	0.80	0.82	0.79
F Statistic	700.03	217.89	1006.50	182.37	80.86	95.99
Regression of Sum of Squares	2.62E+10	1.33E+10	1.27E+10	2.16E+10	1.13E+10	1.03E+10

Y-Intercept	551.14	-127.88	756.10	-2637.39	-2776.37	-2629.16
Uncertainty (Y-Intercept)	992.47	2047.32	742.55	1908.16	3271.67	2369.49
Standard Error for Y Estimate	6114.66	7825.46	3557.13	10892.56	11822.08	10379.59
Degrees of Freedom	47.00	18.00	26.00	47.00	18.00	26.00
Residual Sum of Squares	1.76E+09	1.10E+09	3.29E+08	5.58E+09	2.52E+09	2.80E+09

	All Limbs 2b	**Forelimbs 2b**	**Hindlimbs 2b**	**All Limbs 2c**	**Forelimbs 2c**	**Hindlimbs 2c**
Slope	1.83	1.71	2.03	1.27	1.23	1.32
Uncertainty (Slope)	0.10	0.14	0.14	0.05	0.07	0.08
Correlation Coefficient (R^2)	0.89	0.89	0.89	0.93	0.95	0.92
F Statistic	367.33	151.26	213.21	648.43	345.79	289.64
Regression of Sum of Squares	2.47E+10	1.29E+10	1.17E+10	2.54E+10	1.31E+10	1.21E+10
Y-Intercept	618.26	900.74	43.67	1652.98	1986.94	1142.07
Uncertainty (Y-Intercept)	1325.83	2363.94	1571.50	986.25	1534.95	1335.15
Standard Error for Y Estimate	8205.80	9233.32	7419.28	6255.62	6162.94	6452.82
Degrees of Freedom	47.00	18.00	26.00	47.00	18.00	26.00
Residual Sum of Squares	3.16E+09	1.53E+09	1.43E+09	1.84E+09	6.84E+08	1.08E+09

Supplementary Table S2.5 – List of Taxa Used with Common Names and Latin Names

Latin Name	**Common Name**
Salamandra salamandra	Salamandra
Cryptobranchus alleganiensis	Hellbender
Brachycephalus nodoterga	Saddleback Toad
Sphenodon punctatus	Tuatara
Caiman crocodilus	Nile Crocodile
Osteolaemus tetraspis	Dwarf Crocodile
Crocodylus moreletii	Spectacled Caiman
Crocodylus niloticus	Morelet's Crocodile
Dromaius novaehollandiae	Chukar

Columba livia	Barn Owl
Pica pica	Magpie
Tyto alba	Pigeon
Accipiter nisus	Quail
Coturnix coturnix	Sparrowhawk
Alectoris chukar	Emu
Elephas maximus	Cow
Camelus dromedarius	Elephant
Vicugna pacos	Rhinoceros
Sus scrofa domesticus	Alpaca
Hippopotamus amphibius	Giraffe
Cervus elaphus	Lion
Bos taurus	Cat
Giraffa camelopardalis	Horse
Vulpes vulpes	Pig
Panthera leo persica	Deer
Felis catus	Zebra
Equus quagga	Camel
Equus ferus caballus	Fox
Ceratotherium simum	Hippopotamus

Supplementary Table S2.6 – Examples of Results with Large and Small Animals Removed

	R Squared	Equation	Multiplier
Original Data	0.9877	y=0.5901x0.9865	1.671751
Without Largest	0.9848	y=0.6225x0.9777	1.569478
Without Smallest	0.9754	y=0.7582x0.9592	1.265102
Without Largest and Smallest	0.9636	y=0.969x0.9257	0.955315

Supplementary Table S2.7 – Example of Study Utility Using *Plateosaurus engelhardti*

Plateosaurus	Skeleton	Skin (Combined Estimate)	Skin (Manus and Pes Distinct)
Manus Area	0.0194	0.032398	0.0388
Pes Area	0.0605	0.101035	0.0968
Manus as % of Pes	32.0661157	32.0661157	40.08264

Plateosaurus		
	Body Mass (N)	7384
	CoM (%GAD)	20.43

	Manus Load	1508.5512
	Pes Load	5875.4488
Combined	Manus Pressure	46563.09649
	Pes Pressure	58152.6085
Separate	Manus Pressure	38880.18557
	Pes Pressure	60696.78512

Skeleton	Area	Load	Pressure
Manus	0.0194	1508.5512	77760.37
Pes	0.0605	5875.4488	97114.86
Manus as % of Pes	32.0661157	25.67550584	80.07052

Combined (Skin)	Area	Load	Pressure
Manus	0.032398	1508.5512	46563.1
Pes	0.101035	5875.4488	58152.61
Manus as % of Pes	32.0661157	25.67550584	80.07052

Separate (Skin)	Area	Load	Pressure
Manus	0.0388	1508.5512	38880.19
Pes	0.0968	5875.4488	60696.79
Manus as % of Pes	40.08264463	25.67550584	64.05642

Supplementary References

Myers, P., Espinosa, R., Parr, C.S., Jones, T., Hammond, G.S. and Dewey, T.A., 2006. The animal diversity web. *Accessed October*, *12*(2006), p.2.

Dunning Jr, John B. *CRC Handbook of Avian Body Masses*. CRC press, 1992.

Hutchinson, J. R.. *Crocbase.* DOI 10.17605/OSF.IO/X38NH

Jones, Kate E., Jon Bielby, Marcel Cardillo, Susanne A. Fritz, Justin O'Dell, C. David L. Orme, Kamran Safi, Wes Sechrest, Elizabeth H. Boakes, and Chris Carbone. "PanTHERIA: A Species-Level Database of Life History, Ecology, and Geography of Extant and Recently Extinct Mammals." *Ecology* 90, no. 9 (2009): 2648–2648.

Pires Jr, Osmindo R., Antonio Sebben, Elisabeth F. Schwartz, Rodrigo AV Morales, Carlos Bloch Jr, and Carlos A. Schwartz. "Further Report of the Occurrence of

Tetrodotoxin and New Analogues in the Anuran Family Brachycephalidae." *Toxicon* 45, no. 1 (2005): 73–79.

Wilson, Edward O. "The Encyclopedia of Life." *Trends in Ecology & Evolution* 18, no. 2 (2003): 77–80.

Supplementary Graphs

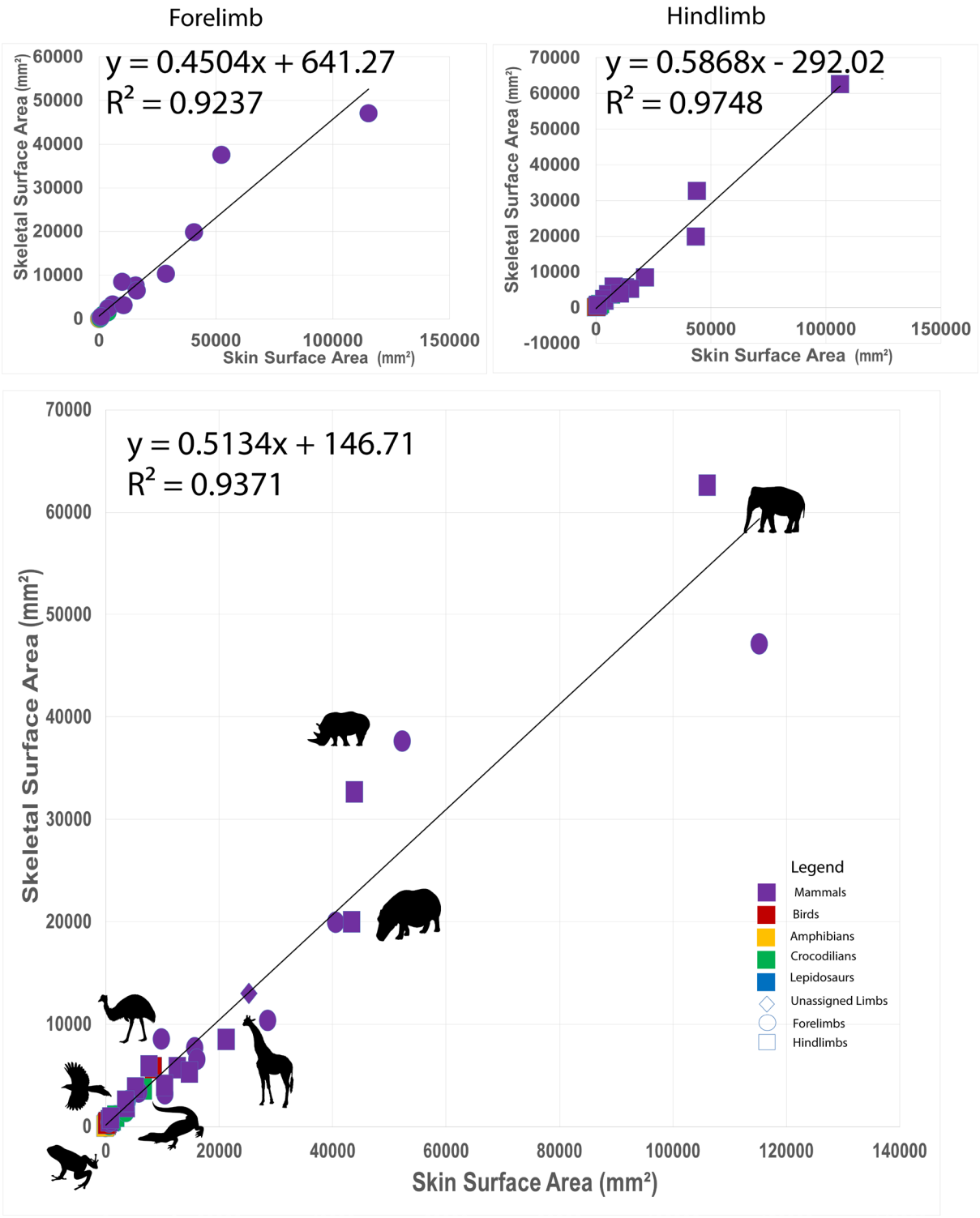

Figure S2.1 Linear plots for projected skin surface area against projected skeletal surface area in pose

1, for forelimbs, hindlimbs, and all limbs. Silhouettes from Phylopic.

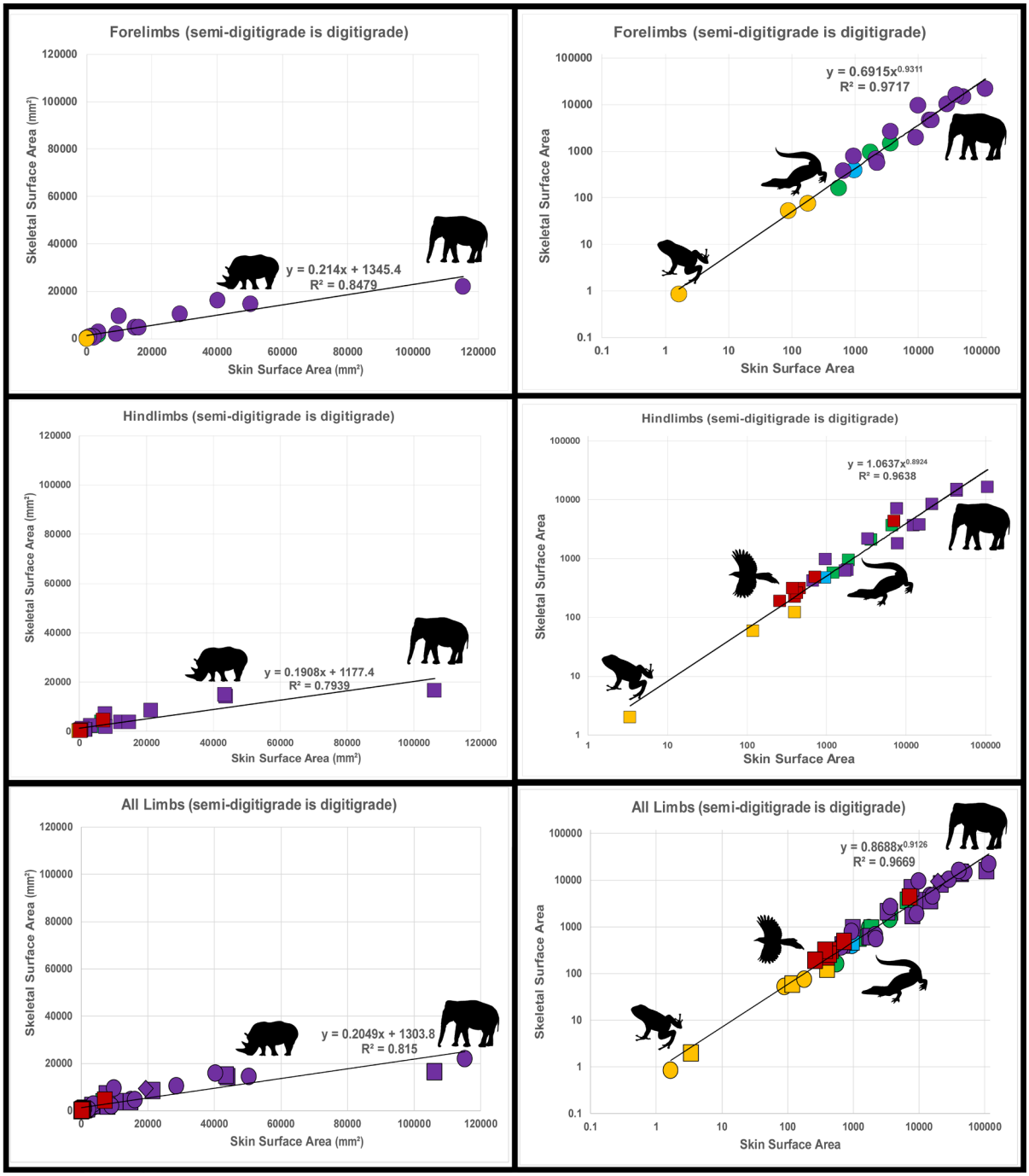

Figure S2.2 Linear and Log10-transformed plots for projected skin surface area against projected

skeletal surface area, in pose 2a, for forelimbs, hindlimbs, and all limbs. Silhouettes from Phylopic.

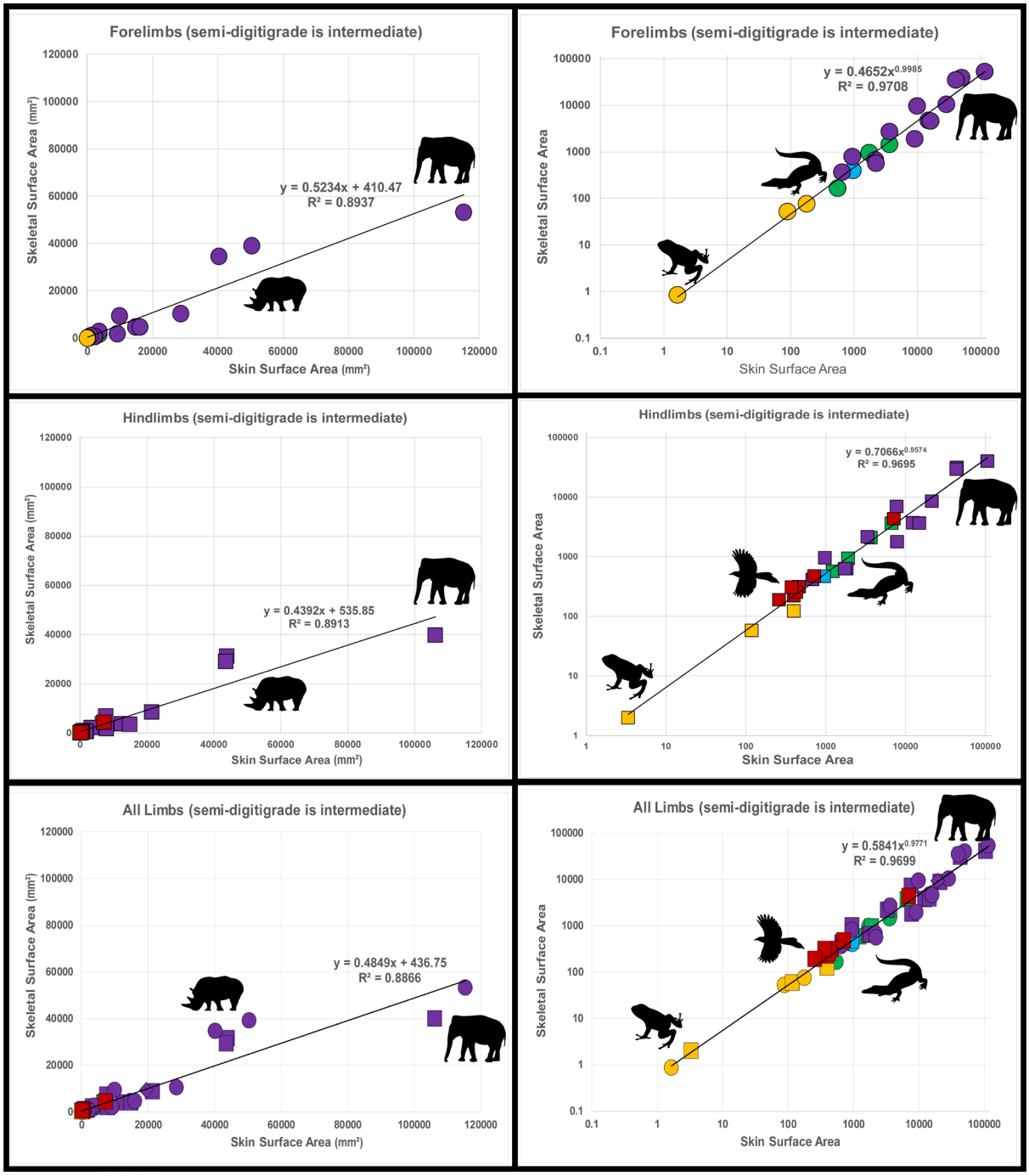

Figure S2.3 Linear and Log10-transformed plots for projected skin surface area against projected

skeletal surface area, in pose 2b, for forelimbs, hindlimbs, and all limbs. Silhouettes from Phylopic.

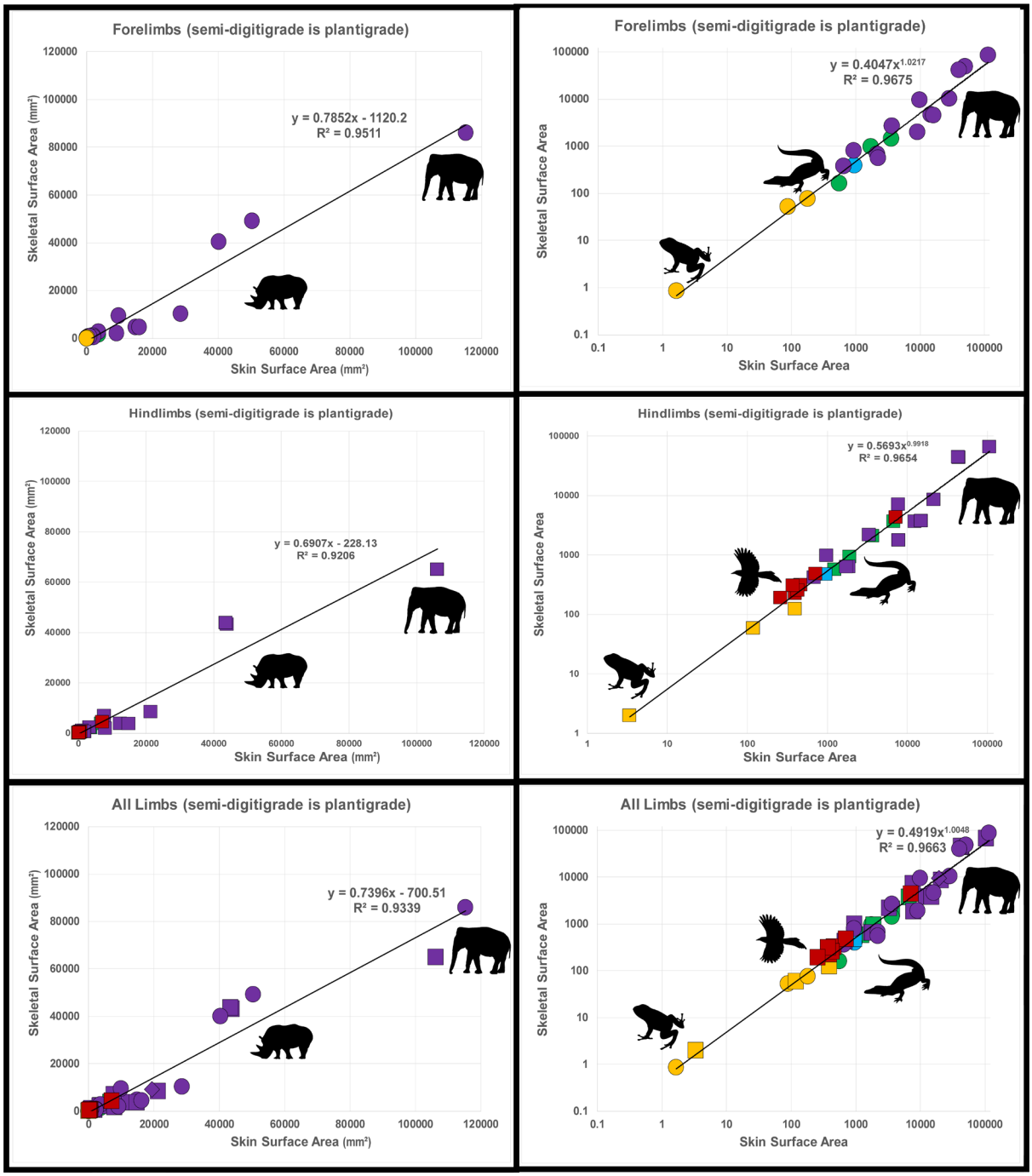

Figure S2.4 Linear and Log10-transformed plots for projected skin surface area against projected

skeletal surface area, in pose 2c, for forelimbs, hindlimbs, and all limbs. Silhouettes from Phylopic.

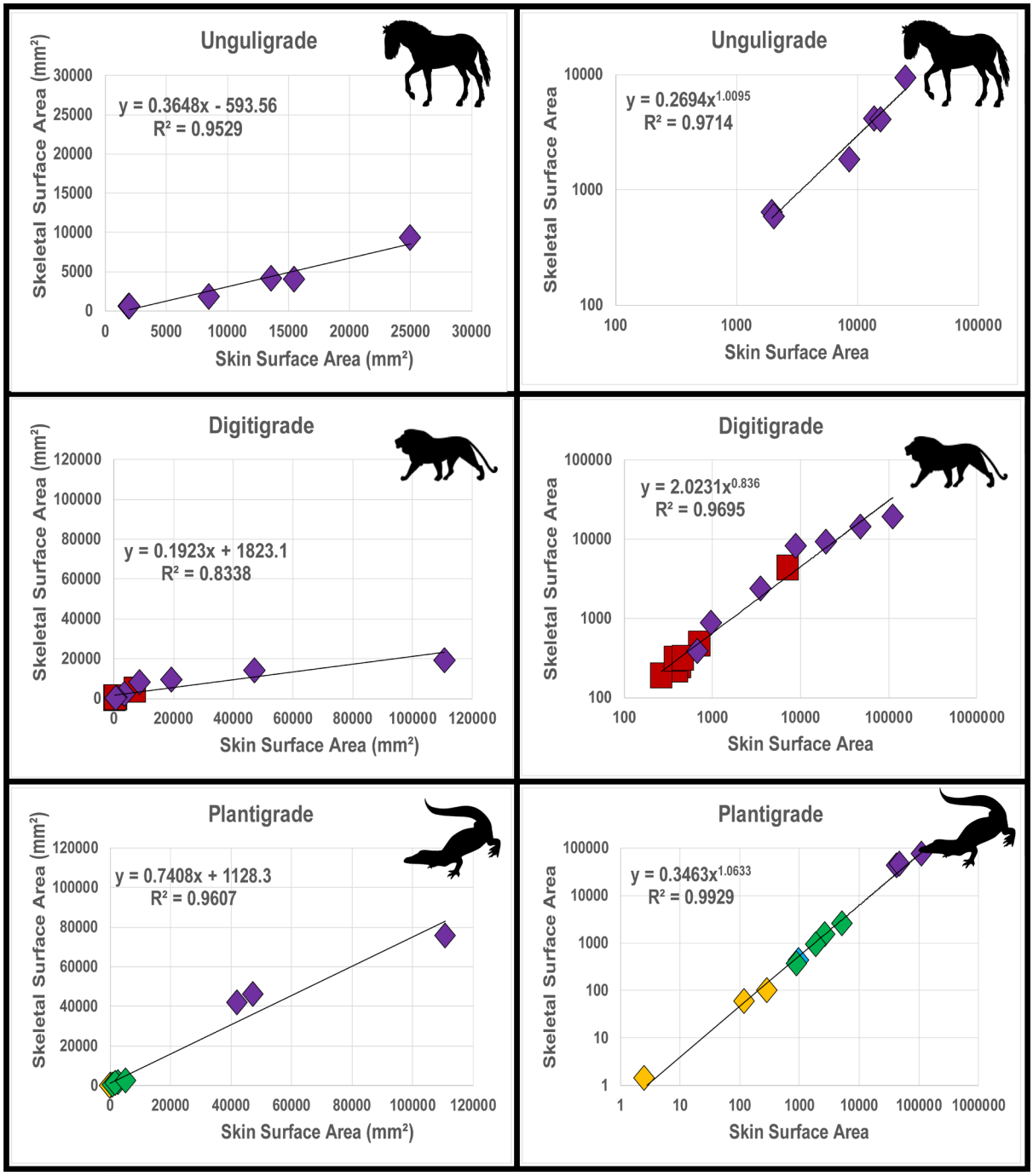

Figure S2.5 Linear and Log10-transformed plots for locomotor mode sub-analysis of projected skin

surface area against projected skeletal surface area, in pose 2. Silhouettes from Phylopic.

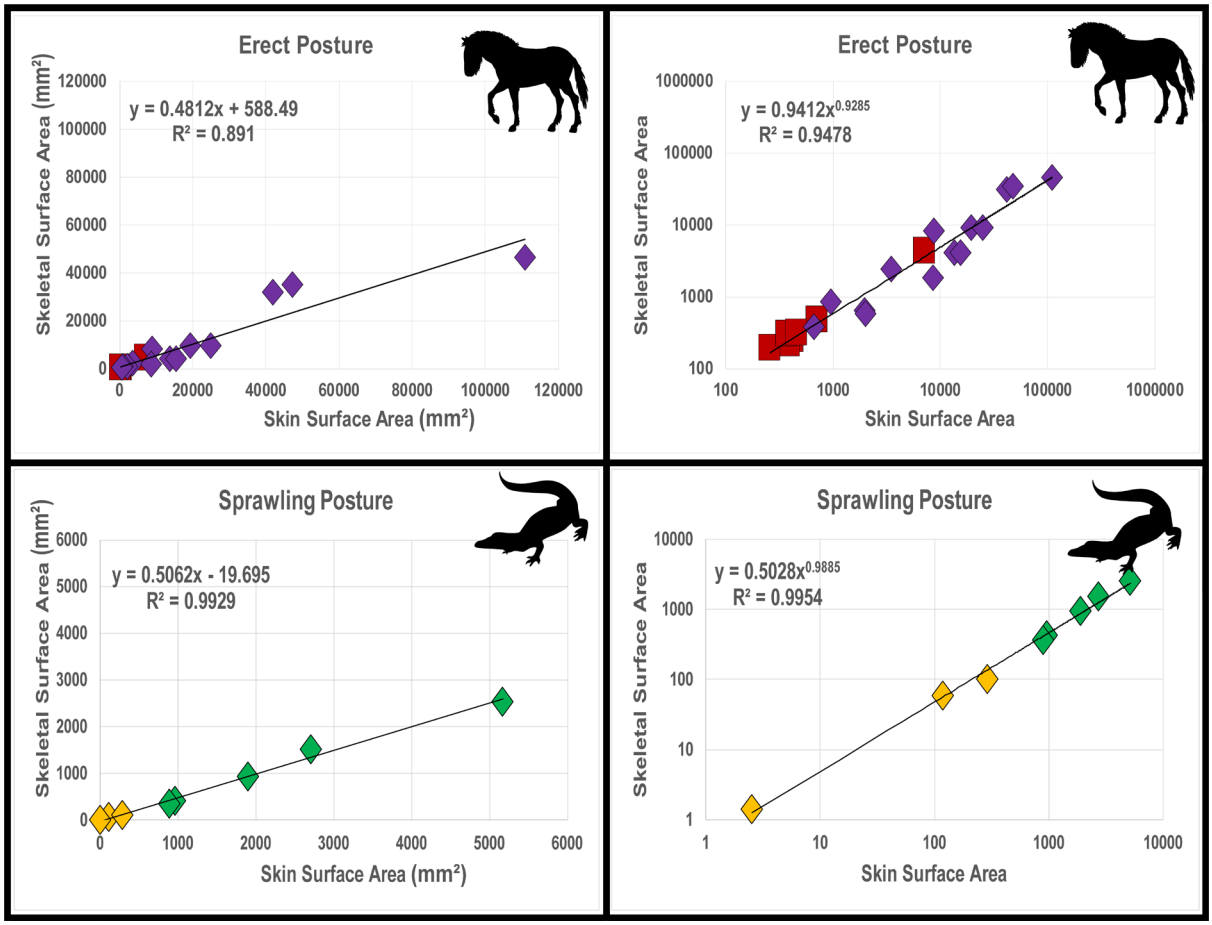

Figure S2.6 Linear and Log10-transformed plots for posture sub-analysis of projected skin surface area

against projected skeletal surface area, in pose 2. Silhouettes from Phylopic.

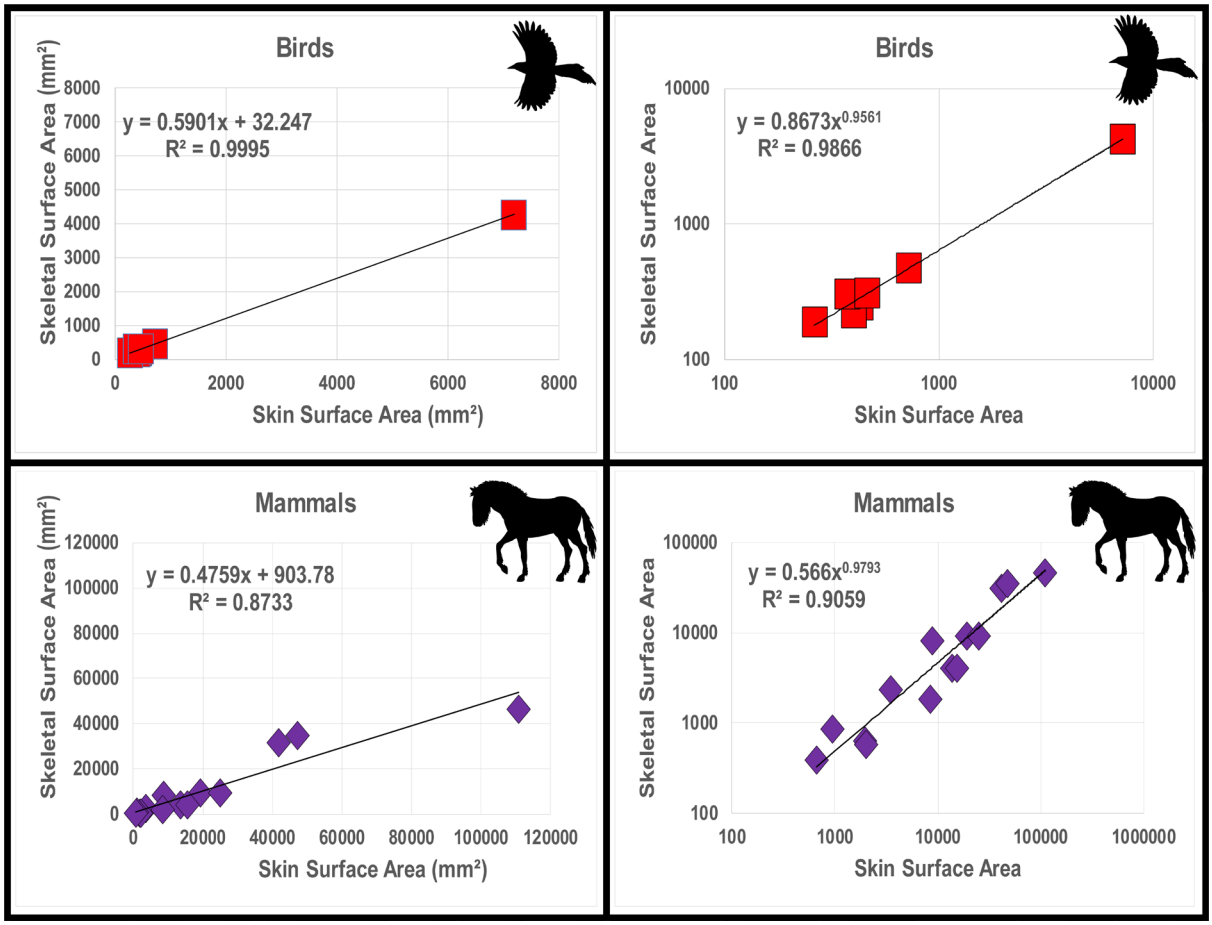

Figure S2.7 Linear and Log10-transformed plots for clade-based sub-analysis of projected skin surface area against projected skeletal surface area, in pose 2. Silhouettes from Phylopic.

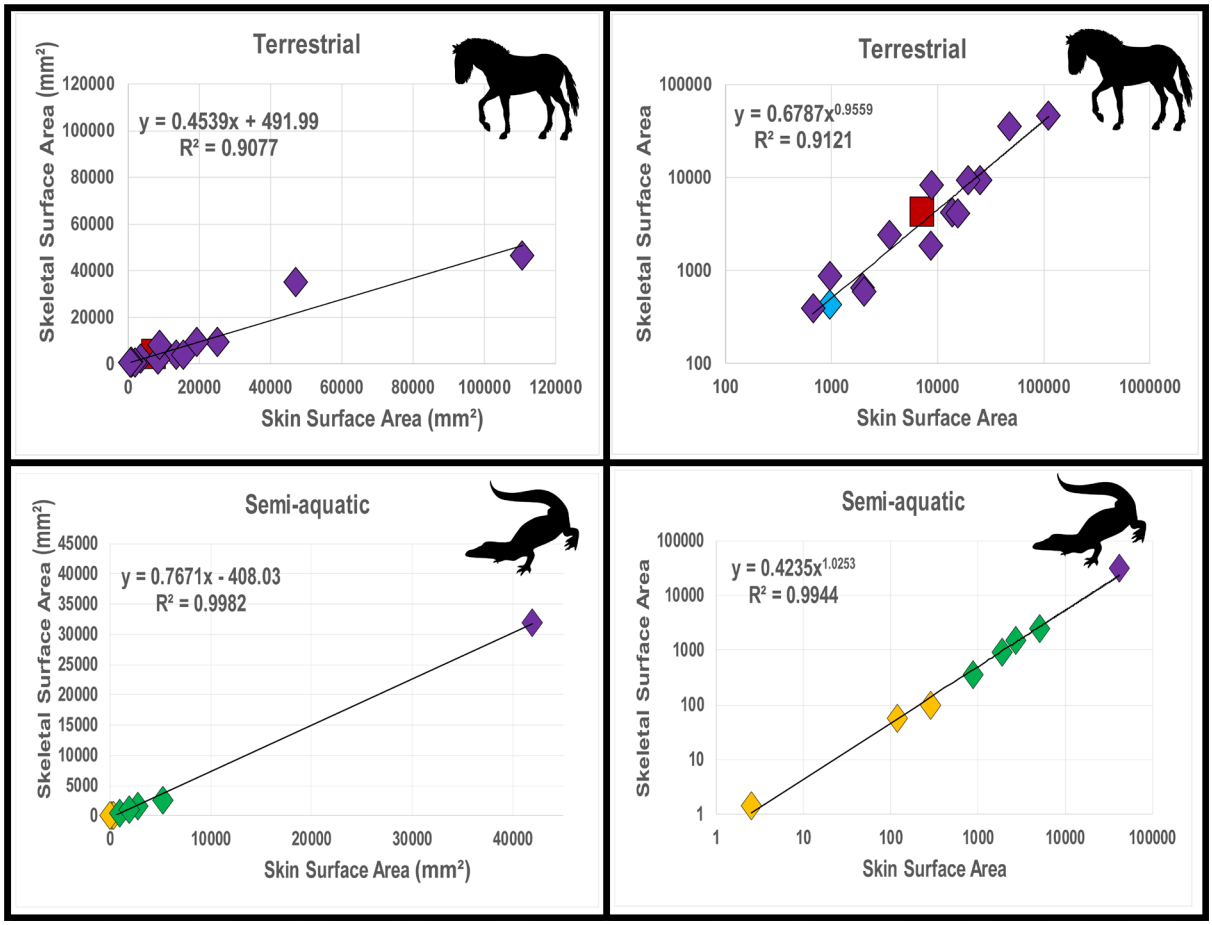

Figure S2.8 Linear and Log10-transformed plots for ecological sub-analysis of projected skin surface area against projected skeletal surface area, in pose 2. Silhouettes from Phylopic.

Presented below are the alpha shape outlines generated via matlab. Outlines are presented for skin surface area and skeletal area in pose 1 (approximate life position), and skeletal outlines for pose 2 (bones laid flat on the horizontal plane).

In some cases (e.g. many crocodilians), pose 1 and pose 2 were identical, as the foot bones are horizontal in both poses.

Large digitigrade/sub-unguligrade animals (Elephant, Hippo, and Rhino) which in life walk on a large fatty pad beneath the foot, had skeletal areas calculated in Pose 2 from just the digits (Pose 2a, as digitigrade), the digits and metatarsals/metacarpals (Pose2b, intermediate) and from the entire Pes/Manus (Pose 2c, as plantigrade).

All units are in mm, except the Tuatara where units are in 0.1mm.

Mammals

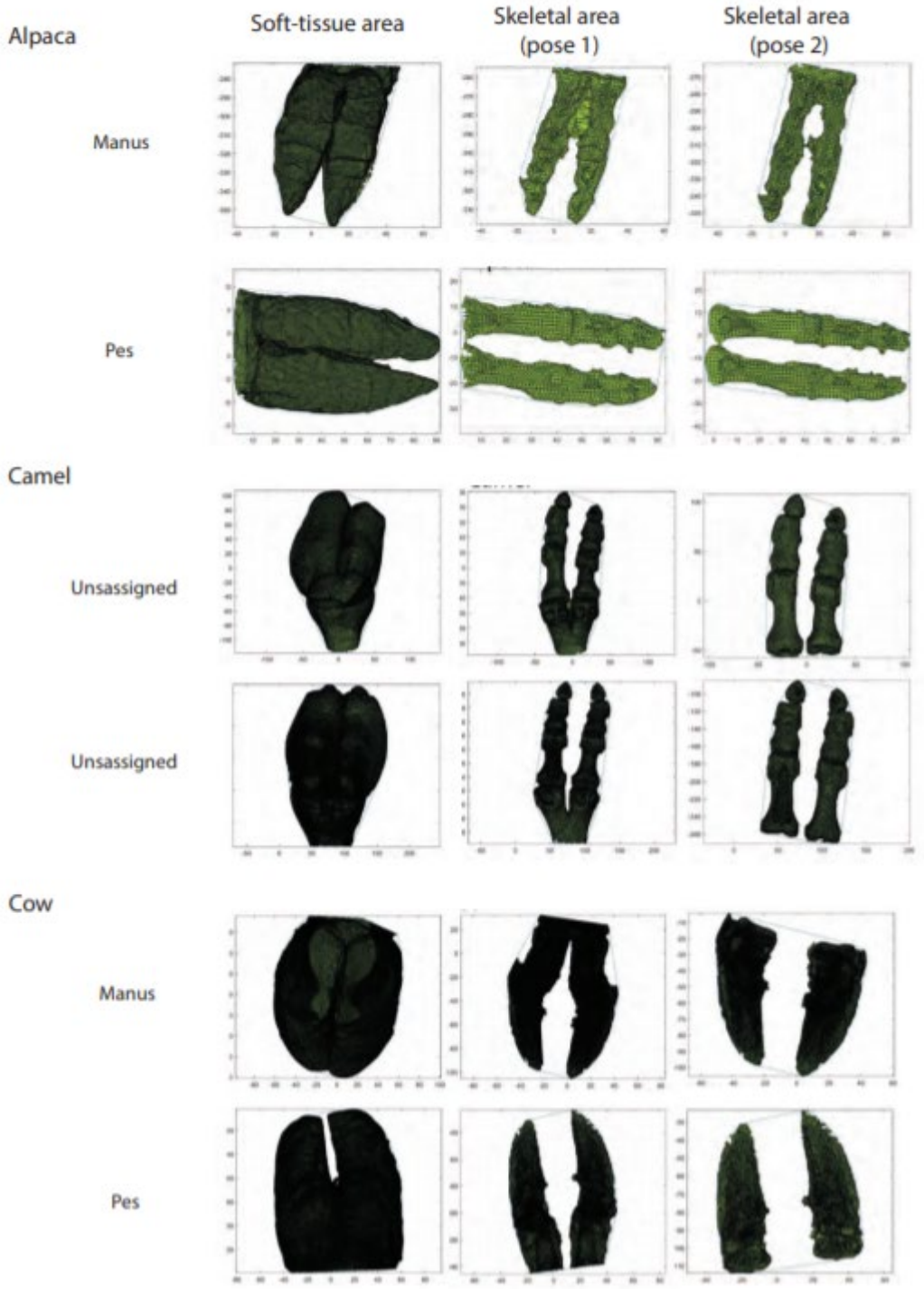
Alpaca
Soft-tissue area
Skeletal area (pose 1)
Skeletal area (pose 2)
Manus
Pes
Camel
Unsassigned
Unsassigned
Cow
Manus
Pes

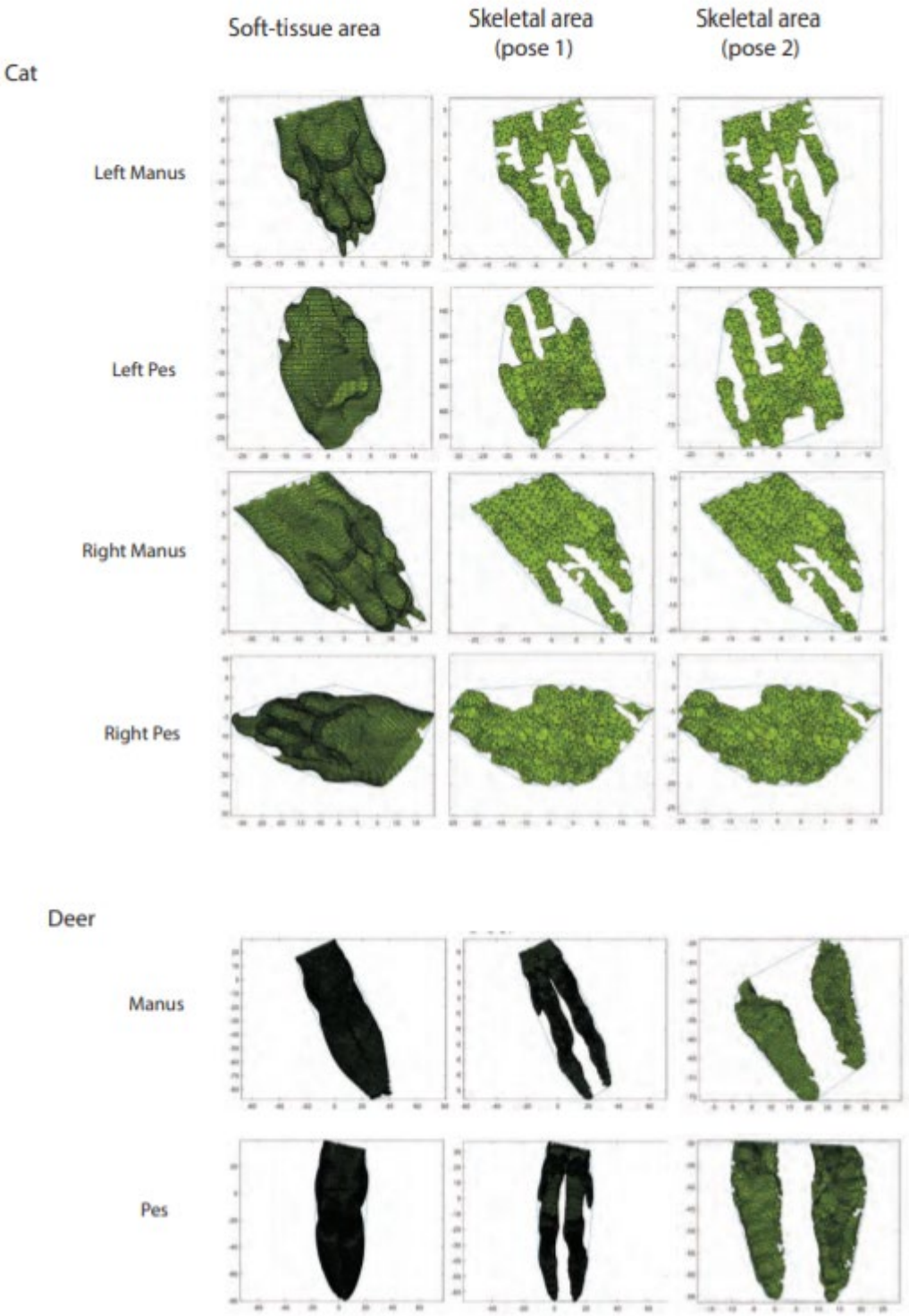
Soft-tissue area
Skeletal area (pose 1)
Skeletal area (pose 2)
Cat
Left Manus
Left Pes
Right Manus
Right Pes
Deer
Manus
Pes

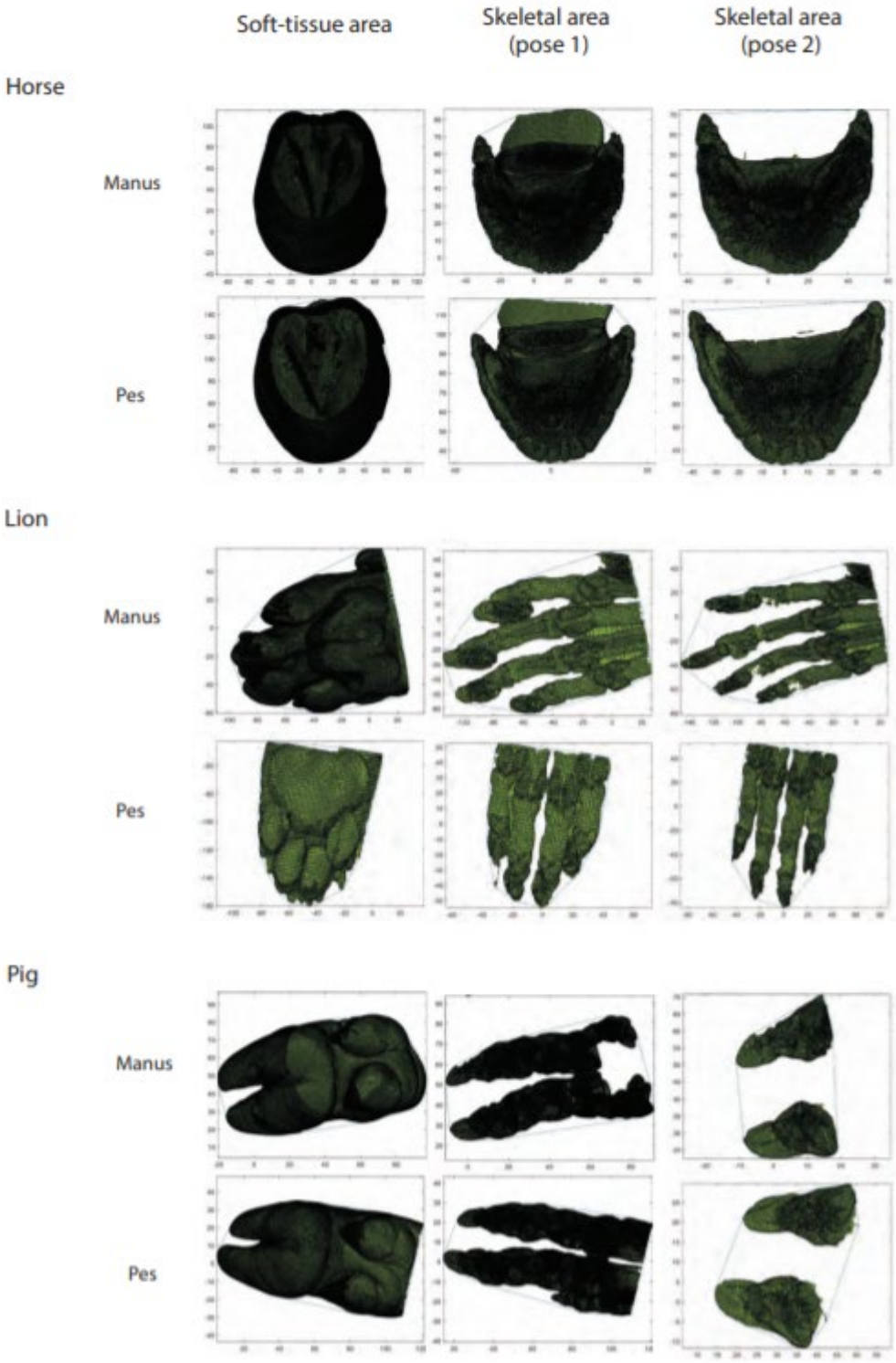
Soft-tissue area
Skeletal area (pose 1)
Skeletal area (pose 2)
Horse
Manus
Pes
Lion
Manus
Pes
Pig
Manus
Pes

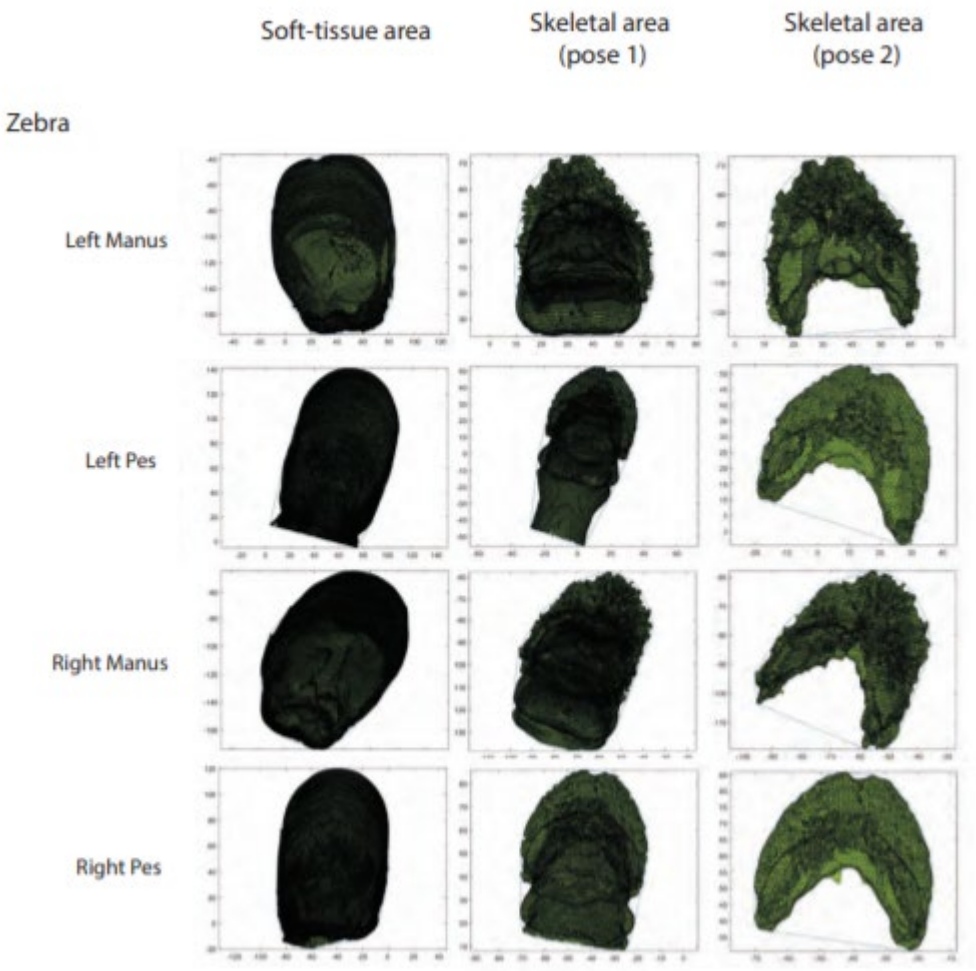
Soft-tissue area
Skeletal area (pose 1)
Skeletal area (pose 2)
Zebra
Left Manus
Left Pes
Right Manus
Right Pes

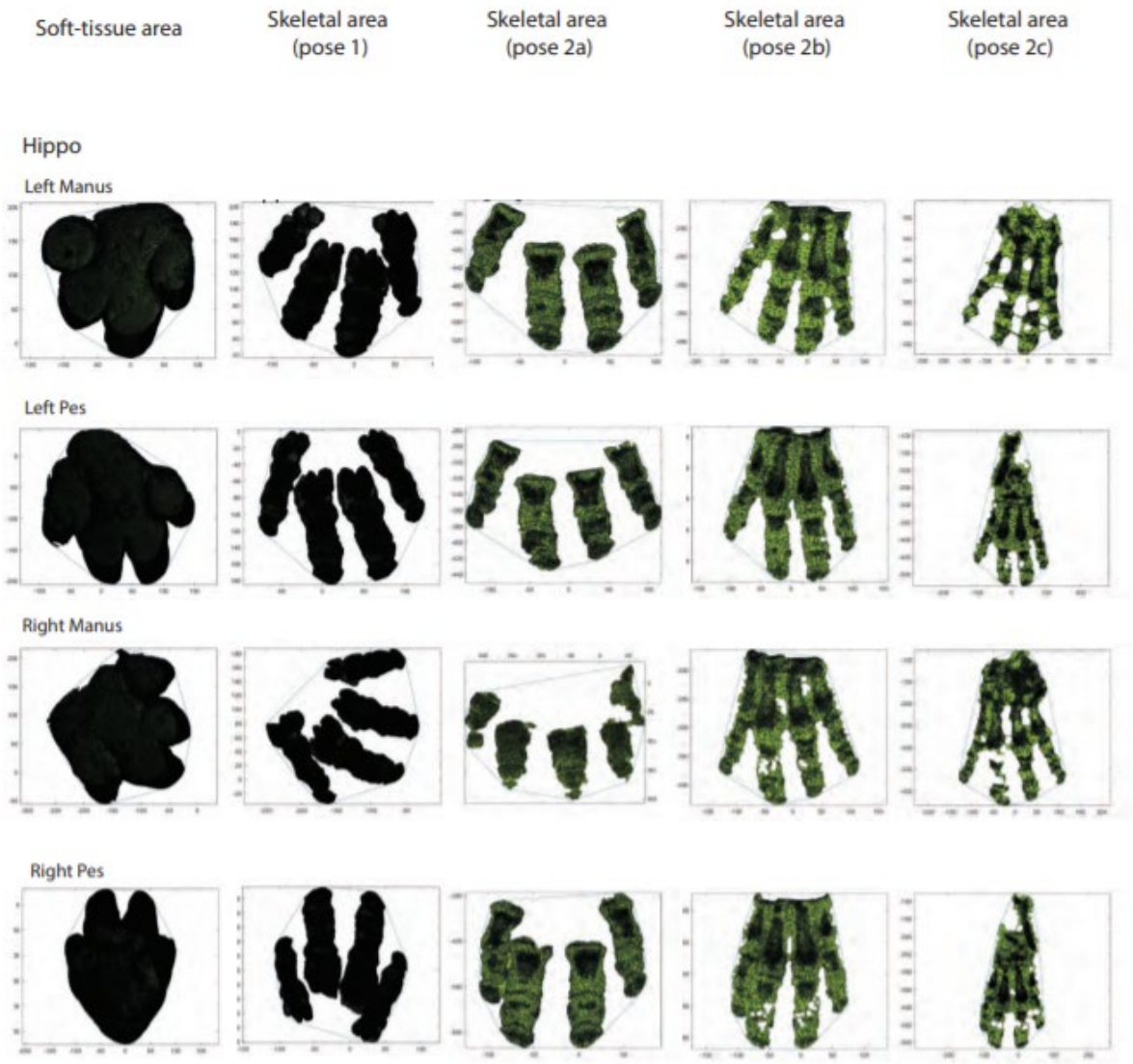
Soft-tissue area
Skeletal area (pose 1)
Skeletal area (pose 2a)
Skeletal area (pose 2b)
Skeletal area (pose 2c)
Hippo
Left Manus
Left Pes
Right Manus
Right Pes

Soft-tissue area	Skeletal area (pose 1)	Skeletal area (pose 2a)	Skeletal area (pose 2b)	Skeletal area (pose 2c)

Elephant

Manus

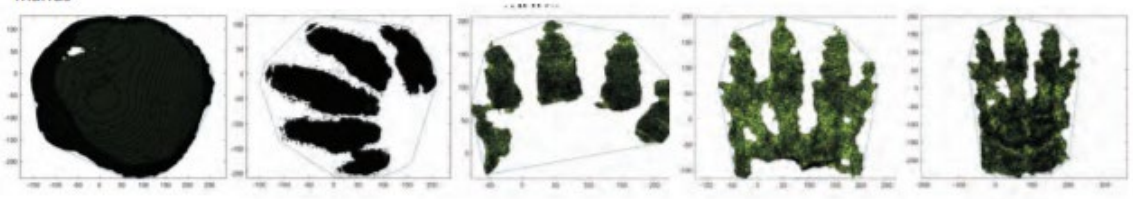

Pes

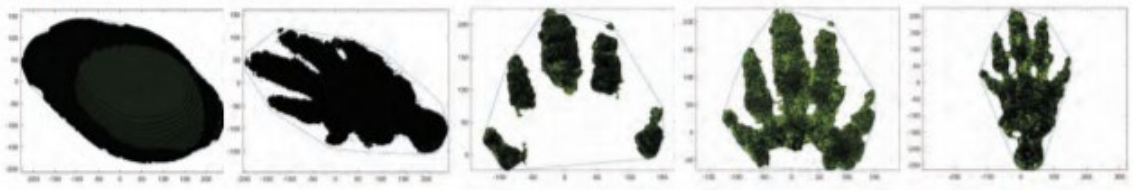

Rhino

Manus

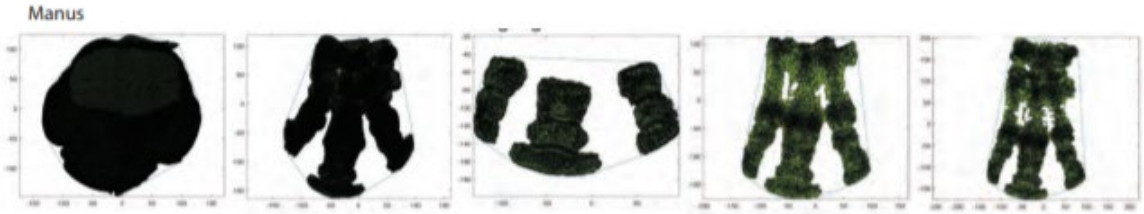

Pes

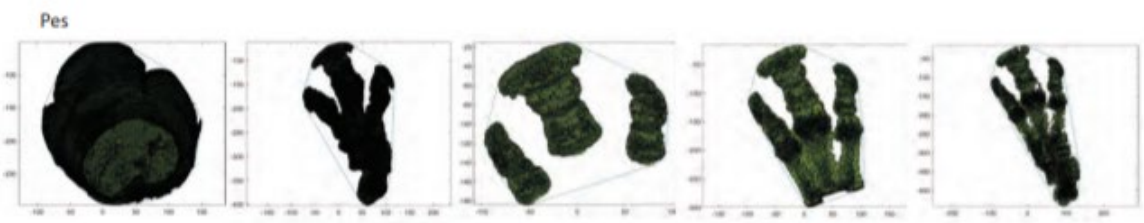

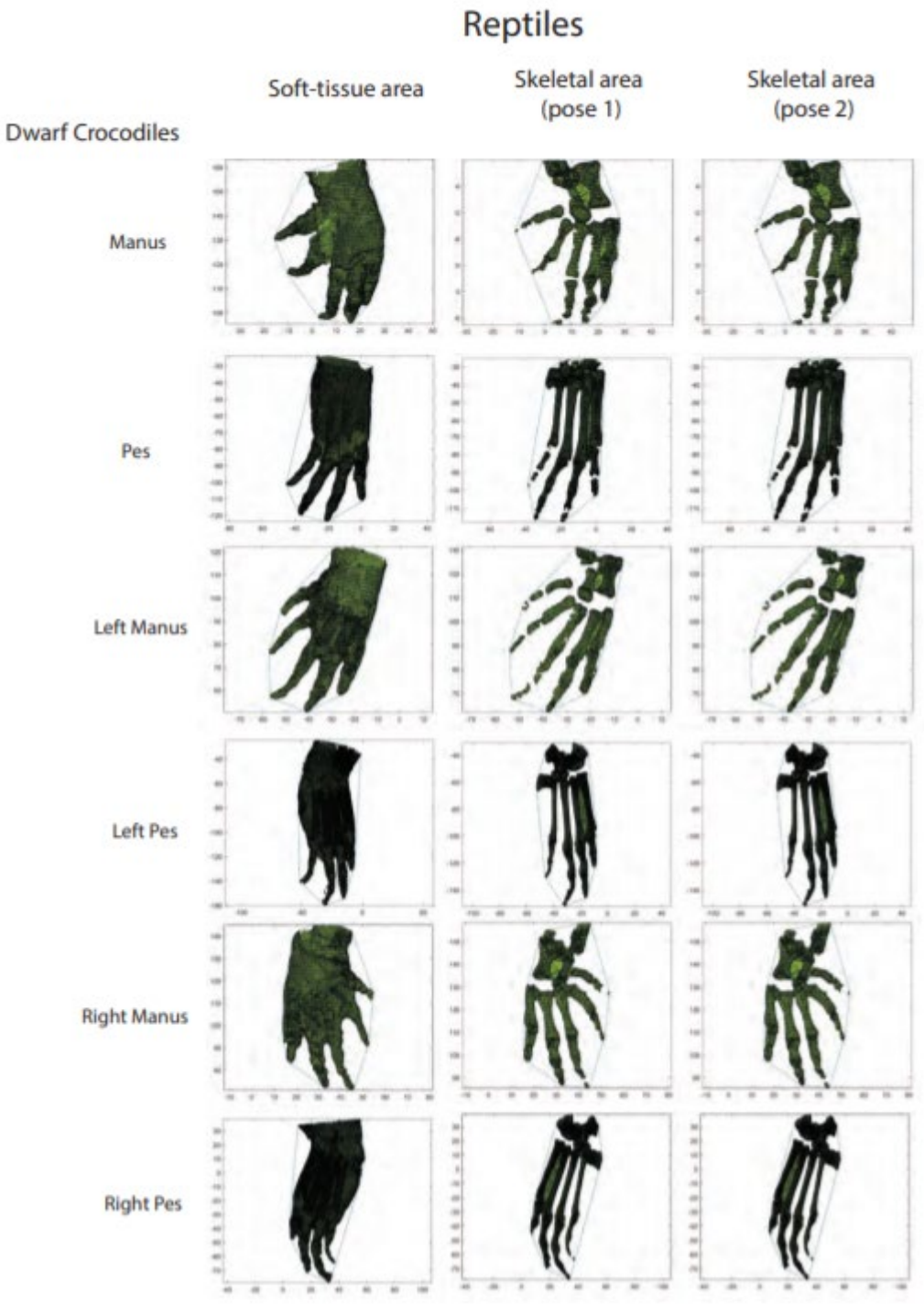
Reptiles
Soft-tissue area
Skeletal area (pose 1)
Skeletal area (pose 2)
Dwarf Crocodiles
Manus
Pes
Left Manus
Left Pes
Right Manus
Right Pes

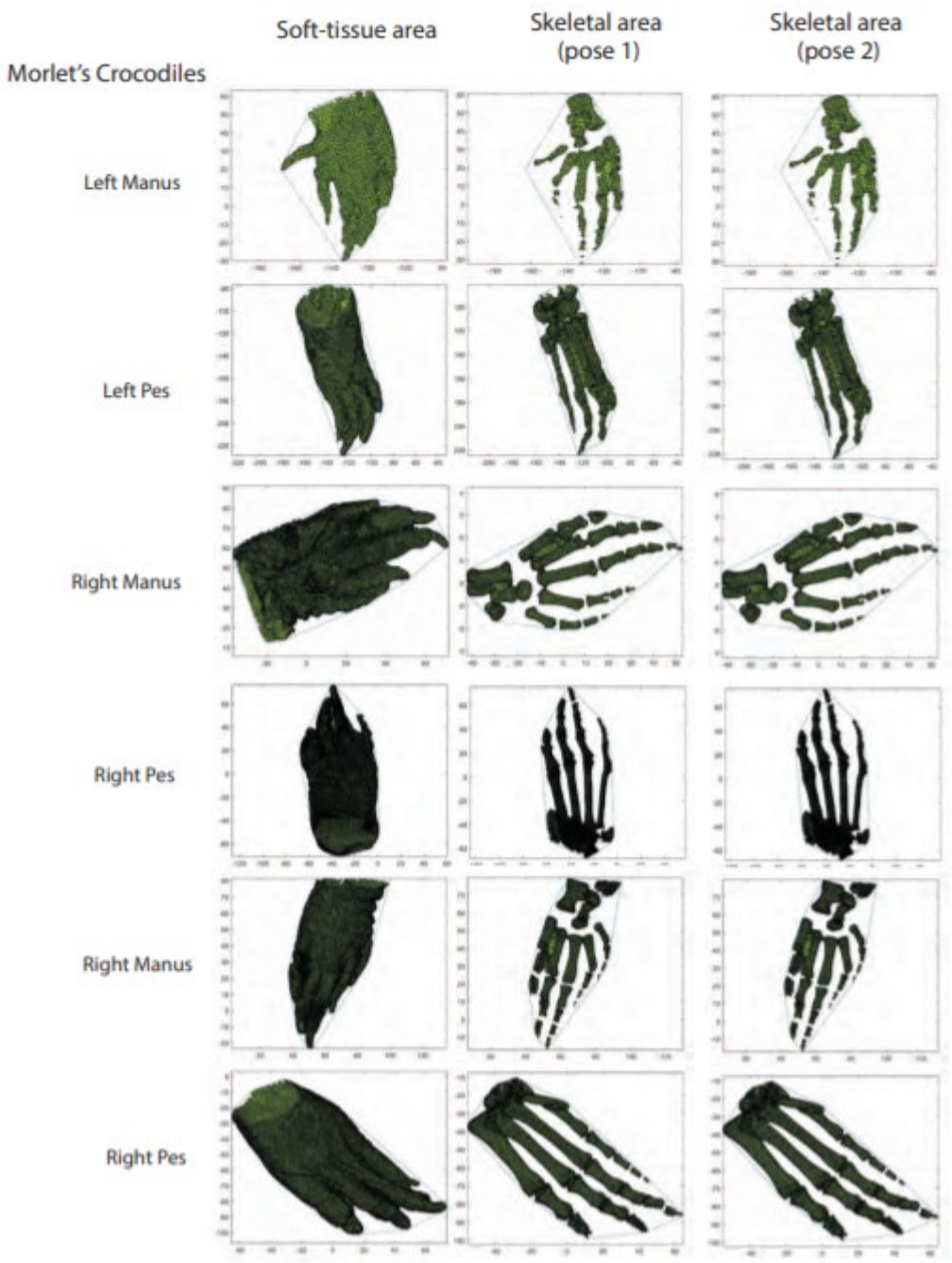
Soft-tissue area
Skeletal area (pose 1)
Skeletal area (pose 2)
Morlet's Crocodiles
Left Manus
Left Pes
Right Manus
Right Pes
Right Manus
Right Pes

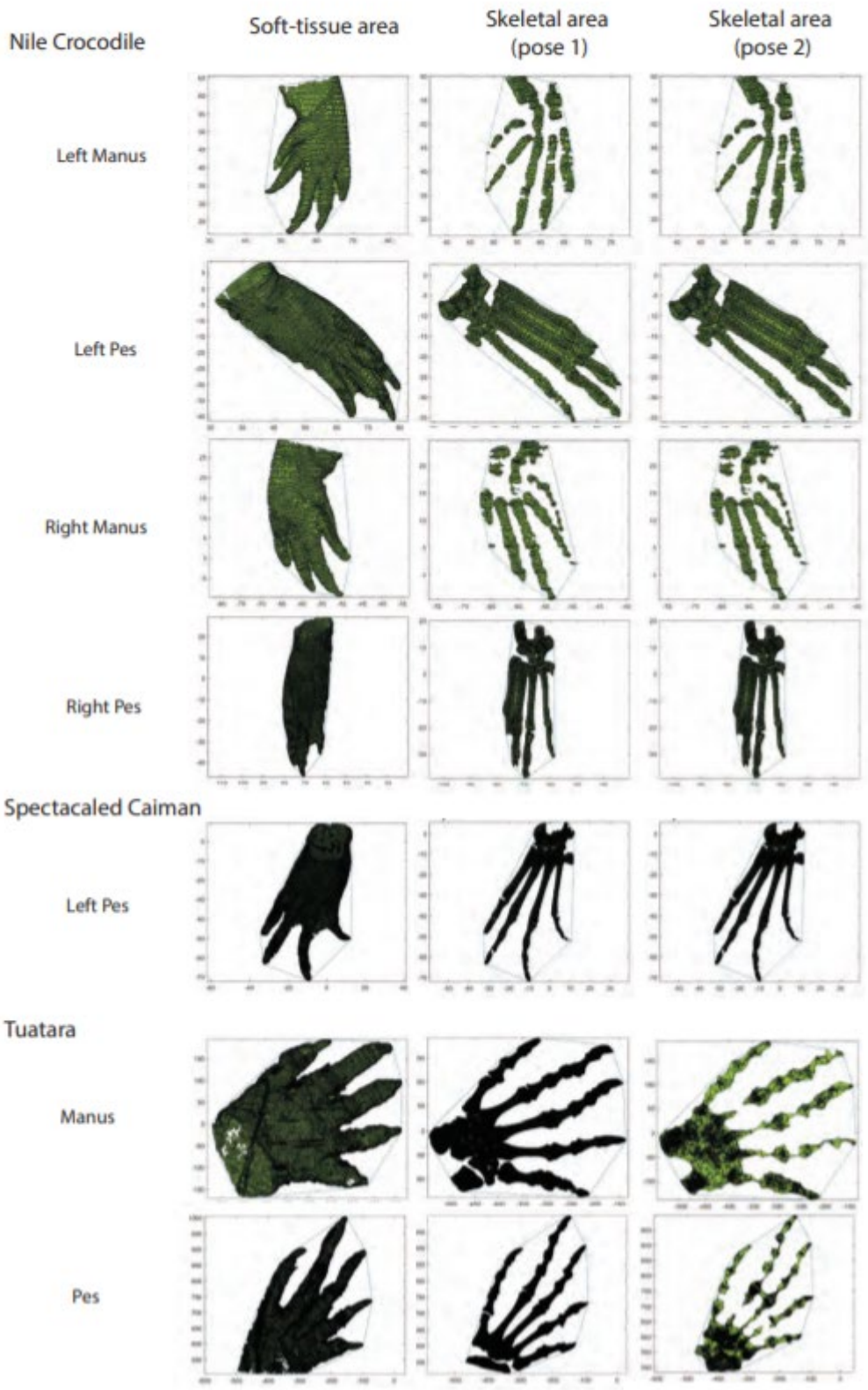
Nile Crocodile
Soft-tissue area
Skeletal area (pose 1)
Skeletal area (pose 2)
Left Manus
Left Pes
Right Manus
Right Pes
Spectacaled Caiman
Left Pes
Tuatara
Manus
Pes

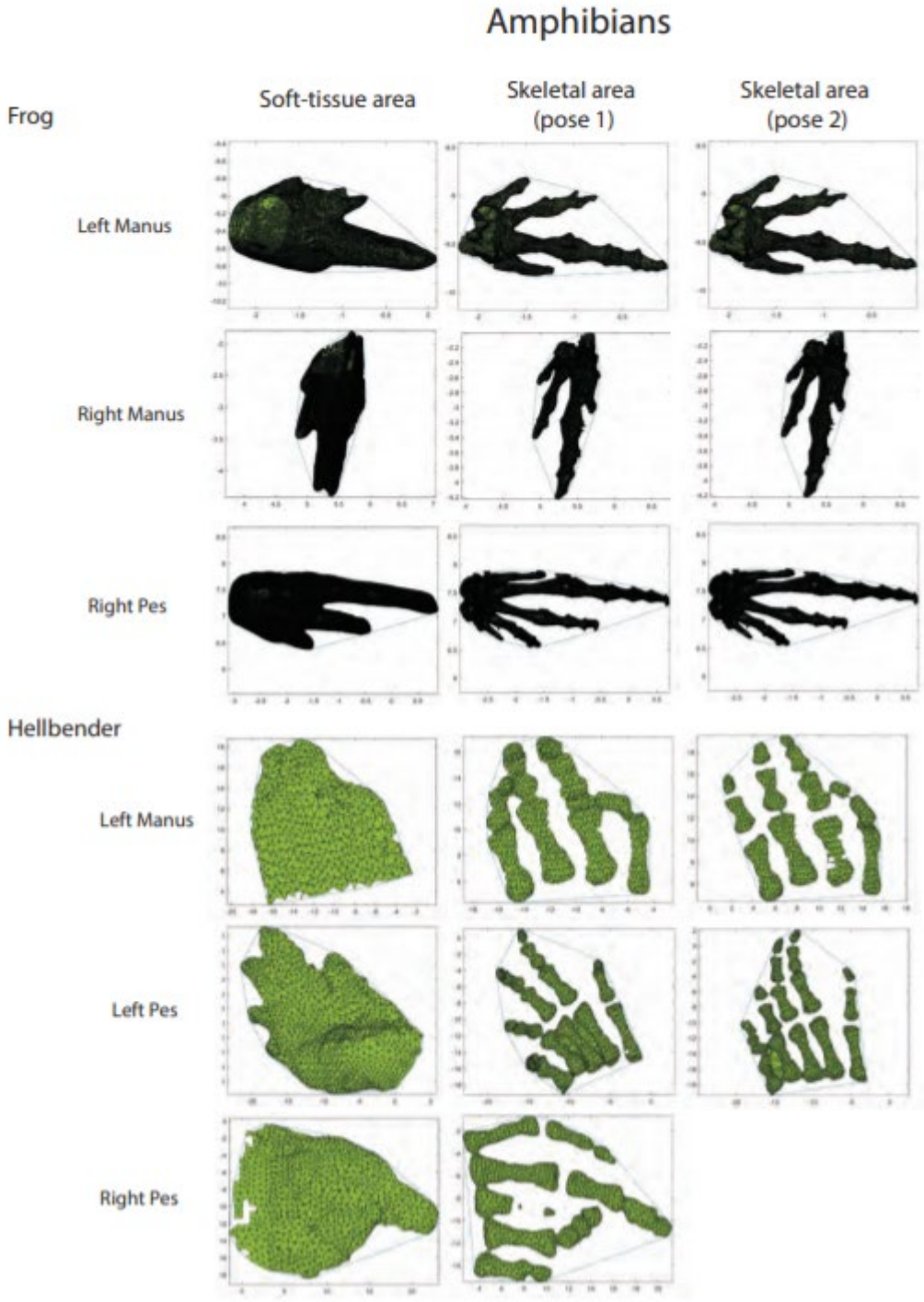
Amphibians
Soft-tissue area
Skeletal area (pose 1)
Skeletal area (pose 2)
Frog
Left Manus
Right Manus
Right Pes
Hellbender
Left Manus
Left Pes
Right Pes

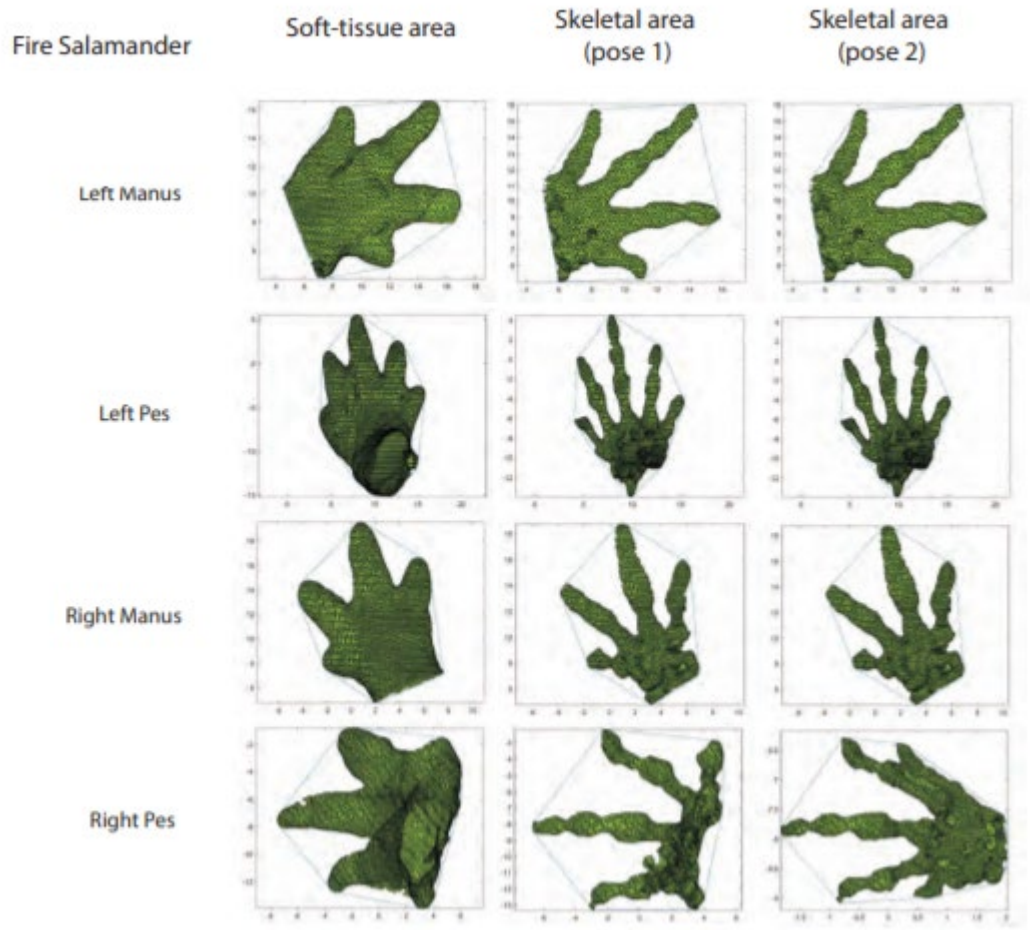
Fire Salamander
Soft-tissue area
Skeletal area (pose 1)
Skeletal area (pose 2)
Left Manus
Left Pes
Right Manus
Right Pes

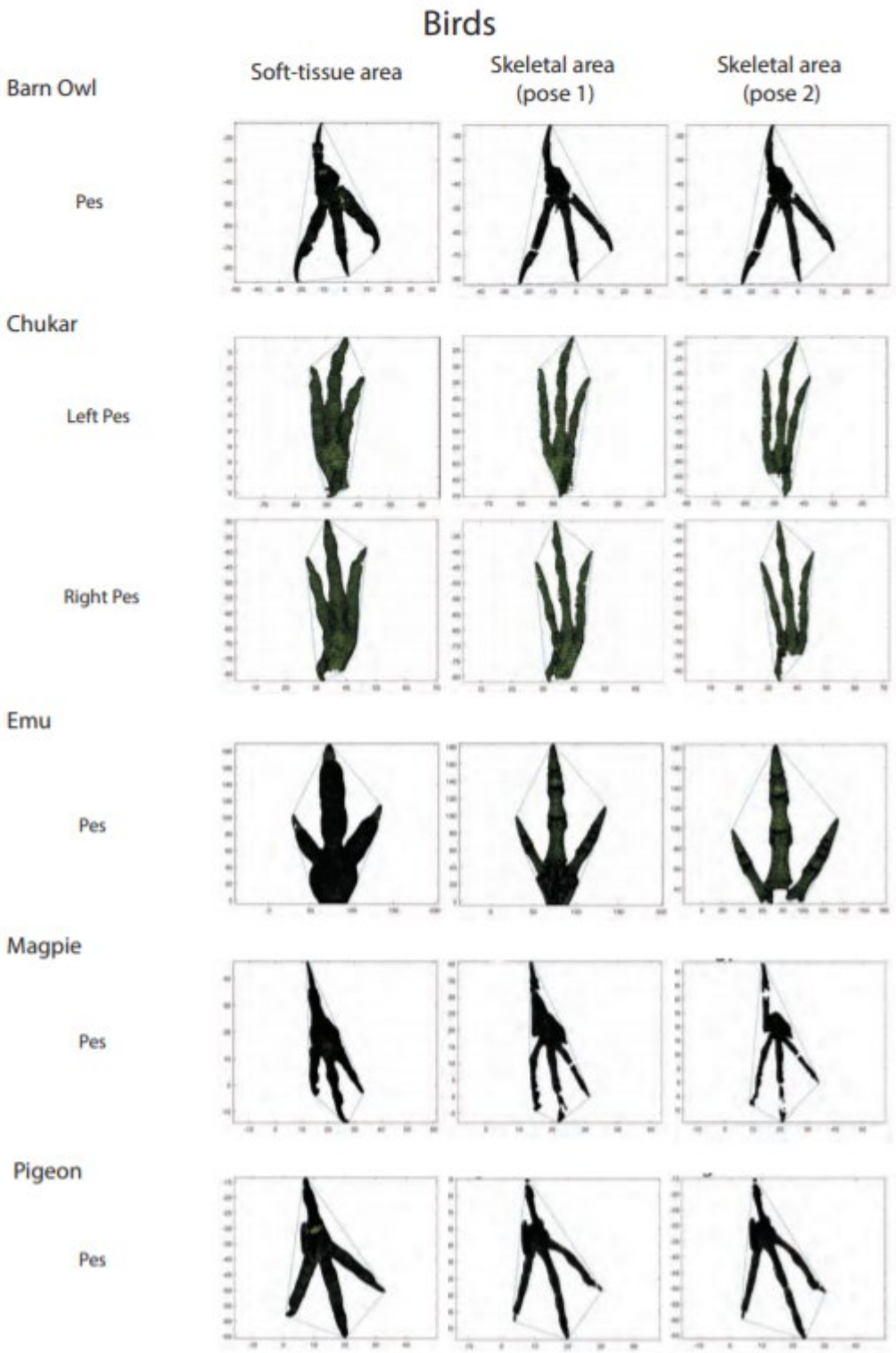
Birds
Soft-tissue area
Skeletal area (pose 1)
Skeletal area (pose 2)
Barn Owl
Pes
Chukar
Left Pes
Right Pes
Emu
Pes
Magpie
Pes
Pigeon
Pes

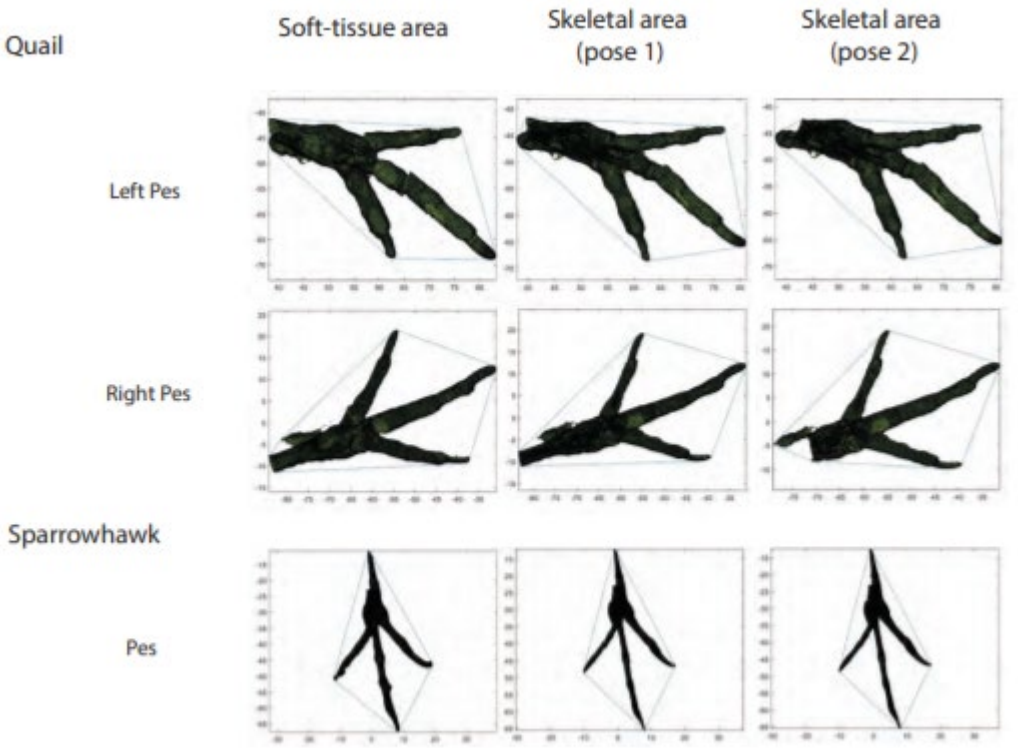
Quail
Soft-tissue area
Skeletal area (pose 1)
Skeletal area (pose 2)
Left Pes
Right Pes
Sparrowhawk
Pes

Chapter 3 Supplementary Material

The following supplementary material contains the following:

1. Tables for phylogenetic comparative methods tests, alongside body mass tests – using generalised least squares to establish the roles of phylogeny and body mass in determining the (lack of) correlations found in Chapter 3 for various foot measurement methods for establishing heteropody in skeletons of extant animals.
2. Contrasting graphs for data using skeletons, and those adjusted for skin as per the formulae for forelimb/hindlimb differences in skin underfoot surface area compared to skeletal underfoot surface area as established in Chapter 2.
3. Images of combined convex hulls of skeletons used to calculate centre of mass in Chapter 3, with locators indicating the positions of the centres of mass, and approximate glenoid and acetabulum positions.

Supplementary Table S3.1 Results for phylogenetic independent constrasts, and phylogenetic generalised least squares statistical tests (with additional tests for effect of body mass) for the different measures of heteropody listed in Table 1 of Chapter 3 using the Grafen Method.

PIC and PGLS Results	PIC						pgls - brownian					pgls - OU					Body Mass Effect				
Manus:Pes Ratio Type	**Multiple R2**	**Adjusted R2**	**CI**	**SE**	**F Statistic**	**F p-value**	**Correlation**	**CI2**	**SE2**	**t value**	**p value**	**Correlation2**	**CI3**	**SE3**	**t value2**	**p value2**	**Correlation3**	**CI4**	**SE4**	**T**	**p**
Functional Foot x CW	0.04269	0.02529	-2.334	1.49	2.453 on 1 and 55 DF	0.1231	-0.092	**-3.1409**	1.769222	-1.775302	0.0814	-0.833	-2.87037	1.624315	-1.767126	0.0828	-0.066	-0.00225	0.021547	-0.1044181	0.9172
Functional Foot x PW	0.05639	0.03923	-2.353	1.298	3.287 on 1 and 55 DF	0.0753	-0.076	**-2.5216**	1.446548	-1.743182	0.0869	-0.787	-1.83585	1.275082	-1.43979	0.1556	0.024	-0.01345	0.03015	-0.4460046	0.6574
Functional Foot Length	0.1193	0.1033	-10.678	3.912	7.451 on 1 and 55 DF	0.00899	-0.222	**-16.33454**	4.645767	-3.516006	0.00009	-0.963	-10.6428	4.168159	-2.553357	0.0135	-0.033	0.00347	0.03711	0.0935217	0.9258
Ungule Length	0.0002155	-0.01703	1.453	4.337	0.1123 on 1 and 52 DF	0.7389	-0.188	**-2.79145**	4.191316	-0.6660077	0.5084	-0.95	-2.70674	3.198277	-0.690798	0.4928	-0.083	-0.07858	0.04858	-1.6174656	0.1121
Digit Length	0.06614	0.04916	-7.583	3.842	3.895 on 1 and 55 DF	0.05346	-0.207	**-14.10787**	4.843347	-2.912836	0.0052	-0.962	-9.91097	4.223648	-2.346543	0.0226	-0.069	0.00945	0.038236	0.2471244	0.8058
Whole Foot Length	0.01358	-0.004354	-2.856	3.282	0.7572 on 1 and 55 DF	0.388	-0.225	**-4.63799**	4.28775	-1.081684	0.2841	-0.966	-2.83119	3.546297	-0.798351	0.4281	-0.032	-0.01891	0.031457	-0.6011158	0.5503
Carpal Width	0.005718	-0.01236	-1.733	3.081	0.3163 on 1 and 55 DF	0.5761	-0.136	**-2.17314**	3.544463	-0.6131088	0.5423	-0.938	-3.06027	3.454012	-0.887005	0.3795	-0.117	-0.01322	0.029668	-0.4454303	0.6578
Heteropody Index (CW)	0.1206	0.1046	0.11679	0.04253	7.54 on 1 and 55 DF	0.00813	-0.147	**0.12071**	0.042512	2.839538	0.0063	-0.95	0.08531	0.041291	2.066122	0.0435	-0.01	-0.00002	0.000186	-0.0972409	0.9229
Heteropody Index (PW)	0.08558	0.06895	0.09532	0.04201	5.147 on 1 and 55 DF	0.02723	-0.149	**0.13188**	0.042862	3.076935	0.0033	-0.935	0.05503	0.037764	1.457246	0.1507	0.024	-0.01345	0.03015	-0.4460046	0.6574

Supplementary Table S3.2 PGLS results for main foot area proxy (functional foot length x carpal width) including body mass analysis, with manually dated tree.

PGLS Analysis

Functional Foot Length x Carpal Width	Brownian Motion	Ornstein-Uhlenbeck	Martin's Correlation	MC with Body Mass
Correlation at Intercept	-0.05	-0.83	-0.81	0.12
Confidence Interval	-0.75	-2.87	-2.79	0.01
Standard Error	1.67	1.62	1.90	0.02
T value	-0.45	-1.77	-1.47	0.37
P Value	0.66	0.83	0.15	0.71
AIC	499.51	439.81		
Log Likelihood	-246.75	-211.41		
Martin's Alpha			58.89	58.89

Supplementary Table S3.3 AIC and log likelighood for phylogenetic generalised least squares statistical tests with Brownian motion, for the different measures of heteropody listed in Table 1 of Chapter 3.

Analysis vs CoM	AIC	Log Likelihood
Functional Foot Length	495.47	-244.74
Ungual Length	478.85	-236.42
Digit Length	438.53	-215.26
Whole Foot Length	508.29	-251.14
Carpal Width	506.64	-250.32
Heteropody Index (using FFL*CW)	499.23	-246.62
Heteropody Index (using FFL*PW)	503.97	-248.98

Supplementary Table S3.4 T-test results comparing heteropody index values for functional foot length between left and right feet.

Skeletons Manus Left vs Right	
T	0.82557
df	52
p	0.4128
alt hypo	true difference in means not equal to 0
95% CI	-37.2341 89.28732
mean of differerences	26.02661

Skeletons Pes
Left vs Right

T	0.48344
df	55
p	0.6307
alt hypo	true difference in means not equal to 0
95% CI	-4.9144 8.039248
mean of differerences	1.562423

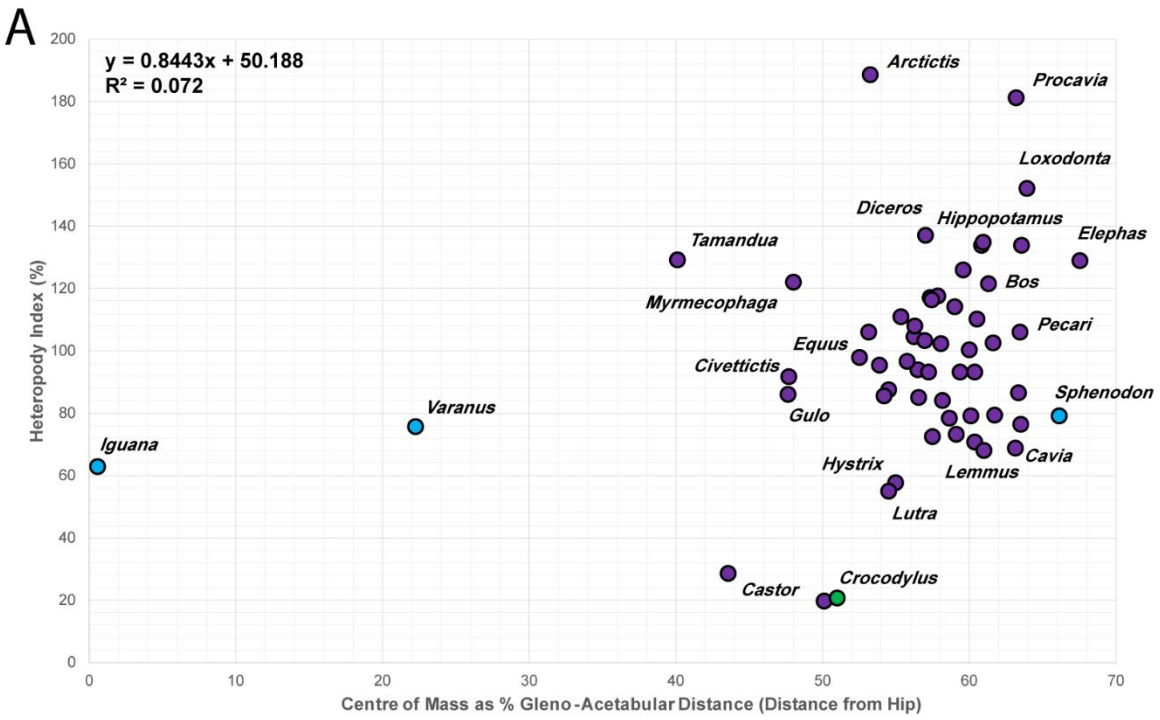

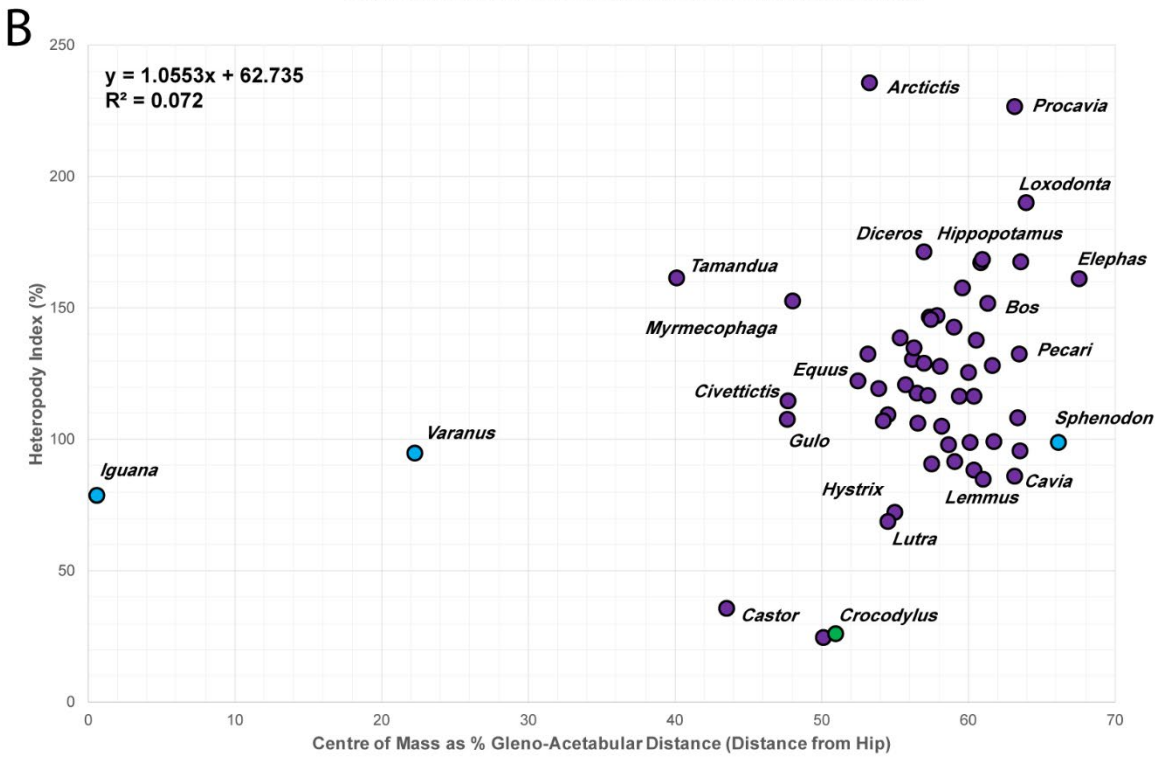

Supplementary Figure S3.1 Main graph (centre of mass position against heteropody index (based on functional foot length multiplied by carpal width) contrasted with the same data adjusted to represent heteropody of *in situ* feet, using the formulae for forelimbs and hindlimbs established in Chapter 2.

Supplementary Figures S3.2-59 Images of combined convex hulls of skeletons used to calculate centre of mass in Chapter 3, with locators indicating the positions of the centres of mass, and approximate glenoid and acetabulum positions.

African Elephant:

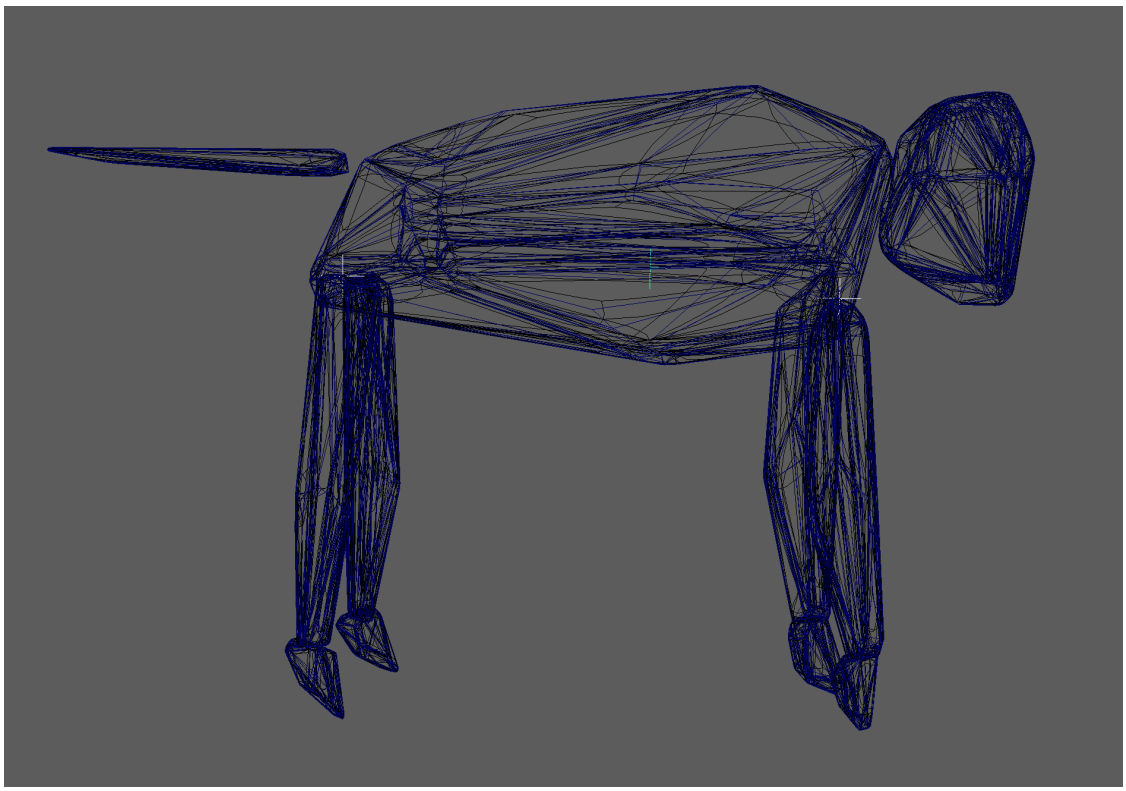

Bison bison - American Bison:

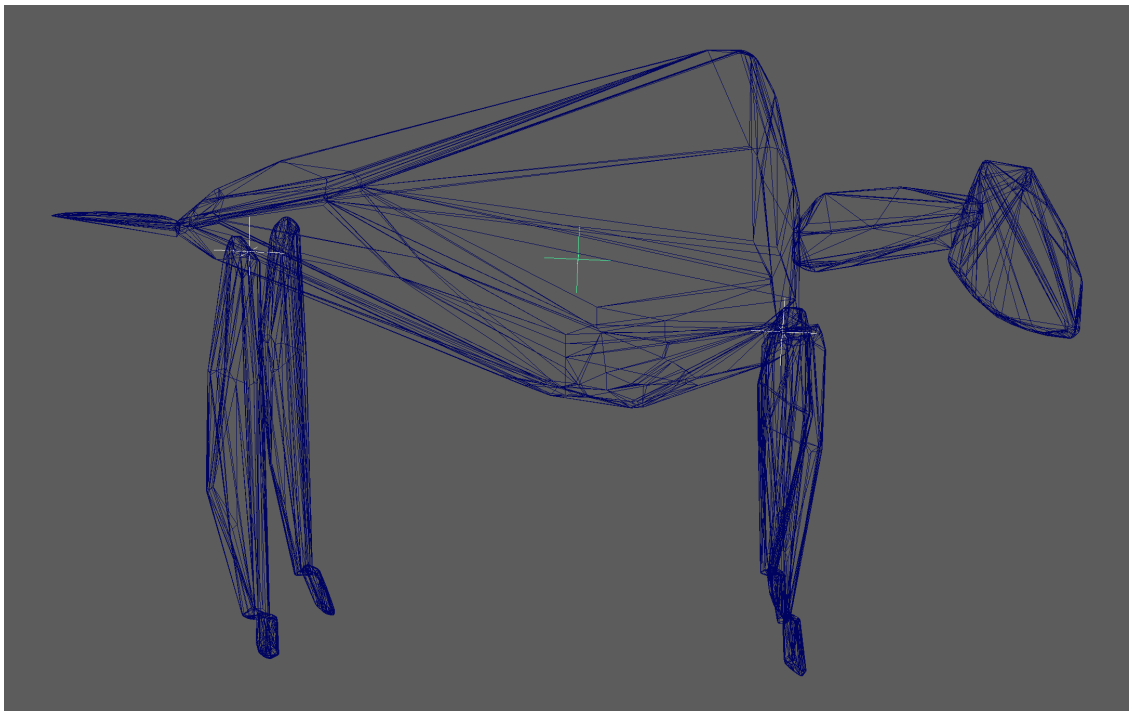

Dasypus novemcinctus - Armadillo:

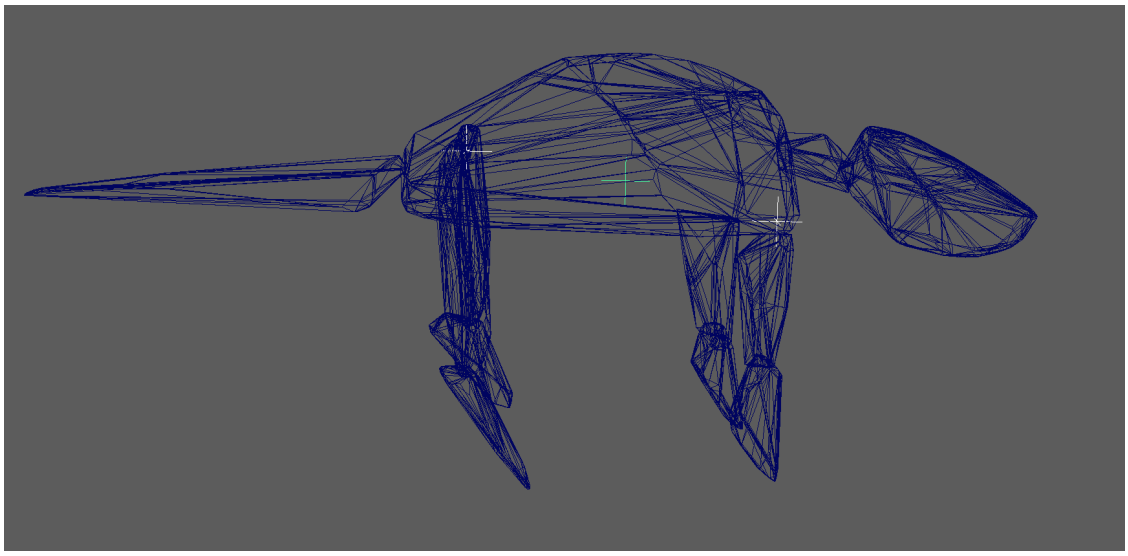

Elephas maximus - Asian Elephant:

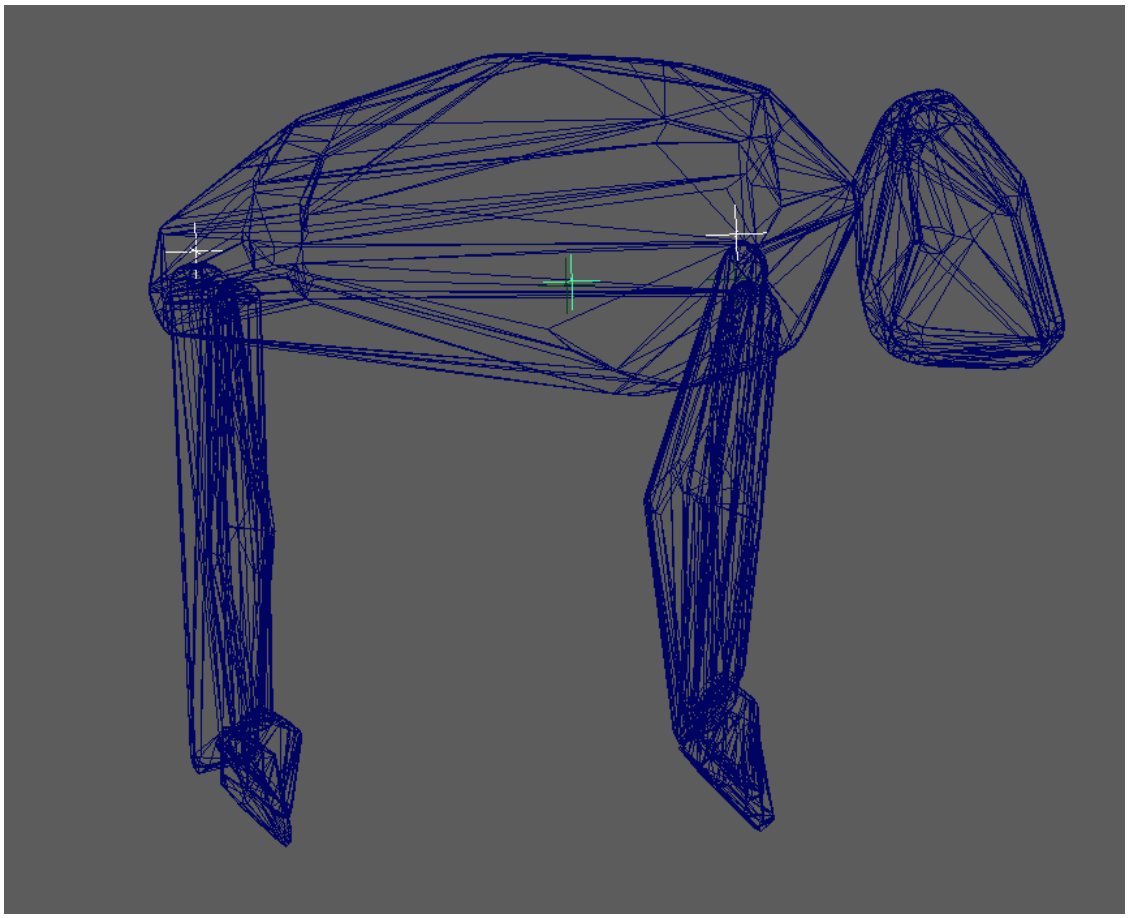

Varanus salvator - Asian Water Monitor:

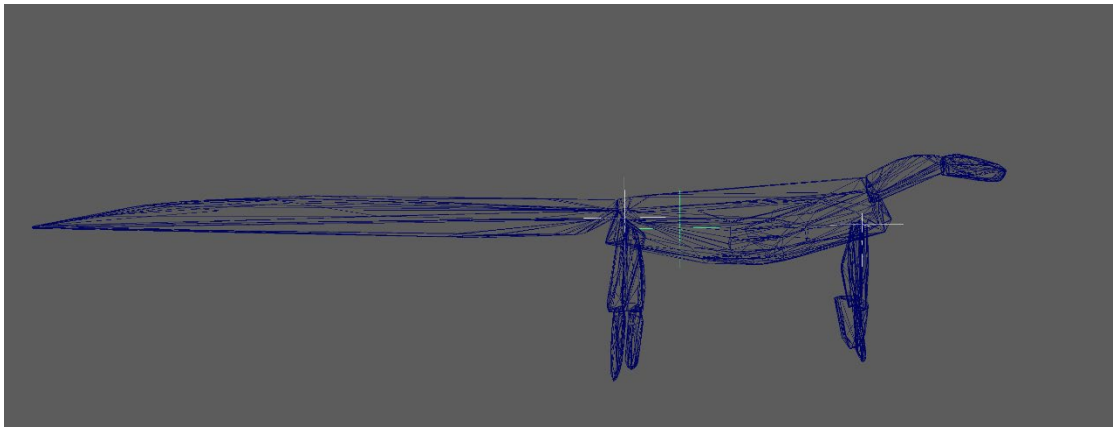

Arctictis binturong - Bearcat:

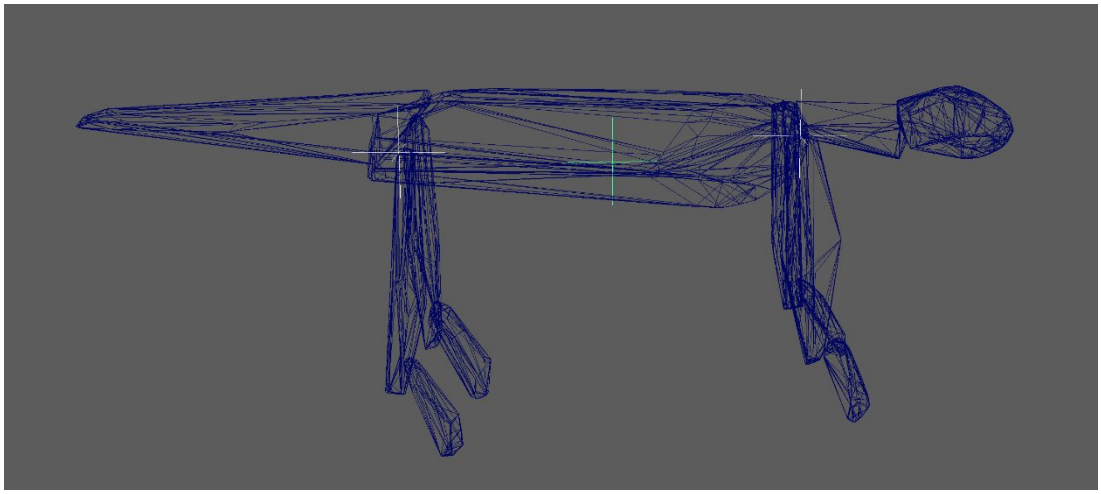

Castor fiber - Beaver:

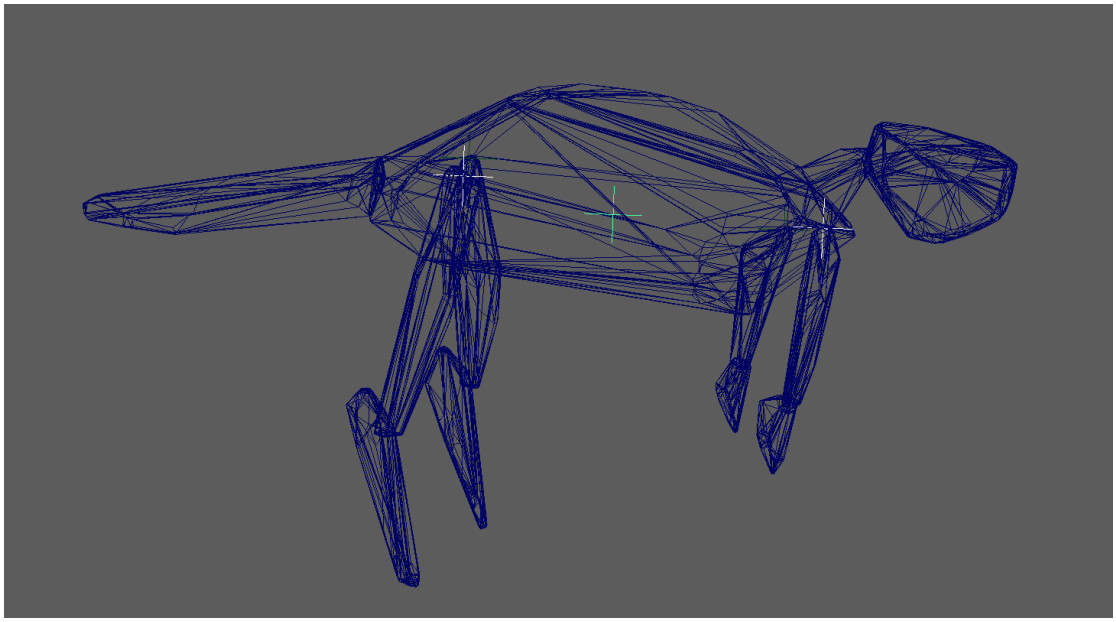

Cephalophus niger - Black Duiker:

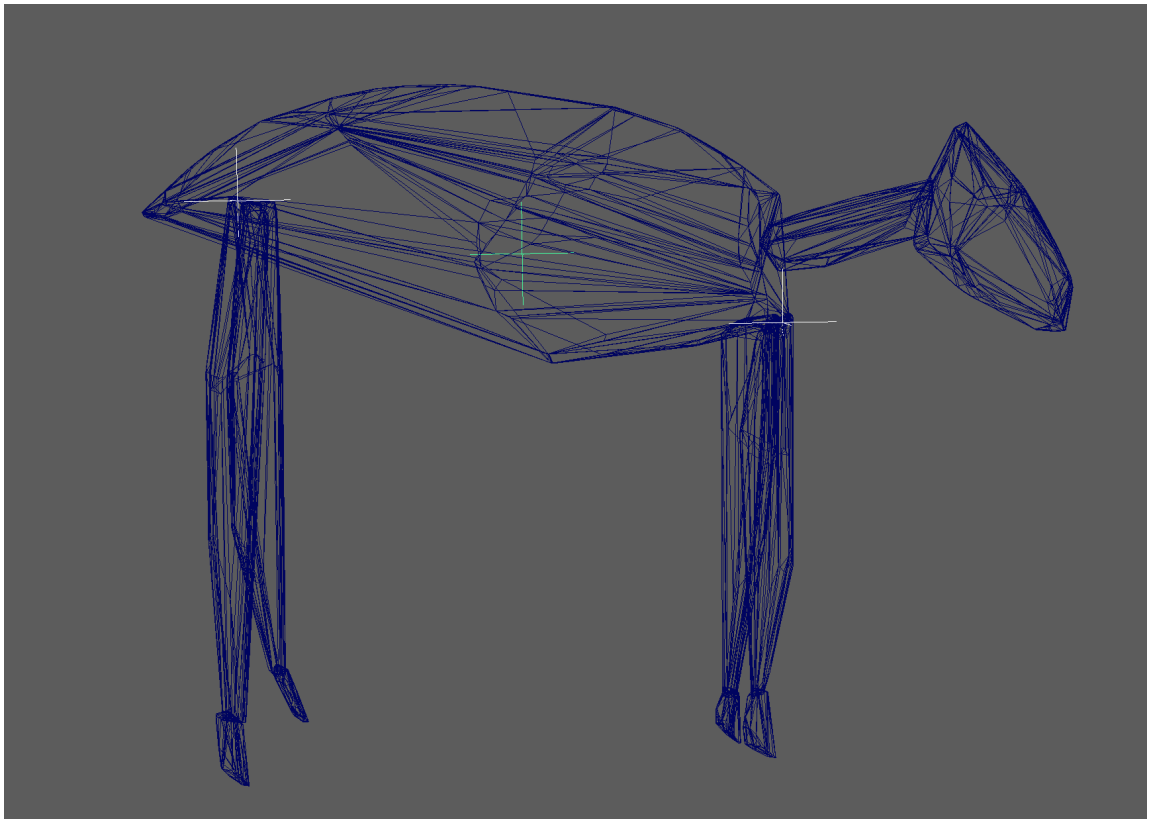

Diceros bicornis - Black Rhino:

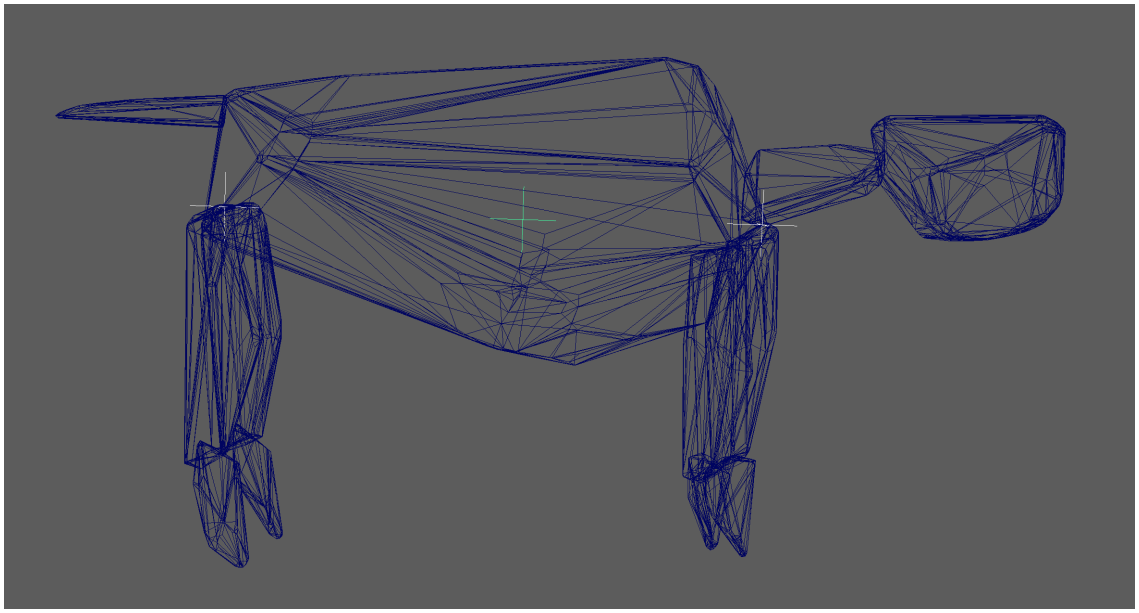

Camelus dromedaries - Camel:

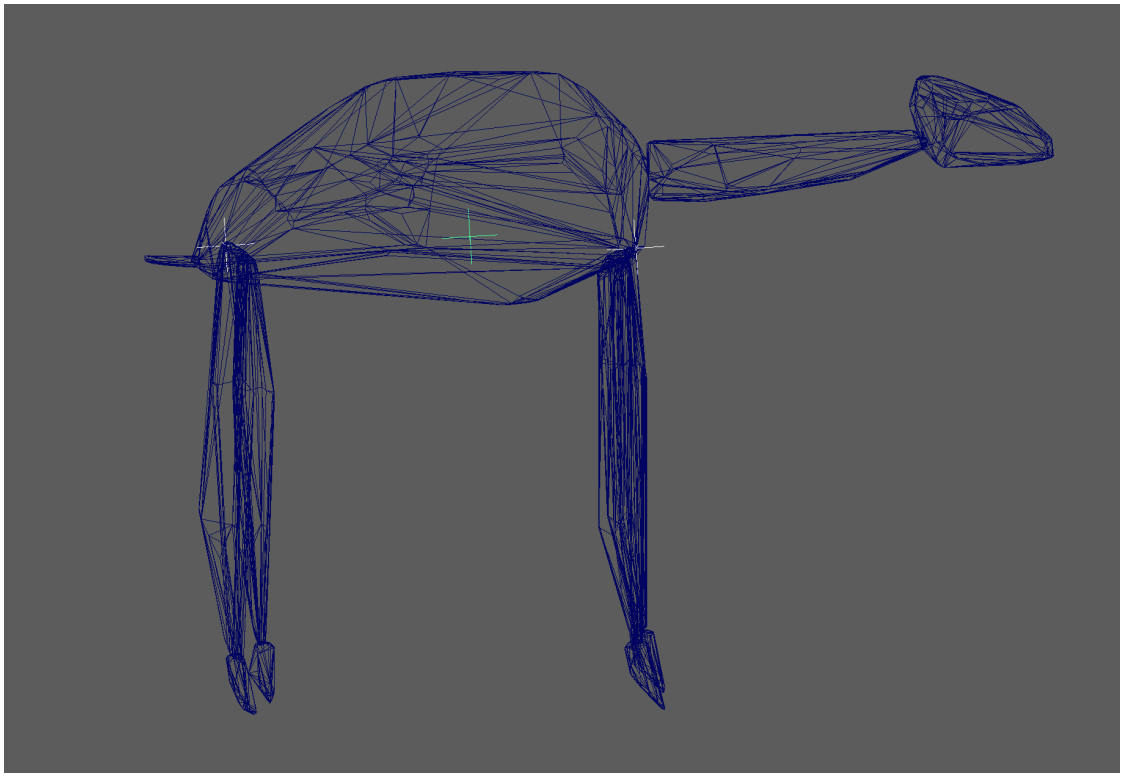

Castor canadensis - Canadian Beaver:

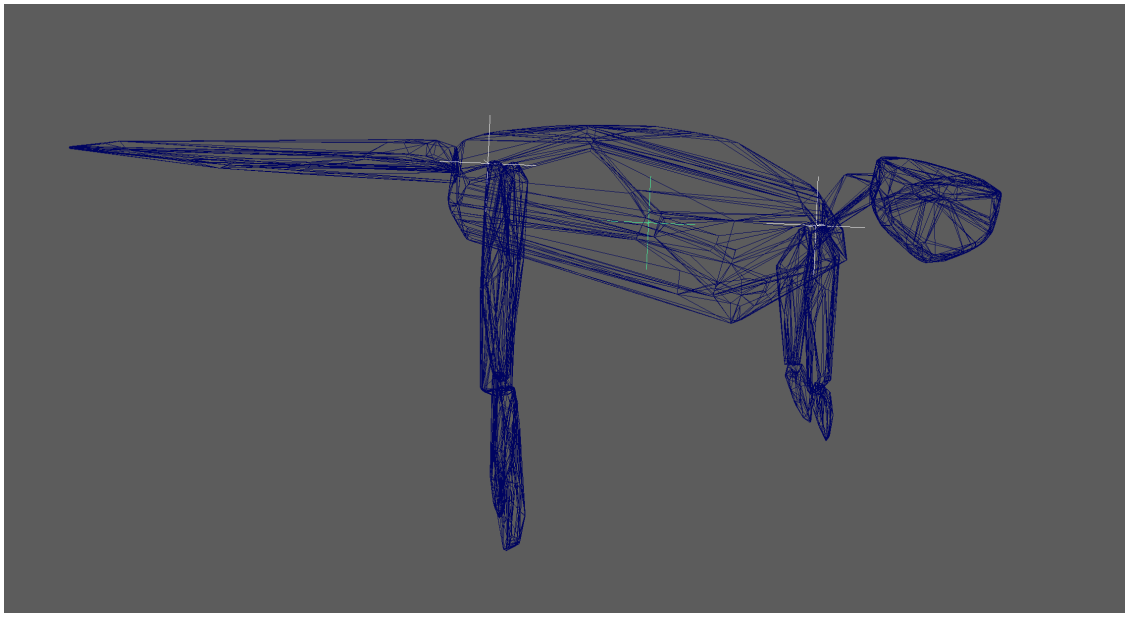

Hydrochoerus hydrochaeris - Capybara:

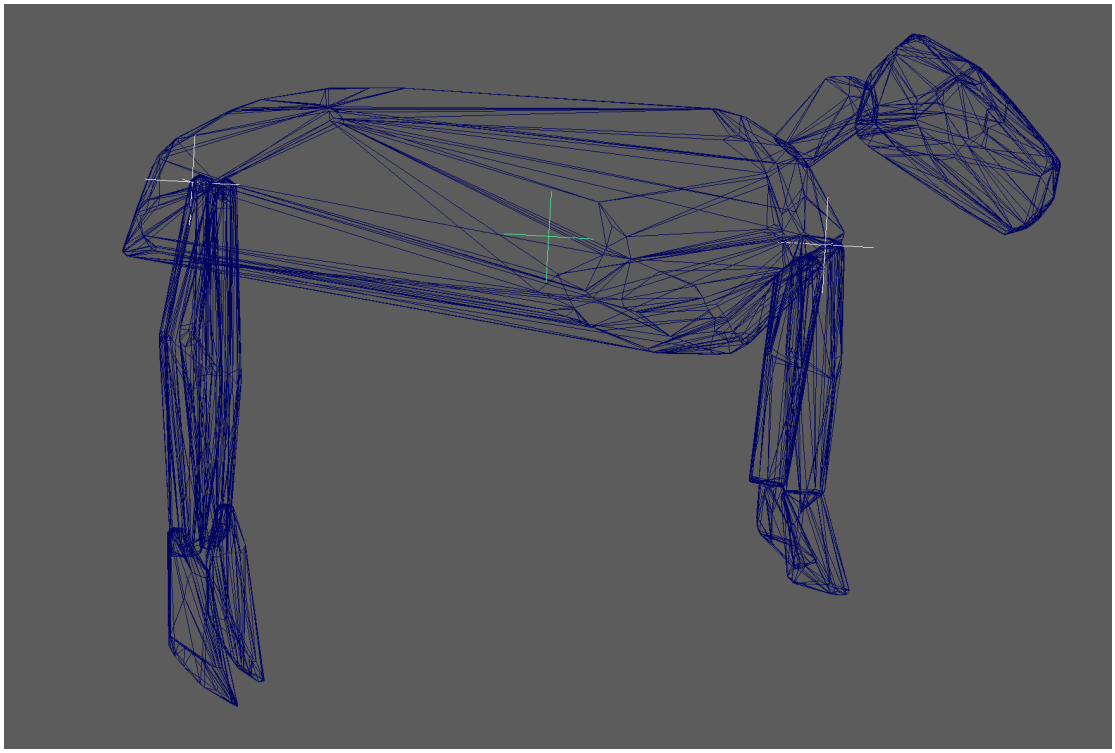

Felis catus - Cat:

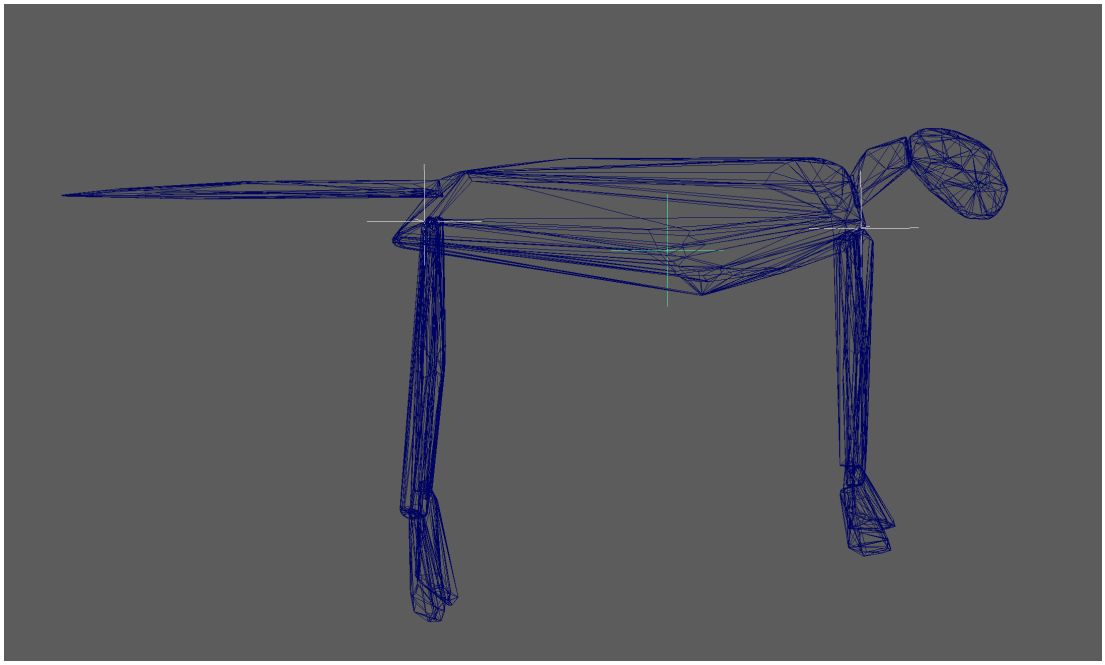

Acinonyx jubatus - Cheetah:

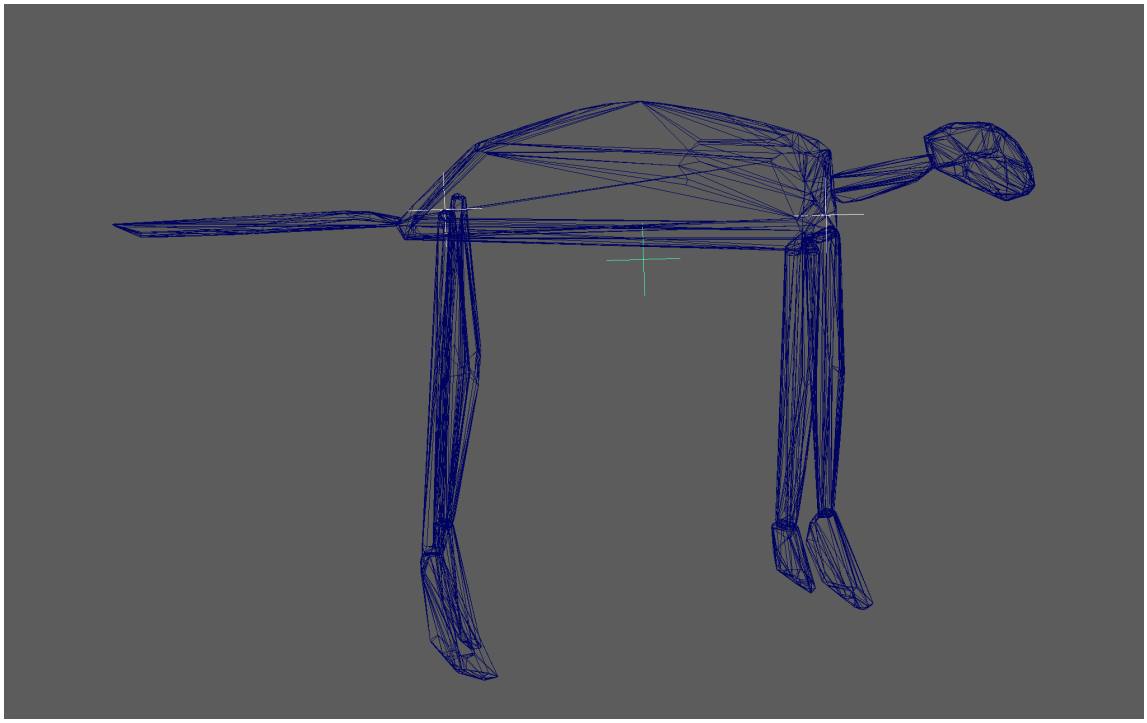

Civettictis civetta - Civet:

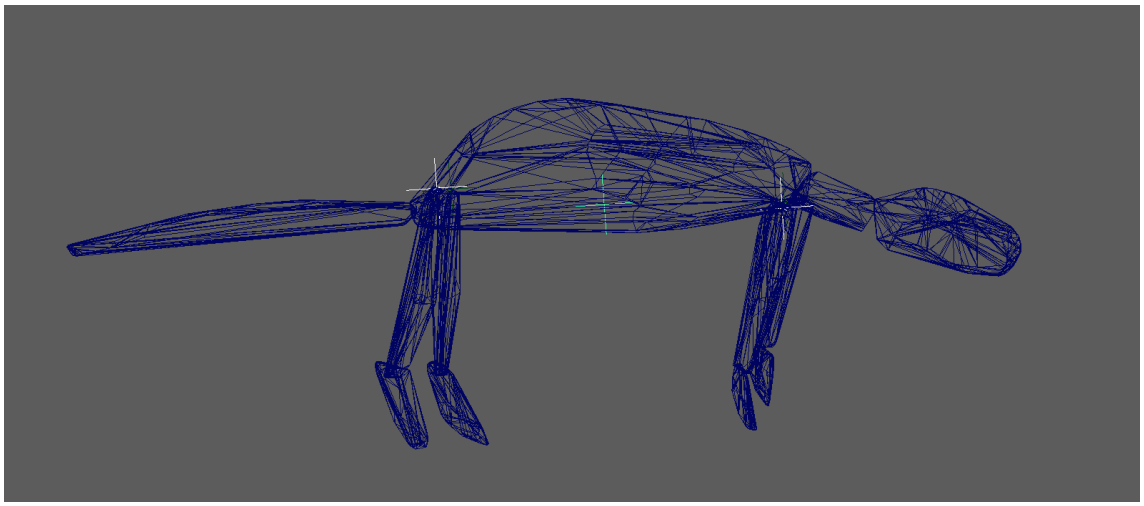

Bos taurus - Cow:

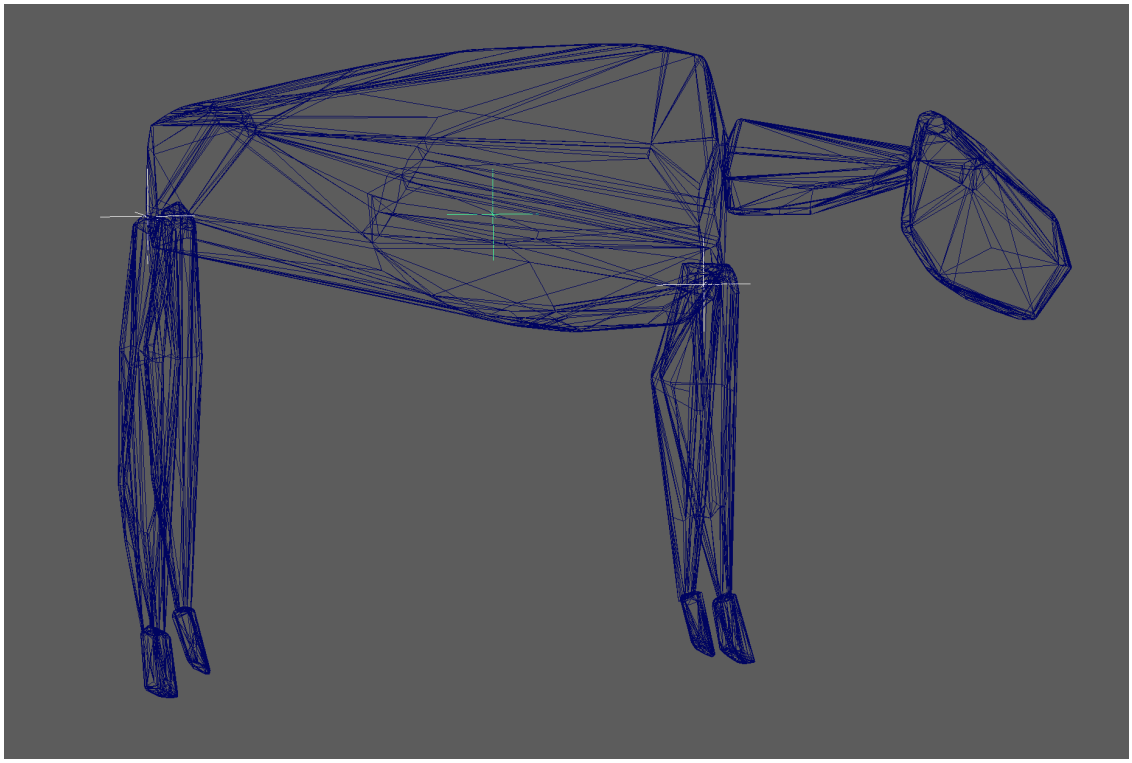

Hystrix cristata - Crested Porcupine:

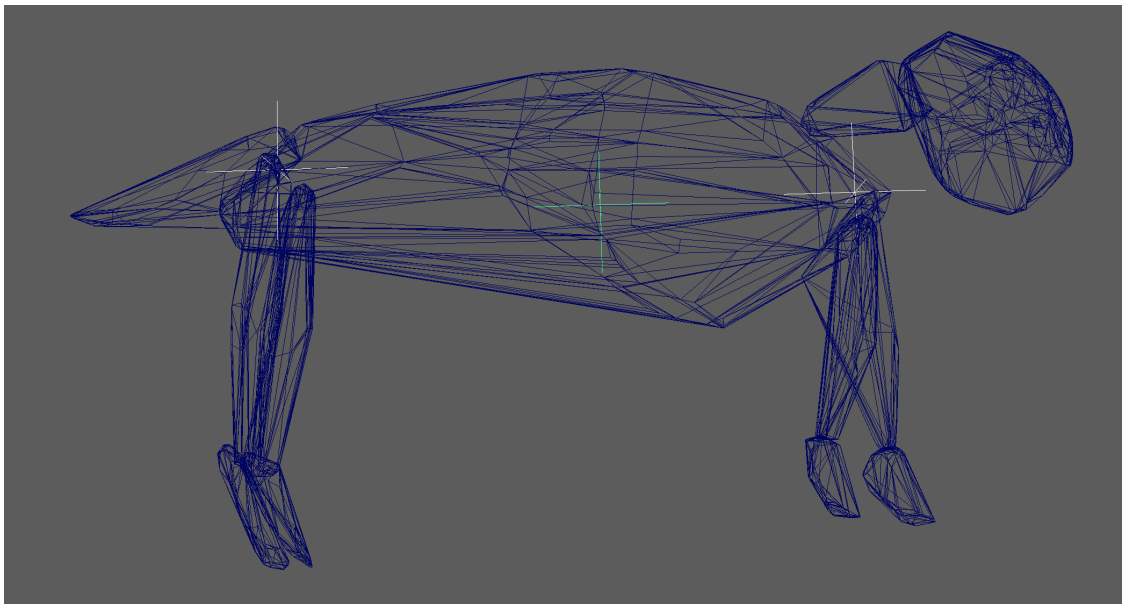

Canis lupus - Dog:

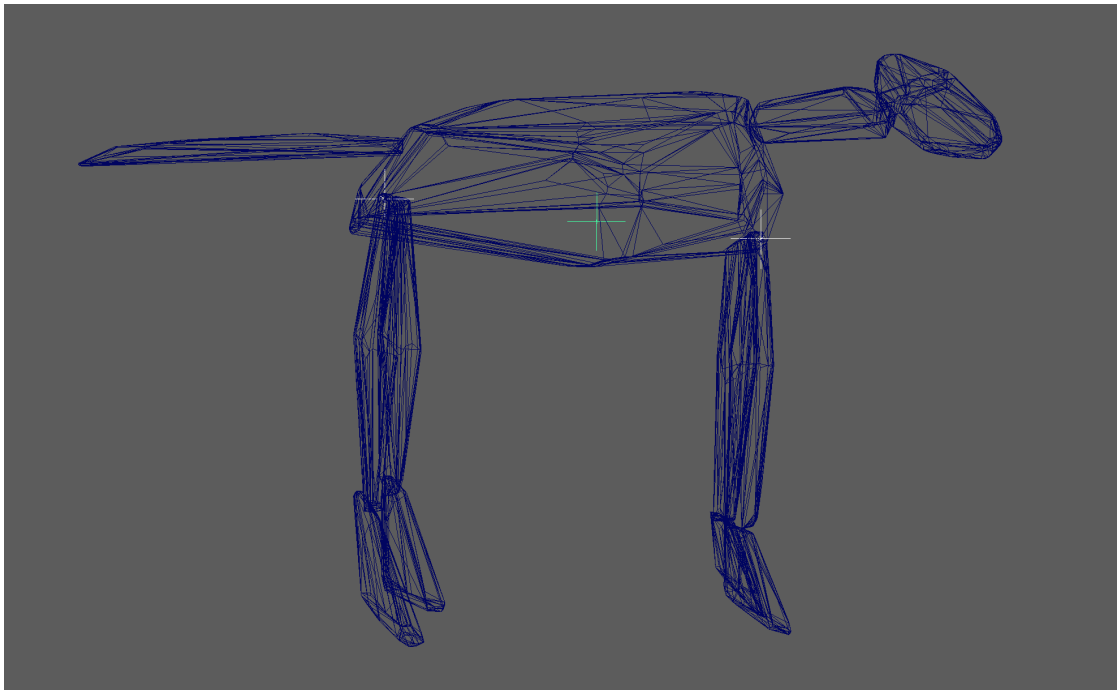

Tachyglossus aculeatus - Echidna:

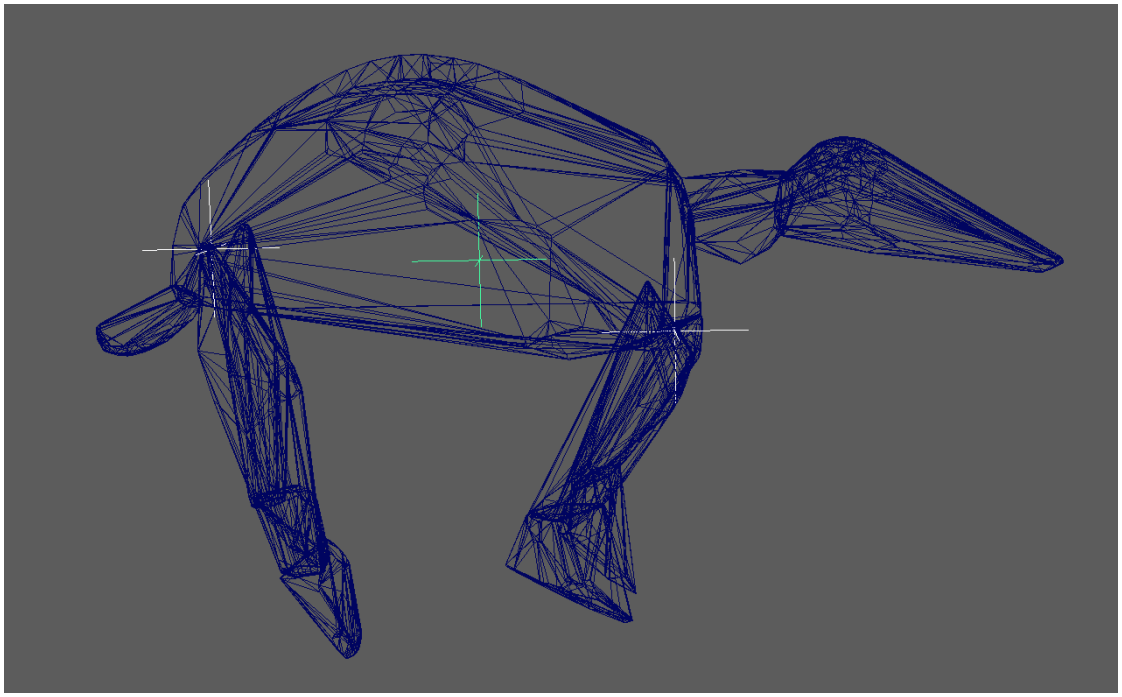

Macroscelides proboscideus - Elephant Shrew:

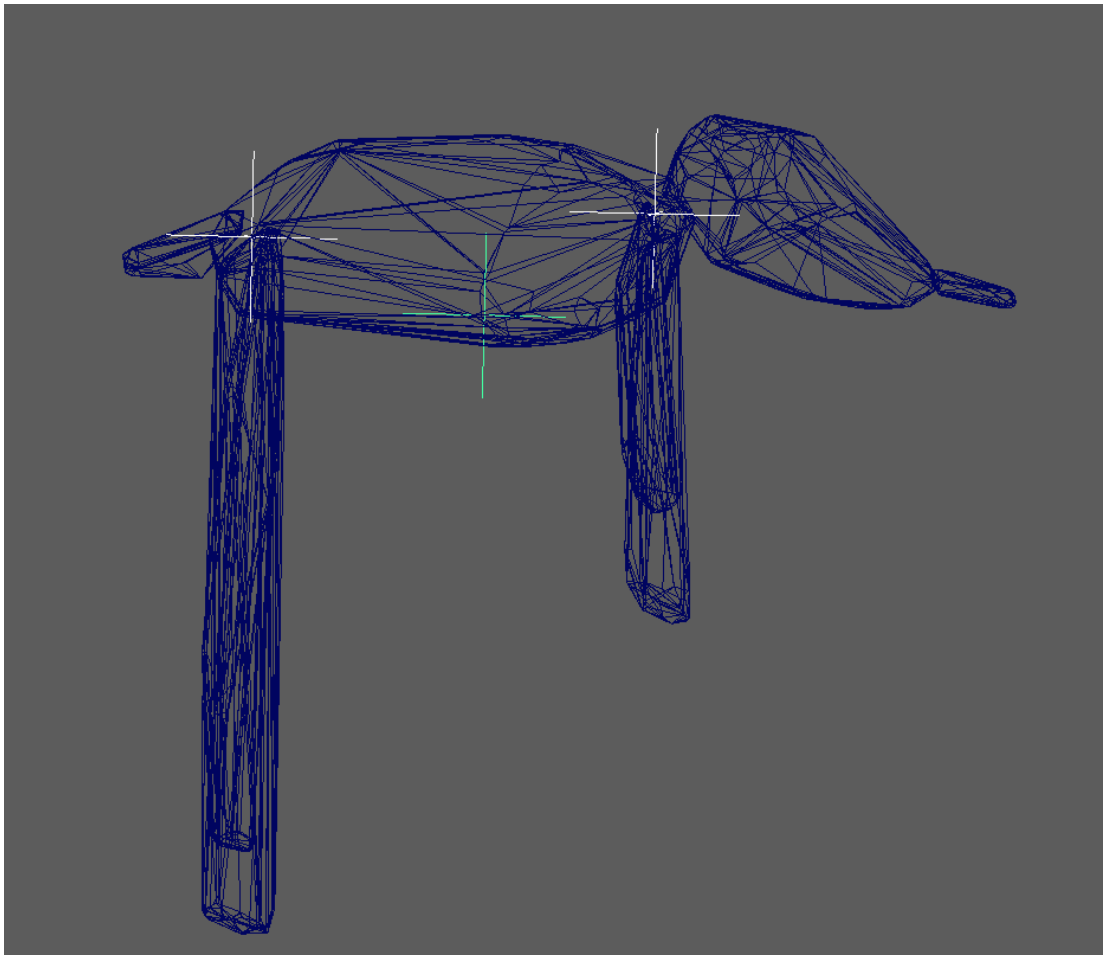

Dama dama - Fallow Deer:

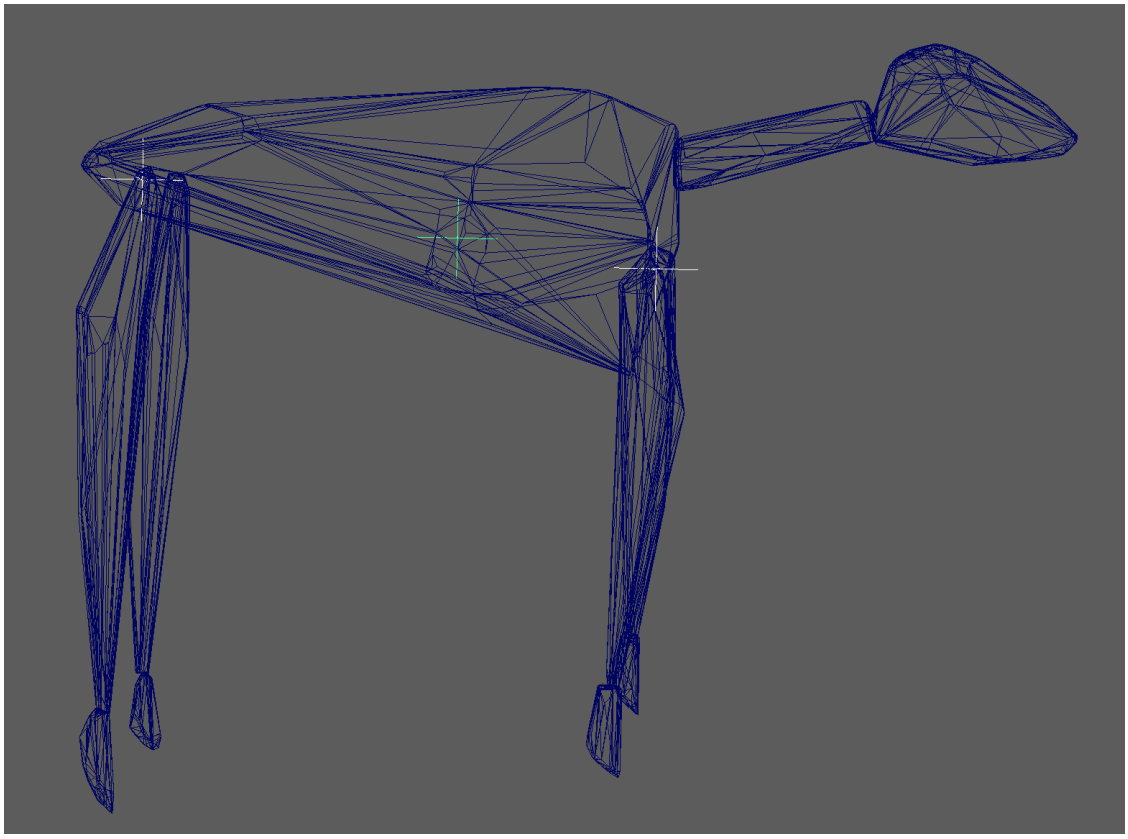

Vulpes vulpes - Fox:

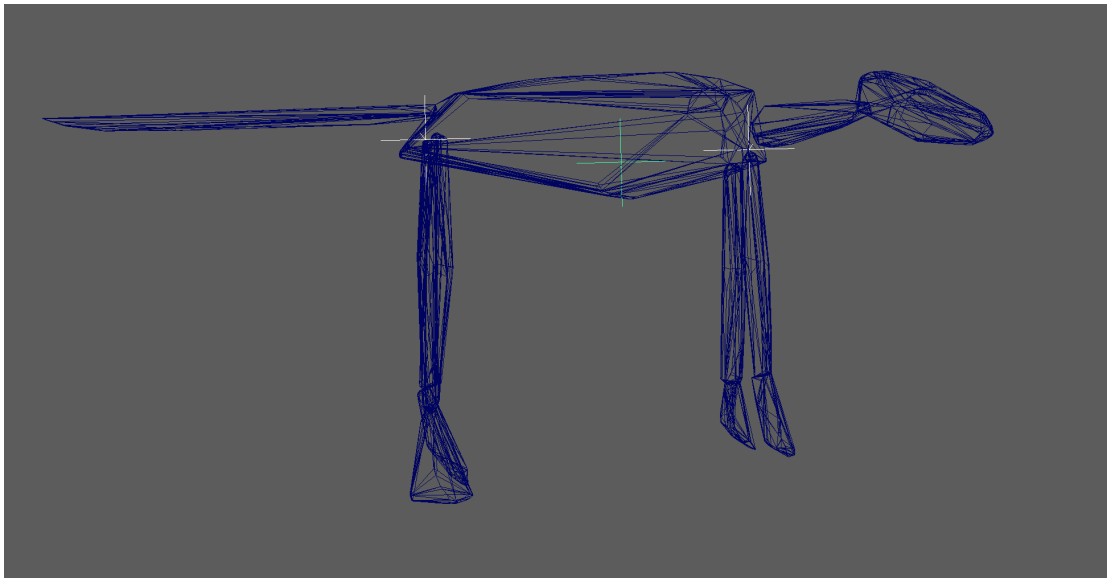

Gazella gazella - Gazelle:

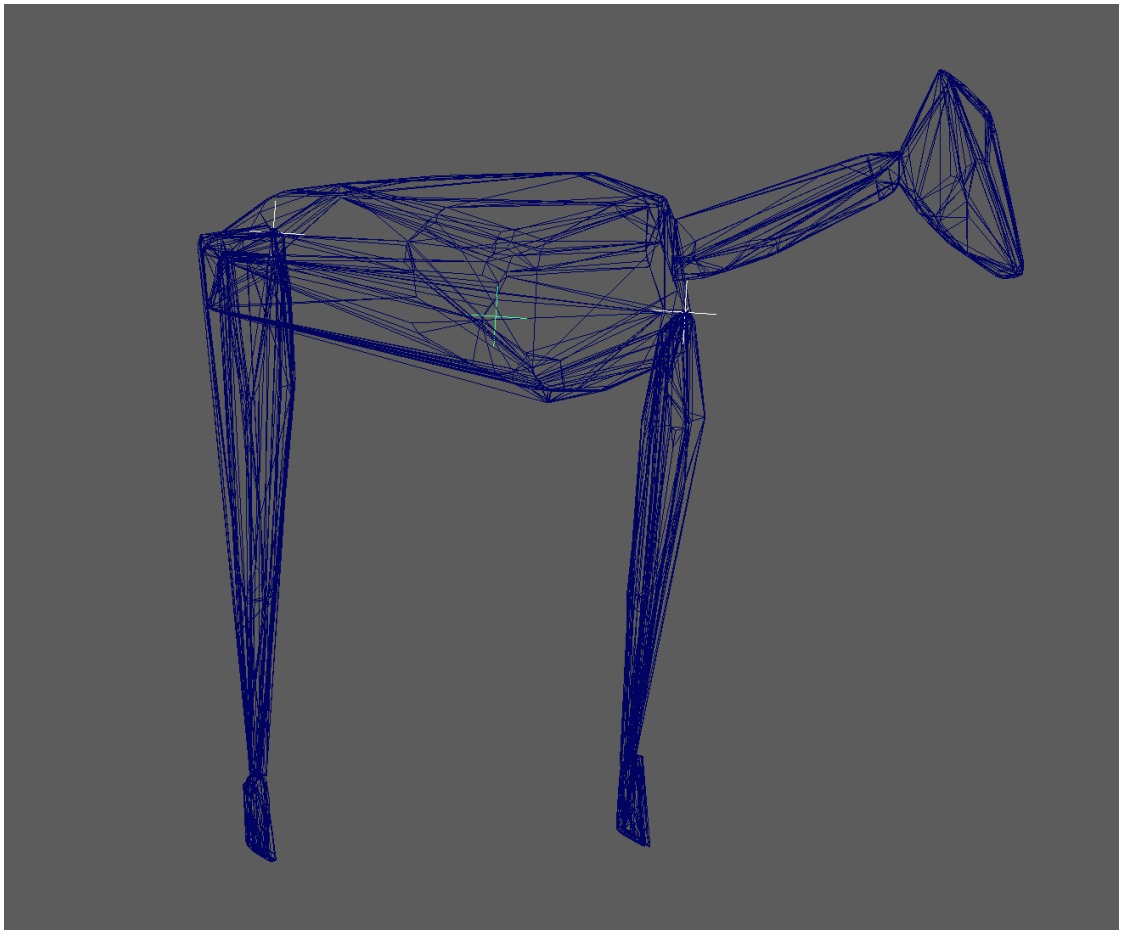

Myrmecophaga tridactyla - Giant Anteater:

Giraffa Camelopardalis - Giraffe:

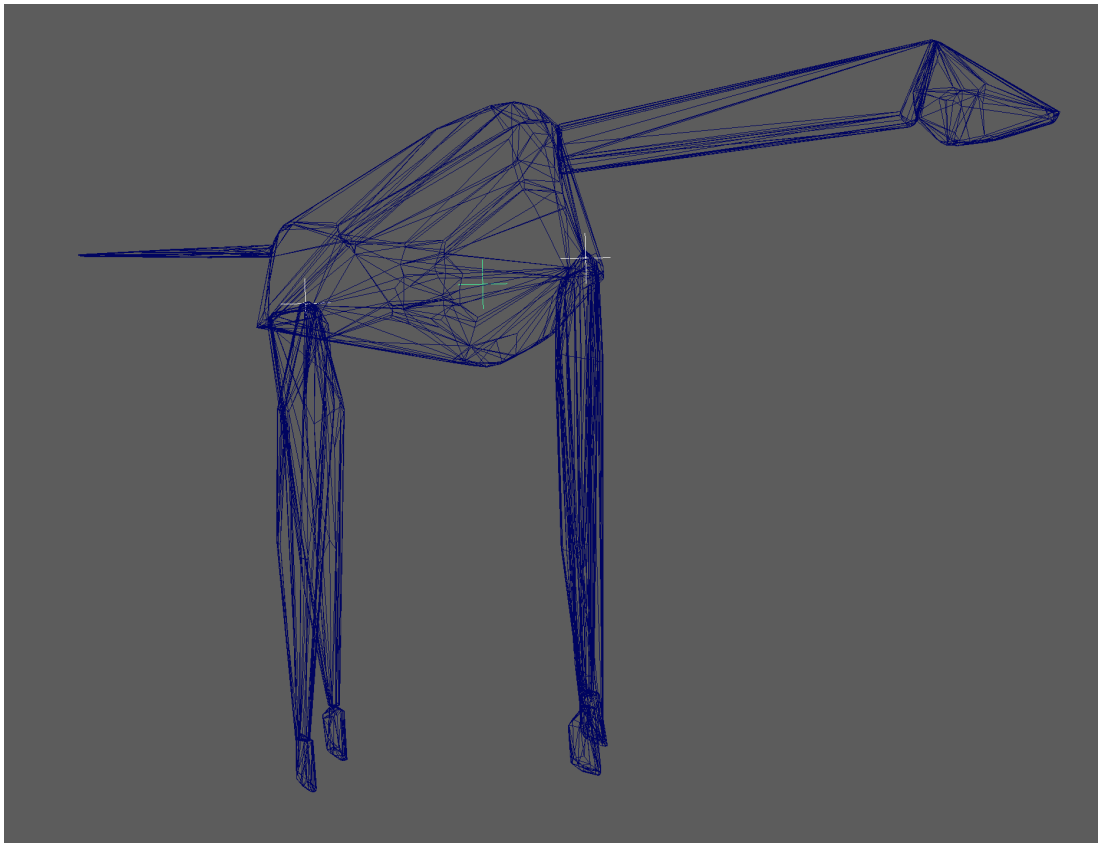

Iguana iguana - Green Iguana:

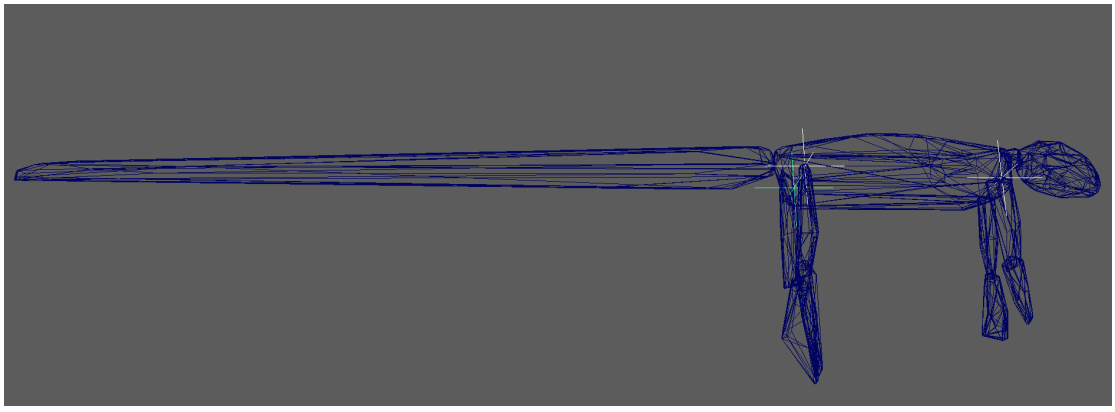

Lama guanicoe - Guanaco Llama:

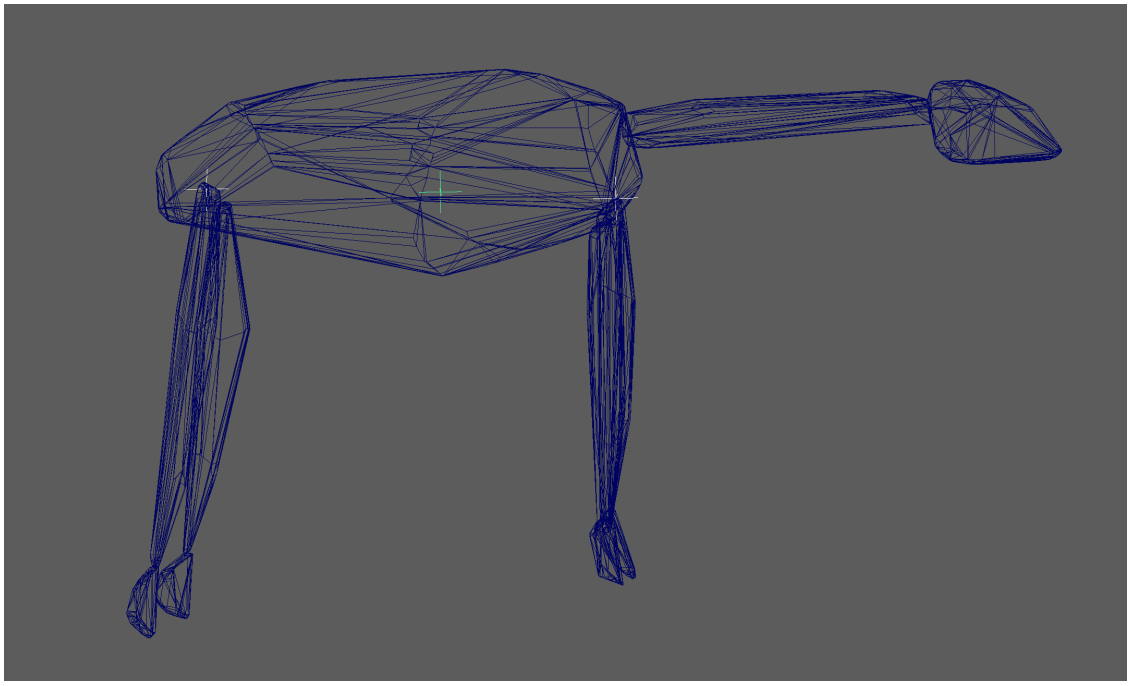

Cavia porcellus - Guinea Pig:

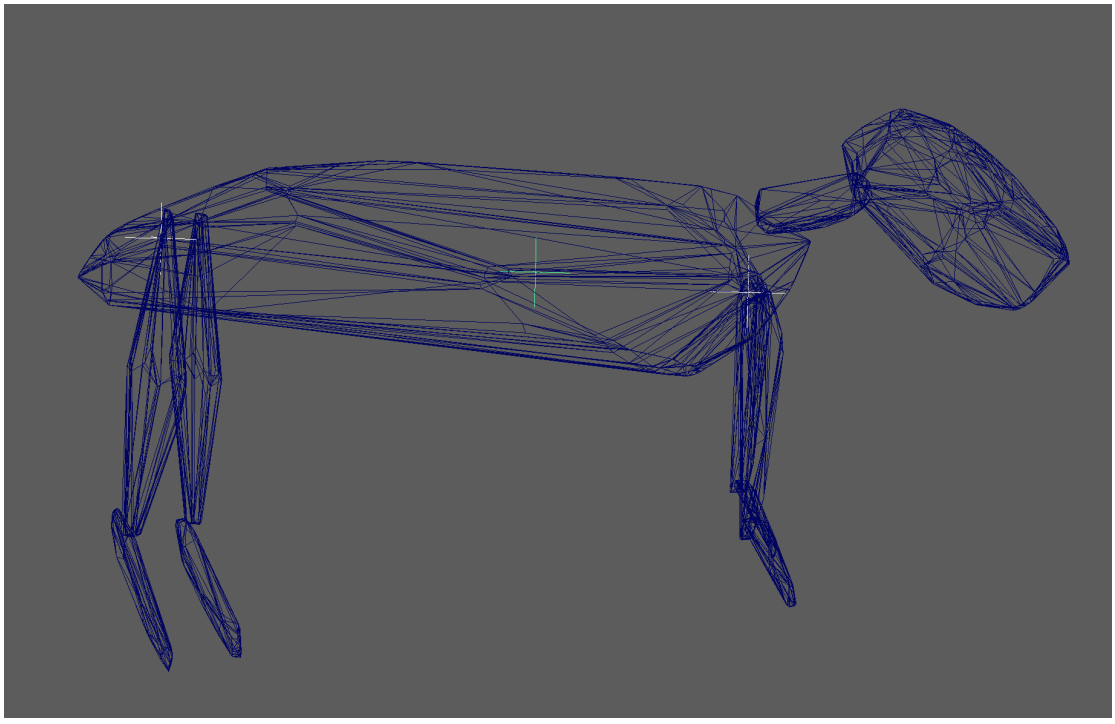

Hippopotamus amphibius - Hippo:

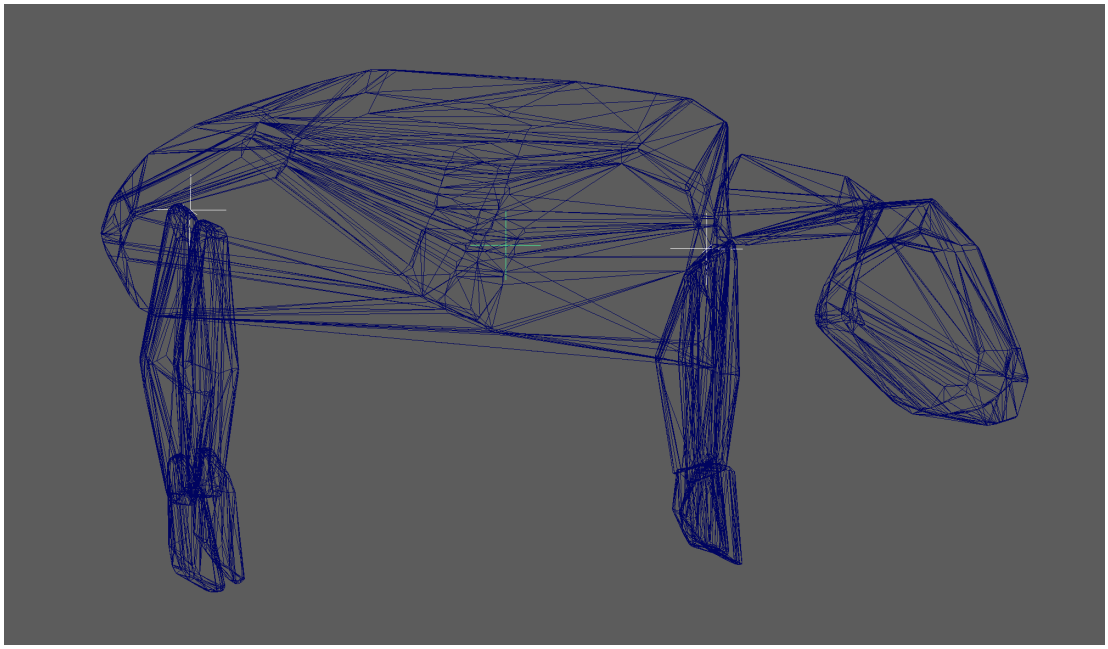

Equus ferus caballus - Horse:

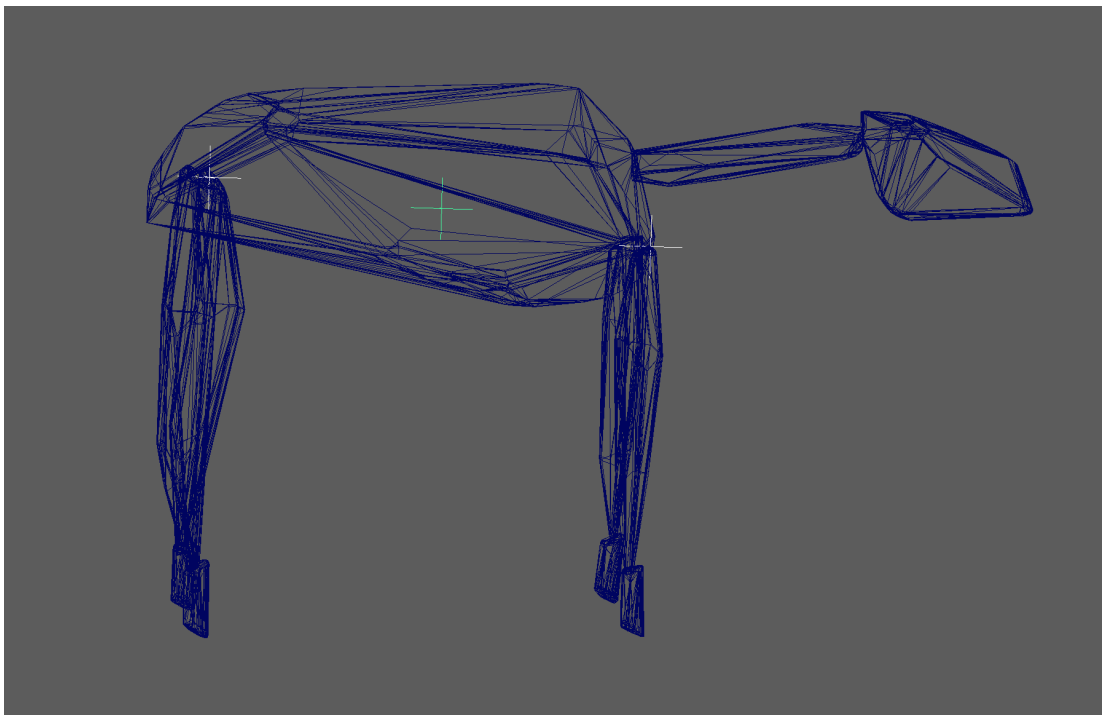

Procavia capensis - Hyrax:

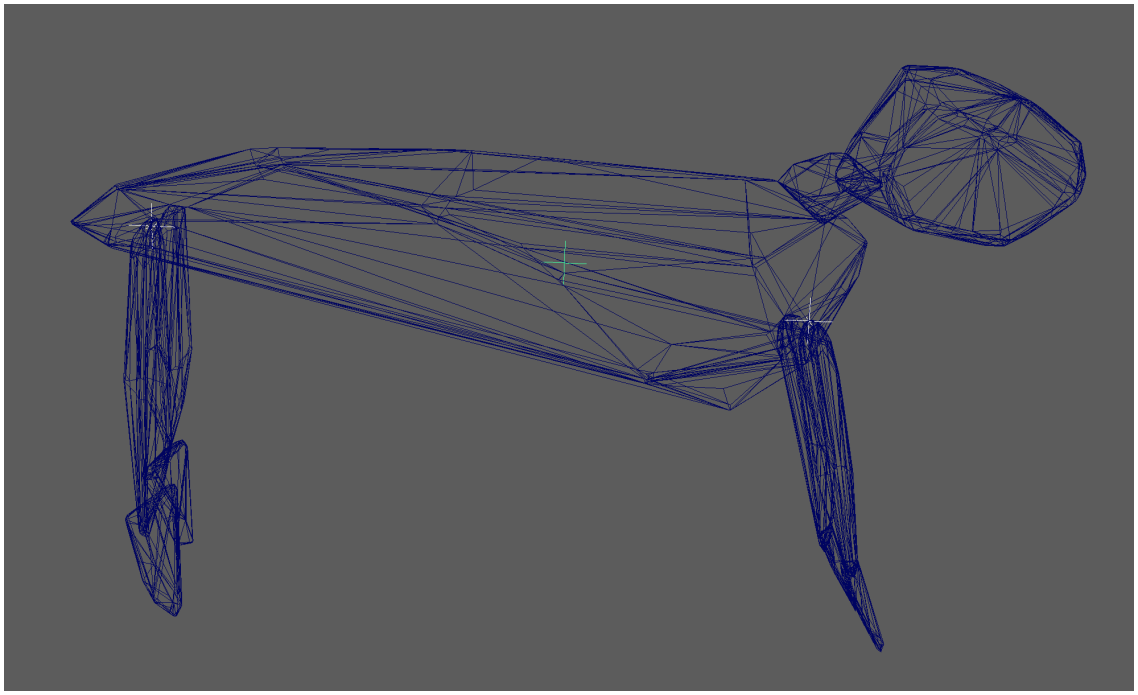

Bos gaurus - Indian Bison:

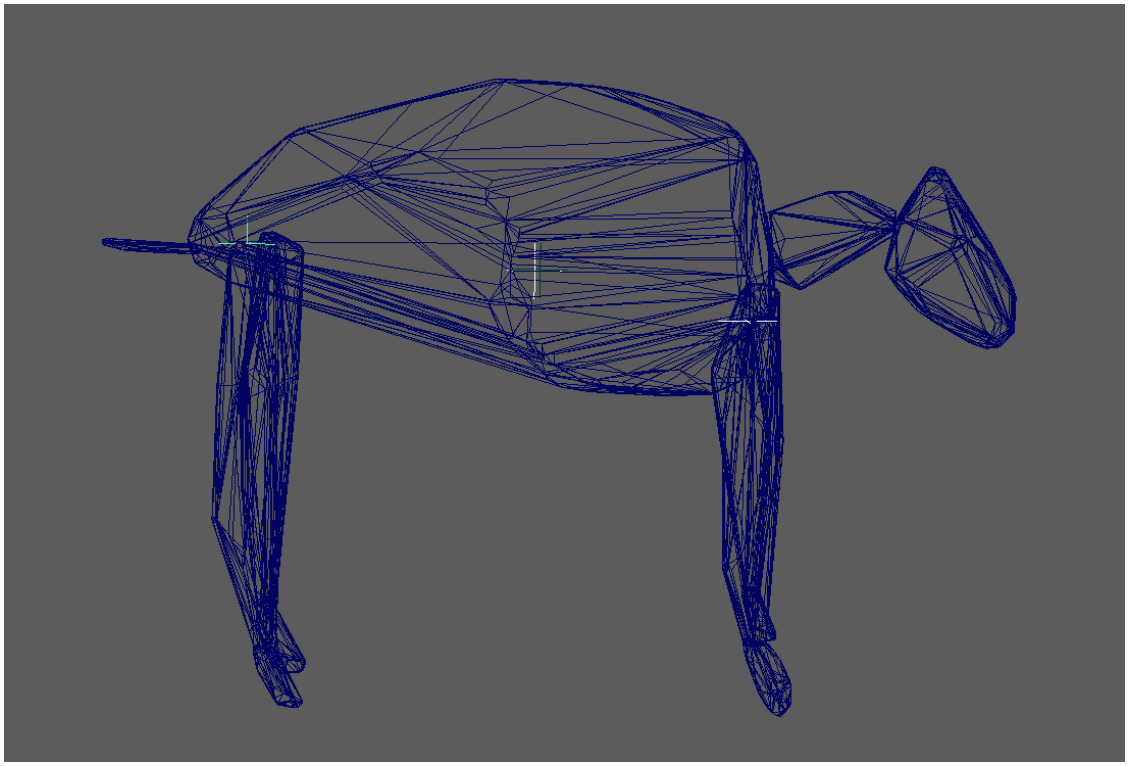

Tragulus javanicus - Javan Mouse Deer:

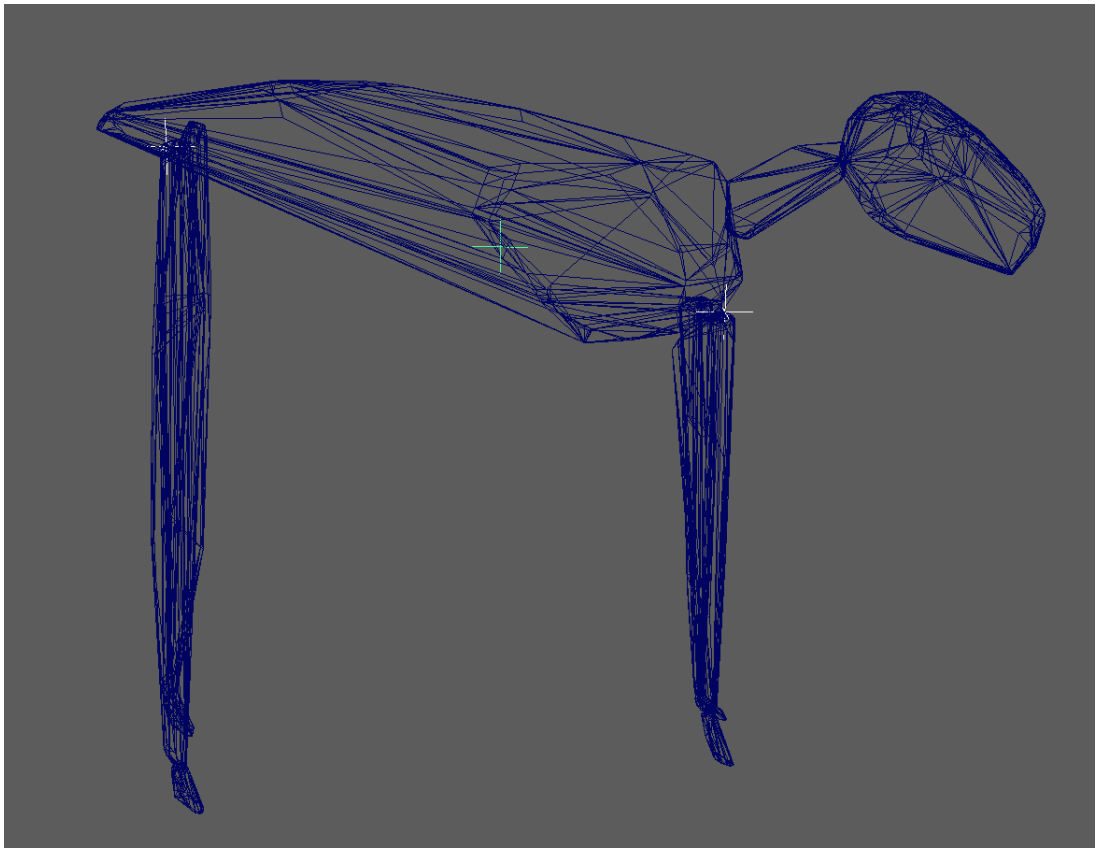

Lemmus lemmus - Lemming:

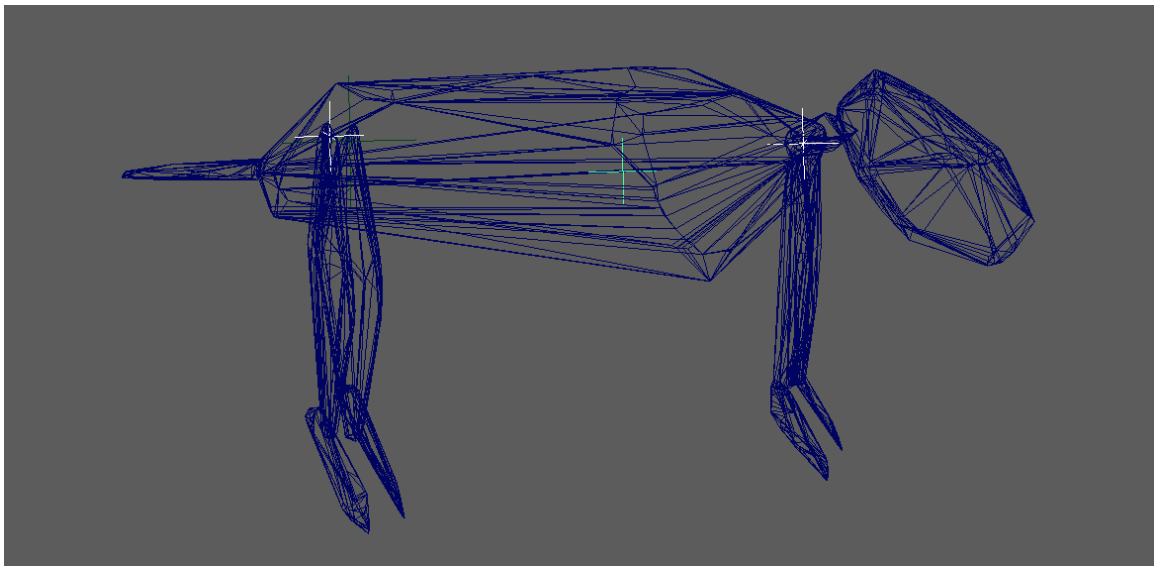

Panthera pardus - Leopard:

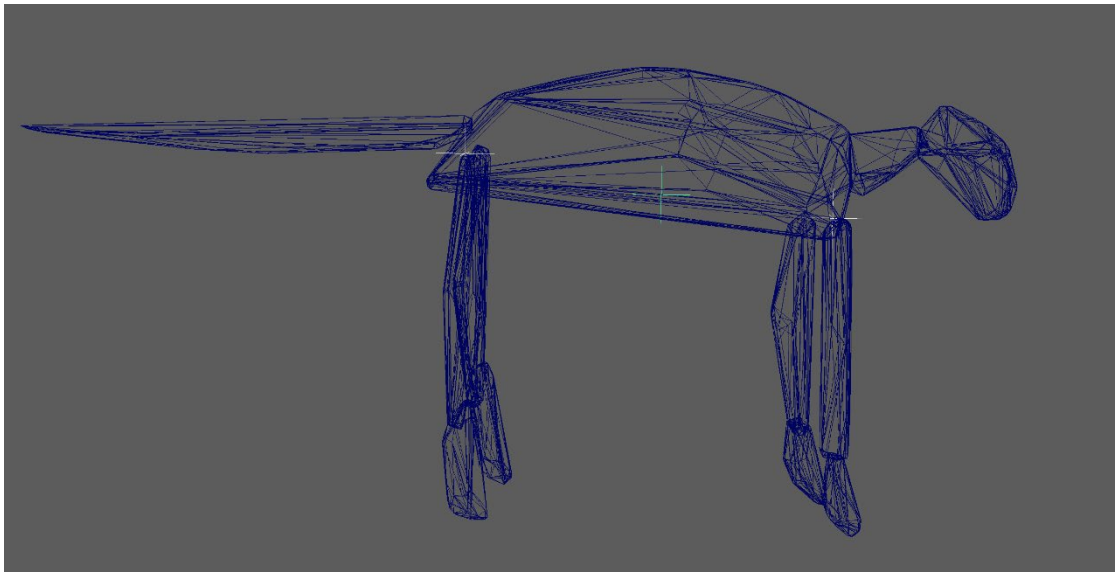

Panthera leo - Lion:

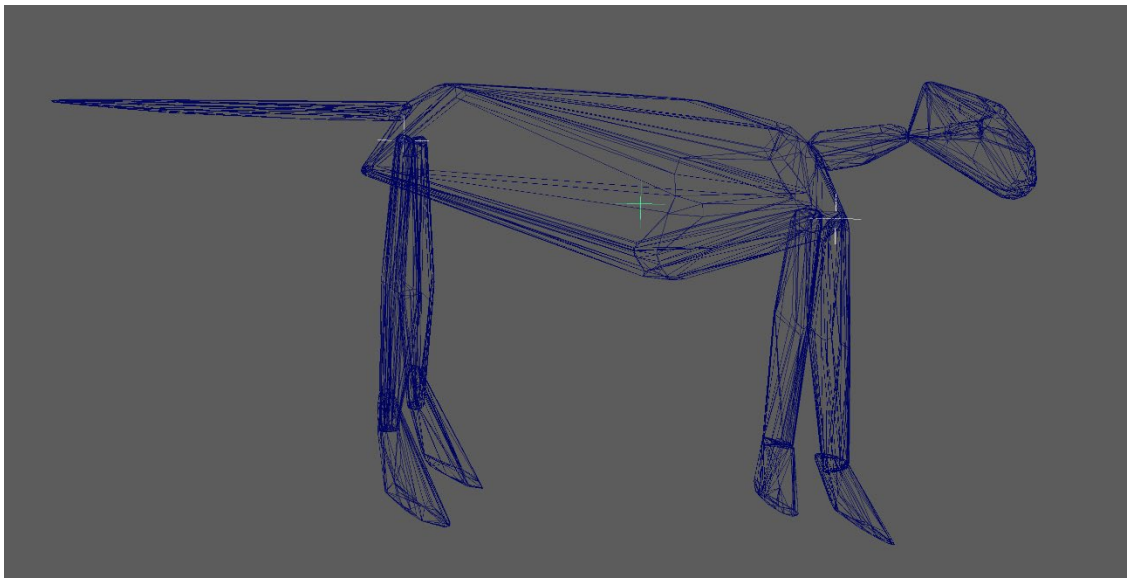

Tapirus indicus - Malayan Tapir:

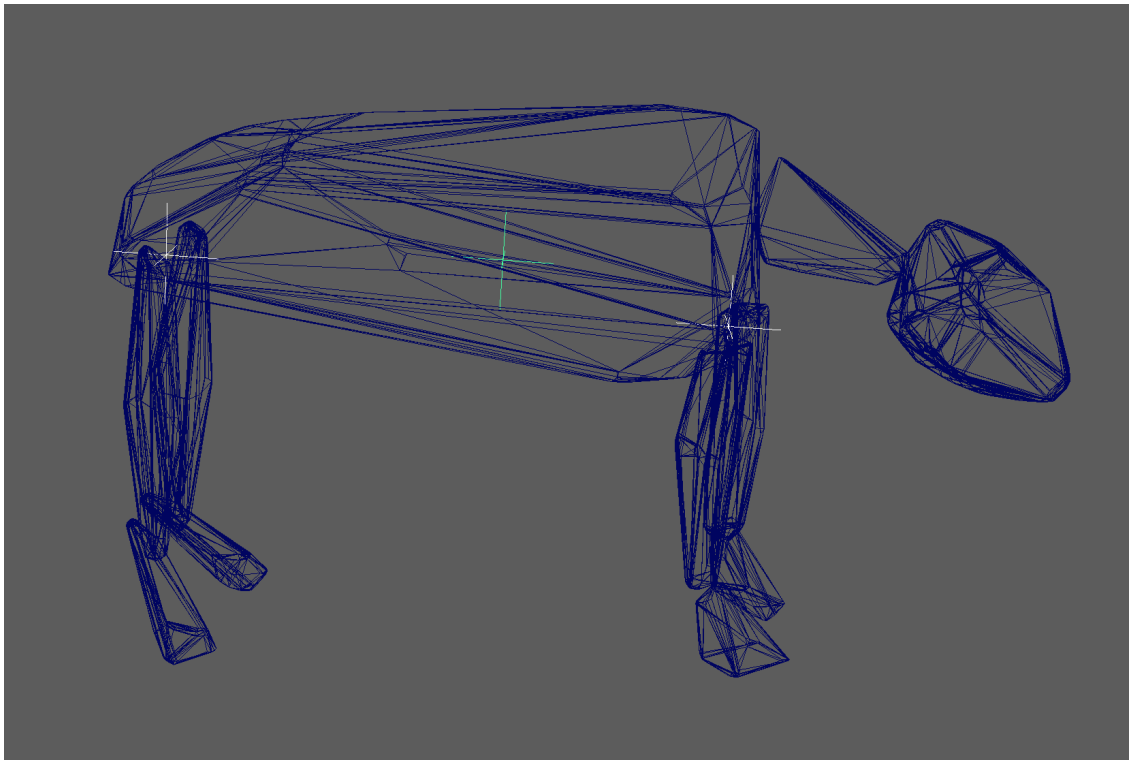

Herpestes edwardsi - Mongoose:

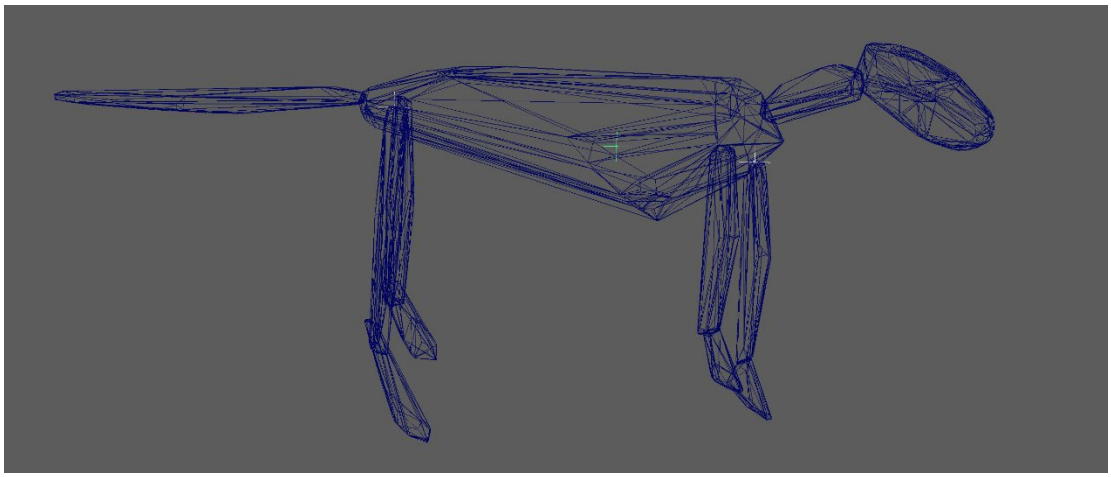

Crocodylus moreletii - Morelet's Crocodile:

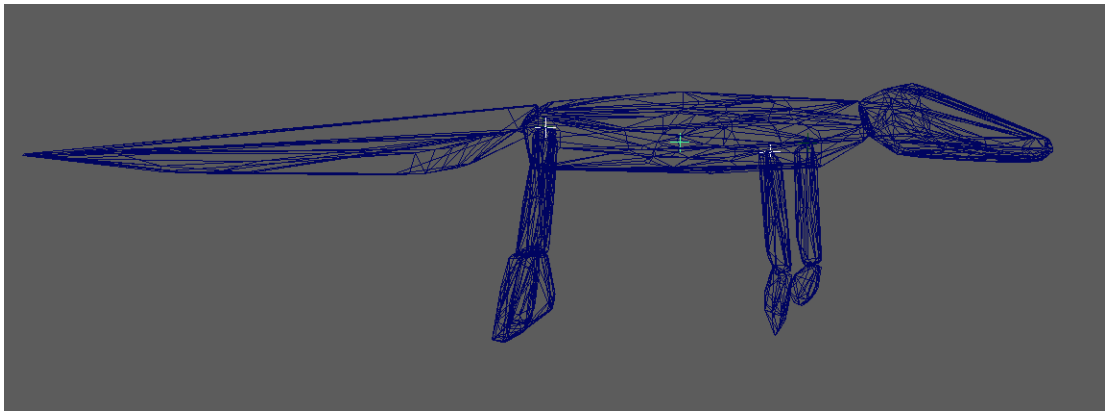

Okapia johnstoni - Okapi:

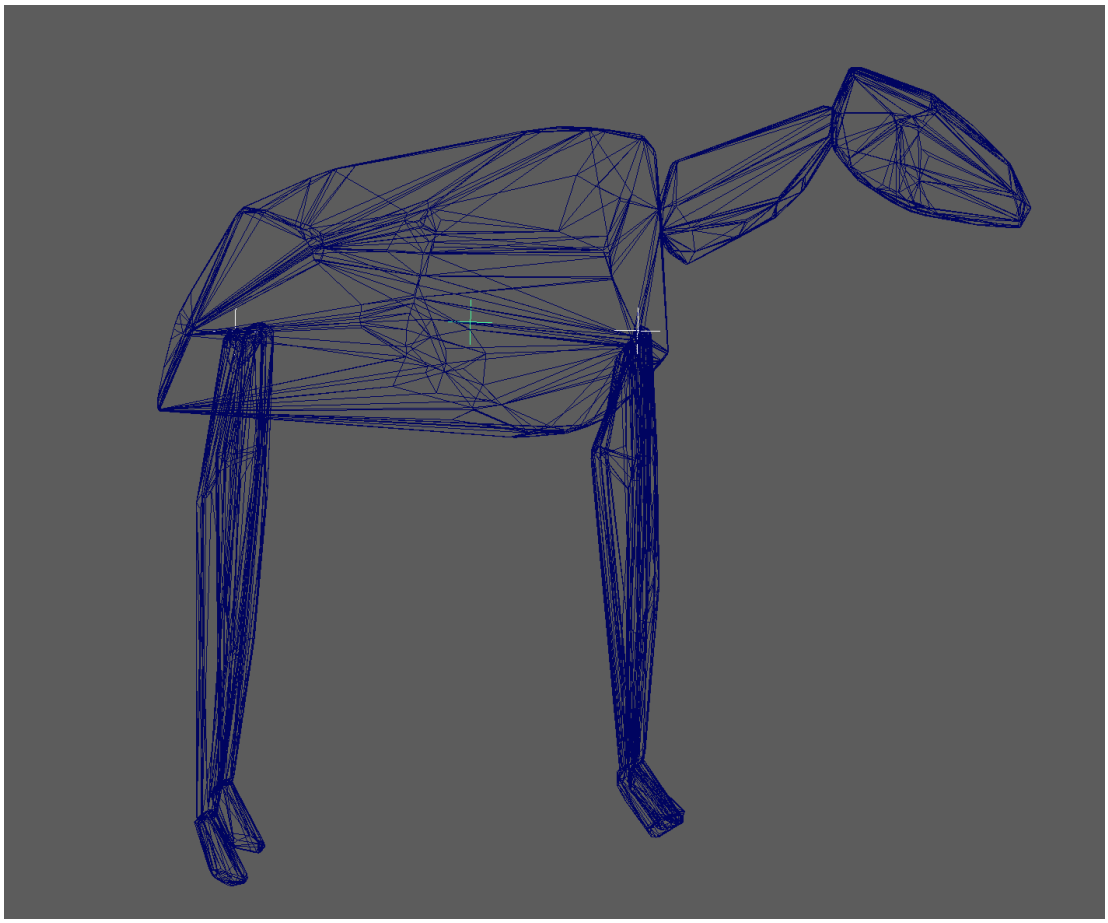

Lutra lutra - Otter:

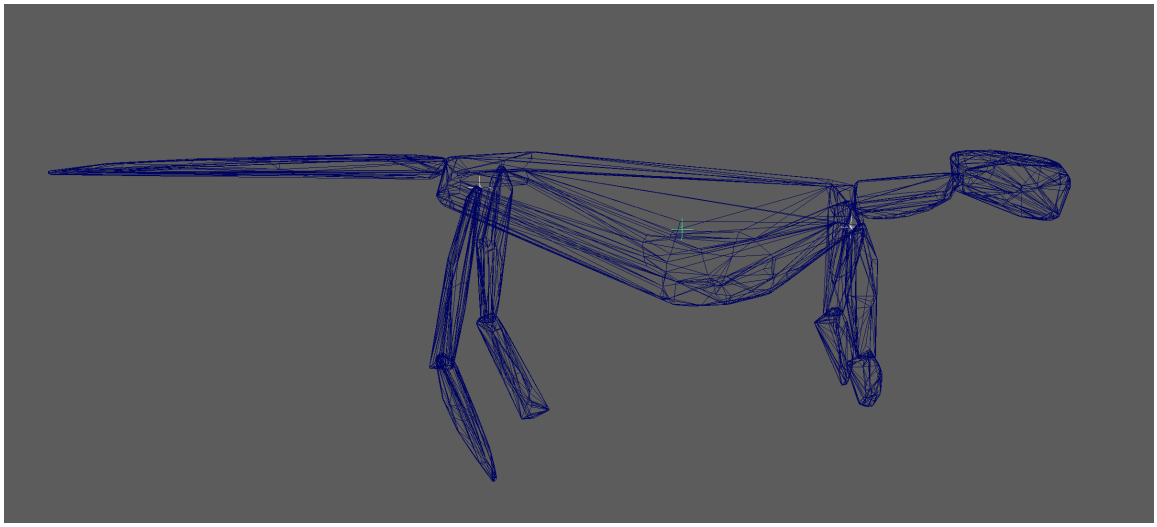

Cuniculus paca - Paca:

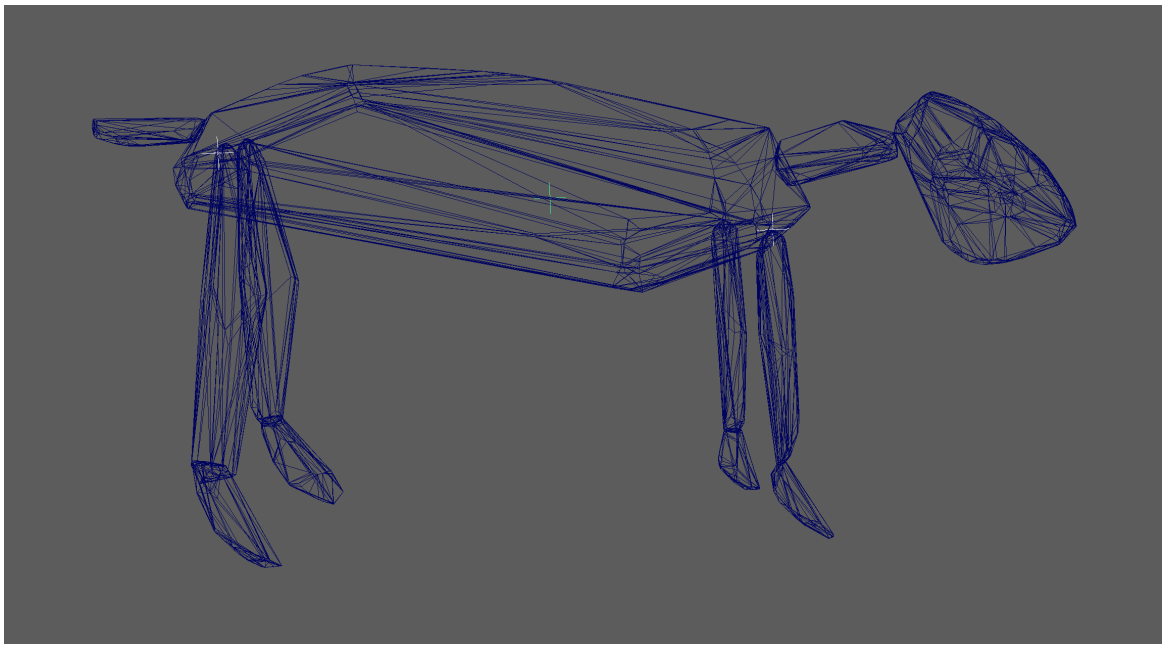

Pecari tajacu - Peccary:

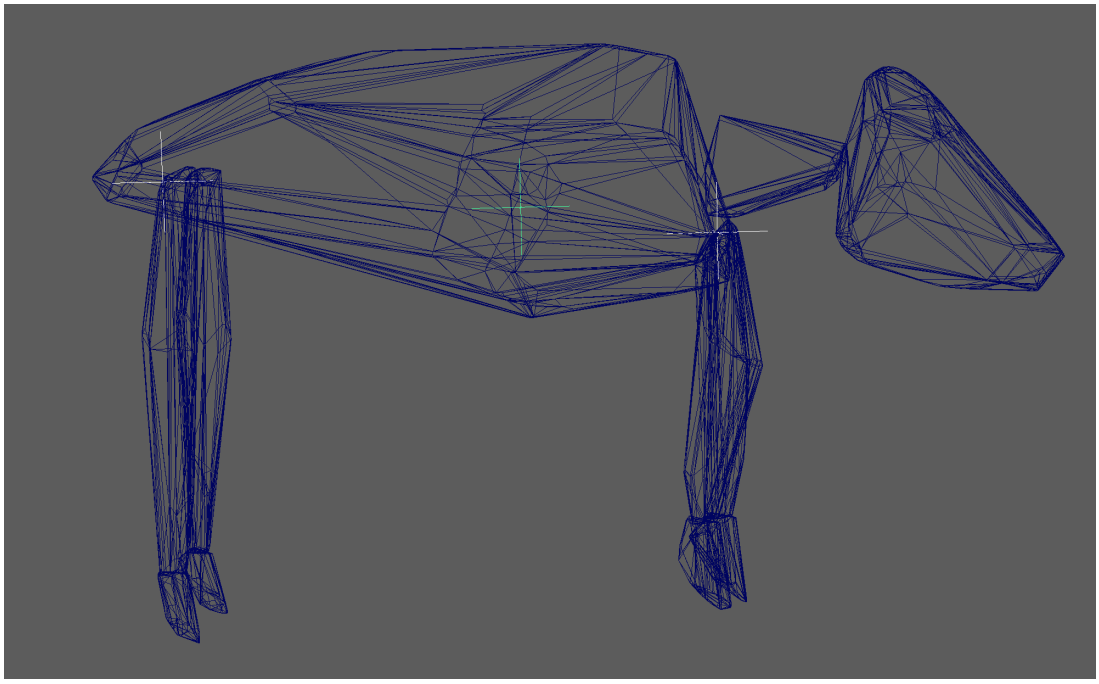

Sus scrofa - Pig:

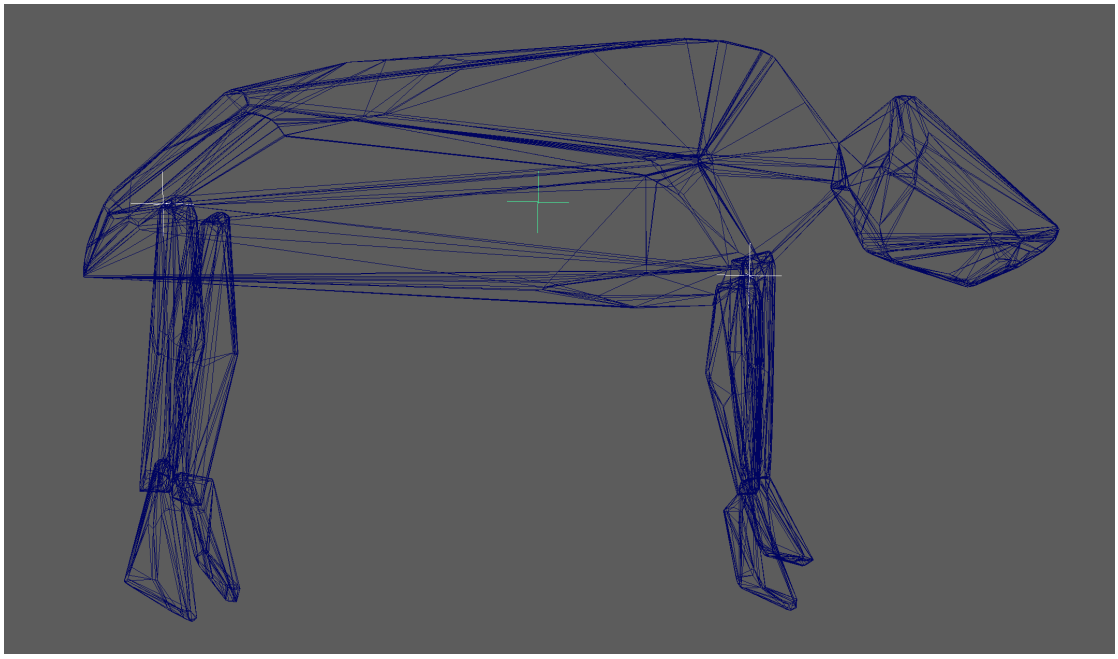

Ursus maritimus - Polar Bear:

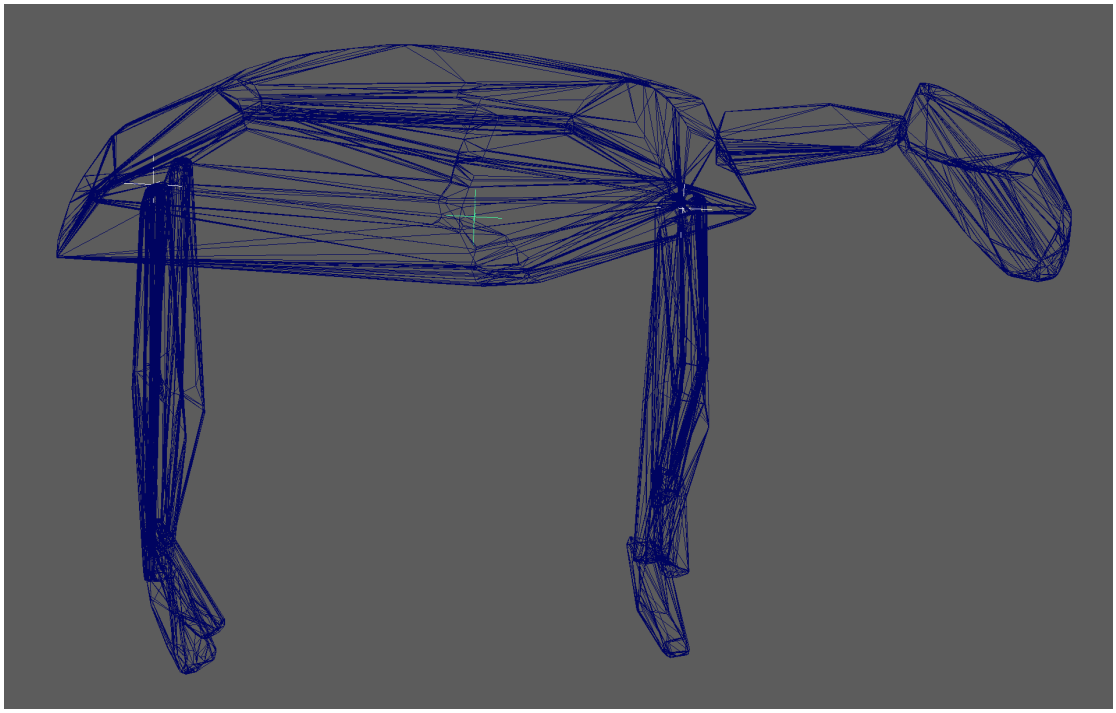

Choeropsis liberiensis - Pygmy Hippo:

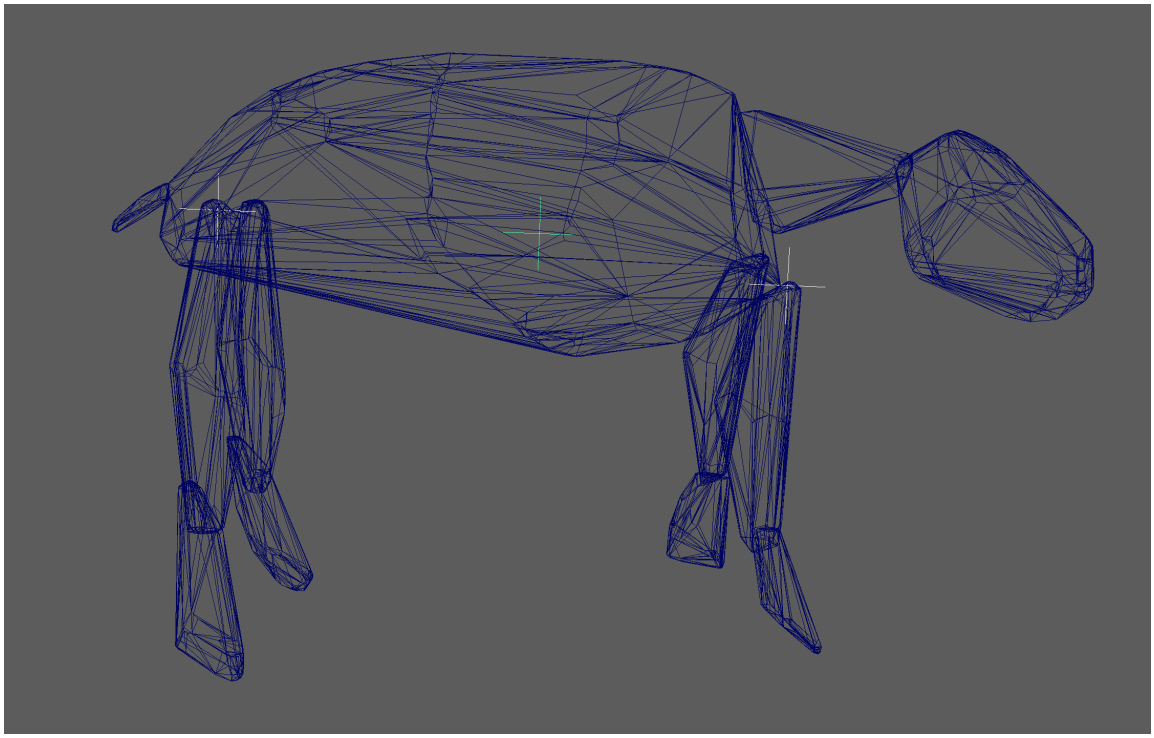

Ovis aries - Ram:

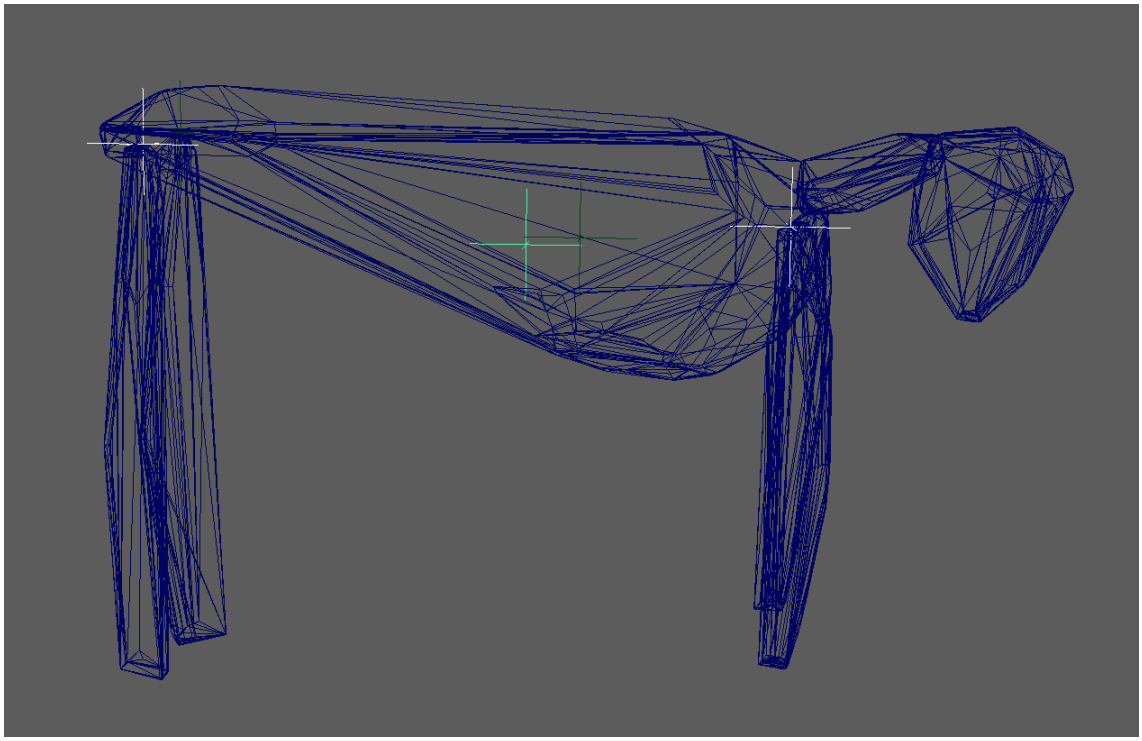

Cervus elaphus - Red Deer:

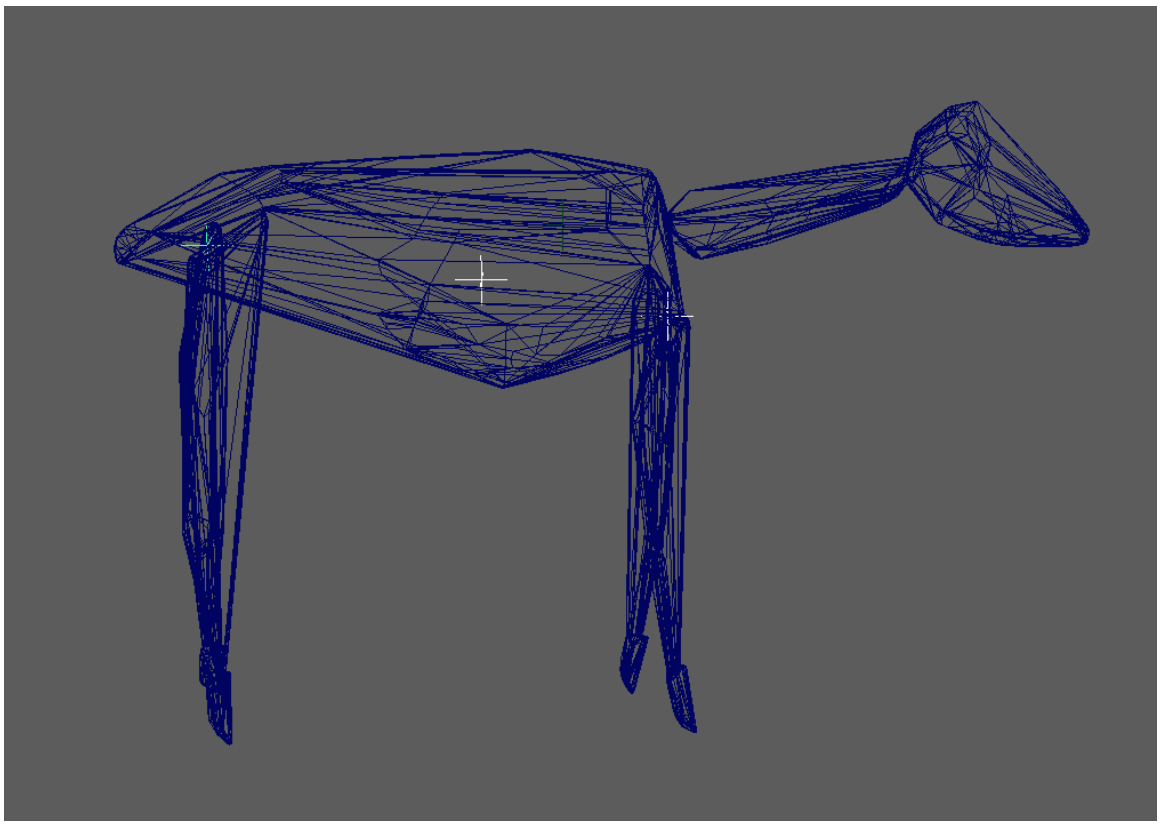

Ailurus fulgens - Red Panda:

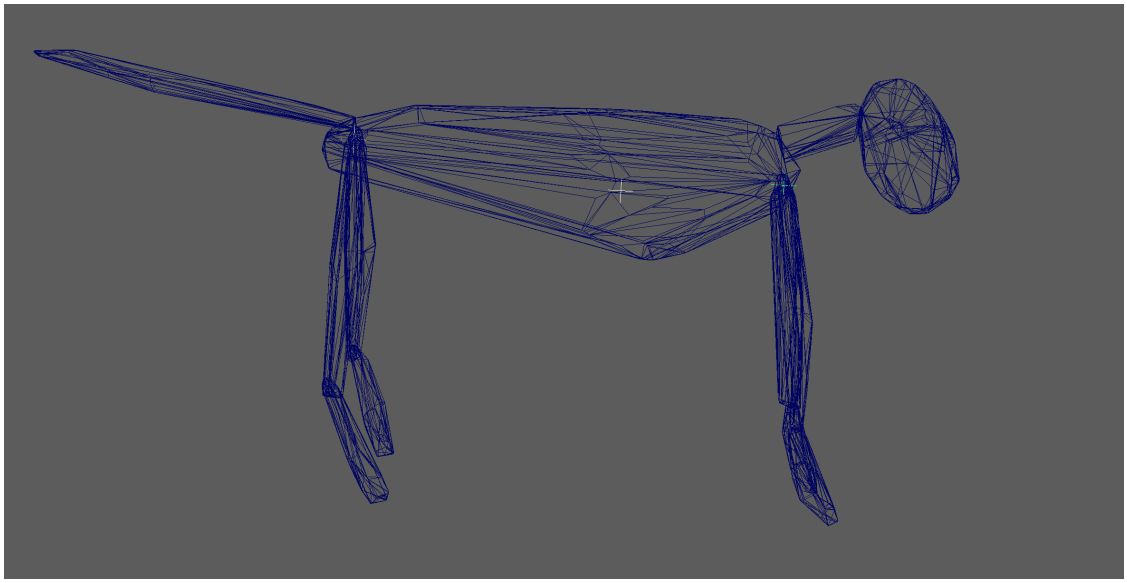

Rangifer tarandus - Reindeer:

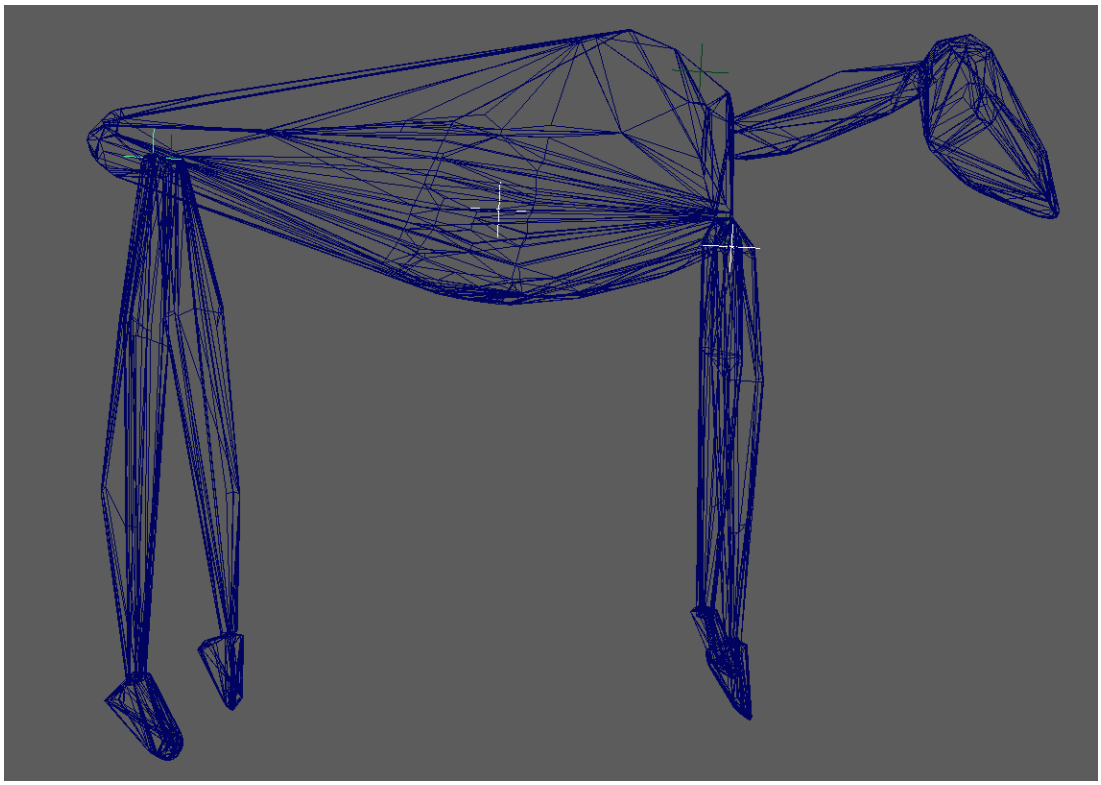

Dicerorhinus sumatrensis - Sumatran Rhino:

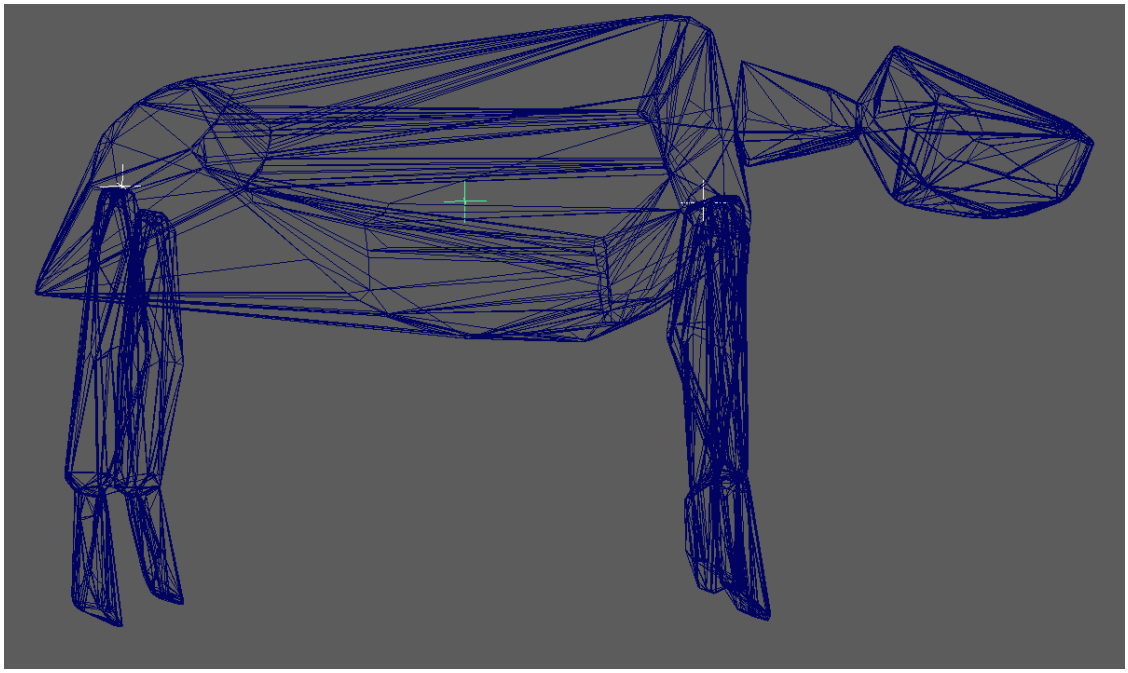

Tamandua tetradactyla - Tamandua:

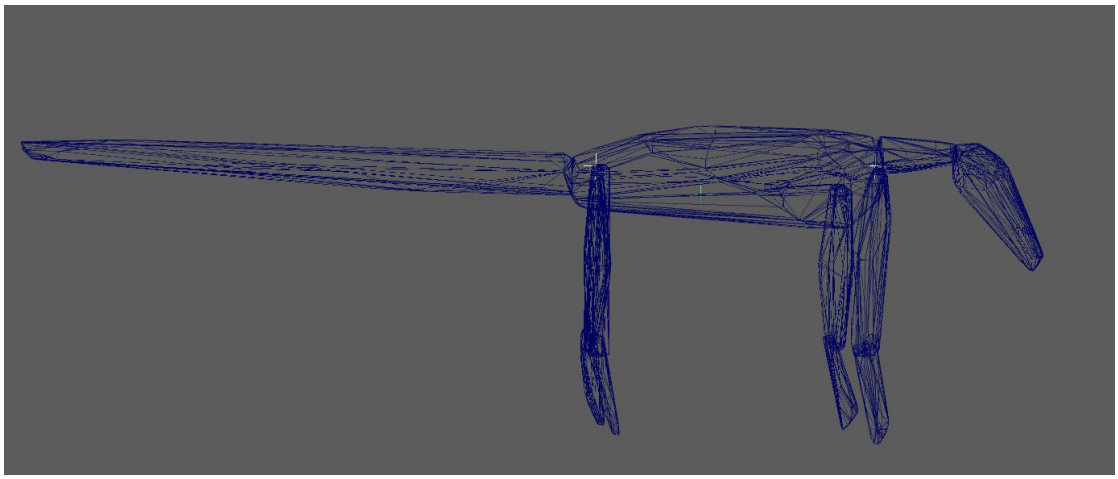

Tapirus terrestris - Tapir:

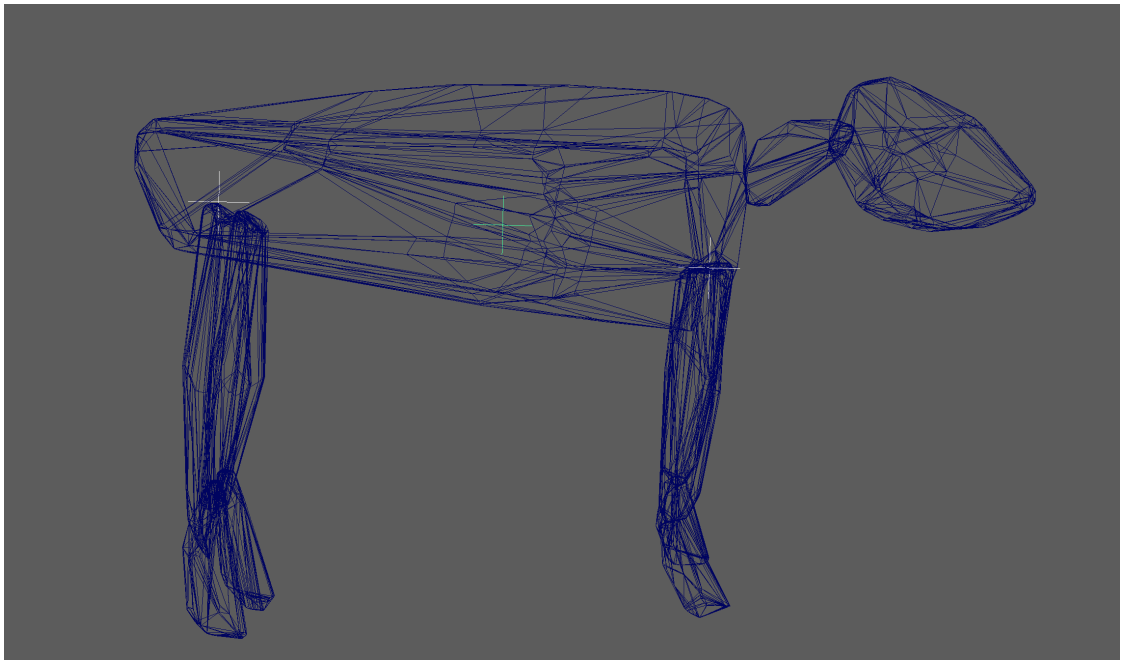

Panthera tigris - Tiger:

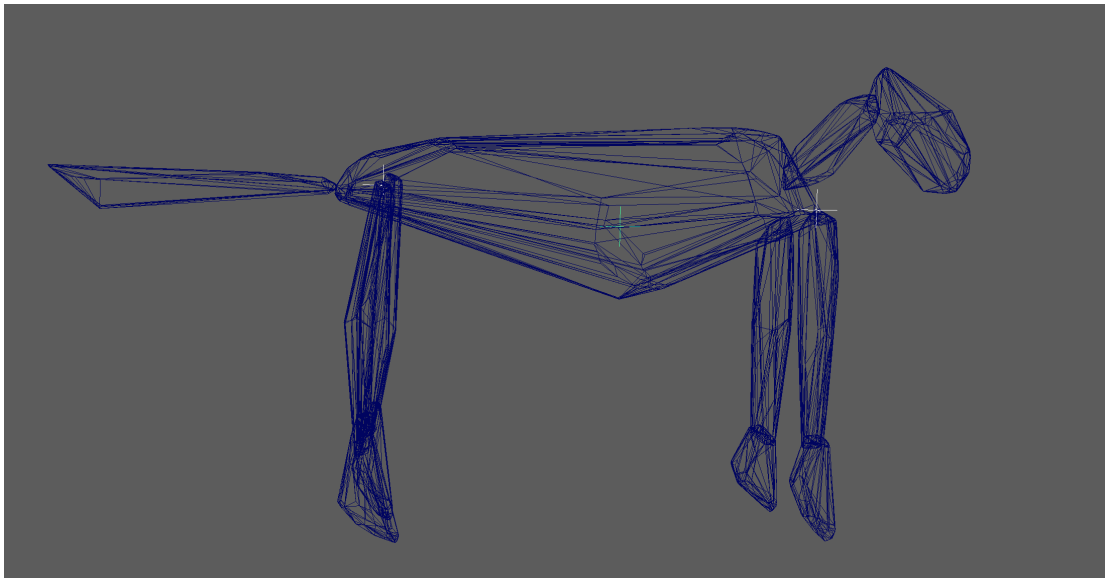

Sphenodon punctatus - Tuatara:

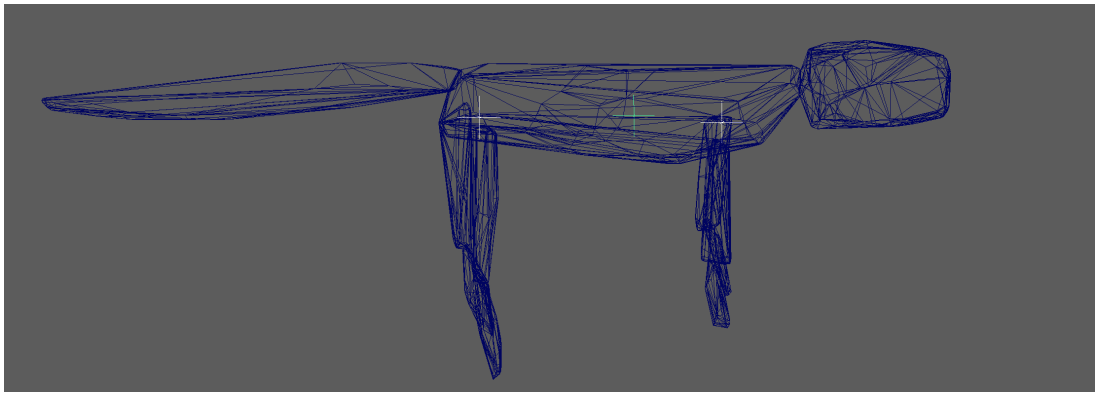

Gulo gulo - Wolverine:

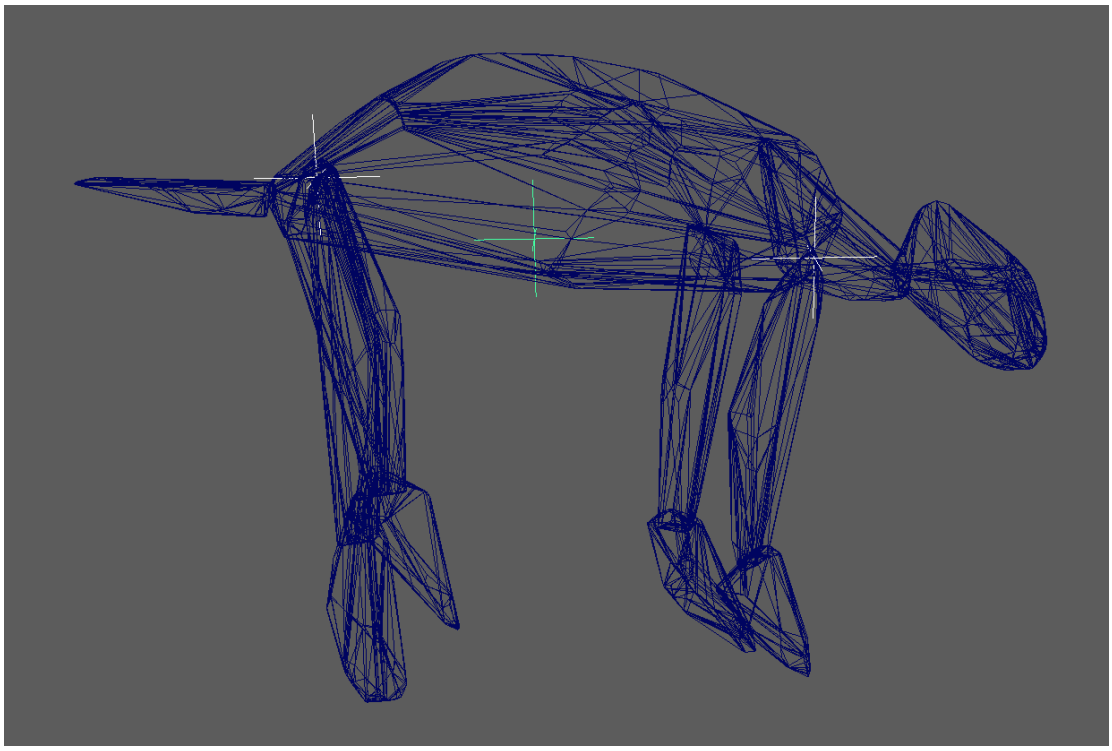

Vombatus ursinus - Wombat:

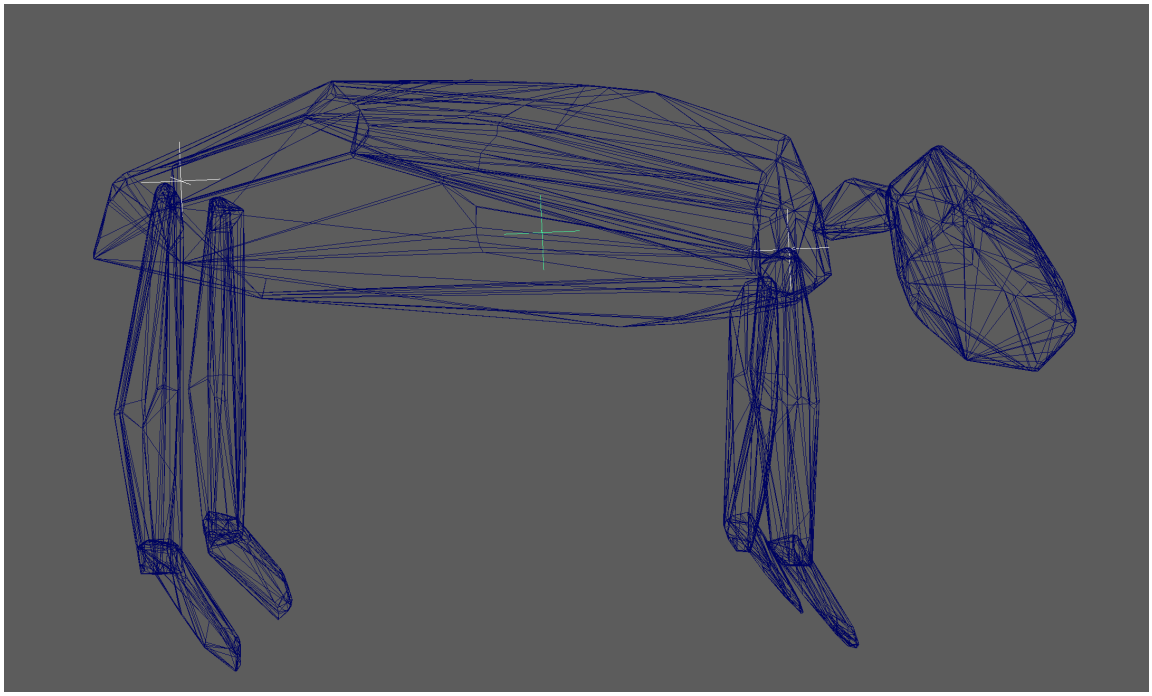

Chapter 4 Supplementary Material

The following supplementary material contains the following:

1. Tables for phylogenetic comparative methods tests for combined data
2. Tables for T-tests for newly-collected data
3. Tables showing raw data collected.

Table S4.1 Table showing results of phylogenetic generalised least squares for tests for newly-collected data combined with data from the literature.

PGLS - Brownian	Correlation	95% CI	P Value	
Area	-0.79	-0.24±0.10	0.04	
Peak Vertical Force	-0.58	-0.06±0.04	0.19	
Peak Pressure	-0.90	-0.11±0.05	0.05	
PGLS - Pagel's Lambda	Correlation	Lambda	95% CI	P Value
Area	-1	-2.23	0.21±0.02	0
Peak Vertical Force	-0.69	0.94	-0.02±0.05	0.68
Peak Pressure	-0.94	0.90	-0.11±0.05	0.08
PGLS - Ornstein-Uhlenbeck	Correlation	95% CI	P Value	
Peak Vertical Force	-0.73	-0.02±0.05	0.67	
Peak Pressure	-0.97	-0.12±0.06	0.07	

4.

5. **Table S4.2** Table showing results of T-tests investigating possible significant differences between manus and pes results for newly-collected data for all relevant variables.

Variable vs CoM	Subject Animal	T Value	DF	P Value	95% CI	95% CI	Mean of Differences
Area	Alpaca	1.57	2	0.26	-17.72	38.10	10.19
Area	Dog	1.00	18	0.33	-2.19	6.18	2.00
Area	Pony	-0.71	2	0.55	-13.63	9.76	-1.94
Area	Goat	8.22	8	3.59E-05	5.60	9.97	7.78
Area	Tapir	2.95	2	0.10	-15.69	83.82	34.06
Peak Force	Alpaca	2.20	3	0.11	-20.33	111.89	45.78
Peak Force	Dog	3.85	19	0.00	7.90	26.70	17.30
Peak Force	Pony	-0.08	3	0.94	-51.81	49.12	-1.34
Peak Force	Goat	4.10	9	2.69E-03	4.53	15.71	10.12
Peak Force	Tapir	3.62	3	0.04	10.89	168.43	89.66
Median Force	Alpaca	2.61	3	0.08	-8.98	90.04	40.53
Median Force	Dog	3.58	19	0.00	6.51	24.84	15.68
Median Force	Pony	1.24	3	0.30	-47.33	107.59	30.13
Median Force	Goat	3.81	9	4.15E-03	4.06	15.93	9.99
Median Force	Tapir	1.26	3	0.30	-118.26	274.1	77.92
Peak Pressure	Alpaca	2.25	3	0.11	-0.19	1.12	0.46
Peak Pressure	Dog	4.59	19	0.00	0.16	0.42	0.29
Peak Pressure	Pony	0.74	3	0.51	-0.56	0.96	0.17
Peak Pressure	Goat	2.52	9	3.30E-02	0.02	0.39	0.21
Peak Pressure	Tapir	1.28	3	0.29	-0.51	1.20	0.34
Median Pressure	Alpaca	2.14	3	0.12	-0.19	1.00	0.40
Median Pressure	Dog	4.16	19	0.00	0.12	0.36	0.24
Median Pressure	Pony	1.44	3	0.25	-0.35	0.94	0.29

Median Pressure	**Goat**	2.85	9	1.90E-02	0.048	0.42	0.23
Median Pressure	**Tapir**	1.01	3	0.39	-0.78	1.51	0.36

6.

1. **Supplementary Table 4.S3** Table showing results of T-tests investigating possible significant differences between left and right results for newly-collected data for all relevant variables.

Variable vs CoM	Subject Animal	T Value	DF	P Value	95% CI	95%CI	Mean of Differences
Area	Alpaca	0.7	1	0.61	-92.95	103.79	5.15
Force	Alpaca	-1.95	1	0.3	-336.32	246.68	-44.82
Pressure	Alpaca	1.13	1	0.46	-5.01	5.99	0.49
Area	Dog	0.76	9	0.47	-4.4	8.82	2.21
Force	Dog	-1.62	9	0.14	-19.09	3.17	-7.96
Pressure	Dog	-2	9	0.08	-0.27	0.02	-0.13
Area	Pony	NOT ENOUGH DATA TO PERFORM TEST					
Force	Pony	NOT ENOUGH DATA TO PERFORM TEST					
Pressure	Pony	NOT ENOUGH DATA TO PERFORM TEST					
Area	Goat	0.26	4	0.81	-5.33	6.41	0.54
Force	Goat	0.73	4	0.5	-10.96	18.8	3.92
Pressure	Goat	1	4	0.37	-0.31	0.66	0.17
Area	Tapir	5.36	1	0.12	-15.63	38.47	11.42
Force	Tapir	4.04	1	0.15	-37.89	73.22	17.67
Pressure	Tapir	-0.45	1	0.73	-1.86	1.73	-0.06

2.

3. **Supplementary Table 4.S4** Table containing raw data, both newly-collected, and from the literature.

New Data	CoM Est (% GAD)	Area (cm2)	Peak Force (N)	Median Force (N)	Peak Pressure (N/cm2)	Median Pressure (N/cm2)
Alpaca - *Vicugna pacos*	56.98	111.05	133.74	140.50	119.51	127.09
Dog - *Canis lupus*	57.36	103.83	126.94	125.27	125.52	122.37
Pony – *Equus ferus caballus*	52.49	92.53	101.58	122.27	111.75	118.43
Goat – *Capra aegagrus herpus*	59.09	140.12	184.07	216.97	134.00	150.82
Tapir – *Tapirus terrestris*	56.57	114.68	143.28	143.52	120.11	124.21

Literature Data	**CoM Est (%GAD)**	**Area (cm2)**	**Peak Force (N)**	**Median Force (N)**	**Peak Pressure (N/cm2)**	**Median Pressure (N/cm2)**
Elephas maximus	58.03	128.08		148.10		117.07
Loxodonta africana	63.92	102.73	116.78		113.36	
Alligator mississippiensis	30		77.36			
Crocodylus porosus	50.98	50.10				
Paleosuchus trigonatus	30	83.65				
Tomistoma schlegelii		48.35				
Tiliqua scincoides intermedia		67.36				
Gerrhosaurus major		55.34				

Varanus komodoensis		69.32		
Varanus exanthematicus		79.54		
Varanus rudicollis		49.45		
Eublepharis macularius		88.75		
Pogona vitticeps		38.69		
Calumma parsonii		62.30		
Furcifer pardalis		135.33		
Shinisaurus crocodilurus		130.71		
Corucia zebrata		69.44		
Smaug warreni			116.25	
Eulamprus quoyii			57.69	
Stellagama stellio			142.61	
Leiocephalus schreibersii			97.14	
Oplurus cuvieri			63.64	
Tropidurus torquatus			47.12	
Varanus exanthematicus			90.69	
Cuora flavomarginata		117.42		
Chaco abingdonii		121.82		
Geochelone platynota		82.30		
Rhinella schneideri		88.14		
Pan troglodytes	59.59		78.33	
Pongo abelii	60.58		80.12	
Chlorocebus pygerythrus			78.56	
Erythrocebus patas			74.83	
Ateles fusciceps	39.78		42.86	
Ateles belzebuth	39.78		39.58	
Lemur fulvus			62.96	
Cercopithecus talapoin	47.84		78.57	
Papio cynocephalus	53.58		60.13	
Macaca fascicularis			97.63	
Papio anubis	53.58		110.14	
Erythrocebus patas			100.85	
Macaca mulatta			88.68	
Callithrix jacchus			116.26	
Cheirogaleus medius			70.64	
Myrmecophaga tridactyla	48.00		169.48	
Ovis aries	59.09		166.03	
Bos taurus	61.34	119.84	123.73	103.24
Addax nasomaculatus			102.38	
Felis catus	51.58	95.69	134.63	140.69
Macropus rufus			38.72	
Monodelphis domestica	63		170.16	
Canis lupus familiaris			149.48	
Rattus norvegicus			95.79	
Mus musculus			108.73	
Equus ferus caballus	52.21	104.31	133.34	117.86
Camelus dromedarius	56.98		100	
Vicugna pacos	56.98	109.01	116.67	107.03
Cervus elaphus	60.54	120.58	140	116.11

Sus scrofa domesticus	63.34	126.10	112.5	89.22
Ceratotherium simum	56.21			265

Chapter 5 Supplementary Material

The following supplementary material contains the following:

1. Figure showing results of osteological analysis with *Shunosaurus* included
2. Images of whole-body convex hulls of dinosaur skeletons where used

Figure 6.S1 Scatter graphs showing linear model regressions for osteological analysis, with heteropody index against centre of mass position as a percentage of gleno-acetabular distance in front of the hip (including *Shunosaurus*). A – analysis with sauropodomorphs and ornithischians. B – analysis with ornithischians alone. C – analysis with sauropodomorphs alone.

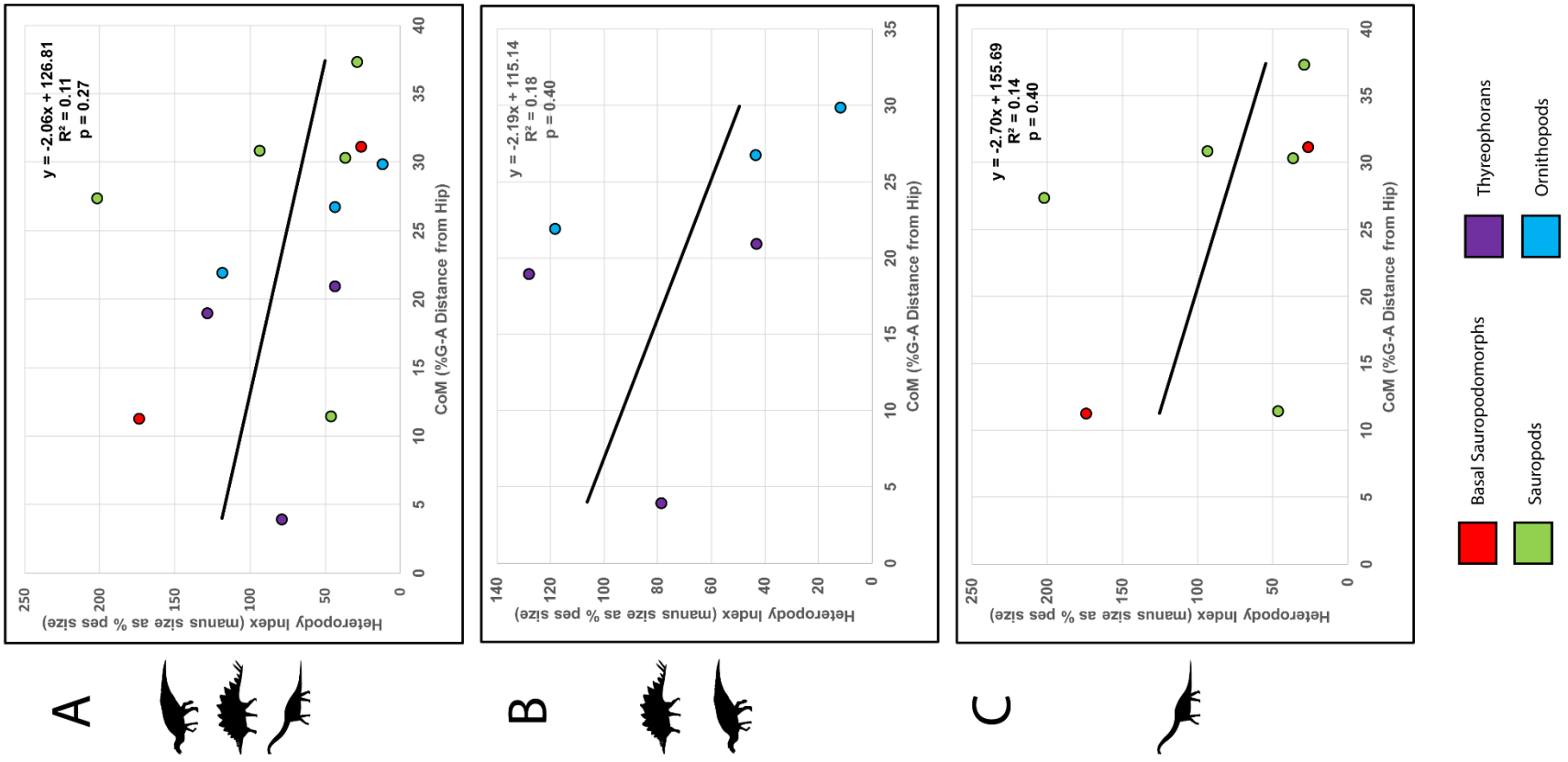

Iguanodon:

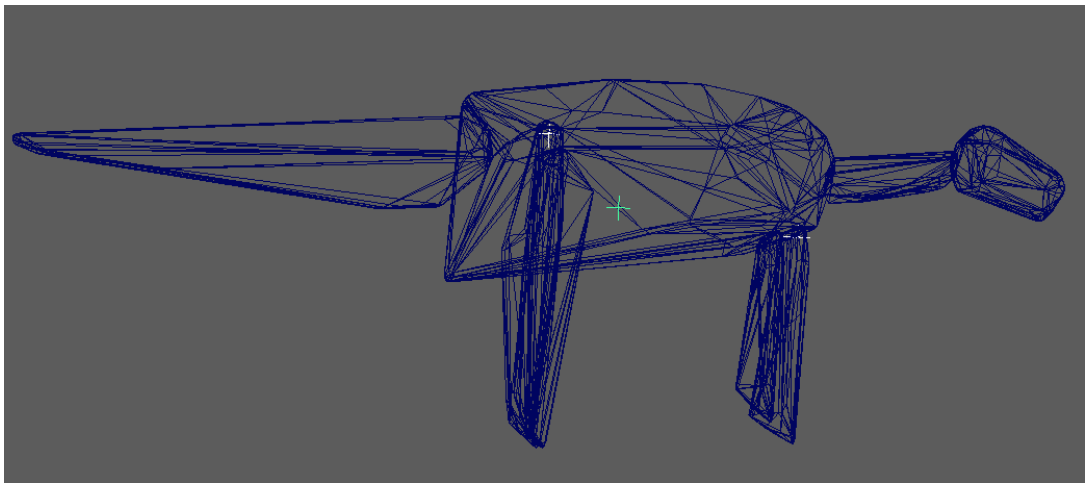

Edmontosaurus:

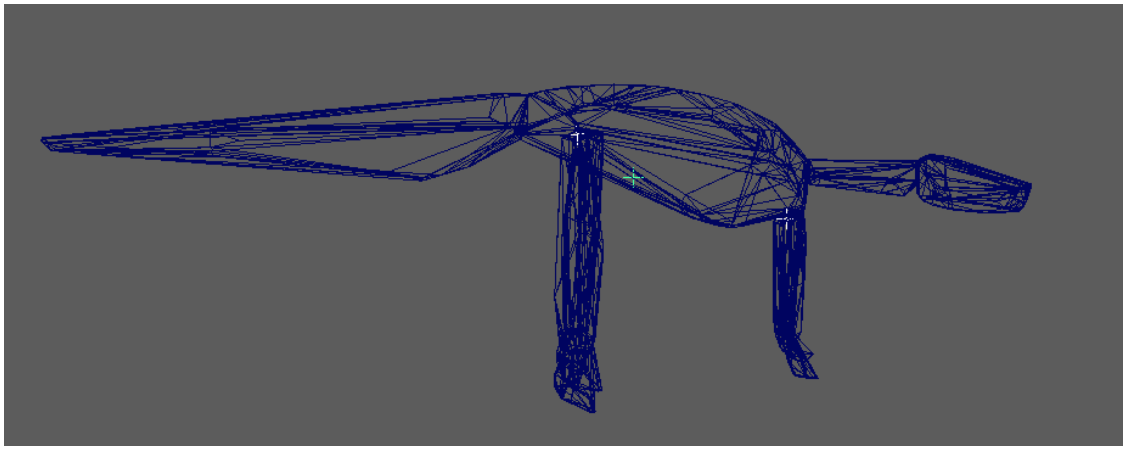

Tenontosaurus: